



HAL
open science

Sources and fluxes of volatile halogenated compounds in highly productive marine areas

Stefan Raimund

► **To cite this version:**

Stefan Raimund. Sources and fluxes of volatile halogenated compounds in highly productive marine areas. Organic chemistry. Université de Bretagne Occidentale, 2010. English. NNT: . tel-01112564

HAL Id: tel-01112564

<https://hal.sorbonne-universite.fr/tel-01112564>

Submitted on 3 Feb 2015

HAL is a multi-disciplinary open access archive for the deposit and dissemination of scientific research documents, whether they are published or not. The documents may come from teaching and research institutions in France or abroad, or from public or private research centers.

L'archive ouverte pluridisciplinaire **HAL**, est destinée au dépôt et à la diffusion de documents scientifiques de niveau recherche, publiés ou non, émanant des établissements d'enseignement et de recherche français ou étrangers, des laboratoires publics ou privés.

Avertissement

Au vu de la législation sur les droits d'auteur, ce travail de thèse demeure la propriété de son auteur, et toute reproduction de cette oeuvre doit faire l'objet d'une autorisation de l'auteur. (cf Loi n°92-597; 1/07/1992. Journal Officiel, 2/07/1992)

UBO

université de Bretagne
occidentale



THÈSE / UNIVERSITÉ DE BRETAGNE OCCIDENTALE

sous le sceau de l'Université européenne de Bretagne

pour obtenir le titre de

DOCTEUR DE L'UNIVERSITÉ DE BRETAGNE OCCIDENTALE

Mention : Chimie Marine

École Doctorale Sciences de la mer

présentée par

Stefan Raimund

Préparée à la Station Biologique de Roscoff,
UMR 7144 AD2M, Equipe chimie marine

Sources and fluxes of volatile halogenated organic compounds in highly productive marine areas

Thèse soutenue le 9 avril 2010:
devant le jury composé de :

Birgit QUACK,
Directrice de recherche, IFM-GEOMAR Kiel / rapporteur

Richard SEMPERE,
Directeur de recherche, Université de la Méditerranée Aix-
Marseille 2 / rapporteur

Pierre LE CORRE,
Professeur Emérite, Université de Bretagne Occidentale /
examineur

Catherine LEBLANC,
Chargée de recherche, Station Biologique de Roscoff /
examineur

Phil NIGHTINGALE,
Professeur, Plymouth Marine Laboratory / examineur

Pascal MORIN,
Chargé de recherche, Station biologique de Roscoff / directeur
de thèse

Ricardo RISO,
Professeur, Université de Bretagne Occidentale / examineur



Table of Contents

Table of Contents	3
List of Figures	7
List of Tables	9
Abstract	11
Acknowledgements	13
1 Introduction	15
1.1 Thesis Goals.....	16
2 VHOC: State of the art	19
2.1 Chemical properties	20
2.2 Sources	21
2.2.1 Biological sources	22
2.2.2 Natural, nonbiological formation of VHOCs.....	24
2.2.3 Anthropogenic sources	27
2.3 Lifetimes in the Troposphere	28
2.4 VHOC contribution to reactive stratospheric halogens	32
2.5 Air-Sea Exchange	35
2.5.1 Henry's law constants	37
2.5.2 Transfer velocity.....	40
2.5.3 Notes on calculations of air mixing ratios	49
3 Methods and Development of the Analytical System	51
3.1 Working with Trace Elements	51
3.2 Sampling Devices.....	51
3.3 Extraction	52
3.3.1 Solid-Liquid extraction.....	52
3.3.2 Liquid-Liquid extraction.....	53
3.3.3 Gaseous-Liquid extraction.....	53
3.4 Purge gas desiccation.....	55

3.5	Preconcentration of the analytes and injection.....	56
3.6	Separation and Detection	57
3.7	Limit of Detection.....	59
3.8	Implemented GC-ECD-System.....	62
3.8.1	Sampling device.....	63
3.8.2	Purge-and-Trap.....	64
3.8.3	Retention times and identification of the compounds	66
3.8.4	Standards.....	67
3.8.5	Summary of the PAT-GC-ECD parameters	69
3.9	Protocols for maintaining the system	70
4	Distribution of Volatile Halogenated Organic Compounds in the Iberian Peninsula	
	Upwelling System	73
4.1	Introduction	73
4.2	Method.....	74
4.2.1	Study Area	74
4.2.2	Physical variables and pigment analysis.....	75
4.2.3	Analysis of volatiles	76
4.2.4	Data analysis.....	77
4.3	Results	78
4.3.1	Upwelling during the campaign and sampling strategy.....	78
4.3.2	Spatial distribution of selected VHOCs	80
4.3.3	SST as grouping variable.....	82
4.3.4	Relationship Between the Compounds.....	83
4.3.5	Vertical distribution of VHOCs compared to environmental parameters	84
4.3.6	Temporal and tide factors in the upper layers.....	88
4.4	Discussion.....	91
4.4.1	Comparison to other studies.....	91
4.4.2	On the different origin of VHOCs	92
4.4.3	Evidence for phytoplanktonic production of VHOCs.....	94

4.4.4	Near shore production: main source for brominated compounds in the upwelling?	97
4.5	Conclusion	98
5	Annual distribution of reactive halocarbons in a tide influenced estuary: Exchange fluxes between ocean and atmosphere	99
5.1	Introduction	99
5.2	Methods	101
5.2.1	Sampling area	101
5.2.2	Sampling strategy	102
5.2.3	Methods for physical, chemical and biological variables	103
5.2.4	VHOC measurements	105
5.3	Results	106
5.3.1	Meteorological variables	106
5.3.2	Environmental data describing seasonality at ASTAN and ESTACADE point	107
5.3.3	Environmental data describing seasonality along a salinity gradient in the Bay of Morlaix	111
5.3.4	Seasonality of VHOC surface concentrations	114
5.3.5	Formation of halocarbons during a diurnal tidal cycle	117
5.3.6	Possible input of halocarbons by a sewage treatment plant at Morlaix	120
5.4	Discussion	122
5.4.1	Comparison to other costal measurements	122
5.4.2	Temporal trends	123
5.4.3	Biogenic sources	125
5.4.4	Different sources along the gradient	129
5.4.5	Sea-air Fluxes	136
5.5	Conclusion	142
6	Physiological function of VHOCs for macroalgae	143
6.1	Summary	147
6.2	Introduction	148
6.3	Material and Methods	150

6.3.1	Algal material and elicitation procedures	150
6.3.2	Conditioning procedure in the laboratory	151
6.3.3	Transient transplantation in the field	152
6.3.4	Aldehydes and volatile halogenated organic compounds (VHOCs) measurements 152	
6.3.5	RNA extraction and RT-qPCR.....	153
6.4	Results	153
6.4.1	Wild and laboratory-grown algae display different defense responses	153
6.4.2	Effect of transient transplantation.....	155
6.4.3	Development of a conditioning procedure in the laboratory	157
6.4.4	The conditioning procedure down-regulated the oligoguluronates-induced release of VOCs	160
6.5	Discussion.....	161
6.6	Acknowledgements.....	166
6.7	References.....	167
7	Conclusions and perspectives	171
8	Literature.....	173

List of Figures

FIGURE 1. STRUCTURAL FORMULA OF STUDIED VHOCS.	19
FIGURE 2. PRIMARY SOURCES OF CHLORINE AND BROMINE FOR THE STRATOSPHERE (FAHEY 2006).	32
FIGURE 3. OZONE DESTRUCTION CYCLE 1.	33
FIGURE 4. MODEL FOR AIR-SEA-FLUXES, ADAPTED FROM LISS AND SLATER (1974).	36
FIGURE 5. TRANSFER VELOCITY OF CO ₂ (BLUE) AND VHOCS (GREEN) USING THE APPROACH OF (LISS AND MERLIVAT 1986)...	42
FIGURE 6. DIFFERENT PARAMETERIZATIONS FOR TRANSFER VELOCITY CALCULATION FOR CO ₂	44
FIGURE 7. COMPARISON OF THREE APPROXIMATIONS FOR Sc CALCULATIONS.	49
FIGURE 8. SCHEME OF AN ELECTRON CAPTURE DETECTOR (ECD).....	58
FIGURE 9. LINEAR RANGE OF AN ECD.....	59
FIGURE 10. ECD RESPONSE, RELATIVE TO THE COMPOUND OF THE HIGHEST RESPONSE (TETRACHLOROMETHANE).....	60
FIGURE 11. SAMPLING DEVICE (WATER), NISKIN-ADAPTER AND FLOW-OPENER	63
FIGURE 12. SAMPLING DEVICE (AIR), GLASS BULB AND SYRINGE.....	64
FIGURE 13. SCHEMATIC PICTURE OF THE ANALYTICAL SYSTEM.	65
FIGURE 14. CHROMATOGRAM OF A STANDARD MIXTURE.	67
FIGURE 15. MOUTON CAMPAIGN 2007 IN THE IBERIAN PENINSULA UPWELLING SYSTEM.	74
FIGURE 16. SATELLITE IMAGE OF SEA SURFACE TEMPERATURE (SST) AND CHL-A CONCENTRATION ON AUGUST 19 TH 2007.....	79
FIGURE 17. SEASURFACE VALUES OF SELECTED VHOCS.	81
FIGURE 18. PRINCIPAL COMPONENT ANALYSIS (PCA) OF ALL NORMALIZED VHOCS DATA.....	82
FIGURE 19. CORRELATIONS OF SELECTED VHOCS WITH ALL VHOCS.	84
FIGURE 20 DEPTH PROFILES FOR THREE DEFINED WATER MASSES.....	85
FIGURE 21. INFLUENCE OF TIME OF THE DAY TO BROMOCARBONS.....	89
FIGURE 22. INFLUENCE OF TIDE TO SELECTED VHOCS IN THE UPPER LAYERS.....	90
FIGURE 23. CORRELATIONS OF SELECTED VHOCS WITH ENVIRONMENTAL VARIABLES.	95
FIGURE 24. CHART DATUM MAP OF THE SAMPLING AREA.	101
FIGURE 25. TIDAL AMPLITUDE [EXPRESSED AS TIDAL COEFFICIENT] AND SAMPLING STRATEGY.	102
FIGURE 26. AIR TEMPERATURE AND SUN RADIATION AT ROSCOFF BETWEEN MAY 2008 AND END OF MAY 2009.....	106
FIGURE 27. WIND VELOCITY [M · S ⁻¹] AND WIND DIRECTION DURING THE FIELD CAMPAIGN 2008/09.....	107
FIGURE 28. SEASONALITY OF SYNOPTIC DATA AT ASTAN AND ESTACADE POINT.	108
FIGURE 29. ANNUAL NUTRIENT LEVELS [μMOL · L ⁻¹] IN THE WESTERN ENGLISH CHANNEL, OFF ROSCOFF.	109
FIGURE 30. ANNUAL DISTRIBUTION OF PIGMENTS [μG L ⁻¹] IN THE WESTERN ENGLISH CHANNEL, OFF ROSCOFF.	110
FIGURE 31. ANNUAL DISTRIBUTION OF CHLOROPHYLL A, PHAEOPIGMENTS AND WATER TEMPERATURE IN THE BAY OF MORLAIX (MAY 2008 TO MAY 2009) ALONG THE SALINITY GRADIENT.	112

FIGURE 32. ANNUAL DISTRIBUTION OF NUTRIENTS IN THE BAY OF MORLAIX (MAY 2008 TO MAY 2009).	113
FIGURE 33. ANNUAL DISTRIBUTION OF BROMINATED HALOCARBONS ALONG A SALINITY GRADIENT IN THE BAY OF MORLAIX....	115
FIGURE 34. ANNUAL DISTRIBUTION OF IODINATED HALOCARBONS ALONG A SALINITY GRADIENT IN THE BAY OF MORLAIX.	116
FIGURE 35. ANNUAL DISTRIBUTION OF CHLORINATED HALOCARBONS ALONG A SALINITY GRADIENT IN THE BAY OF MORLAIX. ...	117
FIGURE 36. DIURNAL TIDAL CYCLE AND LENGTH OF DAYLIGHT AT ROSCOFF DURING THE FIELD CAMPAIGN AT THE <i>ESTACADE</i> POINT.	117
FIGURE 37. CONCENTRATIONS OF CHLORINATED COMPOUNDS AT <i>ESTACADE</i> POINT DURING DIURNAL TIDAL CYCLE.	118
FIGURE 38. CONCENTRATIONS OF BROMINATED COMPOUNDS AT <i>ESTACADE</i> POINT DURING DIURNAL TIDAL CYCLE.	119
FIGURE 39. CONCENTRATIONS OF IODINATED COMPOUNDS AT <i>ESTACADE</i> POINT DURING DIURNAL TIDAL CYCLE.	120
FIGURE 40. COMPARISON OF HALOCARBON CONCENTRATIONS ALONG TWO SALINITY GRADIENTS (PSU VS $\mu\text{MOL L}^{-1}$).	121
FIGURE 41. SEASONALITY OF VHOCs IN THE BAY OF MORLAIX.	124
FIGURE 42. MACROALGAE DISTRIBUTION OFF ROSCOFF AND AROUND ÎLE DE BATZ (NORTH WESTERN PART OF THE BAY OF MORLAIX).	126
FIGURE 43. INFLUENCE OF SALINITY ON VHOC CONCENTRATIONS.	130
FIGURE 44. PIGMENT CONCENTRATIONS [$\mu\text{G L}^{-1}$] ALONG THE SALINITY GRADIENT.	132
FIGURE 45. CORRELATION PLOTS BETWEEN SEAWATER HALOCARBON CONCENTRATIONS.	134
FIGURE 46. CURRENTS IN THE BAY OF MORLAIX.	135
FIGURE 47. SEA-AIR FLUX [$\text{NMOL M}^{-2} \text{D}^{-1}$] OF SELECTED VHOC USING DIFFERENT PARAMETERIZATION FOR THE TRANSFER VELOCITY.	138
FIGURE 48. THE PUTATIVE ROLE OF VANADIUM-DEPENDENT HALOPEROXIDASES (VHPO) IN THE DEFENCE RESPONSE OF KELP..	144

List of Tables

TABLE 1. CHEMICAL PROPERTIES OF VHOCS STUDIED IN THIS WORK.	21
TABLE 2. VHOCS IN THE ATMOSPHERE.	31
TABLE 3. EXPERIMENTAL VARIABLES A, B AND C TO CALCULATE THE TEMPERATURE AND SALINITY DEPENDENT H_D	39
TABLE 4. PUBLISHED VALUES FOR HENRY'S LAW CONSTANT H_D (DIMENSIONSLESS).	40
TABLE 5. MOLECULAR VOLUME [$\text{CM}^3 \text{MOL}^{-1}$] AND SCHMIDT NUMBERS FOR VHOCS AT 15°C.	48
TABLE 6. COMPARATIVE STUDY OF LITERATURE ABOUT DIFFERENT PAT- AND DESICCATION TECHNIQUES.	54
TABLE 7. COMPARATIVE STUDY OF LITERATURE ABOUT DIFFERENT AD- AND DESORPTION TECHNIQUES.	57
TABLE 8. COMPARISON OF ABSOLUTE DETECTION LIMITS [$\text{PMOL} \cdot \text{L}^{-1}$] IN THE LITERATURE.	61
TABLE 9. GENERAL OVERVIEW OF MEASUREMENT CONDITIONS.	69
TABLE 10. VOLATILE HALOGENATED ORGANIC COMPOUNDS DETERMINED IN THE IBERIAN PENINSULA UPWELLING SYSTEM.	77
TABLE 11. MEAN VALUES OF 13 VHOCS IN PMOL/L AND DBM/BF- RATIO IN THE IBERIAN UPWELLING.	87
TABLE 12. PHYSICAL AND CHEMICAL VARIABLES IN THE IBERIAN UPWELLING REGION.	87
TABLE 13. MEAN VALUES OF MARKER PIGMENTS IN THE IBERIAN UPWELLING REGION.	88
TABLE 14. COMPARISON OF VHOCS CONCENTRATIONS IN DIFFERENT REGIONS.	92
TABLE 15. RANGE OF HALOCARBON CONCENTRATIONS MEASURED IN WATER [PMOL L^{-1}] AND COMPARISON WITH PREVIOUS STUDIES.	122
TABLE 16. RANGE OF HALOCARBON MIXING RATIOS [PPTV] MEASURED IN AIR SAMPLES FROM DIFFERENT SAMPLING SITES.	123
TABLE 17. RELEASE OF BROMINE AND IODINE FROM DIFFERENT MACROALGAE, REPORTED BY CARPENTER ET AL. (2000).	127
TABLE 18. SPEARMAN'S RANK CORRELATION (SIGNIFICANCE $P < 0.01$). *	132
TABLE 19. AVERAGE ANNUAL DAILY [$\text{NMOL M}^{-2} \text{DAY}^{-1}$] AND TOTAL [$\mu\text{MOL M}^{-2} \text{YR}^{-1}$] SEA-TO-AIR FLUX IN THE BAY OF MORLAIX. *	139

Abstract

Volatile halogenated organic compounds (VHOCs) constitute a large group of environmental gases that can influence atmospheric chemistry, and have natural and anthropogenic sources. Biological VHOC formation is poorly investigated. In this work the role of plant-plant communication and their influence on VHOC formation was studied. It could be demonstrated that oligoguluronates trigger the formation of VHOC. Plant-plant communication orchestrates the formation of VHOCs: “forewarned” algae react less intensely after perception of an oligoguluronates signal. This might be beneficial for the algae in terms of cost efficiency.

Marine biogenic production of VHOC contributes significantly to the global halogen cycle, and a better knowledge of sources and fluxes of VHOCs is crucial. In this work VHOC distribution was studied in the Iberian upwelling system, and in a mega-tidal influenced and nutrient-enriched estuary on the South-western coast of the English Channel. Both areas are characterized by high primary production and are suspected to be “hot spots” of VHOC formation. Measurements off Portugal showed that halocarbons distribution is related to sea surface temperature and advection processes. Bromocarbon concentrations are affected by tides and had the highest concentrations near the coast. Coastal macroalgae beds are most likely the main source of brominated VHOCs in the upwelling while open-ocean concentrations could be related to phytoplankton production. Evidences were found that iodinated compounds have mainly a bacterial offshore origin. Chlorocarbons have non-biological sources. The postulated high concentrations of biogenic VHOCs were not found. Hence we reject the idea that upwelling regions might be hot spots for VHOC formation due to diatom activity. Annual halocarbon measurements in the English Channel displayed a marked seasonality. Brominated and iodinated compounds showed summer maxima and winter minima, and exhibited elevated concentrations in surface waters during low tide compared to high tide. Chlorinated compounds showed winter maxima and summer minima. Distinct concentration gradients of bromo- and chlorocarbons revealed the occurrence of highly localized sources for both groups. Bromocarbons sources were linked to macroalgae beds, whereas chlorocarbons have mostly airborne sources with higher inputs via the river side. Iodocarbons have unknown unlocalized sources in the Bay of Morlaix. Flux calculations revealed that tidal-influenced and macroalgae-dominated ecosystems significantly contribute to global halogen emissions, especially via bromoform and dibromomethane emissions.

Acknowledgements

I would first like to thank my PhD examining board: Birgit Quack, Richard Sempéré, Phil Nightingale, Catherine Leblanc, Pierre Le Corre and Ricardo Riso. Thanks for having accepted to evaluate my work and for travelling to Roscoff.

This work was supported by a FP-6 Marie Curie Fellowship ESteam (MEST-CT-2005-020737) at the Station Biologique de Roscoff, France.

Et comme réaliser une thèse est un travail d'équipe...

Il y a trois ans et demi, quand j'ai quitté « Rostock de l'est » pour rejoindre « Roscoff de l'ouest », je ne pensais pas trouver dans ce petit village gaulois, une Station qui offre un tel environnement pour travailler tant aux niveaux géographique (pour les mauvaises langues, je ne parle pas QUE des vagues du Dossen et de Moguériec !), scientifique qu'humain.

Après les premiers moments de certaines découvertes surprenantes mais inévitables, comme ma première huître, ma première langue de bœuf, mes premiers repas interminables (mais passent ils leur journée à manger en France??) et mon premier kig ha farz, je me sens maintenant à 50% français, et fin prêt désormais à tester ma première cuisse de grenouille grillée. Bref, pour faire court, ces trois années ont vraiment été incroyables pour moi. J'y ai rencontré des personnes accueillantes, disponibles, chaleureuses, alors, un merci à certaines d'entre elles, pêle-mêle :

Bernard Kloareg, sans qui, toute cette «french adventure» n'aurait pas été possible, ainsi qu'à Michèle Barbier pour leur accueil chaleureux et leur dévouement.

Spécial dédicace pour mon équipe, bien-sûr, qui m'a soutenu jusqu'au bout, mes piliers !:
Pascal, tout d'abord, pour m'avoir si bien accueilli et intégré dans l'équipe, pour m'avoir donné sa confiance et son aide tout au long de cette thèse, et pour m'avoir laissé le temps et la liberté nécessaires pour dompter cette machine récalcitrante !! Merci à toi, Pascal!!

Yann, pour les corrections du manuscrit, les discussions scientifiques et tout le reste...

Et puis aussi Geneviève, Marc, Eric, Thierry, Laure, « re-Yann » et « re-Pascal » pour (dans le désordre) : les analyses de sels nutritifs, la compagnie, les sorties en baie de Morlaix, la patience, les pauses cafés, la bonne humeur, la précieuse aide sur MOUTON, le soutien moral, etc...

Bref, à vous tous, un grand merci pour tous ces moments passés et à venir....

Et aussi :

Le service mer (Laurent, Gilles, Noël, Yann, Wilfried pour avoir été si patients et arrangeants face à mes nombreuses (et tardives !!) demandes)

Jérôme Dabin («THE macro-man» !!!): pour m'avoir créé une incroyable macro Excel

François Thomas « l'homme qui murmurait à l'oreille des algues ».

Philippe Bujard et Jack alias Bob pour leur aide technique et leurs dépannages. Spécial message pour Bob : j'aime tes « guten tag » alsaciens quotidiens !!!

Catherine Leblanc pour les enrichissantes discussions scientifiques.

Eric Thiébaud et Pascal Riera pour leur aide sur les statistiques.

Nicole Guyard pour la recherche d'articles.

Stéphane Hourdez pour son efficacité et sa rapidité pour les corrections de dernière minute!!!

Essylt Louarn, pour m'avoir appris les rudiments de chimie marine, ainsi que le fonctionnement de la machine infernale GC

François Lallier et Stéphane Egée qui ont fait le nécessaire pour que je puisse soutenir cette thèse dans les meilleures conditions possibles

...et tous ceux et celles qui m'ont aidé pendant ces trois années.

Et puis, parce qu'une thèse ne se fait pas sans moments de «décompression», et sans création de liens d'amitié, un big thank à :

The «surfing team» : mon acolyte Jan de Cannes bien sûr, Jean-Marie, Gaëlle et Xavier. – Ca farte??

The «Soirées, apéros team » : Caro, Gauthier, Florentine, Régis, Guillaume, Marjo, Steph Egée, Sab et Rigoul !!!..... et surtout merci d'avoir diverti et occupé ma moitié et ma fille pendant ces longs mois de rédaction. Et les gars, une bonne fois pour toute!: non, en Allemagne, les fêtes ne se passent pas comme dans « la grande vadrouille », on ne saute pas sur une chaise à l'envers en chantant « Aie i aie o »

« My french family », Ninick et Lolo. Merci d'avoir rendu les choses plus faciles par votre présence et votre aide !!!

Les plus forts remerciements je voudrais les adresser à "mon coeur" : Céline. Tu m'as apporté un tel soutien pendant ma thèse qu'il est presque difficile de trouver les mots justes pour te dire "Merci". Merci pour tes mots de soutien, luttant pour moi contre les surprises bureaucratiques quotidiennes, merci d'avoir accepté mes absences virtuelles ces dernières semaines et pour tous ces bons et beaux moments que tu as créés. Cette thèse aurait été tout simplement impossible sans toi.

Und ein paar Worte auf Deutsch....

Ein besonderer Dank geht an Birgit für ihre Unterstützung dieser Arbeit! Unter anderem gilt das für die vielen lehrreichen Hinweise und Antworten alle Fassetten das Thema betreffend. Und natürlich dafür, das Du einige Male die strapaziöse Anreise in die Bretagne in Kauf genommen hast!

Mein Dank gilt dem "pdf-Team": Steffen, Christian, Norbert, Thomas, Lucia und Kathrin haben meiner Literaturdatenbank zur ansehnlichen Größe verholfen. Steffen und Simon sei gedankt für den Einführung in die obskure Parallelwelt der Statistik (es gibt ein Leben vor und nach der PCA!).

Meine kleine Tochter Mona hat mich mit Ihrem Lachen moralisch ungemein unterstützt und hat durch ihre Unkompliziertheit ein kontinuierliches Arbeiten erst ermöglicht.

Besonders möchte ich meinen Großeltern für Alles danken, was Ihr mir ermöglicht habt!

1 Introduction

Volatile Halogenated Organic Compounds (VHOCs) are trace gases that can influence atmospheric chemistry. VHOCs are climatically active and potentially a major source of reactive halogens. These gases may contribute to 20-35% of stratospheric bromine; essentially by the short-lived polyhalogenated compounds CH_2Br_2 and CHBr_3 (Pfeilsticker et al. 2000). Bromine may contribute up to 30 % of ozone depletion in the troposphere and lower stratosphere (Salawitch et al. 2005; Yang et al. 2005). World oceans, via the marine-atmosphere boundary layer have been suggested to be the largest source of natural produced VHOCs to the atmosphere. With the introduction of highly sensitive techniques to detect such traces in the environment (Lovelock 1974), it became clear that, beside anthropogenic sources, Nature produces those gases in significant quantities and qualities. In contrast to anthropogenic halocarbons, VHOC with natural sources are characterized as short-lived compounds with life-times in the range of minutes (e.g. diiodomethane) to about a one year (chloromethane) (Law and Sturges 2006). The transport of these gases to the lower stratosphere results from large-scale ascent in the tropics and rapid deep convection. Thus, the role of VHOCs for stratospheric ozone depletion depends on various factors: (1) the ozone depleting potential of the gas itself (life-time, halogen, and breakdown products), (2) source strength, (3) location of the source (distance to deep convection) and (4) seasonal aspects.

In the last two decades the magnitude of oceanic formation and emissions of certain halocarbons has been estimated in several studies (e.g. Class and Ballschmiter 1988; Lobert et al. 1997; King et al. 2002; Quack et al. 2004; Quack et al. 2007b; Carpenter et al. 2009). Generally, halocarbon concentrations are higher in the coastal regions than in the open ocean. Brominated and iodinated compounds mainly have biological sources in coastal regions. Biological sources are related to macroalgae (e.g. Manley and Dastoor 1987; Laturnus 2001; Palmer et al. 2005), phytoplankton (e.g. Sturges et al. 1992; Tokarczyk and Moore 1994; Moore et al. 1996b) or bacteria (e.g. Amachi et al. 2001; Smythe-Wright et al. 2006; Hughes et al. 2008). Furthermore abiotic processes are an additionally source for marine VHOCs. Photochemical production in surface waters (Richter and Wallace 2004) and anthropogenic discharge (Quack and Wallace 2003) are most important among these processes. Anthropogenic discharge is the strongest source for the long-lived chlorinated halocarbons.

Macroalgae are claimed as the most effective producer for various iodo- and bromocarbon and might contribute up to 70% of global bromoform emissions (Carpenter and Liss 2000). Seaweed incubation experiments have demonstrated that macroalgae produce various halocarbons, and that formation is highly species-dependent (Nightingale et al. 1995; Carpenter et al. 2000). Since macroalgae distribution is restricted to coastal regions, halocarbons have strongly localized sources. Compared to macroalgae production, phytoplankton produces relatively less VHOCs. However, global phytoplanktonic emissions can become significant considering the large size of the open oceans. Beside eukaryotic phytoplankton (mainly diatoms), marine cyanobacteria (e.g. *Prochlorococcus*) might play an important role in the understanding of global halogen budget (Smythe-Wright et al. 2006).

Several studies attempted to estimate global fluxes for a few VHOC and aimed to assess the role of those gases in the global halogen cycle (e.g. Moore and Groszko 1999; Quack and Wallace 2003). However global flux estimates require the knowledge of formation processes and source strength preferably for a large number of geographical regions and ecosystems. Another considerable uncertainty of those flux calculations arise from the high temporal variability of VHOC formation. Indeed, field campaigns are usually limited in temporal resolution. Consequently, measurements in unstudied areas and studies with a high temporal resolution are essential for better halocarbon budget calculations.

The biological formation of halocarbons and the underlying purpose for the involved species still remain unclear. For few species it has been proposed that vanadium-dependent haloperoxidases (vHPOs) are the crucial enzymes for the formation of polyhalogenated compounds (Leblanc et al. 2006). Triggered by H_2O_2 , vHPOs are able to oxidize halides (bromide and iodide primarily) leading to the halogenations of organic substrates. The key to understanding the global halogen cycle can clearly be found in a better understanding of the biological background of the VHOC formation.

1.1 Thesis Goals

This thesis aims at improving the knowledge of sources and fates of volatile halogenated organic compounds in highly productive marine areas. The primary objective was to establish techniques for the determination of trace gases at the *Station Biologique Roscoff*.

The second objective was to study the distribution of organohalides in two different oceanic provinces: a phytoplankton-dominated upwelling region and a macroalgae-influenced coastal region. Upwelling systems are characterized by high primary production, predominantly by diatoms. Moore et al. (1996b) claimed a high potential of those unicellular heterokonts for the formation of VHOCs. However only few studies (Quack et al. 2007a; Quack et al. 2007b) aimed at estimating the source strength of upwelling systems. This work improved our knowledge of VHOC distribution in upwelling areas. During summer 2007 coastal waters off Portugal were studied in order to investigate the origin of halocarbons.

The littoral zones (and especially macroalgae beds) are “hot spots” for VHOC formation. Due to oxidative stress, tides have an influence on VHOC formation in macroalgae beds (e.g. Pedersen et al. 1996). However no high resolution study is made in tidal influenced and nutrient-enriched estuaries. In this work the annual distribution and sea-air fluxes of VHOC along a salinity and nutrient gradient was investigated in the Bay of Morlaix; an estuary with a high nutrient input and a mega-tidal regime at the South-western end of the English Channel.

An additional objective was to study aspects of VHOC formation conditions in the marine model organism *Laminaria digitata*. This work focused on the role of plant-plant communication and their influence on VHOC formation.

2 VHOC: State of the art

Volatile halogenated organic compounds (VHOCs) are naturally emitted or man made gases with high impact on atmospheric chemistry. In this work the focus was on 13 different haloalkanes with generally short life times (range of minutes to days). The range of studied short lived compounds are enlarged by the anthropogenic gases methyl chloroform and tetrachloromethane which have atmospheric lifetimes of several years. Figure 1 shows the structural formula of the VHOCs studied in this work.

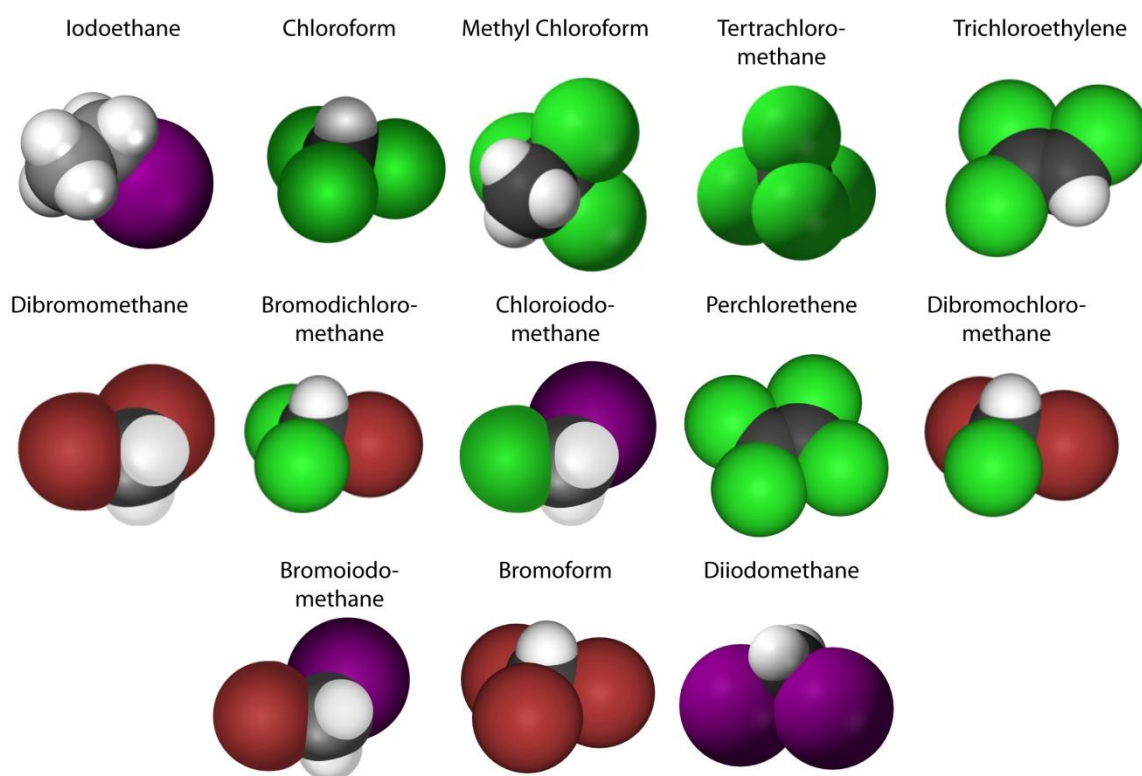


Figure 1. Structural formula of studied VHOCs.

2.1 Chemical properties

VHOCs are chlorinated, brominated, iodinated and fluorinated hydrocarbons with up to four C-atoms as well as chlorinated benzene. The characteristics of the halogen substitutes (F, Cl, Br, I) and their carbon-halogen bond energies, determine the physicochemical properties of the VHOCs.

With increasing molecular weight, carbon-halogen bond energies decrease: the carbon-fluorine bond is very strong and show a high polarity. Iodinated compounds show lowest carbon-halogen bond energies and polarities. The electron-withdrawing effect and the physical size of the halogen substituent influence chemical reactivity of the VHOC. Under standard conditions VHOCs are gaseous or liquid and are generally poorly soluble in water and show increased lipophilicity. The biological consequence of this hydrophogylipophilicity is an increased accumulation in cellular lipids. Hence biological degradation might be reduced since it becomes less accessible for hydrophilic enzymes. A final characteristic of halogens is their potential to alter toxicity of the organohalogen. VHOC are known to have a high toxic, carcinogen, mutagen and teratogenic potential and to causes allergies. It is assumed that biologically produced organohalogens have functions as antibiotics or for protections against feeding pressure or completion. Table 1 gives an overview to chemical properties of those chemicals.

Table 1. Chemical properties of VHOCs studied in this work.

Abbreviation, name, CAS-number, molecular weight [g · mol⁻¹], melting and boiling point [°C], density [g · ml⁻¹], solubility in water [g · l⁻¹] and vapour pressure [hPa, 20°C].

abbr.	Name	CAS	formula	M	MP	BP	ρ	at °C	sol	pc
IE	Iodoethane, Ethyl iodide	75-03-6	CH ₃ CH ₂ I	156.0	-110.9	72.4	1.95	²⁵	4	150
CF	Chloroform, trichloride	Methyl 67-66-3	CHCl ₃	119.4	-63.5	61.2	1.48	²⁰	8.2	213
MC	Methyl Chloroform, 1,1,1-Trichloroethane	71-55-6	CH ₃ CCl ₃	133.4	-33	74	1.32	²⁵	1.3	133
TCM	Tetrachloromethane, Carbon tetrachloride	56-23-5	CCl ₄	153.8	-22.92	76.72	1.59	²⁵	0.8	119.4
TCE	Trichloroethylene, 1,1,2-Trichloroethene	79-01-6	C ₂ HCl ₃	131.4	-73	87	1.46	²⁰	1.1	87.1
DBM	Dibromomethane, Methyl dibromide	74-95-3	CH ₂ Br ₂	173.4	-52.7	96.95	2.50	²⁰	11.7	60
BDCM	Bromodichloromethane, Dichlorobromomethane	75-27-4	CHBrCl ₂	163.8	-57	90	1.98	²⁰	4.5	67
CIM	Chloriodomethane, Chloromethyl iodide	593-71-5	CH ₂ ClI	176.4		108.5	2.42	²⁰		
PCE	Perchloroethene, Tetrachloroethene	127-18-4	CCl ₂ =CCl ₂	165.8	-19	121.1	1.62	²⁰	0.15	19
DBCM	Dibromochloromethane, Chlorodibromomethane	124-48-1	CHBr ₂ Cl	208.3	-22	119.5	2.45	²⁵	5.25	20
BIM	Bromiodomethane, Bromomethyl iodide	557-68-6	CH ₂ BrI	220.8	1	139.5	2.93	²⁰	2.7	14.67
BF	Bromoform, Methyl tribromide	75-25-2	CHBr ₃	252.7	8	149.1	2.89	²⁰	1	6.6
DIM	Diiodomethane, Methyl diiodide	75-11-6	CH ₂ I ₂	267.8	6	181	3.32	²⁰	14	1.13

Compounds are sorted following their retention time in the GC-ECD. Generally retention times are correlated to the boiling point of a compound.

2.2 Sources

About 3800 different organohalogens are known having natural sources (Gribble 2003). Natural sources include biological production by bacteria, fungi, lichen, terrestrial plants, and algae or even by insects and higher animals. In addition volcanoes, forest fires or geothermal processes widen the sources with natural origin. Man made organohalogens have either no natural equivalent or extent the natural sources. VHOCs are used in the chemical industry, in the

agriculture, are by-products of water treatment and are formed during combustion of organic waste.

2.2.1 Biological sources

Biosynthesis of VHOC forms a great number of different compounds and occurs within various organisms. Brominated and chlorinated organohalides outnumber the biological formed iodinated compounds. Even though fluorine is the most abundant halogen in the earth crust, only few biologically produced fluorinated organohalides are known (Key et al. 1997; O'Hagan and Harper 1999).

Methyl transferase (Wuosmaa and Hager 1990; Moore et al. 1996b; Manley 2002) and haloperoxidase (Theiler et al. 1978) are the two known enzyme groups catalyzing biosynthesis of haloalkanes. The enzymatic methylation of halides generates monohalogenated compounds (e.g. iodomethane). Organisms containing haloperoxidases are able to synthesis polyhalogenated compounds (e.g. bromoform or dibromomethane).

Methyltransferase

Monohalomethanes can be formed by enzymatic halogenations of methyl groups. This reaction was described in fungi (Wuosmaa and Hager 1990; Saxena et al. 1998), bacteria (Coulter et al. 1999), terrestrial plants (Attieh et al. 1995; Ni and Hager 1999) and marine algae (Itoh et al. 1997). Methyltransferase in marine algae can use different substrate as methyl donor, such as S-adenosyl-L-methionine (SAM), methionine methyl sulfonium chloride or dimethyl sulfoniopropionate (DMSP). Nonspecific methyltransferases from haptophytes (*Pavlova gyrams*) had been described as capable for the methylation of either bromide or iodide ions. Hence phytoplankton can be discussed as an oceanic source for bromomethane and iodomethane.

Haloperoxidase

Haloperoxidases are able to oxidize halogen anions. Those enzymes are accounted by a great variety of organisms. Asplund et al. (1993) found chloroperoxidases in soil extracts. Moore et al. (1996b) and Wever et al. (1991) detected bromoperoxidases and iodoperoxidases in macro- and microalgae. Hoekstra et al. (1998) described the presence of chloroperoxidase at the natural formation of chloroform by fungi.

While iodoperoxidase is highly specific to iodide, bromoperoxidase is able to use bromide and iodide. Chloroperoxidases are further unspecific and oxidize chloride bromide and iodide (Moore et al. 1996b; Urhahn and Ballschmiter 1998).

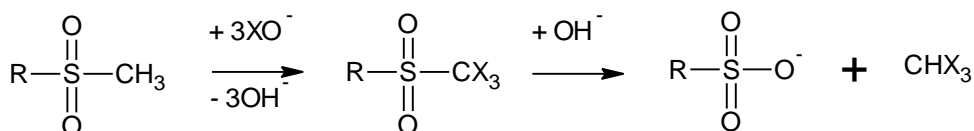
During the enzymatic reaction haloperoxidase form under the presence of halides and hydrogen peroxide, electrophilic halogen species (EHS):

(1)

Cl, Br or I ions

EHS electrophilic halogen species (XO^{\cdot} or R_2NX)

In a second step EHS substitute the H-atom of a carbonyl activated methyl group. Finally this substituted methyl group is split of the originally organic molecule. Urhahn and Ballschmiter (1998) proposed methyl sulfur compounds like methionine or dimethyl sulfoxide (DMSO) as a reagens for sulfo-haloform reaction:



Why organisms produce VHOCs?

In the evaluation of the biological function of halocarbon formation, large uncertainties still remain. Manley (2002) claimed halomethane formation as a metabolic 'accident'. According to this hypothesis, halomethanes are by-products of halogenation by haloperoxidase, which was found in great variety of organisms in different phyla. The main function of haloperoxidase is to protect the cell of harmful reactive oxygen species (ROS) such as hydrogen peroxide (H_2O_2), ozone (O_3) or hydroxyl radical ($\cdot\text{OH}$). Reactive oxygen species may cause damage to vitally important cell molecules, essentially enzymes or genetic molecules. Halogenation reactions by haloperoxidases

are suggested to scavenge H_2O_2 during oxidative stress (Pedersen et al. 1996). Consequently, VHOCs formed by marine algae are secondary waste products in order to lower intracellular ROS levels.

Macroalgae produce hydrogen peroxide as a defence reaction to grazing or as antifouling. In the process, intracellular hydrogen peroxide concentrations overshoot the normal cellular tolerance against those ROS (Theiler et al. 1978; Palmer et al. 2005). Küpper et al. (1998) described a H_2O_2 removal mechanism in *Laminariales* involving the accumulation of iodine. *Laminariales* are able to establish an intracellular iodine concentration gradient, which are more than 30 000 times higher compared to seawater. The iodine uptake is triggered by H_2O_2 and enhanced by adding haloperoxidase. The authors presume extracellular haloperoxidases catalyse the oxidation of iodine in the presence of H_2O_2 . During this reaction, hypohalous acids (HOI and HOBr) are produced. Subsequently, hypohalous acids react with methyl groups and form polyhalomethanes such as dibromomethane or bromoform (Wever et al. 1991).

Küpper et al. (2008) challenged in a later publication the idea of Manley and Pedersen. They proposed instead the hypothesis of a defence function, considering the high microbial toxicity of halocarbons. VHOCs may play a role as grazing deterrent for macroalgae (Gschwend et al. 1985; Wever et al. 1991; Itoh et al. 1997).

Palmer et al. (2005) supported the hypothesis that halocarbon producing algae control the formation of condensation nuclei for coastal cloud formation. Therewith kelp would be able to reduce oxidative stress from sunlight high levels. Pedersen et al. (1996) reported such stress conditions: concentrations of halocarbons were elevated in inter-tidal macroalgae beds during low tide. The authors attribute those findings with dry stress for the macroalgae.

Considered as a whole, it appears that VHOC are produced as response to various biotic and abiotic stresses (Potin et al. 2002; Laturnus et al. 2004; Leblanc et al. 2006).

2.2.2 Natural, nonbiological formation of VHOCs

Abiotic natural formation of halocarbons occurs in the environment without the presence of enzymes. In those processes biotic material can be involved. During the degradation of plant material for instance, methyl halides (mostly CH_3Cl , CH_3Br and CH_3I) are produced abiotically (Hamilton et al. 2003; Wishkerman et al. 2008).

Nucleophilic substitution

Although nucleophilic substitution do not reveal primary sources of VHOCs, it is crucial for some compounds like chloromethane (Moore 2003). From a Pacific Ocean data set it has been deduced that about 15% of global chloromethane flux arise from nucleophilic substitution (Moore and Groszko 1999).

This reaction is a sink for bromomethane and iodomethane in seawater and at the same time a source for chloromethane (Zafiriou 1975). Beside substitution with Cl, hydrolysis is an alternative.

(2)

X	Br or I
Y	Cl, Br or I

Results from Singh et al. (1983a) however do not support this idea. The authors found correlations between bromomethane and chloromethane but no correlations between iodomethane and chloromethane.

A photochemically induced substitution was suggested as a pathway for nucleophilic substitution (Class and Ballschmiter 1987; Class and Ballschmiter 1988). Diiodomethane and dibromomethane can be transformed in mixed halogenated compounds:

(3)

Halocarbons can be produced by oxidation processes during degradation in organic rich waters or sediments (Keppler et al. 2000; Keppler et al. 2003). For the formation of monohalogenated compounds an abiotic reaction mechanism was assumed which is induced by the oxidation of organic matter by iron(III).

Another formation pathway for methyl halides was proposed by White (1982): dimethyl sulfonium propionate (DMSP) dissolve in seawater and react with halide ions. DMSP is an osmolyte detected in prymnesiophytes, dinoflagellates and chrysophytes. However in a kinetic study (Hu and Moore 1996) was shown that these reactions are too slow to have significant influence on oceanic methyl halide productions.

Photochemical formation of iodomethane

Aside biological formation of iodomethane by macro- and microalgae and marine bacteria, photochemical formation is an important pathway for this very short lived VHOC (Richter and Wallace 2004). These authors showed, based on production experiments in the tropical Atlantic that 50% of the average air-to-sea flux of iodomethane is caused by photochemical formation. Recently, Wang et al. (2009) measured spatial and seasonal variation of iodomethane in the NW Atlantic and could not demonstrate the dominance of photochemical formation over other pathways. These two studies demonstrate that the photochemical formation of VHOCs depends on high light intensities. In a light-dependent production pathway, ultraviolet radiation drives the formation of CH_3 -radicals and iodine atoms in seawater. The following reaction was then suggested by Moore and Zafiriou (1994):

(4)

Geogenic sources

Volcanoes and other geothermal processes are known to emit a great variety of halogenated organic compounds (Gribble 1996; 1998; Jordan et al. 2000). The latter authors found about 100 chlorinated, 25 brominated, five fluoride and four iodinated compounds in fumaroles and lava gas samples from four different volcanoes (Etna, Iwojima, Kuju, Satsuma, Vulcano). Gribble (2003) (see reference therein) reported rocks and minerals containing small amounts of haloalkanes. When rocks are crushed during natural erosion or mining operation these haloalkanes are released to the atmosphere and may contribute significantly to global halogen emissions.

2.2.3 Anthropogenic sources

In the last century halogenated compounds were widely used in the chemical industry and the global production is constantly increasing. World chlorine production and consumption for instance was estimated to 48 million tons in 1996 and is increasing about 3.4% annually (Stringer and Johnston 2001). Halogenated compounds like 1,2-dichloroethane and chloroethene are precursors for the production of polymers such as polyvinyl chloride (PVC). Other industrial application for halogenated compounds (such as chloromethane, chloroethanes, chlorobenzene or chlorofluorocarbons) includes the usage as flame retardants, biocides, solvents, degreaser and dielectric fluids.

Biocides and solvents

Due to their chemical properties VHOCs are potentially toxic to life. Many pesticides or fungicides are halogenated compounds. Bromomethane for instance was used as fungicide (Clerbaux and Cunnold 2006) mostly in underdeveloped countries. Due to its high ozone depleting potential the use in agriculture is globally prohibited since 2005.

Many chlorinated solvents are highly necessary for industrial applications. Chloroform and tetrachloromethane are degreasing agents and therefore have been used in dry-cleaning of clothes.

Water treatment and bleaching

Chlorine is used in industry for various purposes such as bleaching agent for pulp and paper production, the treatment of waste and drinking water or antifouling agent of seawater for cooling water in power plants. Since the beginning of the 20th century, drinking water is treated with hypochlorite (ClO^-). About 6% of global chlorine production is used for this assignment and lead to a remarkable reduction of water-borne diseases (Stringer and Johnston 2001). However chlorination of drinking water is responsible for the formation of various polyhalogenated hydrocarbons and thereby it is an important source of anthropogenic VHOCs. Hypochlorite is an effective oxidizing agent and capable to breakdown complex organic compounds such as peptides, humic and fulvic acids.

If hypochlorine is released in the marine environment – due to the presence of bromine – ClO^- is converted to BrO^- and finally form brominated halomethanes. Helz and Hsu (1978) found elevated

concentrations of bromoform, chloroform, bromodichloromethane and dibromochloromethane in the Balck Water estuary (Maryland, USA) and assumed it was due to the discharge of a wastewater treatment plant upstream. Indeed, oxidative water treatment is usually the most important antropogenic source for VHOCs (Rook 1977; Fogelqvist and Krysell 1991; Krysell and Nightingale 1994; Quack and Suess 1999).

Biomass burning

Combustion of biomass like savanna fires in southern Africa can be related to methyl halide (e.g. CH_3Cl , CH_3Br and CH_3I) emissions (Andreae et al. 1996). Burning of biomass itself is a natural process mostly induced by spontaneous fire lightning. However today's biomass burning is about 90 % man made and therefore the dominant factor (Koppmann et al. 2005). Organohalogens are emitted to the atmosphere during combustion of organic material (e.g. fire clearance or incineration of municipal waste). Gribble (1999) calculated that 30% stratospheric bromine budget can be traced back to biomass burning. Those emissions of bromomethane are in the same range than marine emissions.

The formation of organohalogens is restricted by the availability of halogens in the plant tissues and the quality of the burning process. Hamilton et al. (2003) described the abiotic formation of chloromethane in the presence of chlorine, in which the plant component pectin acts as a methyl donor. It was observed that emissions were dramatically increased at high temperature. It can be assumed that similar processes are causal for the release of CH_3Br and CH_3I . Also, the formation of polyhalogenated compounds can be the result of incomplete burning (Lobert et al. 1999).

2.3 Lifetimes in the Troposphere

Halogenated compounds are chemically converted in the atmosphere by photochemical products (hydroxyl radicals, ozone and nitrogen oxides) or by uv-radiation. The final products are reactive halogen species (Chameides and Davis 1980):

(5)

Among this group of reactive halogen gases, one can distinguish hydrogen halides (HI, HBr, HCl, HF), halogen nitrates (e.g. BrONO₂ or ClONO₂), halogen monoxides (e.g. ClO, BrO) and atomic halogens (e.g. Br atoms).

The lifetimes of halogenated gases is determined by their chemical conversation.

Table 2 shows lifetimes, burdens and sources for VHOCs. It must be pointed out that lifetime are correlated to latitudes: for iodomethane for instance average lifetimes are reported in the range between 4-8 days (Zafiriou 1974; Yvon-Lewis and Butler 2002). Due to lower uv-radiation at higher latitudes the lifetimes can increase up to two weeks (Blake et al. 1999).

While naturally produced VHOCs are typically short lived with lifetimes in the order of months, some VHOCs with anthropogenic origin are photochemically stable with lifetimes of several years. Some iodinated compounds have remarkably short lifetimes, for example diiodomethane has a lifetime of several minutes. This is mainly due to the fact that photolytic degradation is the main factor responsible for decomposition of iodocarbons. For instance, photolysis of iodomethane is about 100 times faster than degradation by hydroxyl species. As a consequence to short lifetimes, iodinated compounds have low effects on stratospheric ozone depletion.

Table 2. VHOCs in the atmosphere.

Published atmospheric lifetimes, burdens and sources (Mossinger et al. 1998; Clerbaux and Cunnold 2006; Law and Sturges 2006).

	Lifetimes [d]	Estimated Burden [Gg]	Source	Estimated Source [Gg yr ⁻¹]
Bromomethane	255		N(A)	
Chloromethane	365		N(A)	
Iodomethane	7	1.7-4.8 (I)	N (A)	180 (I) open ocean 66 (I) anthropogenic
Iodoethane	4	0.5 (I)	N	
Chloroform	150	66-210 (Cl)	AN	588 (Cl) total 320 (Cl) seawater 196 (Cl) soil
Methyl Chloroform	1825		A	
Tetrachloromethane	9500		A	
Trichloroethylene	4.6		A	
Dibromomethane	0.6	18-22	N	
Bromodichloromethane	78	1.3-1.5	N(A)	17 (Cl) open ocean 19 (Br) open ocean
Chloriodomethane	0.1		N	95 (I) open ocean 27 (Cl) open ocean
Perchloroethene	99	17-160	A	313 (Cl) industry 16 (Cl) ocean 2 (Cl) fossil fuel
Dibromochloromethane	69	0.8-2.3 (Br) 0.2-0.5 (Cl)	N(A)	5 (Cl) open ocean 23 (Br) open ocean
Bromiodomethane	45 minutes		N	
Bromoform	26	11-18 (Br)	N(A)	800 (Br) total 28 (Br) industry
Diiodomethane	5 minutes			

Lifetimes determine the ozone depleting potential of VHOCs. Chloromethane and bromomethane are long lived compounds and contribute significantly to stratospheric reactive halogen species (Clerbaux and Cunnold 2006). Both are natural produced halocarbons with longer photochemical lifetimes (8 month to one year) than the average large-scale transport time (about 6 month) through the troposphere (Law and Sturges 2006). Chloromethane shows 20 times higher atmospheric concentrations than bromomethane (Adams et al. 1998). However bromomethane

has about 50 times more effective ozone depleting potential than chloromethane (Butler 1995). Hence the ozone depleting potential of both gases is in the same range.

Decomposition of chlorinated and brominated compounds by photolysis is slow. Hydroxylation dominates the formation of those reactive halogens (Mossinger et al. 1998). Hence the longer lived chlorinated and brominated compounds are able to reach the stratosphere and therefore have a high ozone depleting potential.

2.4 VHOC contribution to reactive stratospheric halogens

The ozone destruction potential of chlorofluorocarbons (CFCs) was firstly described by Molina and Rowland (1974). About 10 years later their severe warning became reality with the discovery of a substantial ozone hole over Antarctica (Farman et al. 1985). Since then the focus was enlarged to other halones like haloalkanes. Those compounds are a large source for reactive halogen species which are causal for ozone depleting (see Figure 2).

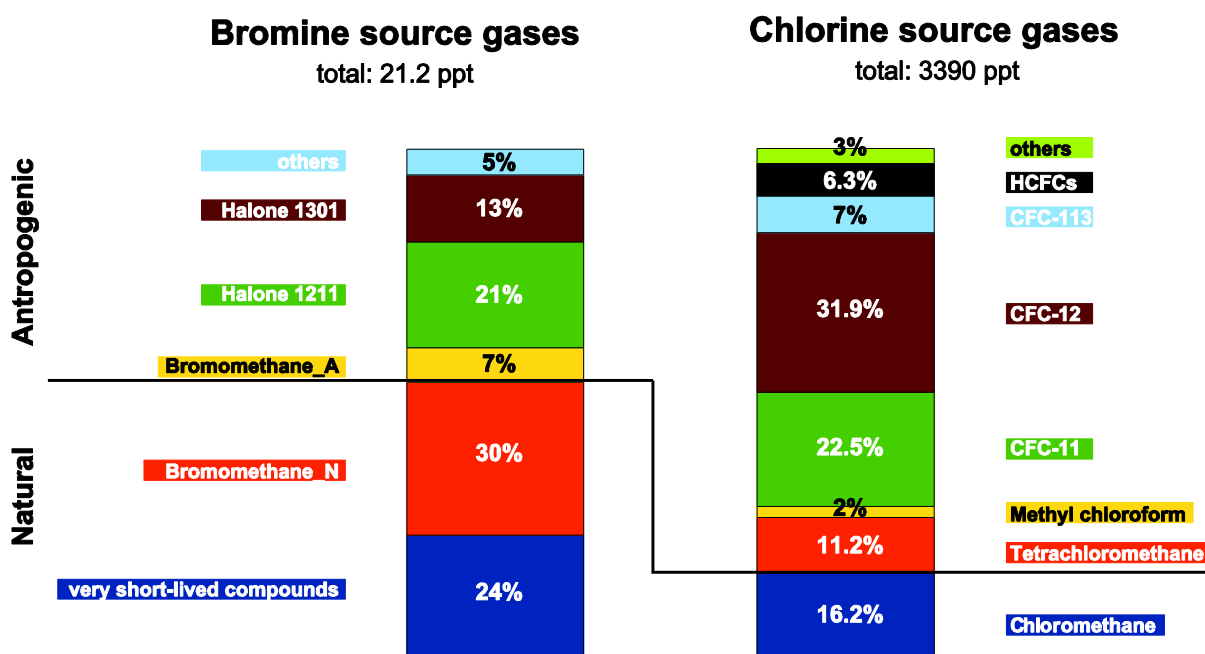


Figure 2. Primary Sources of chlorine and bromine for the stratosphere (Fahey 2006).

The mixing ratio of chlorinated compounds is about 150 times higher than those of brominated compounds. However, both halocarbon groups have a comparable ozone depleting potential. The reason for that is the high efficiency of brominated compounds in ozone degradation. Both groups have different origins: brominated compounds have strong natural sources whereas chlorinated compounds are largely manmade.

Due to short life times, atmospheric concentrations of iodinated compounds decrease with increasing altitude (Davis et al. 1996; Blake et al. 1999). Hence the impact on stratospheric ozone depleting seems to be limited. However during deep convection events – a strong vertical mixing, which are common in the tropics – iodinated compounds might reach the lower stratosphere (Solomon et al. 1994).

The chemical reactions of ozone depleting are shown in Figure 3. In the stratosphere the ozone cycle is driven by sunlight: uv-radiation breaks apart oxygen-oxygen bonds in molecular oxygen and ozone. The first reaction is ending in ozone formation while the latter destruct ozone. However reactive halogens shift this equilibrium towards a forced formation of oxygen molecules.

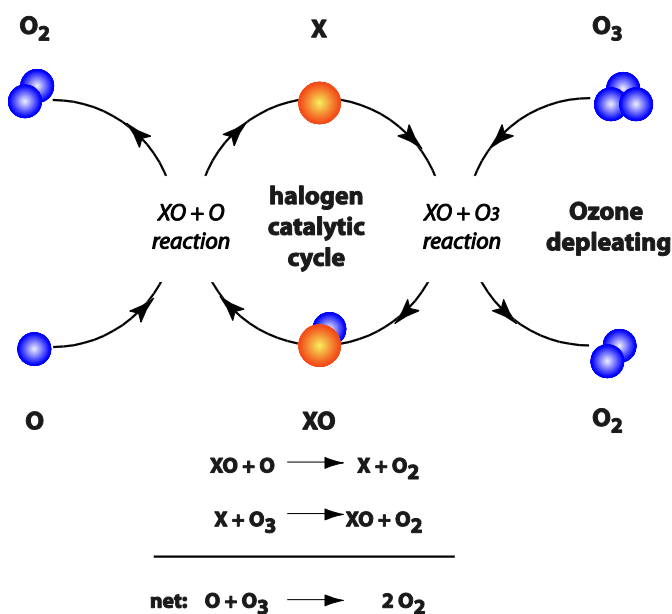


Figure 3. Ozone destruction cycle 1.

X ≡ halogen. Adapted from Fahey 2006. This cycle is of significance for stratospheric ozone depleting at intense uv-radiation (middle to lower latitudes).

As Figure 3 clearly demonstrates halogens have a catalytic function. One chlorine atoms for instance, are able to destruct 10^5 ozone molecules. Since those reactions depend on high uv-radiation levels, it is assumed that those processes are restricted to middle and lower latitudes.

In higher latitudes (Polar Regions), uv-radiation is less intense. Moreover halogen monoxide concentrations are elevated compared to lower latitudes. Hence two other cycles are proposed for those regions. In the first cycle halogen monoxides of the same kind react with each other. The remaining product is deconstructed by visible light ($\lambda = 380-780\text{nm}$):

(6)

In another cycle two halogen monoxides with different halogen substitutes react with each other:

or

(7)

Other ozone depleting processes are related to the presence of halogen nitrates (XONO_2) and hydrogen halides (HX). Both groups do not react directly with ozone but can be transformed to reactive compounds. Therefore they are claimed as reservoir gases for reactive compounds.

2.5 Air-Sea Exchange

The air-sea interface is the crucial barrier for the transport of gases between the atmosphere and the oceans. For instance, halocarbons produced in the marine environment influence atmospheric concentrations of those gases, whereas some sites in the ocean are known sinks for VHOC. Hence air-sea flux calculations are essential for budgeting halogens globally. The chemical properties of those gases determine the potential transfer rates between ocean and atmosphere. VHOCs are slightly water soluble gases and have a low hydrolysis potential. The exchange between air and sea is determined by diffusion processes at the air-sea-interface. Different models were developed to describe this transport. Whitman (1923) proposed a two-film theory, which was taken by Liss and Slater (1974) and modified for environmental purpose. This model is physically unrealistic but able to simplify and to explain transfer processes that may occur between both interfaces (Nightingale 2003). Following this model atmosphere and water are separated by two thin laminar layers: a gas film as the lowest atmospheric layer and a liquid film as topmost water layer. Figure 4 shows exchange processes in both directions: saturated oceans and low atmospheric concentration resulting in a net flow toward the atmosphere. Alternatively, high atmospheric concentrations together with low water concentrations resulting in a reverse flow towards the ocean.

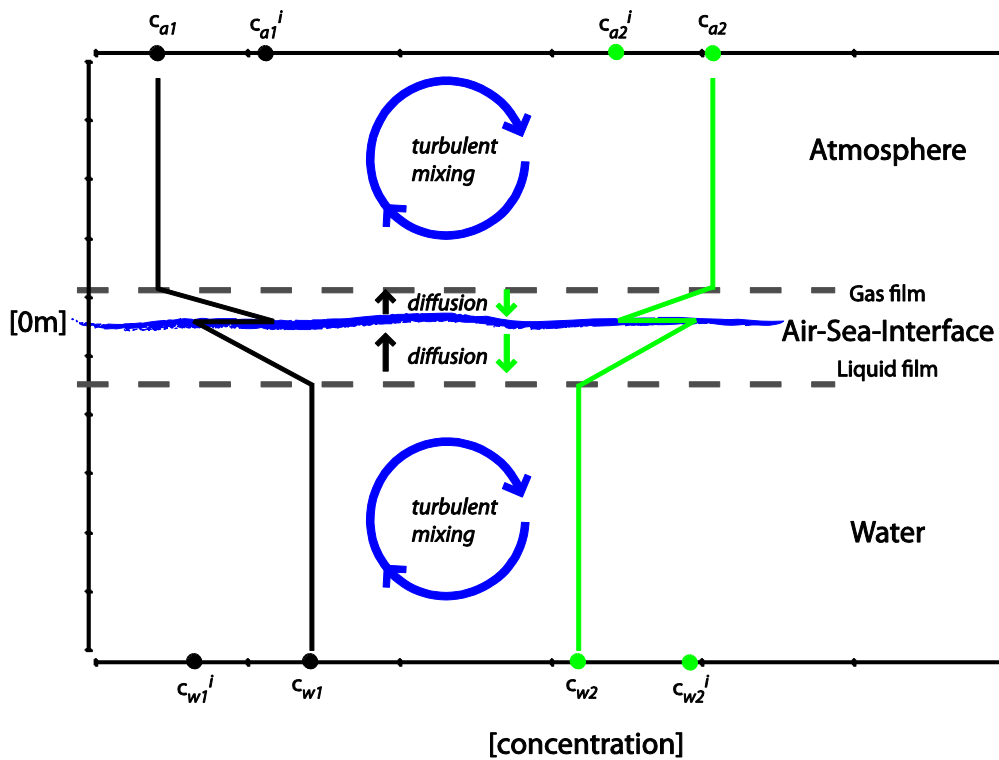


Figure 4. Model for air-sea-fluxes, adapted from Liss and Slater (1974).

Ordinate: Depth and altitude respectively. Abscissa: gas concentration. Black line: net flow to the atmosphere. Green line: net flow to the ocean. c_a and c_w are concentrations in water and air. c_{ai} and c_{wi} are concentrations in air-sea-interface.

A flux passing those thin laminar films is the result of a concentration gradient between atmosphere (c_{a1} or c_{a2} respectively) and water (c_{w1} or c_{w2} respectively). The laminar films act as two coupled resistances. Whereas water as well as atmosphere are claimed to be well mixed with a rapid internal exchange by Eddy diffusion, the two laminar films feature a distinct concentration gradient with a relatively slow internal exchange by molecular diffusion. Consequently it can be assumed that the transfer resistance is negligibly low in the water and atmosphere. In contrast the transfer resistance is high in the two laminar films and determines the total transfer velocity k . However, since VHOC are hydrophobic molecules with high Henry's Law constant values (Mackay et al. 1979), transfer resistance in the gas film can be neglected. Therefore Liss and Merlivat (1986) claimed water transfer velocity (k_w) can be equalized with the total transfer velocity (k_t). The transfer velocity is determined by different variables of velocity like wind and

friction velocity as well as variables describing the sea surface like wave types or surface films (Frew et al. 2002; Tsai and Liu 2003). Summarizing the above, the flux (F) is expressed as:

$$\text{---} \tag{8}$$

F	flux	[nmol m ⁻² d ⁻¹]
k _w	transfer velocity	[m d ⁻¹]
c _a	concentration in water	[p mol dm ⁻³]
c _w	concentration in air	[p mol dm ⁻³]
H _d	Henry's law constant	[dimensionless]
ΔC	concentration anomaly	[p mol dm ⁻³]

2.5.1 Henry's law constants

Henry's law constants (or coefficients) express the air-water equilibrium partition coefficient of a gas in a dilute aqueous solution (Staudinger and Roberts 2001). Only at the air-sea-interface, water and atmospheric VHOC concentrations are at equilibrium and related by Henry's law constant H_d:

$$\text{---} \tag{9}$$

	water concentration in the interface	[p mol dm ⁻³]
	air concentration in the interface	[p mol dm ⁻³]

One can find different forms of *Henry's law* constant in the literature. In this work all collected values are expressed as dimensionless air-to-liquid concentration ratio H_d. When necessary values were converted using the following formula:

$$\text{---} \tag{10}$$

H	Henry constant	[Pa · m ³ · mol ⁻¹ or atm · m ³ · mol ⁻¹]
R	gas constant	[8.314 Pa · m ³ · mol ⁻¹ · K ⁻¹]

or

$$[8.205 \cdot 10^{-5} \text{ atm} \cdot \text{m}^3 \cdot \text{mol}^{-1} \cdot \text{K}^{-1}]$$

T seawater temperature [K]

The dependence of H_d (H respectively) upon temperature and salinity were described by different authors. Hunter-Smith et al. (1983) described a linear relationship between the logarithm of H_d and the reciprocal of temperature. The authors determined air-sea fluxes for chloroform, iodomethane, tetrachloromethane and methyl chloroform and proposed the following equation:

$$\frac{\text{unknown } H_d}{\text{known } H_d} = \frac{T_1 - T_2}{T_1} \quad (11)$$

T1 seawater temperature for unknown H_d [K]

T2 temperature for known H_d [K]

A similar relationship was proposed by Singh et al. (1983b). Like for the formula of Hunter-Smith et al. (1983) salinity was not considered in the formula:

$$\frac{\text{unknown } H_d}{\text{known } H_d \text{ at } 25^\circ\text{C and } 0 \text{ PSU}} = \frac{T - 25}{T} \quad (12)$$

T seawater temperature for unknown H_d [$^\circ\text{C}$]

In oceanic environments salinity has a minor effect on H_d (Moore et al. 1995). However in estuaries which are characterized by a clear salinity gradient this factor needs to be considered. Hence in this work the following causal relations reported by Mackay and Shiu (1981), Moore et al. (1995) and Dewulf et al. (1995) were used:

	—	(13)
a,b,c	experimental variables	
T	seawater temperature	[K]
S	salinity	[PSU]

Table 3 gives values for the variables a, b and c. Values from Dewulf et al. (1995) were taken directly from the literature. Sander (1999) showed that H_d -values for iodomethane and iodoethane are identical. Therefore, we used the experimental variables a, b and c of iodomethane for the calculations of iodoethane (values from Moore et al. 1995). Moore et al. (1995) claim that salinity has only a minor effect on H_d , and therefore did not give any values for the variable c. Here we calculated those variables using the solver of Excel (method of minimizing the deviance). In the literature no values for bromiodomethane are available. Therefore we estimated some H_d - values regarding to known values of compounds with similar chemical properties (vapour pressure and boiling point) and calculated the variables a, b and c.

Table 3. Experimental variables a, b and c to calculate the temperature and salinity dependent H_d .

	a	b	c	Reference
IE	-4338	13.05	0.0086	Sander 1999
CF	-4142	12.01	0.0059	Dewulf et al. 1995
MC	-3834	12.35	0.0090	Dewulf et al. 1995
TCM	-4073	13.72	0.0081	Dewulf et al. 1995
TCE	-3648	11.12	0.0081	Dewulf et al. 1995
DBM	-4418	11.43	0.0086	Moore et al. 1995
BDCM	-4678	12.76	0.0086	Moore et al. 1995
CIM	-4305	11.10	0.0086	Moore et al. 1995
PCE	-4528	14.66	0.0108	Dewulf et al. 1995
DBCМ	-4914	13.34	0.0086	Moore et al. 1995
BIM	-4944	13.14	0.0094	<i>estimated</i>
BF	-4973	12.86	0.0094	Moore et al. 1995
DIM	-5006	12.47	0.0094	Moore et al. 1995

Table 4 shows literature values for the *Henry's law constants* we used for flux calculations. Generally, these values are smaller in cold and less salty waters. High H_d values increase the volatility/solubility-ratio. In parallel the transfer from water to the gas phase is elevated with high H_d values. Values for iodoethane were estimated according to Sander (1999).

Table 4. Published values for Henry's Law constant H_d (dimensionless).

Values measured in aqueous solution with marine PSU.

	0 / 2 °C		10 °C		18.2/20 °C		Reference
IM	0.076	± 2.6%	0.136	± 2.6%	0.225	± 2.5%	Moore et al. 1995
IE	0.076		0.136		0.225		Sander 1999
CF	0.056	± 2.4%	0.091	± 2.6%	0.145	± 1.2%	Moore et al. 1995
MC	0.280	± 9.6%	0.410	± 2.8%	0.650	± 7.8%	Dewulf et al. 1995
TCM	0.430	± 5.8%	0.680	± 12.1%	1.010	± 2.5%	Dewulf et al. 1995
TCE	0.130	± 3.5%	0.210	± 4.2%	0.320	± 0.8%	Dewulf et al. 1995
DBM	0.011	± 0.9%	0.021	± 0.8%	0.034	± 0.6%	Moore et al. 1995
BDCM	0.025	± 1.0%	0.045	± 1.2%	0.079	± 2.8%	Moore et al. 1995
CIM	0.012	± 1.4%	0.022	± 0.4%	0.036	± 0.9%	Moore et al. 1995
PCE	0.240	± 6.1%	0.380	± 2.8%	0.640	± 6.8%	Dewulf et al. 1995
DBCM	0.012	± 1.0%	0.024	± 1.0%	0.042	± 0.7%	Moore et al. 1995
BIM	0.009		0.018		0.032		<i>estimated</i>
BF	0.006	± 1.1%	0.012	± 0.7%	0.022	± 0.9%	Moore et al. 1995
DIM	0.004	± 2.0%	0.007	± 1.1%	0.013	± 1.4%	Moore et al. 1995

2.5.2 Transfer velocity

In the literature several approaches are known to estimate the transfer velocity (Smethie et al. 1985; Liss and Merlivat 1986; Wanninkhof 1992; Wanninkhof and McGillis 1999). As mentioned above the transfer velocity depends on different environmental variables like wind speed and friction velocity, wave types, occurrence of surface films or bubble formation. However wind speed is described as the major factor and is easy to integrate in a model. Models explain measured transfer velocities of a model gas depending on wind speed. Consequently it is necessary to correct this calculated transfer velocity:

(14)

transfer velocity for a model [cm · h⁻¹]
 cv correction value, depending on windspeed

Below we will explain and compare different approaches to estimate k_{Wm} -values. Then we will describe calculations to adapt k_{Wm} -values to k_W , using the so called Schmidt number.

Linear approaches for k_W estimations

Smethie et al. (1985) proposed a simple linear model to describe the relationship of wind velocity and transfer velocity. They assumed no flux at low wind speed (below 3 m · s⁻¹):

for $u \leq 3$ (15)

for $u > 3$

u wind velocity [m · s⁻¹ at 10m above seasurface]

This equation was deduced from transfer velocities of CO₂ at 20°C. Since the model of Smethie et al. (1985) is very simplified the use of this equation is uttermost limited in the literature.

Liss and Merlivat (1986) combined a field data set of Wanninkhof et al. (1985) with wind tunnel experiments. They proposed three linear equations for the k_{Wm} -calculations, depending on sea surface conditions:

for $u \leq 3.6$ (16)

for $3.6 < u \leq 13$

for $u > 13$

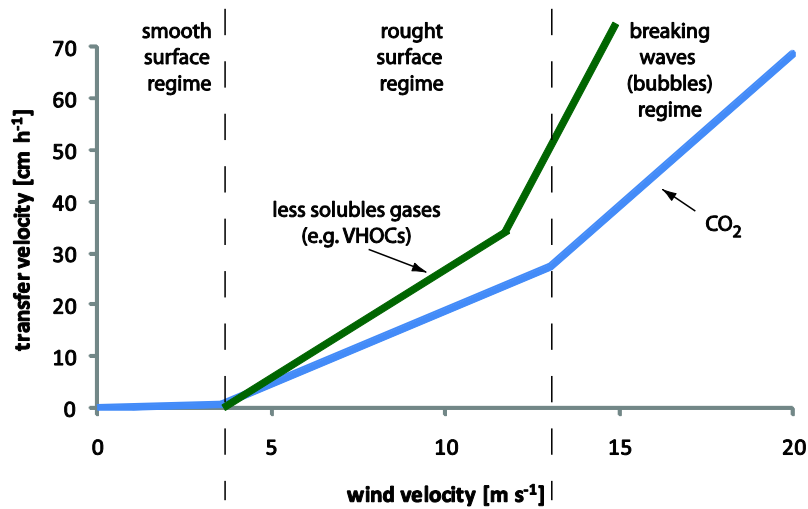


Figure 5. Transfer velocity of CO₂ (blue) and VHOCs (green) using the approach of (Liss and Merlivat 1986).

Nonlinear approaches for k_w estimations

Wanninkhof (1992) introduced an empirical nonlinear relationship between wind and transfer velocity of CO₂. For steady winds the following equations was proposed:

(17)

The author suggested an additional formula with modifications accounting wind conditions by longer term observations. If the average wind velocity of a sampling site is known the following model fit better flux estimation:

(18)

$$\text{average wind velocity} \quad [m \cdot s^{-1} \text{ at } 10m \text{ above seasurface}]$$

Since wind speed is subjected to permanently changing conditions formula (18) might give more reliable results. Moore et al. (1996a) compared both calculations and showed that measured wind speeds at the time of sampling do not necessarily reflects the wind conditions at the sampling

side over a longer period. This period however, should be taken into account when calculating a flux from the water column towards the atmosphere at a given sampling site.

Nightingale et al. (2000a) and Frost and Upstill-Goddard (2002) proposed a quadratic relationships with resulting k_{wm} values, which are centred between Liss and Merlivat (1986) and Wanninkhof (1992). The approximation of Nightingale for the gas transfer coefficient is computed:

(19)

Wanninkhof and McGillis (1999) introduced a nonlinear approach and suggested a cubic relationship between flux and wind speed:

(20)

McGillis et al. (2001) modified this computation and submitted the following formula, which fitted best to measured data:

(21)

Comparison of the different approaches to calculate k_w

To demonstrate the implications of different approaches modelling k_{wm} values, we plotted CO_2 curves of four different authors in Figure 6. At low wind speeds ($<3 \text{ m s}^{-1}$) the model of McGillis et al. (2001, denoted as M01) gives highest values, whereas Liss & Merlivat (1986, denoted as LM86) and Wanninkhof & McGillis (1999, denoted as WM99) show lowest values. The model of Wanninkhof (1992, denoted as W92) gives medium values. At low wind speed ($3 \text{ m s}^{-1} < u < 8 \text{ m s}^{-1}$) highest values are calculated with W92. Other models give lower values (factor about 1.75). At moderate wind conditions ($8 \text{ m s}^{-1} < u < 14 \text{ m s}^{-1}$) W92 still modulate highest values whereas LM86 deviate strongly from all other models and gives lowest values. Both cubic models (WM99 and MG01) return median values. At strong wind conditions ($u > 14 \text{ m s}^{-1}$) the linear model differ

towards low values compared to the W92 whereas the cubic models differ towards high values compared to the W92.

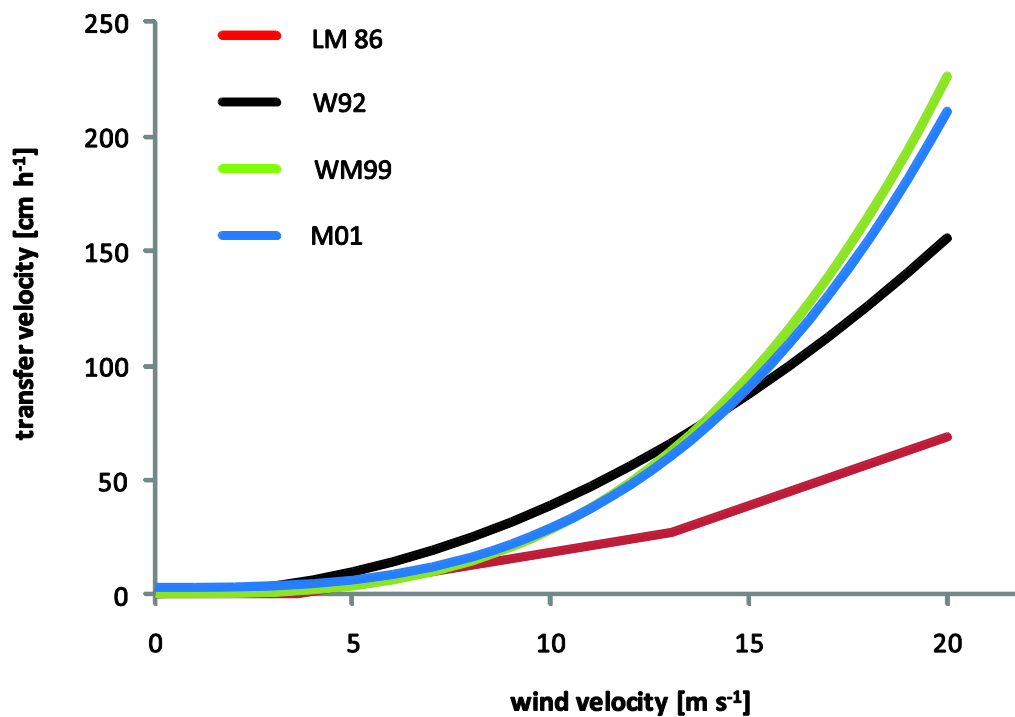


Figure 6. Different parameterizations for transfer velocity calculation for CO₂.

The variances between the different models are remarkable on a global scale. Moore et al. (1996a) compared different approaches for oceanic chloromethane emissions and found variances in the range of Tg. At high wind speeds for instance, cubic models might overestimate k_w values whereas the linear models could underestimate k_w . At moderate wind speeds, the W92 model might overestimate k_w values. In paragraph 5.4 different models are discussed.

Model correction with Schmidt numbers and wind speed

As mentioned before calculated k_{wm} -values are valid only for a model gas at a certain temperature and salinity. Transfer velocity estimations are usually based on CO₂ at 20°C. In order to describe the model gas the so called *Schmidt number* is utilized. The *Schmidt number* is expressed as the ratio of kinematic viscosity of seawater to the molecular diffusivity of a

compound in the same medium. The kinematic viscosity is defined as dynamic viscosity divided by the density. *The Schmidt number* depends mainly on temperature but only marginal on salinity.

(22)

Sc	Schmidt number
ν	kinematic viscosity
D_v	molecular diffusivity

The models of Smethie et al. (1985) and Liss and Merlivat (1986) based on *Schmidt numbers* of $Sc = 600$; the value for CO_2 at 20°C in distilled water. In the nonlinear models however approximations were made for marine environments with higher *Schmidt numbers* ($Sc = 660$).

The causality between k_w , k_{wm} and Sc are expressed in the following equation and depends on wind conditions:

(23)

N	– for most conditions
	– for very low wind speed
Schmidt number for the model gas	600 for linear approaches
	660 for nonlinear approaches

In different wind speed conditions *Schmidt number* conversations differ in their exponent. In the literature an exponent of -0.5 are suggested for the most common conditions. However at calm weather this exponent needs to made allowance for lower transfer velocity. Hence an exponent of -0.67 is suggest for wind speeds lower than $3.6 \text{ m} \cdot \text{s}^{-1}$ (Holmen and Liss 1984; Clark et al. 1995; Crusius and Wanninkhof 2003).

Below we present three approximations to calculate Schmidt numbers for the k_w -correction.

An approach described by Kuß (1994) and Quack (1994) deviated Schmidt numbers for VHOCs from those of CO_2 . The authors relied on a calculation from Jahne (1980) who described the dependence of Sc (for CO_2) on temperature:

$$\frac{Sc(T)}{Sc(298.15)} = \left(\frac{298.15}{T} \right)^{1.7} \quad (24)$$

Schmidt number at temperature T [dimensionless]

T absolute temperature, seawater [K]

In a following step, these authors used a ratio described by Atkins (1986). This ratio explains the interrelation of the Schmidt number with the molecular weight of two compounds:

$$\frac{Sc(\text{VHOC})}{Sc(\text{CO}_2)} = \sqrt{\frac{M(\text{CO}_2)}{M(\text{VHOC})}} \quad (25)$$

Schmidt number. CO_2 at temperature T

Schmidt number. VHOC at temperature T

molecular mass. CO_2 [44.01 g mol⁻¹]

molecular mass. VHOC [g mol⁻¹]

From equation (24) and (25) the following final equation was deduced:

$$\frac{Sc(\text{VHOC})}{Sc(\text{CO}_2)} = \left(\frac{298.15}{T} \right)^{1.7} \sqrt{\frac{M(\text{CO}_2)}{M(\text{VHOC})}} \quad (26)$$

A second approach to obtain Sc -values for VHOCs was based on measurements of diffusivity of bromomethane in seawater at different temperatures (DeBruyn and Saltzman 1997a). With these

measurements the authors yields an equation for a given halocarbon in a temperature range between 5 and 30°C:

$$\text{temperature} \quad \text{for temperature range 5-30°C} \quad (27)$$

[°C]

With one known *Schmidt number* other Sc-values can be calculated for different VHOCs using an equation initially proposed by Wilke and Chang (1955):

$$\text{---} \quad \text{---} \quad \text{for temperature range 5-30°C} \quad (28)$$

molecular volume of compound A [cm³ mol⁻¹]

molecular volume of compound B [cm³ mol⁻¹]

Schmidt number of compound A

Schmidt number of compound B

The molecular volume of a compound can be estimated with the additive method of Le Bas (Reid et al. 1987). Table 5 shows the calculated V_A-values.

Equation (27) and (28) leads to:

$$\text{---} \quad (29)$$

A third approach was introduced by Khalil and Rasmussen (1998). These authors describe the dependence of Sc on temperature and molecular mass:

(30)

M	Molecular mass	[g · mol ⁻¹]
T	temperature	[°C]

In Table 5 values are given for the three different Sc-calculation. Depending on the compound Sc-values differ up to a factor of 1.7 between the calculations. Low Sc values calculated after Wilke and Chang (1955) results in higher transfer velocity values.

Table 5. Molecular volume [cm³ mol⁻¹] and Schmidt numbers for VHOCs at 15°C.

	VA	Sc	Sc	Sc
	molecular volume after Le Bas	Khalil and Rasmussen (1998)	DeBruyn and Saltzman (1997), Wilke and Chang (1955)	and Atkins (1986), Jähne (1980)
Iodomethane	62.9	1587.02	1014.34	1440.27
Iodoethane	85.1	1663.61	1216.04	1509.78
Chloroform	92.3	1455.45	1276.77	1320.86
Methyl chloroform	114.5	1538.54	1453.03	1396.27
Tetrachloromethane	113.2	1652.10	1443.11	1499.33
Trichloroethylene	107.1	1526.89	1395.94	1385.70
Dibromomethane	76.2	1754.00	1138.06	1591.81
Bromodichloromethane	94.7	1705.01	1296.59	1547.35
Chloriodomethane	83.8	1769.11	1204.86	1605.52
Perchloroethene	128	1715.23	1553.52	1556.63
Dibromochloromethane	97.1	1922.45	1316.20	1744.68
Bromiodomethane	86.2	1979.50	1225.45	1796.46
Bromoform	99.5	2117.67	1335.63	1921.85
Diiodomethane	96.2	2180.06	1308.87	1978.47

Figure 7 shows the dependence of the three different approximations for Sc -calculation for bromoform on temperature.

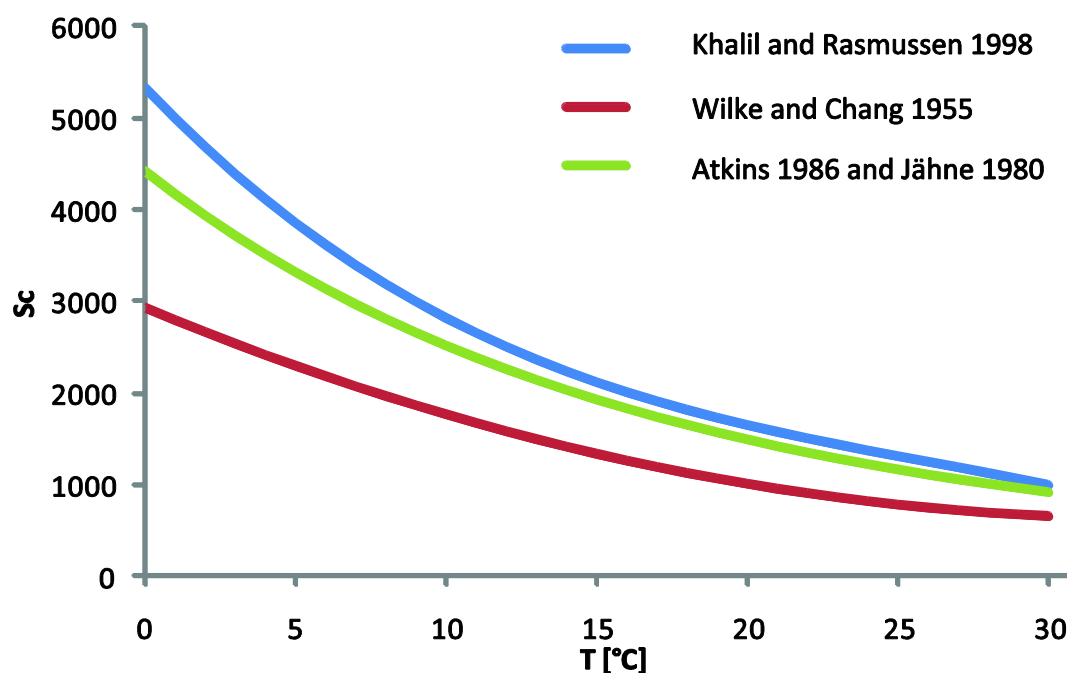


Figure 7. Comparison of three approximations for Sc calculations. Here values for bromoform are given as a function of temperature.

In this work we use the equations of Wilke and Chang (1955) and DeBruyn and Saltzman (1997a). This calculation gives higher flux values but we assume that the basic principle (derivation of another halogarbon) might reflect best the real *Schmidt number* for VHOCs.

2.5.3 Notes on calculations of air mixing ratios

Although part-per-notation is not a SI-unit (international system of units), parts per trillion (ppt) is commonly used in atmospheric chemistry. Another drawback of the part-per-notation is disaccords due to the different meanings in short and long scales for numbers: for most languages in continental Europe billion has the value of 10^{12} and trillion of 10^{18} . English language-speaking countries however using short scale notation with billion = 10^9 and trillion of 10^{12} . Consequently ppt for instance stands for $1 \cdot 10^{-12}$.

Though part-per-notation do have some strong advantages to express air concentrations: in contrast to the metric units (e.g. $\text{ng} \cdot \text{m}^{-3}$), ppt is not influenced by temperature, pressure or molecular weight. This has a crucial benefit, since gas mole fractions of different atmospheric layers are directly comparable.

Beside ppt, pptv (part per trillion by volume) are present in the literature too as a unit for gas mole fraction. However both units are identical for the purposes in atmospheric chemistry. Since mole and volume fraction are identical for ideal gases (and practically identical for most gases) pptv can be calculated under standard temperature and pressure (STP = 1013.25 mbar and 273.15 K) using the following equation:

$$\text{pptv} = \frac{m_{\text{gas}}}{V \cdot M} \cdot V_m \quad (31)$$

V_m	standard molar volume of ideal gas at STP	[22.413996 L/mol]
m_{gas}	mass of the VHOC	[pg]
M	molecular weight of the VHOC	[g · mol ⁻¹]
V	Volume of the sample at STP	[dm ⁻³]

Calculations for air concentrations must consider real temperature and pressure. The sample volume at STP can be calculated using following equation:

$$V_s = \frac{V_{\text{STP}} \cdot p}{T} \quad (32)$$

V_s	Sample volume	[dm ⁻³]
T	absolute temperature	[K]
p	pressure	[mbar]

3 Methods and Development of the Analytical System

3.1 Working with Trace Elements

VHOCs occur as trace elements in the atmospheric and marine environment. Common concentrations range at $\text{pmol} \cdot \text{L}^{-1}$ -level for water samples and pptv for air samples. To illustrate this concentration range, Wikipedia gives the following figure: Parts per trillion “is equivalent to one drop of water diluted into 20, two-meter-deep Olympic-size swimming pools ($50,000 \text{ m}^3$)”. Hence working with trace elements requires very careful handling to avoid pollution of the sample or the analytical cycle. Desorption of pollutants and adsorption of analytes from/towards materials must be considered as a challenging problem. Materials and cleaning procedures should be adapted with regards to their interfering potential. Borosilicate glassware and stainless steel are preferable to plastic material. In order to maintain high analytical precision, the analytical cycle must be absolutely gastight towards the atmosphere.

The low environmental concentrations pose a challenge for the detection: usually air- and water concentrations are below the detection limit; including the most sensitive methods. Direct injection of water samples onto the capillary column was tried (Grob and Habich 1983) but emerged as unsuitable for halocarbon measurements. For detection, the analytes needed to be preconcentrated: in a first step, the analytes are separate from the medium. Then, in a second step the concentrated analytes are chromatographically separated and finally measured by a specific detector.

The following paragraphs give a review on different techniques necessary for halocarbon measurements. For a better understanding, theory is explained succinctly for techniques and apparatus. Finally the implemented methods are described.

3.2 Sampling Devices

Air and water samples can be stored in special sample vessels or syringes. It should be noted that the risk of contamination or the loss of analytes is highest between sampling and injection

in the analytical cycle. Sample contact with ambient air must be avoided at all time. The material of the sample device should not interfere with the analytes. Different techniques are described for rapid shipboard measurements for water samples, including glass ampoules (Bulsiewicz et al. 1998; Pruvost et al. 1999; Vollmer and Weiss 2002), PVC bottles and syringes (Bullister and Wisegarver 2008) or glass vials (Martinez et al. 2002a). Samples should be stored in dark to avoid photolytic degradation. Low temperatures reduce biological and chemical reactions. For longtime storage samples can be frozen in stainless steel containers (Zoccolillo and Rellori 1994), treated with mercury chloride (Gschwend et al. 1980) or hydrochloric acid (Dewulf and VanLangenhove 1995). However latter mentioned sample treatments must be critically examined. Mercury chloride is highly toxic and will stop biological (bacterial) activities in the samples thus chemical reactions are not influenced.

For a review on different water sampling techniques, see Dewulf and VanLangenhove (1997). For air collection, several types of containers can be used, including metal canisters, gas-tight syringes or glass vessels. Ras et al. (2009) give and detailed review about different sampling techniques for air samples.

3.3 Extraction

3.3.1 Solid-Liquid extraction

Halocarbons in seawater can be extracted and preconcentrated using a solid sorbent. Duinker (1993) described such a technique for the detection of PCBs (polychlorinated biphenyls) in seawater: several hundreds of litres of filtered seawater flow through a trap filled with a sorbent (XAD-2). In a second step an organic solvent (acetonitrile-water mixture) is used to wash the analytes from the trap. After distillation of the acetonitrile-water mixture, the distillate is purified by HPLC. Then the remaining PCB-extract (1 ml) is analysed by GC-ECD after a final distillation.

Solid phase microextraction (SPME) is another common used preconcentration technique (Page and Lacroix 1993; James and Stack 1997; Popp and Paschke 1997; Grote et al. 1999). The analytes are trapped on the microextractor, which contains fine fibers of chemically modified

fused-silica. Finally, this microextractor is introduced directly in the injector of the GC. SPME can be adopted for gaseous samples as well.

3.3.2 Liquid-Liquid extraction

Halocarbons can be extracted from a liquid medium by a liquid solvent (e.g. pentane). Originally introduced by Eklund et al. (1978) this technique was frequently used until the nineties of the last century (e.g. by Abrahamsson and Klick 1990). Even though the extraction procedure is simple, the method has some crucial technical drawbacks: the separation of the two phases can be interfered in organic rich water by the formation of emulsions. Furthermore it is often necessary to insert high volumes of solvent for high extraction efficiency. This however disagrees with the aimed preconcentration of the analytes.

3.3.3 Gaseous-Liquid extraction

In this method an inert gas (nitrogen, helium, argon) is used to separate analytes from a liquid medium. The technique was described by Swinnerton et al. (1962) for the first time. Since then, this technique became the main technique used for the determination of halocarbons. The gaseous-liquid extraction is differentiated into two groups:

In the static headspace extraction a water sample is given into a gas tight container. An adequate headspace is left and replaced by an inert gas. The container is shaken until equilibrium between the water phase and the headspace is reached. This equilibrium depends on the temperature, the partial pressure and the salinity and is describes by the Henry's Law (see 2.5.1). The Henry's Law constant determine the precision of the method: low gas-to-liquid concentration ratios causes low gas phase concentrations and therefore accuracy can be limited. Larger headspace volume might solve this problem (King et al. 2000). Static headspace techniques had been developed for incubation experiments (Itoh et al. 1997; Manley and de la Cuesta 1997; Amachi et al. 2001) and for environmental samples (Drewer et al. 2008; Jakubowska et al. 2009).

Dynamic headspace extraction, or purge-and trap (PAT), is the most commonly used technique to extract halocarbons from water. This method is characterised by low detections limits caused by high effective preconcentration of the analytes. PAT is subdivided in three steps:

firstly, an inert gas (e.g. helium) stripes the analytes from a sample. Then, water vapour is removed from the gas flow downstream. Finally, the analytes are focused in a trap on a sorbent bed or in a cold trap. Several factors influence the extraction efficiency: high extractions rates can be achieved by high gas flow and purging temperature, fine bubble sizes (determined by pore size and salinity) and by a purge gas with a low water solubility (e.g. helium). Moreover compounds with lower water solubility show (c.f. 2.1) higher extraction rates from the sample. Table 6 gives a comprehensive overview of PAT-techniques used by different authors for halocarbon measurements as well as the one used during this thesis.

Table 6. Comparative study of literature about different PAT- and desiccation techniques

Reference	Volume [ml]	Purge gas	Flow [ml · min]	Time [min]	Temperature [°C]	Desiccation
Lepine and Archambault (1992)	5	Helium	40	8	RT	dry purging
Krysell and Nightingale (1994)	18.8	N (H doped)	55	20	RT	nafion
Laternus 1995	50	Helium	80	30	RT	potassium carbonat (2°C)
Ekdahl and Abrahamsson, 1997	27.8	Nitrogen	50	4	70	condenser, Mg(ClO ₄) ₂
Pruvost et al. 1999	30	Nitrogen	90	20	RT	condenser, Mg(ClO ₄) ₂
Miermanns et al. 2000	25	Helium	10		50	condenser (-15°C)
Quack et al. 2004	88	Helium	40	20	up to 80°C	nafion
This work, 2007	30	Nitrogen	90	20	RT	condenser, Mg(ClO₄)₂
This work, 2008	10	Helium	90	20	RT	condenser, Mg(ClO₄)₂

A distinction is drawn between on-line and off-line methods. The term on-line denotes a direct linking between the purge-and-trap, the injection and the gas chromatographic separation and detection. On-line methods are characterized by low external contamination. On the other hand, off-line means a spatial and temporal separation between extraction and detection. Off-

line methods lend itself for field work: samples can be taken and prepared (extracted) in the field. Moreover extracts can be stored much longer than raw samples.

The two following paragraphs – gas desiccation and trapping – are restricted to headspace extraction.

3.4 Purge gas desiccation

Stripping the analytes from the aqueous phase has a negative side effect: significant amounts of water vapour are purged together with the analytes. This water can decrease the trapping potential of the adsorbent, plug cold traps, interfere the separation process or lower the detector sensitivity. Moreover when the moisture is condensing inside fine tubes, some portions of the analytes might be trapped in these water drops. Analyzing air samples causes less problems with water vapour, since the amount of water is considerably lower.

In the literature several techniques are described to remove water vapour from the gas flow, downstream the purge chamber. Condensers (Zlatkis et al. 1973; Werkhoff and Bretschneider 1987; Pankow 1991; Tessier et al. 2002), micro sieve traps or desiccants are used to remove high portions of water vapour. Latter technique covers the use of different chemicals such as potassium carbonate (Schall and Heumann 1993; Laturus 1995; Giese et al. 1999); sodium carbonate, magnesium perchlorate (Novak et al. 1973; Simmonds 1984; Doskey 1991; Murphy et al. 2000; Tokarczyk and Saltzman 2001) or silica gel (Klamm and Scheil 1989). Alternately nafion drying membranes are described as effective and simple devices for the removal of water vapour (Tanzer and Heumann 1992; Janicki et al. 1993; DeBruyn and Saltzman 1997b; Richter and Wallace 2004).

Different methods can be combined, thus resulting in a better gas drying (Ekdahl and Abrahamsson 1997; Groszko 1999; Pruvost et al. 1999). These authors used condenser followed by magnesium perchlorate traps. Christof et al.(2002) connected a condenser, a nafion dryer and a magnesium perchlorate in series.

Each water removal procedure was reported as suitable for the determination of volatile halocarbon. In the present work, a Graham condenser was used together with a magnesium perchlorate trap downstream.

3.5 Preconcentration of the analytes and injection

After the extraction and desiccation process, analytes are preconcentrated in special traps. Two trap configurations can be distinguished: 1.) on cryotrapping, analytes freeze out at very low temperatures. Cold traps – open narrow bore stainless steel tubes (Pruvost et al. 1999; Carpenter et al. 2000) or glass tubes, filled with glass beads or glass wool (Camel and Caude 1995; Laturnus et al. 2000) – are cooled with liquid nitrogen or dry ice (Bulsiewicz et al. 1998). For desorption, traps are heated rapidly in order to achieve a simultaneous injection of all analytes onto the column.

2.) on sorbent trapping, analytes are focused on a compound sorbent bed, composed of one or more (Sanchez and Sacks 2003) specific sorbents. Benefits of this technique are the high trapping temperature and the lipophilic character of sorbent. Some of those traps work at ambient temperature and do not require desiccation of the gas flow. Sorbents are either carbon or polymer based materials. Carbonaceous sorbents are: Carbopack/Carbosieve (Dewulf et al. 1996), Carbotrap (Urhahn and Ballschmiter 2000), Carboxen (O'Doherty et al. 1993) and microcharcol filters (Atlas and Schauffler 1991). Polymerious sorbents are: Tenax TA (Li et al. 1999), Tenax GR (Quack and Suess 1999), Porapak N (Wallace et al. 1994) or Poraplot Q (Quack et al. 2004). For sorbent trapping, thermo desorption requires high temperatures for complete unload of the analytes. A comparative literature study is shown in Table 7.

Table 7. Comparative study of literature about different ad- and desorption techniques.

Trap	Focussing		Desorption	Reference		
stainless capillary tube	steel	cooling mixture (ice-salt)	-10	heat gun	un-stated	Laternus 1993
Tenax TA		liquide nitrogen	-196	boiling water	80	Laternus 1993
Tenax GR		liquide nitrogen	-120	electric resistance	200-250	Kuss 1994
stainless capillary tube	steel	liquide nitrogen	-150	boiling water	100	Krysell, M. and P. D. Nightingale , 1994
different adsorbents		unspecified	5-10	unspecified	140	Ekdahl and Abrahamsson, 1997
stainless capillary tube	steel	cooling mixture: acetone/liquid nitrogen	-94	boiling water	100	Pruvost et al. 1999
fused silica tube	capillary	liquide nitrogen	-120	electric resistance	200	Miermanns et al. 2000
Tenax TA		dry ice	-40	electric resistance	220	Christof et al. 2002
Tenax TA		ambient temperature	<38°C	electric resistance	250	Janicki et al. 2002
Poraplot Q mesh)	(80-100	liquide nitrogen	-70	electric resistance	170	Quack et al. 2004
stainless capillary tube	steel	dry ice	-78	boiling water	100	This work, 2007
Glass Beads mesh)	(80-100	liquid nitrogen	-120	boiling water	100	This work, 2008

3.6 Separation and Detection

The separation of halocarbons is carried out by gas chromatography and different capillary columns. Helium and nitrogen can be used as carrier gas (mobile phase). A great variety of capillary columns (stationary phase) are applied for separation: lengths (24-105m), inner diameter (mega bore and narrow bore) and the choice of film material influence the analytical performance. Additionally, temperature and flow programming are used to obtain optimal separation in a minimum of time.

Flame ionisation detectors (FIDs), electron capture detector (ECDs) and mass spectroscopy (MS) can be exert for determination of halocarbons. FIDs are used to determine organic compounds and are suitable for gas chromatography (Bianchi et al. 1991). However they are about three orders of magnitude less sensitive compared to ECD and unspecific for a great variety of organic substances. Thus, peaks of nonhalogenated organic compounds may

interfere with those ones of halocarbons. Since MS detectors has reached similar or even better sensitivities compared to ECD, this detector are gaining popularity nowadays (Wevill and Carpenter 2004; Jakubowska et al. 2009; Ras et al. 2009). When working in the *single ion mode*, the detection is compound specific and inert to interfering compounds.

The ECD – a device invented by Lovelock (1958) – enable to detect electronegative compounds (such as VHOCs) in a carrier gas. Figure 8 shows a general scheme of an ECD. A beta emitter (radioactive ^{63}Ni) ionize the make-up gas; usually nitrogen. As a result of this ionization, a stable cloud of free electrons are established in the detector cell. After applying a potential between anode and cathode, the free electrons move to the anode and generate a standing current. When electronegative compounds are flushed into the detector cell, the compounds react with the electron cloud by capturing free electrons and reduce the current between the collector anode and the cathode. However this primordial setup is limited in the linear detector response.

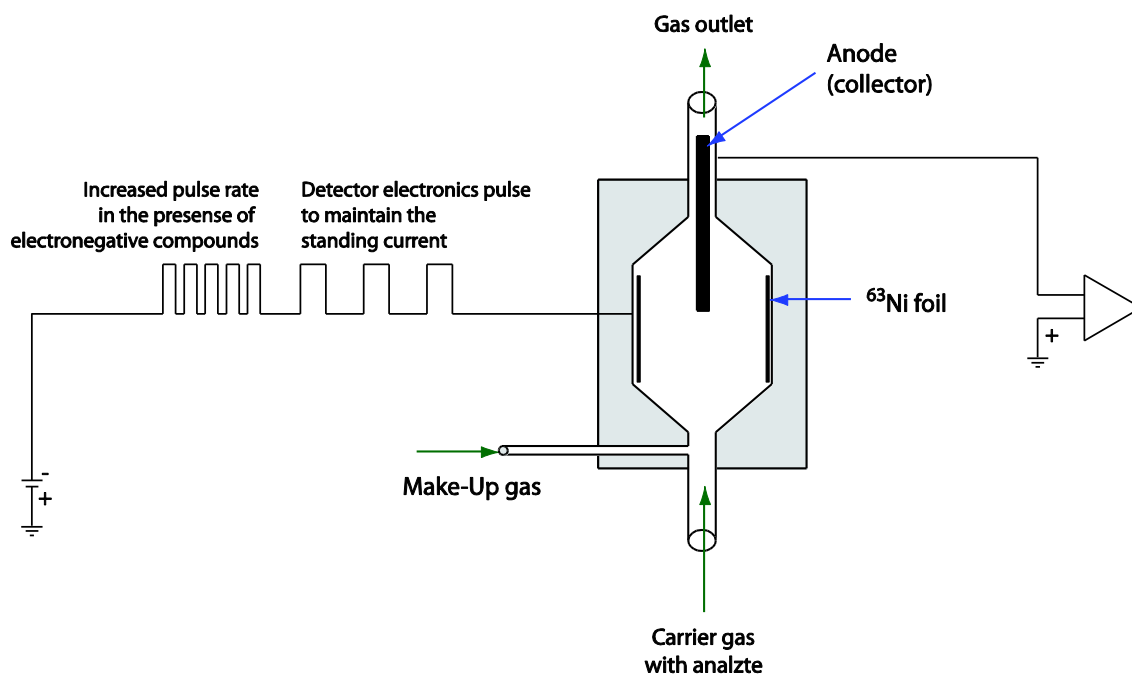


Figure 8. Scheme of an Electron Capture Detector (ECD)

Hence, more recent ECDs work with pulse modulation: a defined standing current value is generated by periodically pulsing of a potential. If the current drops below the defined standing current value, the number of pulses are modified until the defined current values is maintained. When the electron density is decreased by electronegative compounds, the pulse rate is increased until reaching the standing current. Its advantage is that the number of free electrons remains constant. Hence adequate numbers of electrons are given even at high analyte concentrations. Thus the linear detector response is enlarged. Finally the pulse rate is detected and converted to an output signal. This output signal is directly proportional to the concentration of the analyte ($\text{fmol} \cdot \text{s}^{-1}$) and the analyte. The detector response increases in the order $\text{F} < \text{Cl} < \text{Br} < \text{I}$ and with the numbers of halogens in a compound by a factor 10. Figure 9 illustrates the detector response on the amount of substance.

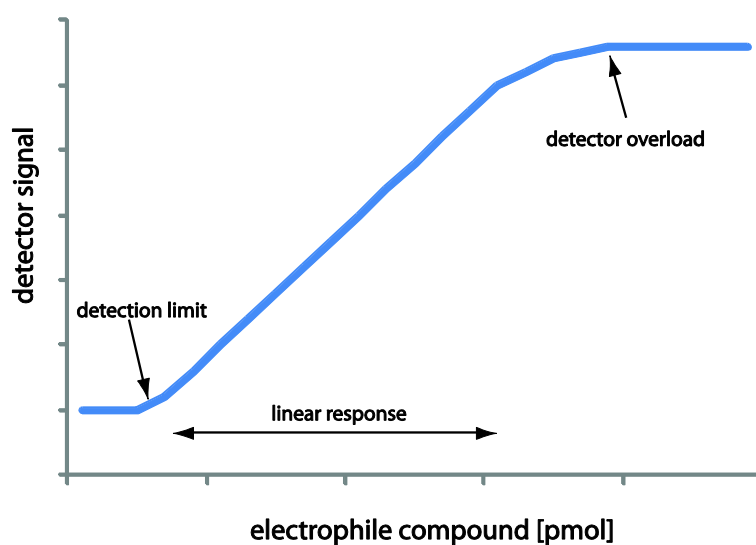


Figure 9. Linear range of an ECD.

3.7 Limit of Detection

The absolute detection limit is defined as the lowest verifiable quantity of a substance, while the relative detection limit (or method detection limit) is expressed as lowest detectable concentration of an analyte (Omenetto et al. 1996). For ECD, the limit of detection (LOD) is

usually estimated as signal-to-noise ratio of 3:1 (three times the standard deviation of a significant number of blanks). The detection limit is depending on the detector response of a compound and the bleeding of the capillary column (constant loss of coating phase of the inner column). High column bleeding results an elevated background noise. Low detector response increases the detection limit. Figure 10 demonstrates the sensitivity of the ECD used in the present work to twelve different VHOC. Signal intensities of VHOC were determined by measuring standards with the same number of substance (100 pmol). Finally, the relative detector response was expressed as the ratio to the compound with the highest response (tetrachloromethane).

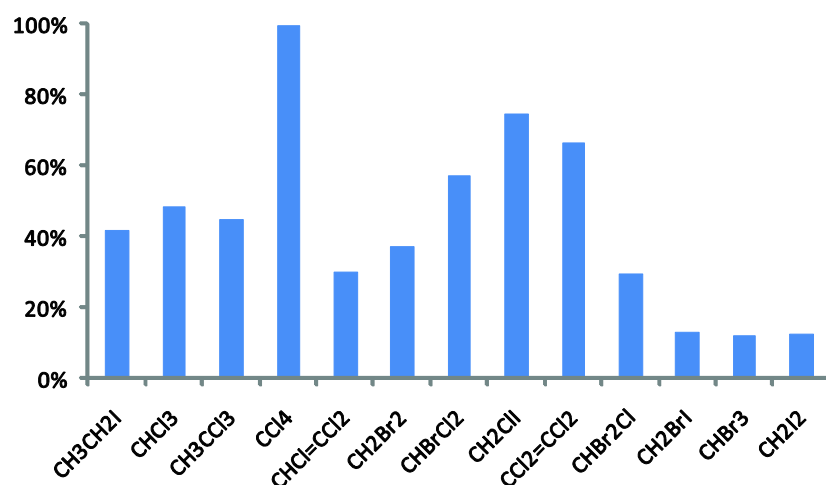


Figure 10. ECD response, relative to the compound of the highest response (tetrachloromethane).

While tetrachloromethane, chloriodomethane and perchloroethene showed highest responses, bromiodomethane, bromoform and diiodomethane was found to have lowest sensitivities.

In Table 8, published applications of various extraction and detection techniques are compared with regards to detection limits. Abrahamsson and Klick (1990) used liquid-liquid extraction combined with ECD. Static headspace extraction and ECD detection were used by Gotz et al. (1998) and Kuivinnen and Johansson (1999). Purge-and-trap combined with mass spectrometry is another common applied technique (Ekdahl and Abrahamsson 1997; Miermans et al. 2000; Christof 2002). Most usually used is the combination of purge-and-trap extraction together with ECD (Krysell and Nightingale 1994; Kuß 1994; Ekdahl and Abrahamsson 1997; Pruvost et al. 1999; Cocquempot 2004).

Table 8. Comparison of absolute detection limits [$\mu\text{mol} \cdot \text{L}^{-1}$] in the literature.

	Abrahamsson and Klick 1990	Kuivinen and Johansson 1999	Gotz 1998a	Miermans et al. 2000	Christof 2002	Ekdahl and Abrahamson 1997
	liquid-liquid ECD	headspace ECD	Headspace-ECD	PAT-MS	PAT-MS	PAT-MS
$\text{CH}_3\text{CH}_2\text{I}$	4.49					1,00
CHCl_3	16.75	837.66	167.53	16.75	0.78	0,10
CH_3CCl_3	1.50	749.63	37.48	44.98	0.84	0,80
CCl_4	0.33	650.11	32.51	13.00	0.59	0,50
$\text{CHCl}=\text{CCl}_2$	3.04	761.11	76.11	38.06	0.76	0,50
CH_2Br_2	2.31				1.50	1,00
CHBrCl_2	1.22	610.39	12.21		1.12	0,90
CH_2ClI	0.17					1,00
$\text{CCl}_2=\text{CCl}_2$	0.42	603.14	60.31	18.09	0.60	0,30
CHBr_2Cl	0.96	480.12	9.60		0.78	0,70
CH_2BrI						
CHBr_3	0.79	791.36	11.87		0.83	2,00
CH_2I_2	1.49					2,00

continued

	Ekdahl and Abrahamson 1997 PAT-ECD	and Kuß 1994 PAT-ECD	Krysell and Nightingale 1994 PAT-ECD	Pruvost 1999 PAT-ECD	This work PAT-ECD
CH ₃ CH ₂ I	0.002			0.03	0.1
CHCl ₃	0.0006		1.68	0.59	0.58
CH ₃ CCl ₃	0.001		0.30	0.52	0.1
CCl ₄	0.0003		0.07	0.02	0.05
CHCl=CCl ₂	0.002	0.0001	0.61	0.23	0.1
CH ₂ Br ₂	0.002	0.002	0.12	0.06	0.09
CHBrCl ₂	0.001	0.001	0.06	0.03	0.11
CH ₂ ClI	0.001			0.11	0.03
CCl ₂ =CCl ₂	0.0002	0.000	0.06	0.04	0.06
CHBr ₂ Cl	0.002	0.037	0.10	0.05	0.07
CH ₂ BrI			0.45		0.15
CHBr ₃	0.03	0.285		0.67	0.43
CH ₂ I ₂	0.002			0.34	0.09

Usually detection limits are given as method detection limit (as a concentration). However it must be considered that high sample volumes result in a lower detection limit. It is clearly visible that liquid-liquid and static headspace extraction show the lowest performance. Formerly, GC-MS shows about three orders of magnitude higher detection limits compared to GC-ECD (Ekdahl and Abrahamsson 1997). Highest performance was achieved by purge-and-trap and ECD. The technique used by Ekdahl and Abrahamsson (1997) and Kuß (1994) showed lowest detection limits for VHOCs. In recent time GC-MS methods reached the level of GC-ECD (Li et al. 2001; Bravo-Linares and Mudge 2009).

3.8 Implemented GC-ECD-System

As stated above, high performance of the analytic system is required for the determination of halocarbons. For the method development, we benefited of previous technical development by Cocquempot (2004) for his former work. The following considerations were made for the method development:

- User-friendly handling and maintaining, achieving by simplifying the design
- High analytical precision
- Avoiding of potentially contaminants
- Filed work ready

3.8.1 Sampling device

In a preliminary study we tested a sampling device introduced by (Pruvost et al. 1999; Cocquempot 2004). However we found important drawbacks in the handling and performance, the main disadvantage being the low gas tightness. Our new device is based on the work of Bulsiewicz et al. (1998). We changed the direction of in- and outlet, modified the diameter of the retainer for the glass ampoule (8 mm) and mounted quick connectors (Swagelok).

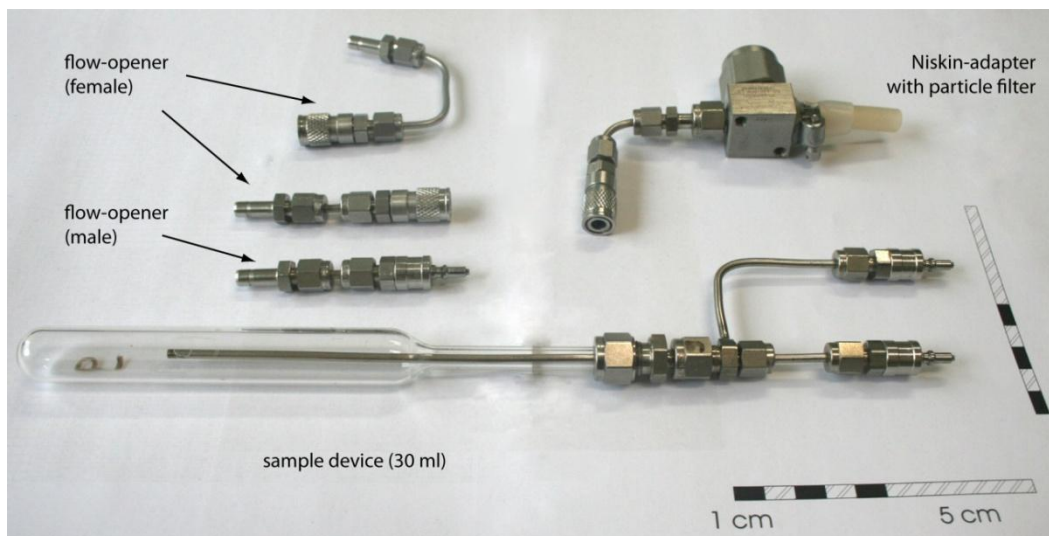


Figure 11. Sampling device (water), Niskin-adapter and flow-opener

The new device is absolutely gastight for several days and sufficient gastight for several weeks. Samples are easy to connect to the Niskin bottle and to the analytical system. The precise volume was determined gravimetrically, after filling the sampling device with de-ionised water.

Sample for air measurements were taken in 250 ml glass bulbs (Figure 12). Both ends were closed with Swagelok quick connectors. Air samples were taken using a 500 ml syringe and a special adapter. The sample device was flushed with ambient air (at least five times their own volume) before closing. Then, the sample devices were mounted at the analytical circle as specified for the water samples. A protection cover was mounted around the glass bulb. A protection cover was mounted around the glass bulb.



Figure 12. Sampling device (air), glass bulb and syringe.

3.8.2 Purge-and-Trap

In a preliminary study we tested different materials for applicability. Glass tubes with OD 6mm appeared highly fragile. Higher wall thickness and higher OD (8mm) solved this problem. Saltwater carrying tubes were connected to Swagelok ball-valves, while Valco rotor-valves were used for gas lines.

Figure 13 shows the analytical cycle: the purge gas enters the analytical system at valve V1 (VALCO, 2C6UWE). The following check valve prohibits contamination caused by back flush. Then, the purge gas flow passes V2 (SS-43YTFS2) and V3 (SS-41GXHLS2). Samples are attached with quick connections to the analytical circle. The sample is pushed towards the purge

chamber, passing a particle filter (SS-2TF-LE), V4, V2 and the glass frit (pore size 4) of the purge chamber.

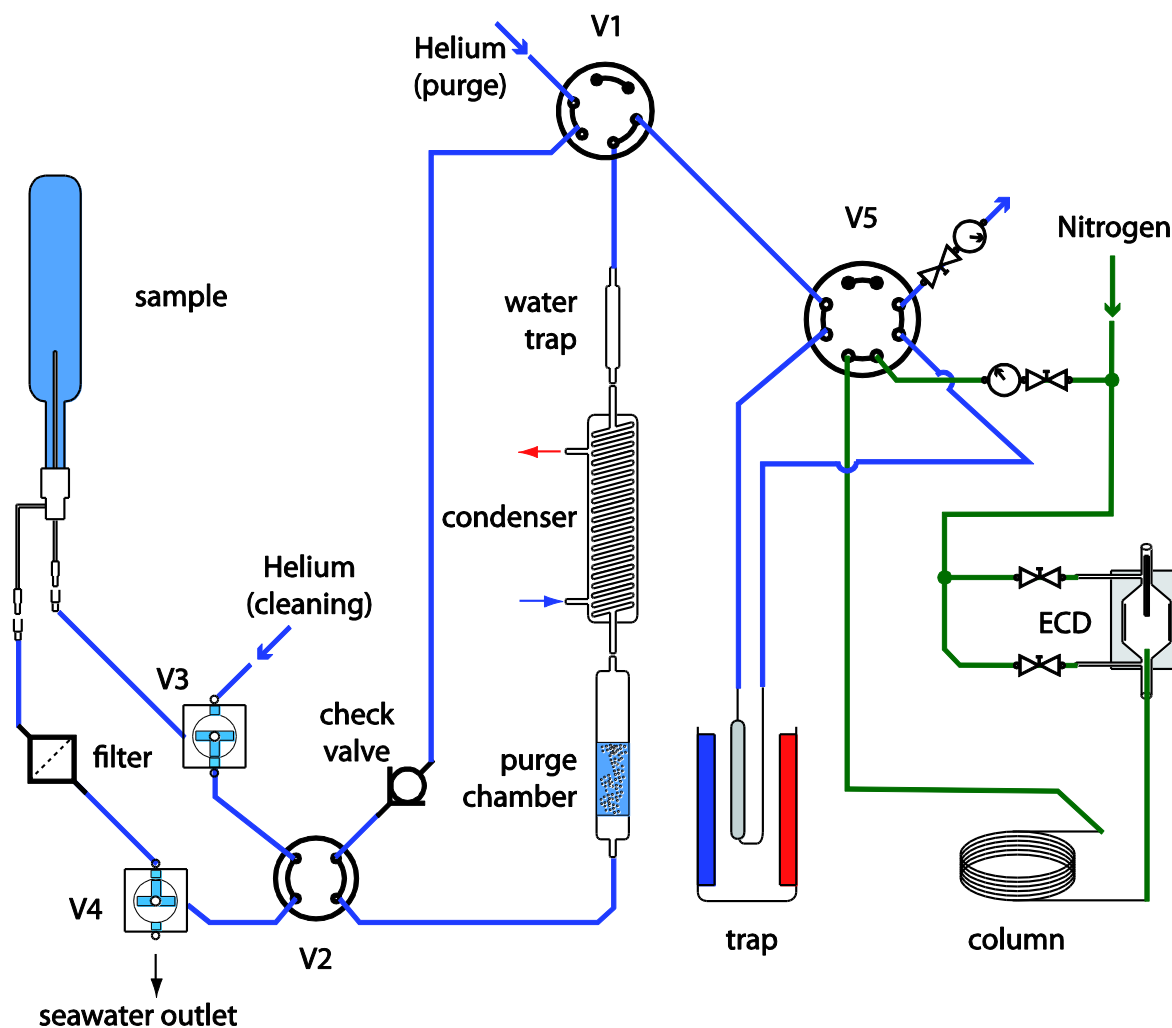


Figure 13. Schematic picture of the analytical system.

When the entire sample is injected in the purge chamber, V2 is turned and the sample device can be removed from the system. Then, the purge gas extracts the analytes from the water. A Graham condenser and a magnesium perchlorate trap remove the water vapour from the gas stream. The Graham condenser is held at about 1°C. The perchlorate trap consists of a glass

tube, the desiccant, and glass wool used as stopper. A simple glass tube (8mm OD) emerged as the ideal configuration: glass bulbs with small OD are difficult to load with desiccants. The analytes were focused in a cryotrap. For the MOUTON campaign (see chapter 4), no liquid nitrogen was available for cryotrapping. Therefore, dry ice was given in a Dewar vessel, together with the trap (empty stainless steel tube). For the work in Brittany (see chapter 5), the trap (glass tube filled with glass beads) was cooled with liquid nitrogen. After 20 min (80 min for air) of purging, valve V5 (VALCO, A4C8WE) was turned and the trap was heated in hot water. Now nitrogen flushes the analytes from the trap in the column. The water is released from the purge chamber, passing V2 and V4. The sample inlet can be cleaned using the valves V3 and V4: a pump is connected to V3 and evacuate remaining water drops and air. Then V3 and V4 are turned at the simultaneously and helium flushes in the circle. This procedure is repeated several times.

The analytes are injected by thermodesorption from the trap (3 min) onto the column. The gas chromatograph used was a Chrompack CP 9000, with an ECD. The oven was temperature programmed for the time of separation. For 10 minutes, the oven was kept isothermally at 70°C. Then, the temperature was ramped at 10°C · min⁻¹ for 8 minutes. For the final 10 minutes, the oven was held isothermally at 150°C.

3.8.3 Retention times and identification of the compounds

VHOCs are identified by comparison of the retention times of a sample with standards of particular compounds. The separation quality of a compound and its retention times can be modified by adjusting the oven temperature and the carrier gas flow; different capillary columns were not available. Halocarbons elute regarding to their boiling point. Therefore, compounds with similar boiling points are difficult to separate. Figure 14 shows a chromatogram of a standard mixture. The analytes eluted in the following order: [1] iodoethane, [2] chloroform, [3] methyl chloroform, [4] tetrachloromethane, [5] trichloroethylene, [6] dibromomethane, [7] bromodichloromethane, [8] chloriodomethane, [9] perchloroethene, [10] dibromochloromethane, [11] bromiodomethane, [12] bromoform and [13] diiodomethane.

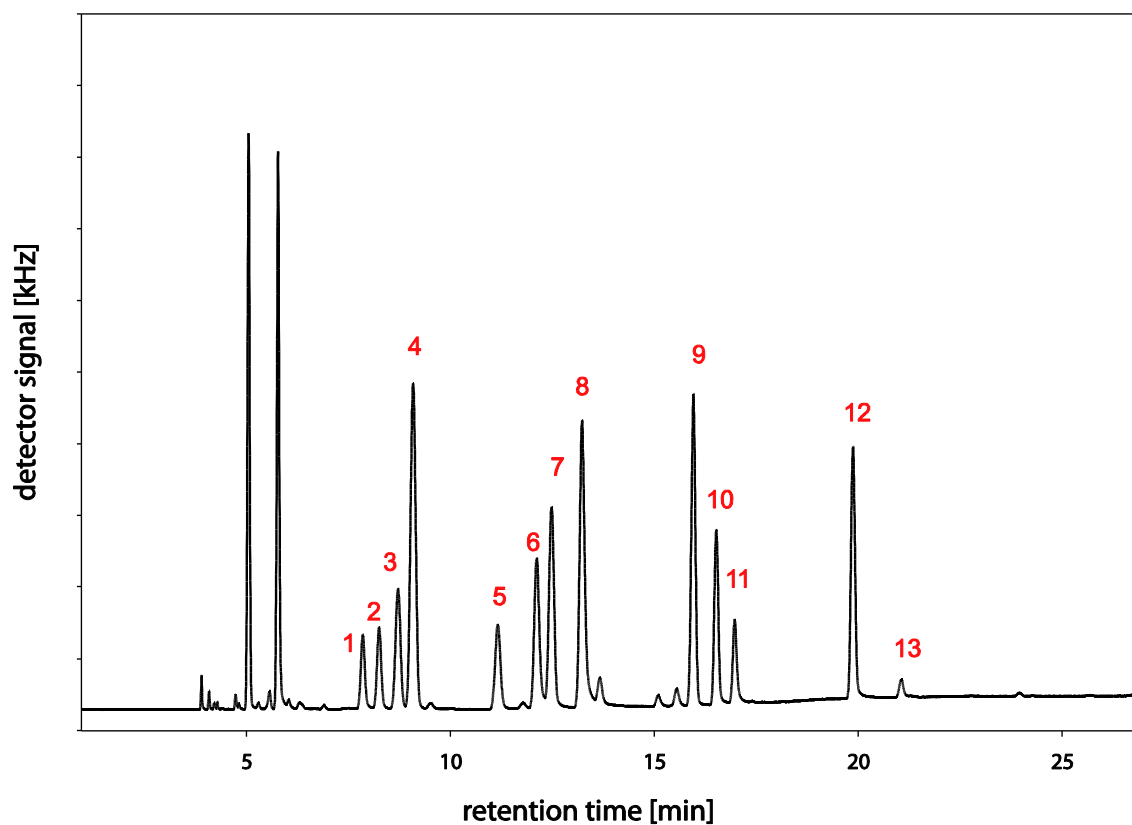


Figure 14. Chromatogram of a standard mixture.

3.8.4 Standards

Calibration of halocarbon measurements is a highly discussed matter in the halocarbon community (see SOLAS Halocarbon Intercalibration Workshop, London 2008). Generally, calibration can be carried out with gas standards (Happell and Wallace 1997) or with liquid standards (Abrahamsson et al. 2004).

Pruvost (2001) and Cocquempot (2004) described a technique for the preparation of liquid standards, which we used at the beginning of this study, too: A mixture of standards (EPA 624, Supleco, $100 \mu\text{g} \cdot \text{ml}^{-1}$) was diluted 1000 times with methanol (Suprasolv, Merck) using a microsyringe. Though, several halocarbons of interest (iodoethane, dibromomethane, chloriodomethane, bromiodomethane and diiodomethane) were missing in this mixture.

Thus pure compounds were volumetrically diluted in several steps and added to the diluted standard mixture.

However, we found several drawbacks for this technique: the EPA standard contains a broad range of halocarbons. It is likely that very volatile compounds (such as chloroform) show higher lost rate over time, compared to less volatile compounds (such as bromoform). Moreover some compounds had to be diluted in four steps that cause a high systematic error.

We used methanol standards (Carlo Erba), obtaining a concentration of $1000 \mu\text{g} \cdot \text{ml}^{-1}$. Those standards were prepared gravimetrically and transferred in special vial. These vials have narrow bored openings for minimizing lost of headspace. The working standard mixture was prepared in one dilution step for each compound. Standards were injected in special injection devices, which are closed with a PTFE/silicon septum and a screw cap. Those injection devices were filed with volatile free filtered seawater and finally treated as normal samples. Thus, this approach does not require the determination of recovery rates.

3.8.5 Summary of the PAT-GC-ECD parameters

Table 9 summarize all parameters for sampling, the PAT and the GC used during this thesis.

Table 9. General overview of measurement conditions.

Purge-and-Trap	
Purge chamber	Custom made (Pyrex, frit porosity class 4)
Purge gas	Nitrogen (MOUTON campaign) Helium (bay of Morlaix campaign)
Purge Flow	90 ml · min ⁻¹ at ambient temperature 20 min for water samples 80 min for air samples
Desiccation	Graham condenser (1°C) and magnesium perchlorate trap
Cryotrapping	Empty stainless steel tube ; 100 cm, 1/16 inch OD 3 0.03 inch ID; -79°C (MOUTON campaign) Glass beads, DMCS, 80-100 mesh (Bay of Morlaix campaign)
GC-ECD	
Chromatography System	Chrompack CP 9000
Software	Maestro 2.4
capillary column	Fused silica megabore DB-624 column (75 m x 0.53 mm ID, 3 mm film thickness, J & W Scientific, Rancho Cordova, CA, USA)
Flow	6 ml · min ⁻¹ (nitrogen)
Detector	63Ni electron capture detector (ECD), model 902A
Detector temperature	300°C
Make up and detector cell purge gas	Ultrapure nitrogen; 99.995%, filtered successively on molecular sieves (13X, 4 Å), an activated carbon cartridge and a metallic oxygen trap (Alltech, Arlkington Heights, IL, USA)
Make up Flow / Purge Flow (detector cell)	35 ml · min ⁻¹ / 15 ml · min ⁻¹
Sample	
Device	Custom made; borosilicate glass (OD: 8-20 mm); stainless steel tube 1/8 inch OD; Swagelok quick connectors
Water	30 ml (MOUTON campaign) 10 ml (Bay of Morlaix campaign)
Air	250 ml
Storage	dark at 4°C, measured within 12 h maximum

3.9 Protocols for maintaining the system

Glassware

All glassware was cleaned in several steps: glassware was treated with diluted sulphuric acid and ultrasonic bath. After it was rinsed with deionised water and cleaned with ethanol. Finally all glassware was heated to 220°C for several hours and covered in aluminium foil. Polluted glass frits were treated with high concentrated sulphuric acid (back flush) with reapplications.

Stainless steel tubs

New tubs (1/8" and 1/16") were heated to 220°C for several hours and flushed with ultrapure nitrogen. Aged tubes were replaced frequently.

Sampling devices

Sampling ampoules were rinsed several times with deionised water. Glass parts were cleaned additionally in an ultrasonic bath. Demounted ampoules were heated at 200°C (maximum for the Swagelok quick-connectors) for several hours. Gas cylinders were checked for water vapour, filled with nitrogen and hold at overpressure.

PAT System

At the end of a campaign, the entire system was rinsed with deionised water by injection via sampling ampoules. Then the system was closed downstream and hold at overpressure. Particulate filters were cleaned with deionised water (back flush) and heated at 200°C.

Possible contaminations were identified with test-blanks (running analyses without a sample). Suspicious parts were successively replaced each followed by a test-blank followed. Alternatively, parts of the analytical cycle were separated. Then, the remaining cycle was tested for purity.

Gas

Ultrapure nitrogen (99.995%, Air Liquide, France) was filtered successively on molecular sieves (13X, 4 Å), followed by an activated carbon cartridge and a metallic oxygen trap (Alltech, USA).

Detector

Because of the age of the entire GC, the ECD required intense maintenance. In case of elevating detector senility, a standard cleaning protocol was conducted. This involved mainly heating at 400°C and an elevated gas flow. Alternatively the collector was cleaned mechanically by superfine sandpaper and methanol. This cleaning procedure was performed considering safety precautions for radioactive materials (beta emitter).

4 Distribution of Volatile Halogenated Organic Compounds in the Iberian Peninsula Upwelling System

4.1 Introduction

Upwelling systems are characterized by high primary production, predominantly by diatoms. In laboratory experiments it could be shown that some diatoms synthesise bromoperoxidase and iodoperoxidase, two key enzymes for the formations of halocarbons. It was demonstrated that cultures of marine diatoms produce various brominated and iodinated compounds (Moore et al. 1996b). Hence it can be assumed that upwelling regions are potentially hot spots for halocarbon formation.

Halocarbon distribution in upwelling systems has been poorly studied. Recently, Carpenter et al. (2009) and Quack et al. (2007a; 2007b) observed elevated dibromomethane and bromoform concentrations in the Mauritanian upwelling. Both studies hypothesised that biological sources like diatom abundance or macro algae beds were the major source for brominated halocarbons. However, underlying factors for VHOC distribution patterns remain poorly understood.

Upwelling systems are well suited to investigate the formation of halocarbons by different phytoplankton groups, especially due to the absence of macroalgae. However, advection and convection of water masses into the upwelling may eliminate possible relations between VHOC concentrations and phytoplankton biomass: (1) convection elevates cold, nutrient rich waters and may reduce VHOC concentration in surface waters, (2) advection transports VHOC-rich coastal waters towards the upwelling (Carpenter and Liss 2000), (3) advection from the upwelling to the open ocean influences VHOC levels and (4) floating macro algae may cause increased VHOC levels far from the coast line (Moore and Tokarczyk 1993).

In this work, halocarbon distributions were investigated in the Iberian Peninsula Upwelling System during a campaign along the coast off Portugal, which took place in summer 2007 (August 11th to September 14th) within the framework of the *Modélisation océanique d'un théâtre d'opérations navales* (MOUTON) program on the French research vessel *Pourquoi pas*.

Here we present spatial, vertical and temporal distribution of VHOCs in the Iberian upwelling system in summer 2007. Environmental variables are analysed for their possible influence on the VHOC distribution. Different potential sources four different VHOC groups are identified.

4.2 Method

4.2.1 Study Area

The study area extended from 39.1 to 42.8°N and 8.9 to 11.1°W. In this area we sampled 69 stations along three different transects and four additional 30-hours stations (see Figure 15).

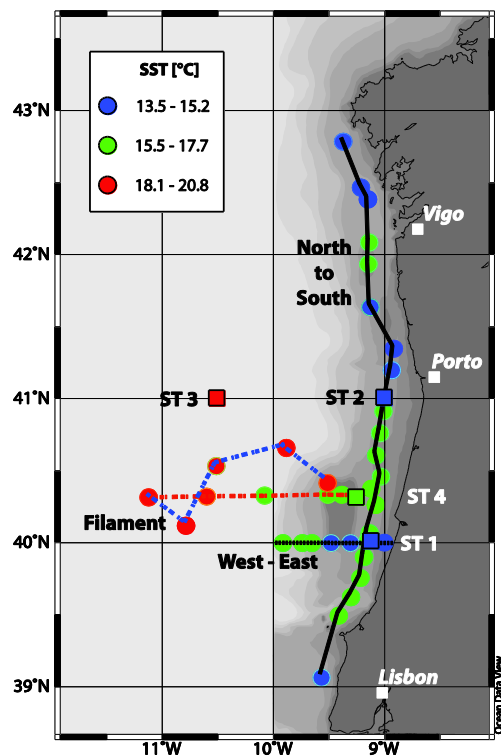


Figure 15. Mouton campaign 2007 in the Iberian Peninsula Upwelling System.

Tracks and 30-hours stations were grouped by sea surface temperature. Dots represent position of a CTD-station. Lines reflect tracks of the cruise (solid line: north to south track within the upwelling; dotted black line: west to east track followed 40°N degree of latitude from the open ocean toward the upwelling; dashed red line: track followed a filament, way there; dashed blue line: filament track, way back. Framed squares: 30-hours stations ST 1 and ST 2 within the upwelling; ST 3 in the open ocean; ST 4 in intermediate water masses.

The Iberian Peninsula Upwelling System is the northern extent of the Canary Upwelling. It ranges from about 36°N to about 46°N and from the Iberian coast to roughly 24°W (Perez et al. 2001). During summer north/northwesterly tradewinds generate a southward flow, which results in an offshore Ekman transport. This Ekman transport is responsible for the upwelling of cold and nutrient enriched waters from 100-300 m depth to the surface along the coastline (Smyth et al. 2001). Upwelling events are usually strongest in the north of the Iberian Peninsula Upwelling system (off Cap Finisterre) and are often related to westward flowing advections. These so called filaments are bands of cold and less salty waters which can reach as far as 100 km westward (Coelho et al. 2002).

Samples were taken using a 12-bottle CTD rosette (10-L-Niskin bottles). At each station, up to five samples were collected at different levels of the water column: surface, upper thermocline, maximum of chlorophyll, lower thermocline and bottom depth. Samples were taken to determine VHOC concentrations, pigment composition and nutrient levels. Physical variables and meteorological data were recorded simultaneously.

Various sea surface temperature (SST) satellite images revealed that the strength of upwelling off the Iberian Peninsula shows intense fluctuation on multiday dimensions. The main sampling took place between August 14th and 25th with high wind velocity and a resulting strong upwelling. Sampling in a filament and 30h stations took place during calm weather conditions between September 4th and 9th with moderate upwelling.

4.2.2 Physical variables and pigment analysis

Physical variables were recorded simultaneously by the CTD rosette and meteorological sensors of the vessel. Oxygen values were calibrated by independent sampling and Winkler titration. Pigments were analysed using a HPLC technique described by Wright et al. (1991). A HPLC system was used from THERMO spectrasystem equipped with a C18 (CLI) inverse column. One litre of sample was filtered at -200mbar onto a 25 mm GF/F filter. Filters were stored at -196°C in liquid nitrogen. Extraction of pigments was conducted with cold methanol (-20°C) for 12 hours. Detection limits range between 0.002 µg/mL for Chl *b*, Chl *c*2 and Alloxantin and 0,013 µg/mL for beta-Caroten. Pigments identification and quantification was done by comparing retention times and peaks areas and adsorption spectra obtained using certified standard solutions from DHI Group, Denmark.

Samples for nutrient analysis were taken in 125 ml polyethylene bottles, pre-treated with hydrochloric acid and deionised water, and finally rinsed with the sea water to analyse. These bottles have been kept at -20°C in darkness until the analysis were carried out. For nutrient analysis a semi-automated system was used (TECHNICON, autoanalyser II). The following nutrients were determined:

- Silicic acid (Si(OH)_4): following the protocol of Fanning and Pilson (1973).
- Nitrate (NO_3^-) and nitrite (NO_2^-): as described by Bendschneider and Robinson (1952) and Wood et al. (1967). Firstly, nitrite concentrations were determined. Then, nitrate was reduced to nitrite and finally the nitrite concentration was measured. The difference between both gives the nitrates concentration.
- Phosphate (PO_4^{3-}): as defined by Murphy and Riley (1962).

4.2.3 Analysis of volatiles

VHOCs were analysed using a purge-and-trap technique and GC-ECD (Chrompack CP 9000) modified after Pruvost et al. (1999). The purge-and-trap-loop was altered and Valco valves were replaced by highly saltwater resistant Swagelok models. Sampling devices were modified according to Bulsiewicz et al. (1998). These new sampling devices (30 ml) were highly gastight; leak tests showed tightness for over a week. In contrast to Bulsiewicz, sampling devices were directly connected to the Niskin bottle and to the purge-and-trap-loop respectively via Swagelok miniature quick connectors. The connector between Niskin-bottle and sampling device comprises a filter element with 15 μm pore size, to remove larger particles. Samples were stored in the dark at 4°C and finally analyzed within four hours after sampling.

Volatiles were extracted by purging with ultra-pure nitrogen for 20 min at a flow of 90 ml min^{-1} . Purging took place at ambient temperature in a purge chamber, which contained a glass frit (Pyrex 4). The gas flow was dried downstream using a condenser (held at 2 °C) and a magnesium perchlorate trap.

Volatiles were concentrated in a stainless steel capillary tube (150 cm) at -78°C and subsequently injected into a gas chromatographic column by thermodesorption (100°C, backflush). Separation of the compounds was performed using a capillary column (fused silica megabore DB-624, 75 m, 0.53 mm id, 3 mm film thickness, J & W Scientific, flow: 6 ml min^{-1} ultra pure nitrogen) and a

temperature program (10 min at 70°C, rising for 8 min to 150°C and stable for 7 min at 150°C). Quantification of volatiles was performed by external liquid standards (EPA 624 mix standards, AccuStandard; iodoethane, dibromomethane, chloriodomethane, diiodomethane, bromiodomethane Carlo Erba). Liquid standards were diluted in seawater and treated like a normal sample.

Table 10 shows the studied VHOC and gives the detection limits for each of them.

Table 10. Volatile Halogenated Organic Compounds determined in the Iberian Peninsula Upwelling System.

VHOC	Abbr.	Molecular formula	LoD [pmol L ⁻¹]
Iodoethane	IE	CH ₃ CH ₂ I	0.1
Chloroform	CF	CHCl ₃	0.58
Methyl chloroform	MC	CH ₃ CCl ₃	0.1
Tetrachloromethane	TCM	CCl ₄	0.05
Trichloroethylene	TCE	C ₂ HCl ₃	0.1
Dibromomethane	DBM	CH ₂ Br ₂	0.09
Bromodichloromethane	BDCM	CHBrCl ₂	0.11
Chloriodomethane	CIM	CH ₂ CI	0.03
Perchloroethene	PCE	CCl ₂ =CCl ₂	0.06
Dibromochloromethane	DBCM	CHBr ₂ Cl	0.07
Bromiodometahane	BIM	CH ₂ BrI	0.15
Bromoform	BF	CHBr ₃	0.43
Diiodomethane	DIM	CH ₂ I ₂	0.09

* LoD: Limit of Detection.

4.2.4 Data analysis

Multivariate methods such as principal component analysis (PCA) or cluster analysis are useful statistical tools to simplify complex data set by reducing the number of potential correlations between variables (Mudge 2007, see there detailed information about statistical methods). In order to determine physical, chemical and biological variables, which could explain the distribution of VHOC we attempt to visualize possible groupings in our dataset. In a first step, a cluster analysis was performed in order to estimate a possible clustering within the dataset. Various variables were treated with a K-means-cluster analysis, including time of the day, water

temperature, sea surface temperature (SST), salinity, density, bottom depth, sampling depth and Chlorophyll *a* concentration.

In a second step, a PCA was carried out in order to evaluate similarities between variables of our data set. Here, we computed a PCA for a data set of normalized VHOC values. As a result of the PCA, similarities between the sampling stations formed distinct clusters. Hence we estimated the factor, which might be causal for this clustering. For that, we combined results from the cluster analysis with the PCA. It appeared that SST was the crucial factor.

Consequently in a third step variable correlation matrices were performed for each SST-cluster. Data were analyzed performing one-way and factorial ANOVA with subsequent post-hoc Tukey's honestly significant difference method for unequal sample size. For the comparison of only two data sets, paired t-tests were performed.

Pearson correlation cross tables were calculated in order to determine the extent to which two variables show linear proportionality to each other. For all statistical tests and techniques *Statistica* (Release 8.0) and *Primer E* (Release 5) were used.

Detailed information about multivariate exploratory techniques (such as PCA or cluster analysis) are given by Legendre (1998), whereas Sokal and Rohlf (1995) gives a comprehensive introduction about univariate analysis (such as ANOVA or Pearson correlations).

4.3 Results

4.3.1 Upwelling during the campaign and sampling strategy

Sampling strategy (for results see Figure 15) was defined by evaluating satellite images (Figure 16). Both Chl-*a* concentration- and SST-images indicated a proceeding upwelling and phytoplankton bloom along the coast of Portugal.

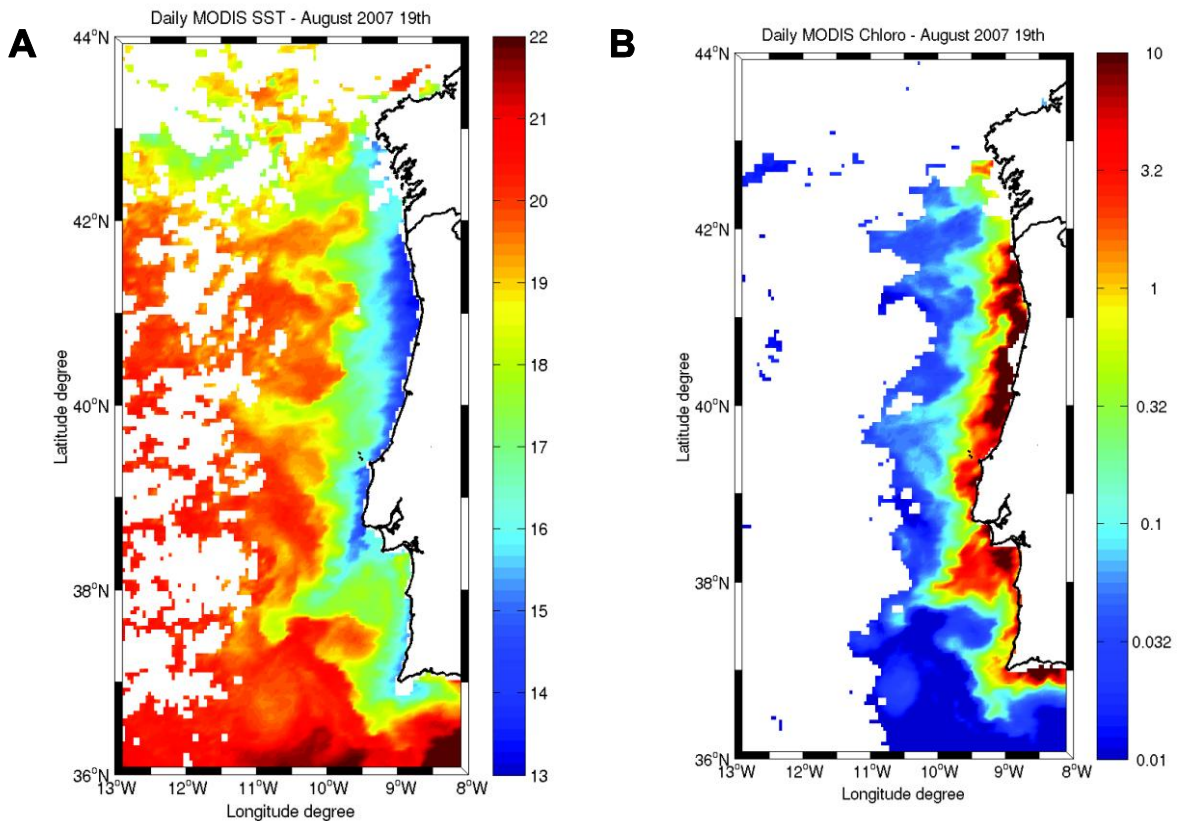


Figure 16. Satellite image of sea surface temperature (SST) and Chl-a concentration on August 19th 2007.

Source: Data from the MODIS satellite (NASA); plot computed by V. Rossi, CNRS/LEGOS, Toulouse, France. A: Blue reflects low SST (13°C), red high values (23°C). White is cloud cover. B: Red reflects high Chl-a concentration, blue reflects low Chl-a concentration. White is cloud cover.

The north-to-south track followed a 100 m bottom depth isoline and was located within the upwelling. This track was chosen in order to investigate VHOC concentrations within the maximum of phytoplankton density. The west-to-east track followed 40°N degree of latitude from the open ocean toward the upwelling. This track was chosen to investigate differences between coastal influenced upwelled waters and nutrient depleted open ocean waters. A distinct offshore filament was sampled heading westwards at 40.4°N. This track was completed by sampling outside the filament heading eastwards. Additionally, samples were taken at four 30 h stations (ST 1 – 4). Station 1 (40°N, 9.1°W) and 2 (41°N, 9°W) were located within the upwelling. Station 3 (41°N, 10.5°W) was a reference point in the open ocean. Station 4 (40.3°N, 9.2°W) was located just outside the upwelling.

Satellite images indicated that sea surface temperature decreased in the first two weeks of the campaign compared to the previous weeks, indicating that upwelling took place before the start of the campaign. A satellite sea-surface temperature image taken on August 19th showed clear upwelling conditions occurring in the studied area (Figure 16, A). Distinctive upwelling took place along the Iberian Peninsula from Cap Finisterre to 37°N with highest convection about 41°N. A clear temperature gradient is visible from the open ocean (around 21°C) towards the coast (less than 15°C). Filaments were visible at 37.5°N, 40°N and 41.5°N. These cold water bands extend from the Iberian coast up to 12°W and are characterised by temperatures significantly lower than the surrounding water masses. Satellite images of Chl-*a* concentrations indicated a phytoplankton bloom along the Iberian Peninsula (see Figure 16, B). Concentrations were highest near the coastline (more than 3.5 µg/L) and low in the open ocean (two orders of magnitude lower). Coupled to upwelling and advection, a meandering structure of the phytoplankton density is clearly visible all along the coast. During the last week of the campaign, upwelling conditions were still evident although wind velocity decreased (less than 10 m/s) and sea surface temperatures increased by several degrees along the coast.

4.3.2 Spatial distribution of selected VHOCs

Sea surface concentrations for selected VHOC measured during the MOUTON campaign are presented in Figure 17.

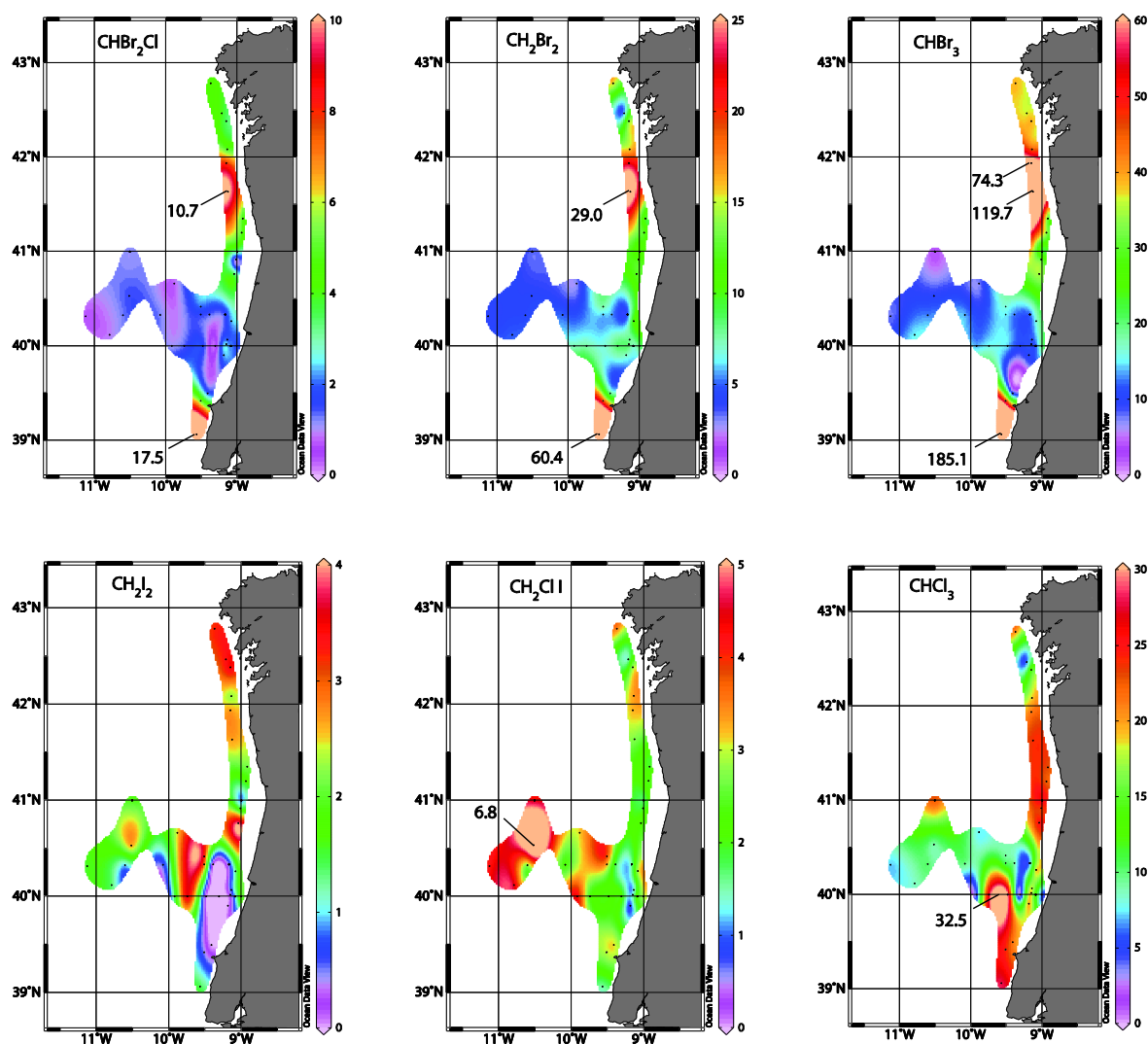


Figure 17. Seasurface values of selected VHOCS.

Dibromochloromethane (CHBr_2Cl), dibromomethane (CH_2Br_2), bromoform (CHBr_3), chloroform (CHCl_3), chloriodomethane (CH_2ClI) and diiodomethane (CH_2I_2) in pmol L^{-1} . Colour scales with different concentration range. Stations with values out of scale are labelled.

Generally, concentrations of brominated compounds were high along the coast and low in the filament and in the open ocean. The highest values were found between 41°N and 42°N and around 39.5°N ($185.1 \text{ pmol L}^{-1}$ for bromoform, 60.4 pmol L^{-1} for dibromomethane and 17.5 pmol L^{-1} for dibromochloromethane).

Concentrations of iodinated compounds were about the same range than dibromochloromethane (surface mean of 2.7 pmol L⁻¹ for chloriodomethane and 1.5 pmol L⁻¹ for diiodomethane). The highest surface concentrations of chloriodomethane were recorded in the open ocean far from the coastline (up to 6.8 pmol L⁻¹). Other sampling sites with elevated chloriodomethane values were located in the upwelling at 42°N and at the northernmost station (4.5 pmol L⁻¹). Diiodomethane levels were elevated in open ocean waters (up to 4.2 pmol L⁻¹) and at two stations near the coast. Chloroform levels were the highest among the chlorinated compounds (surface mean of 16.9 pmol L⁻¹). Values were elevated in the upwelling between 40.5 and 42° N (up to 23.9 pmol L⁻¹) and south of 40°N. The highest chloroform concentration was recorded at the junction between upwelling and intermediate water masses at 40°N (32.5 pmol L⁻¹). Concentrations were low in the open ocean and in the filament structure.

4.3.3 SST as grouping variable

In order to evaluate VHOC distribution patterns we performed cluster analyses and a principal component analysis (PCA). The result of the PCA was used to visualize relationships among studied VHOCs and their sampling sites (Figure 18).

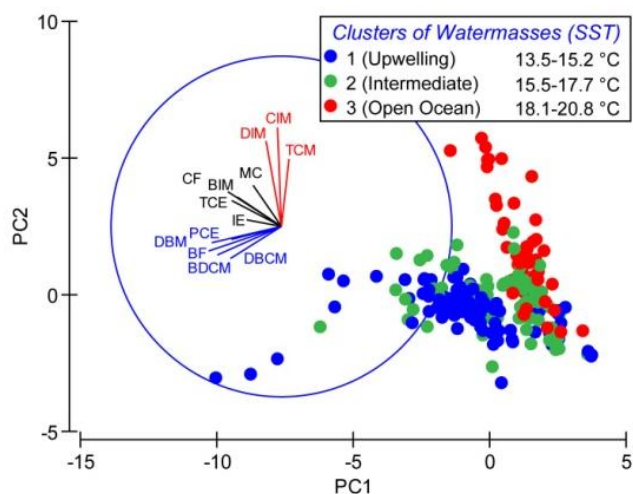


Figure 18. Principal Component Analysis (PCA) of all normalized VHOC data.

Similarities among VHOC are plotted as vectors, while similarities between the sampling sites are plotted as dots. Samples are grouped by SST-clusters. For abbreviations of VHOC see Table 10. Correlations to the principal component PC1 (x-axis) explain 32 % of the data and correlations to the principal component PC2 (y-axis) explain about 17% of all data.

Diiodomethane, chloriodomethane and tetrachloromethane are best explained by PC2 and show high similarities among themselves. Dibromomethane, bromoform, dibromochloromethane, bromodichloromethane and perchloroethene formed a second cluster, which is related to PC1. A third cluster is composed of iodoethane, bromiodomethane, 1,1,2-trichloroethene, methyl chloroform and chloroform. This group however is not well explained by the PCA model. Because of the marginal vector length of perchloroethene and tetrachloromethane, correlations to PC1 and PC2 are low.

Figure 18 illustrates clear similarities between various samples sites. Here we found that sample sites form three clusters. In order to demonstrate the underlying feature of this data spreading, we overlaid the plot with results of a cluster analysis. From the studied physical variables sea surface temperature (SST) was determined as a factor that could best explain the distribution pattern of the sampling sites. Other variables (e.g. salinity or chlorophyll a) did not reflect the clustering of the sampling sites. SST values form three clusters and reflected different water masses: The *upwelling water mass* reflect stations with a SST-mean of 14.5 °C (see also Figure 15). These stations were located were close to the coast of the Iberian Peninsula. The *Intermediate water mass* attributed stations with a SST-mean of 16.4°C. Those stations were located either close to the coast line (aged upwelled waters) or in the filament (cold waters mixed with open ocean waters). The *Open ocean water mass* featured a SST-mean of 19.7°C. All stations were located in the far off Iberian coast.

4.3.4 Relationship Between the Compounds

Similarities between VHOCs were shown in the PCA model (see Figure 18). In order to evaluate correlations in-between gases, we calculated Pearson correlations matrices. In Figure 19 we present those correlations of three representative halocarbons to all other VHOCs. Brominated compounds are well correlated among each other in all water masses. Highest correlations were found between dibromomethane and bromoform in intermediate water masses. Clear correlations between iodinated compounds were remarkable between chloriodomethane and diiodomethane in the open ocean and less articulated in intermediate water masses. In the upwelling however, no significant correlations were found among iodinated compounds. Correlations between chlorinated compounds were weak. The highest correlations were visible between methyl chloroform and chloroform in the upwelling.

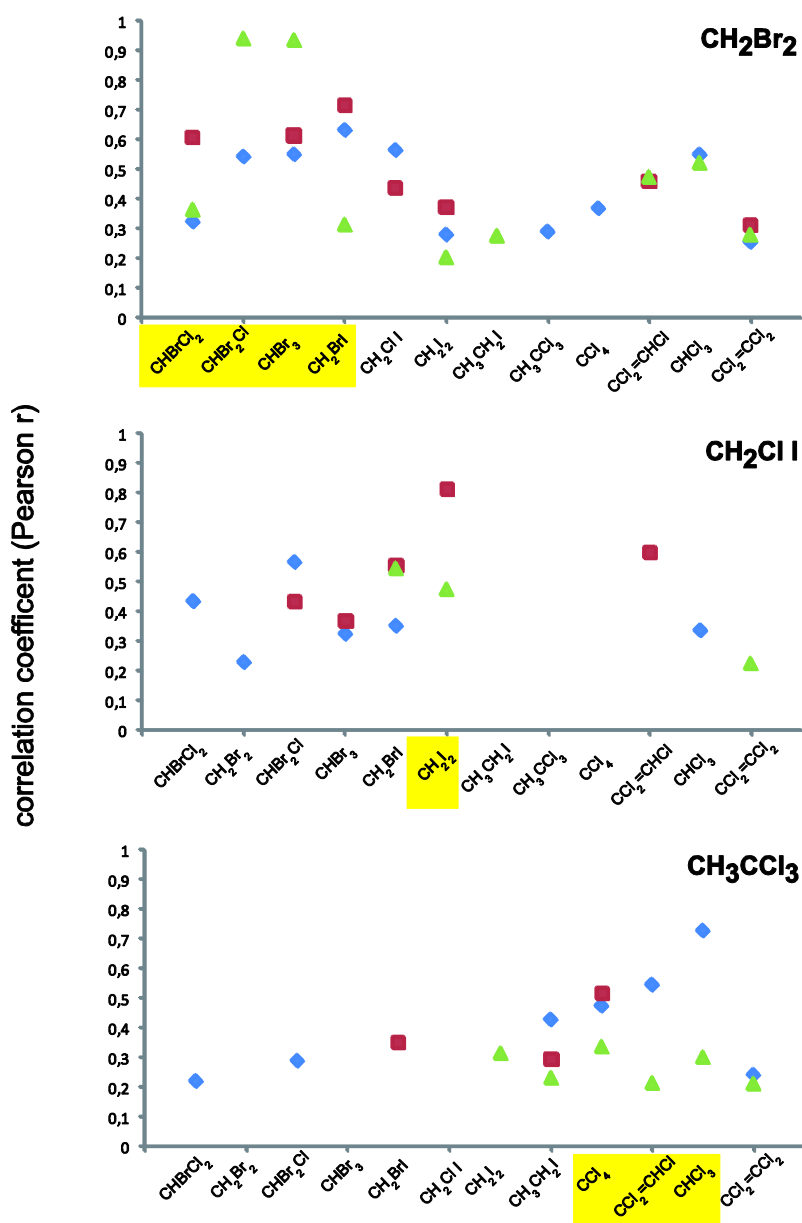


Figure 19. Correlations of selected VHOCs with all VHOCs.

Results of cross-tabulation tables of Pearson r correlation coefficients for all VHOCs. Significant level $p < 0.05$. The correlation cross table was calculated for all samples. Data are clustered in three different water masses: Upwelling (blue), intermediate water (green) and open ocean (red). Remarkable correlations are indicated in yellow.

4.3.5 Vertical distribution of VHOCs compared to environmental parameters

Based on the three water mass types (as defined above), we studied the vertical distribution of VHOCs and environmental parameters in each water mass. Figure 20 shows the distribution of

representative halocarbons and synoptic data. Sampling depth was a highly significant factor for most variables. More detailed information is given in Table 11, Table 12 and Table 13. There, VHOCs and environmental variables are grouped by different water mass and depth (mean values of all samples from surface to thermocline and samples below the thermocline).

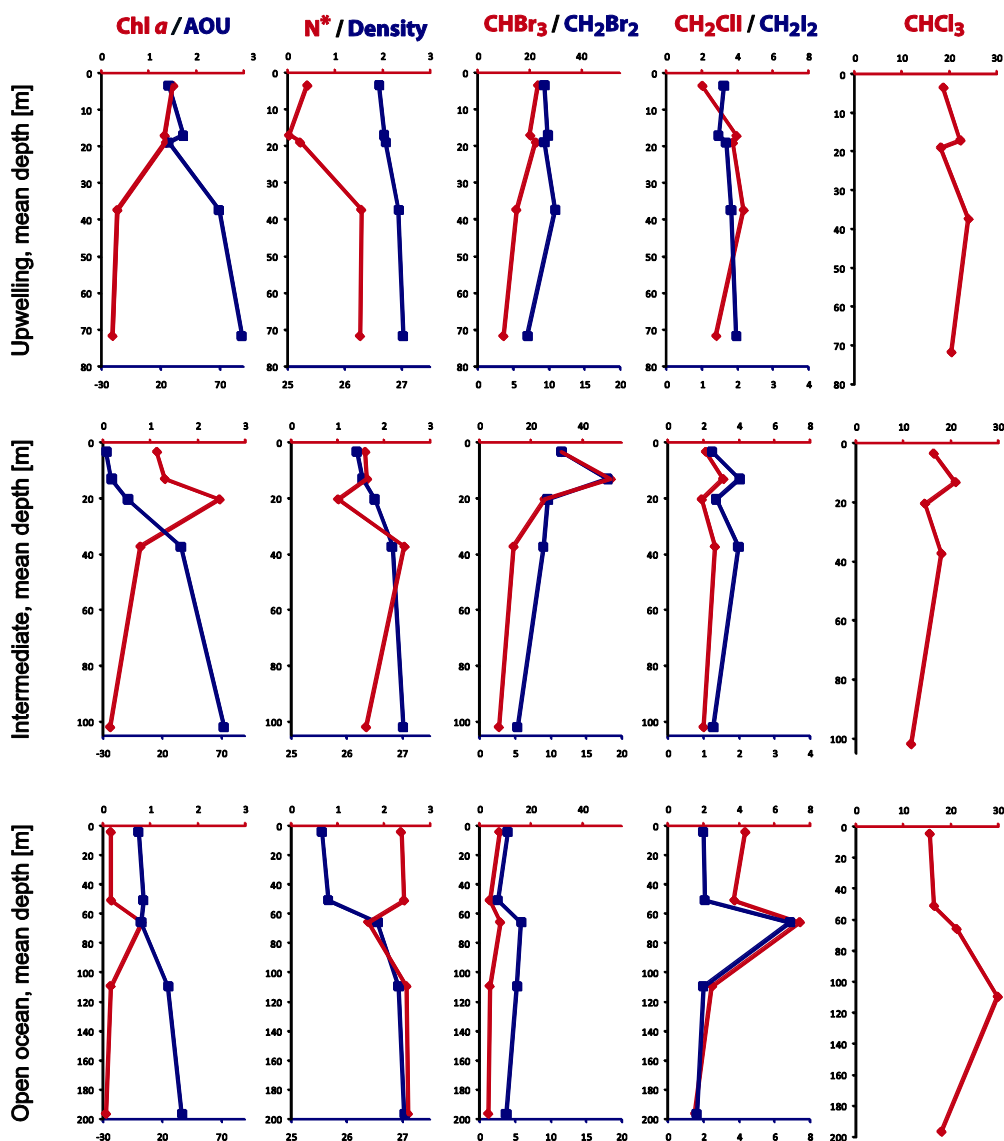


Figure 20 Depth profiles for three defined water masses.

Mean values of chlorophyll a [$\mu\text{g} \cdot \text{L}^{-1}$], AOU [$\mu\text{mol} \cdot \text{L}^{-1}$], N^* [$\mu\text{mol} \cdot \text{L}^{-1}$], density [σ] and selected VHOC [$\text{pmol} \cdot \text{L}^{-1}$] in the three defined water masses at five depth. Row 1: Upwelling waters. Row 2: Intermediate waters. Row 3: Open ocean waters. Values expressed as mean of samples of surface, upper thermocline, maximum of chlorophyll, lower thermocline and bottom. Red lines use primary x-axis (above, red). Blue lines refer to secondary x-axis (below, blue). Note: CIM concentration at open ocean province had different scale from the other provinces.

In the upwelling, σ -values showed a deep mixing without a clear pycnocline (Figure 20, row 1). Maxima of Chl-*a* were observed in the first 20 m ($1.5\mu\text{g L}^{-1}$) and reached very low values in the deeper layer below 40 m. The apparent oxygen utilisation (AOU) was negatively correlated to Chl-*a*: values were low near the surface and in the Chl-*a* maximum whereas AOU-values increased with depth. N^* (a linear combination of nitrate and phosphate; see (Gruber and Sarmiento 1997)) is a benchmark for the marine nitrogen cycle. Low N^* -values reflect a nitrate loss whereas high values indicate nitrogen fixation. In the upwelling, N^* showed the same pattern as AOU: the lowest values were found in surface waters and in the Chl-*a* maximum. Bromocarbons showed no clear peak in the water column. While dibromomethane did not vary significantly with depth, bromoform concentrations were significantly lower in the deeper layer compared to the upper layer (factor 2.4, $p=0.001$). Variations of chloriodomethane, diiodomethane and chloroform did not vary significantly with depth in the upwelling.

In the intermediate water mass (Figure 20, row2), the water column was weakly stratified (pycnocline at about 20 m). However, a clear Chl-*a* maximum was recorded at 20-m depth and corresponded to a minimum N^* -value. AOU values were significantly elevated below the pycnocline. For all gases, maximum values were measured just above the Chl *a* maximum. Values of brominated compounds were up to 6.7 times higher here compared to the deeper layer values. Iodinated compounds and chloroform showed maxima just above and below the Chl-*a* maximum. However variations of diiodomethane and chloroform did not vary significantly with depth.

In the open ocean (Figure 20, row3), the water column was clearly stratified. The pycnocline (66 m) corresponded with the Chl-*a* maximum. N^* -values were in average 1.5 times higher in the upper layers of the open ocean compared to the upper layer in the identified intermediate water mass, indicating a lower loss of nitrogen in the open ocean. At the Chl-*a* maximum however, N^* values were significantly lower, in average 1.5 times than in all other water layers. Brominated compounds showed no clear maxima throughout the water column. Concentrations were low compared to coastal waters (about 3 times lower for the surface concentrations). However, bromocarbon concentrations were significantly higher at the Chl-*a* maximum. Iodinated compounds showed maximum values at the Chl-*a* peak. Values were 2-5 times higher there compared to all other depth, and 2.7 – 3.2 times higher compared with the coastal waters.

Chloroform showed a maximum concentration below the pycnocline (2 times higher compared to surface waters).

Table 11. Mean values of 13 VHOC in pmol/L and DBM/BF- ratio in the Iberian Upwelling.

Data (n_{total} =239) grouped by sampling depth (Cluster 1: surface to maximum of chlorophyll, n=152; Cluster 2: below maximum of chlorophyll, n=87) and SST (group SST1: Upwelling, T < 15.3 ; group SST2: Intermediate, 15.4 > T < 18°C; group SST3: Open Ocean, T>18.1°C).

	Surface to Thermocline				Below Thermocline			
	Entire Data	Upwelling	Intermediate	Open Ocean	Entire Data	Upwelling	Intermediate	Open Ocean
CH ₃ CH ₂ I	1.12	1.14	1.33	0.73	0.88	1.31	0.65	0.56
CHCl ₃	17.81	19.24	16.14	18.54	18.36	21.9	13.9	20.96
CH ₃ CCl ₃	4.92	4.57	5.48	4.46	5.18	5.42	5.18	4.73
CCl ₄	5.86	3.66	6.12	8.81	3.4	2.34	3.27	5.72
C ₂ HCl ₃	8.59	8.67	8.8	8.11	7.39	8.1	7.64	5.5
CH ₂ Br ₂	9.18	9.42	11.48	4.77	6.89	8.59	6.61	4.18
CHBrCl ₂	2.44	3.45	2.51	0.76	2.28	2.98	2.34	0.8
CH ₂ ClI	2.97	2.04	2.15	5.84	1.94	1.73	2.22	1.76
CCl ₂ =CCl ₂	1.73	2.27	1.6	1.13	1.88	2.39	1.65	1.4
CHBr ₂ Cl	2.79	3.22	3.27	1.32	2.04	2.77	1.83	1.07
CH ₂ BrI	1.67	2.08	1.37	1.55	1.72	2.06	1.82	0.84
CHBr ₃	22.19	21.68	31.09	7.36	9.26	11.93	9.54	3.48
CH ₂ I ₂	2.21	1.62	1.41	4.52	1.71	1.91	1.53	1.72
CH ₂ Br ₂ /CHBr ₃	0.41	0.43	0.37	0.65	0.74	0.72	0.69	1.2

Table 12. Physical and chemical variables in the Iberian Upwelling region.

For data grouping see Table 11.

	Surface to Thermocline				Below Thermocline			
	Entire Data	Upwelling	Intermediate	Open Ocean	Entire Data	Upwelling	Intermediate	Open Ocean
SST [°C]	16.38	14.46	16.37	19.66	16.38	14.46	16.37	19.66
Salinity [PSU]	35.74	35.68	35.69	35.92	35.76	35.76	35.77	35.76
Temp [°C]	15.56	14.16	15.71	17.48	13.04	12.93	13.2	12.89
Oxygen [mL/L]	245.37	224.2	264.66	239.58	198.92	183.39	198.91	230.0
AOU [μmol L ⁻¹]	4.71	32.91	-15.43	1.18	63.99	80.14	63.16	33.73
Turbidity [NTU]	0.37	0.65	0.35	-0.01	0.12	0.16	0.14	-0.03
Nitrate [μmol/L]	3.14	7.35	1.59	0.37	10.48	12.5	10.05	8.08
Silicate [μmol/L]	1.76	3.13	1.06	1.27	4.71	5.82	4.53	3.25
Phosphate [μmol/L]	0.3	0.62	0.19	0.08	0.72	0.86	0.69	0.53
N* [μmol/L]	1.14	0.19	1.34	2.07	1.89	1.57	1.85	2.52

Table 13. Mean values of marker pigments in the Iberian Upwelling region.

For data grouping see Table 11.

	Surface to Thermocline				Below Thermocline			
	Entire Data	Upwelling	Intermediate	Open Ocean	Entire Data	Upwelling	Intermediate	Open Ocean
chla	1466.93	1774.72	1584.17	577.78	457.66	550.0	426.88	no data
chlb	115.21	101.82	122.25	111.39	33.94	30.13	35.21	no data
chlc2	172.1	233.48	178.96	52.61	42.09	72.25	32.04	no data
chlc3	100.14	90.95	112.52	71.11	38.19	43.63	36.38	no data
fuco	708.24	907.86	797.26	86.17	251.38	329.13	225.46	no data
but	35.15	18.8	35.71	58.67	9.56	8.63	9.88	no data
perid	83.48	87.71	96.76	30.44	28.63	29.38	28.38	no data
hex	114.37	64.1	117.06	183.17	27.5	11.63	32.79	no data
diadino	96.82	102.12	113.93	28.67	30.5	34.13	29.29	no data
allo	20.01	21.7	22.92	7.17	6.38	12.88	4.21	no data
lut	11.24	12.68	13.73	0.28	5.69	1.88	6.96	no data
zea	44.33	32.9	40.55	75.33	7.81	7.75	7.83	no data
caro	40.93	52.34	42.78	16.72	10.88	6.38	12.38	no data

4.3.6 Temporal and tide factors in the upper layers

Diurnal and tidal variations of VHOC concentrations were investigated by calculating ANOVAs of all samples taken in the upper layers (sea surface to thermocline). Again, the data set was divided into the three different water masses.

In order to investigate the factor time, samples were sorted by the sampling time and divided in four groups: night, day, and intermediates. All samples taken in between 2h after sunset and 2h before sunrise were defined as “night samples”. All samples taken in between 2h after sunrise and 2h before sunset were defined as “day samples”. Intermediate times were defines as morning or evening samples. Results of the ANOVAs indicate that the factor time has significant effects (Figure 21) on bromocarbons. In the upwelling, values were significantly higher after sunset (factor 1.5 to 1.8; p-values between 0.002 and 0.055) and stayed rather low during the rest of the day. Intermediate waters showed higher concentrations between dusk and night, compared to the period between dawn and daytime (factor 1.8 to 2.1). Diurnal variations of bromocarbons in the open ocean were less clear. Variances for dibromomethane and dibromochloromethane are small (factor 1.1 and 1.2) and statistically not significant. Bromoform however showed a significantly elevated concentration during night-time (factor 2, p = 0,05). Time of the day showed no significant influence on iodocarbons and chloroform (data not shown).

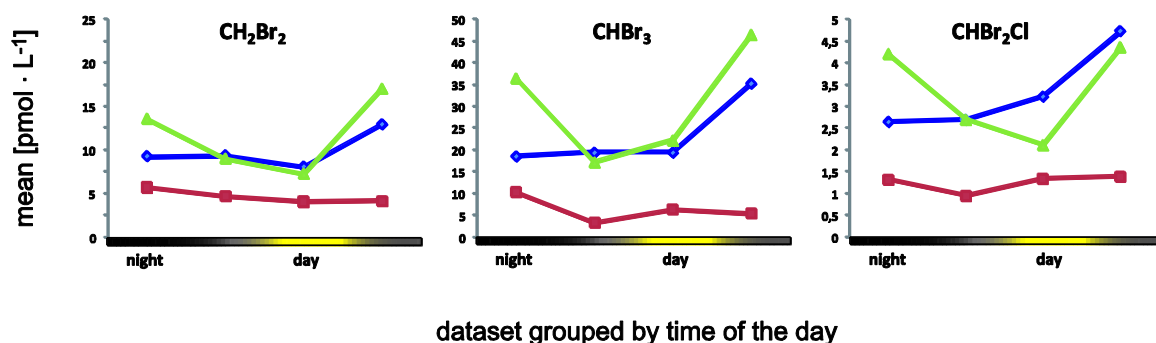


Figure 21. Influence of time of the day to bromocarbons.

Mean values of four different times of the day (night, day, and intermediates) for samples from the surface to the thermocline. Night and day were defined as two hours before sunrise and sunset, respectively.

In order to investigate the factor tide, samples were sorted by the sampling time and divided in four groups: high tide, low tide, incoming mid tide and outgoing mid tide. Sampling times were compared with tide tables, provides by SHOM (*Service hydrographique et océanographique de la marine*) for different places along the Iberian coast. Figure 22 illustrates clear effects of tide on VHOC levels within the upwelling. Upwelling values of brominated compounds were significantly elevated when water flowed back from the coast to the open ocean. In intermediate water masses the effect is still noticeable but statistically less significant. Similarly to brominated compounds chloroform and iodinated compounds showed elevated concentrations in the upwelling during the outgoing tide. In intermediate water masses however, values of chloriodomethane and diiodomethane were significantly elevated at incoming tide. Generally, in intermediate water masses, effects are noticeable and are not significant in the open ocean.

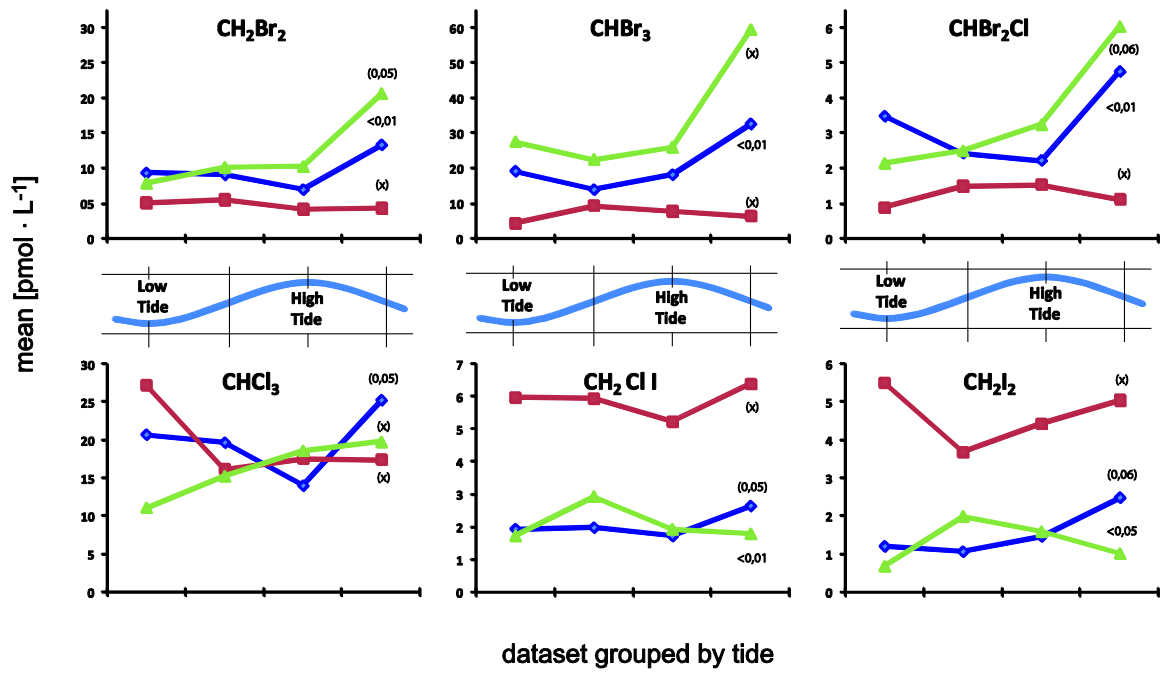


Figure 22. Influence of tide to selected VHOCs in the upper layers.

Blue lines: in the upwelling. Green lines: intermediate waters. Red line: open ocean. Mean- and p-values are plotted against four tidal steps (low tide, incoming mid tide, high tide, outgoing mid tide). Non-significant effects are expressed as (x). Significant levels are expressed in parentheses (p-values).

4.4 Discussion

This is the first study of volatile halogenated organic compounds in the Iberian Upwelling, and presents a comprehensive number of brominated, iodinated and chlorinated volatiles in an upwelling system. Our data show that multivariate effects are causal for the distributions of VHOCs. Here we present evidence for different VHOCs sources, which are each causal for the production of a certain group of VHOCs. This study demonstrates for the first time the effect of tide on VHOCs distribution.

4.4.1 Comparison to other studies

Although a wide range of marine regions were investigated for VHOC levels, only a few studies focused on upwelling regions: Class and Ballschmiter (1988) measured bromocarbons and tetrachloromethane near the West African coast (25°N 16°W). The Mauritanian Upwelling was investigated by Quack et al. (2007b) between 17.0 and 20.5 °N in April/March 2005 and by Carpenter et al. (2009) between 16 and 35°N in May/June 2007. Both studies were focused on bromoform and dibromomethane and found similar mean values (see Table 14).

Our values however, were about a factor 2 higher than data reported for the Mauritanian Upwelling, and were rather similar to coastal water values reported for the African Upwelling.

The only study which studied various VHOC along the Iberian Peninsula, were restricted to the shoreline and did not measured in the upwelling(Martinez et al. 2002b). These authors focused on monitoring different anthropogenically produced VHOCs and reported results as class distribution and maximum values. Consequently these results give a broad representation for nonnatural coastal inputs of chlorinated volatiles but are less comparable to our results.

Table 14. Comparison of VHOC concentrations in different regions.

Mean values in pmol · L⁻¹.

	African Coastal Upwelling	Mauritanian Upwelling	African Coastal Upwelling	North Atlantic	east Atlantic	English Channel	Irish Sea	Antarctic waters	Portugal coast
	25°N 16°W (03/1985)	17-20.5°N 16-19°W (04-05/2005)	16-35°N 14-24°W (05-06/2007)	53-59°N 7-13°W (06-07/2006)		50°N 4°W (2002-2004)	53°N 4°W (2004-2005)	70-72°S 9-11°W (12/2003)	(1999-2000)
	Class and Ballschmiter 1988	Quack et al. 2007	Carpenter et al. 2009			Archer et al. 2007	Bravo-Linares and Mudge 2009	Carpenter et al. 2007	Martinez et al. 2002
CH ₃ CH ₂ I						1.5	^f 9.5	^g	
CHCl ₃							141.77	^g	167.53 ^x
CH ₃ CCl ₃							0.92	^g	12.22
CCl ₄	6.5	^a					3.4	^g	117 ^x
C ₂ HCl ₃							2.64	^g	98.94 ^x
CH ₂ Br ₂	5.77	^a 4.9	^a 3.4	^c 1.1	^e		5.45	^g	
		5.8	^b 3	^d 1.9	^f				
			1.4	^e 15.6	^g				
CHBrCl ₂	6.1	^a					5.06	^g	
CH ₂ ClI						10.8	^f 0.91	^g 0.7	^g
CCl ₂ =CCl ₂							13.13	^g	78.41 ^x
CHBr ₂ Cl	9.6	^a					17.3	^g	
CH ₂ BrI						1.2	^f	0.8	^g
CHBr ₃	23.74	^a 10.7	^a 11.5	^c 3.4	^e		214.23	^g 56.7	^g
		9	^b 14.4	^d 6.7	^f				
			3.5	^e 68.3	^g				
CH ₂ I ₂						2.5	^f 2.71	^g 4.2	^g

* ^a depth 0-12m; ^b depth 14-50m; ^c upwelling; ^d Canaries; ^e open ocean; ^f shelf and far coast; ^g coastal; ^x coastal and river, not specified, maximum values.

Based on various oceanic data, production of VHOCs has highly localized sources. Saturations are highest in littoral zones, mainly in macro-algae beds. Furthermore, seawater concentrations vary greatly with seasons (Archer et al. 2007) and hence comparisons of different studies might be challenging. Contrary to the assumptions of a strong phytoplankton production in upwelling regions, we report values intermediate between coastal and open ocean values.

4.4.2 On the different origin of VHOCs

Results from the principal component analysis (see Figure 18) showed similarities between three sample sites and between VHOCs. It was shown that sample sites cluster in three groups:

upwelling, intermediate water masses, and open ocean. Moreover we showed high similarities between VHOCs indicating similar sources for three different groups: (1) bromocarbons, (2) two iodocarbons (chloriodomethane and diiodomethane) and (3) the remaining VHOCs (mostly chlorocarbons).

Similarities between VHOCs (Figure 18) and correlations among them (Figure 19) indicated common sources for brominated compounds. Highest correlations between brominated compounds (see Figure 19, row 1) were recorded in samples with the highest concentrations (intermediate water masses). In intermediate water masses correlations to other gases were not significant or negligibly low. Hence for this region it can be assumed that bromoform, dibromomethane and dibromochloromethane do have the same origin. Contrary to intermediate water masses, correlations between brominated compounds were less pronounced in the open ocean and the upwelling. Thus an additional and more compound-specific source (and/or sink) can be assumed for both water masses.

Dibromomethane/bromoform ratios were calculated by several authors (Carpenter and Liss 2000; Quack et al. 2007b; Carpenter et al. 2009; Jones et al. 2009). Dibromomethane/bromoform slopes were found to be lower in coastal regions and are caused by different sources: macroalgae-produced bromocarbons cause a lower slope whereas slopes are higher in phytoplankton-dominated regions. Our results supported these findings (Table 11).

Iodocarbons (Figure 19, row 2) show clear correlations among each other: the highest correlation was observed between chloriodomethane and diiodomethane in open ocean waters, a region where the highest concentrations were measured for both gases. Hence both halocarbons do have the same origin and this origin is located in the open ocean. In a recent study it was shown that both compounds can be formed in the presence of dissolved iodine, dissolved organic matter and ozone (Martino et al. 2009).

The correlations of chlorocarbons (Figure 19, row 3) did not show clear patterns. For example, we present correlations of methyl chloroform to all other VHOCs. The highest correlations (methyl chloroform and chloroform) were observed in the upwelling whereas just one significant correlation was observed in the open ocean. Consequently, a common source for chlorinated

volatiles might be connected to the shoreline. Martinez et al. (2002b) reported a high coastal input of anthropogenic chlorocarbons at several places in Portugal.

4.4.3 Evidence for phytoplanktonic production of VHOCs

Correlations between different VHOC groups and chlorophyll (fluorescence sensor) were found for brominated and iodinated compounds (see Figure 23). Moreover, we found a good correlation between both VHOC groups and both biological markers N* and AOU. These correlations were clearly visible for the open ocean and less pronounced in the upwelling or in intermediate water masses. These results indicate that the formation of brominated and iodinated compounds was usually coupled to photosynthetically produced oxygen and nitrogen loss; both caused by phytoplankton activity. The absence of strong correlations in the upwelling and intermediate water could have two explanations: either the main source for brominated and iodinated compounds was non-biological or, and more likely, the formation of those compounds was locally separated. Main sources of bromo- and iodocarbons are likely coastal zones of the Iberian Peninsula. Water masses are transported westwards containing elevated concentrations of those compounds.

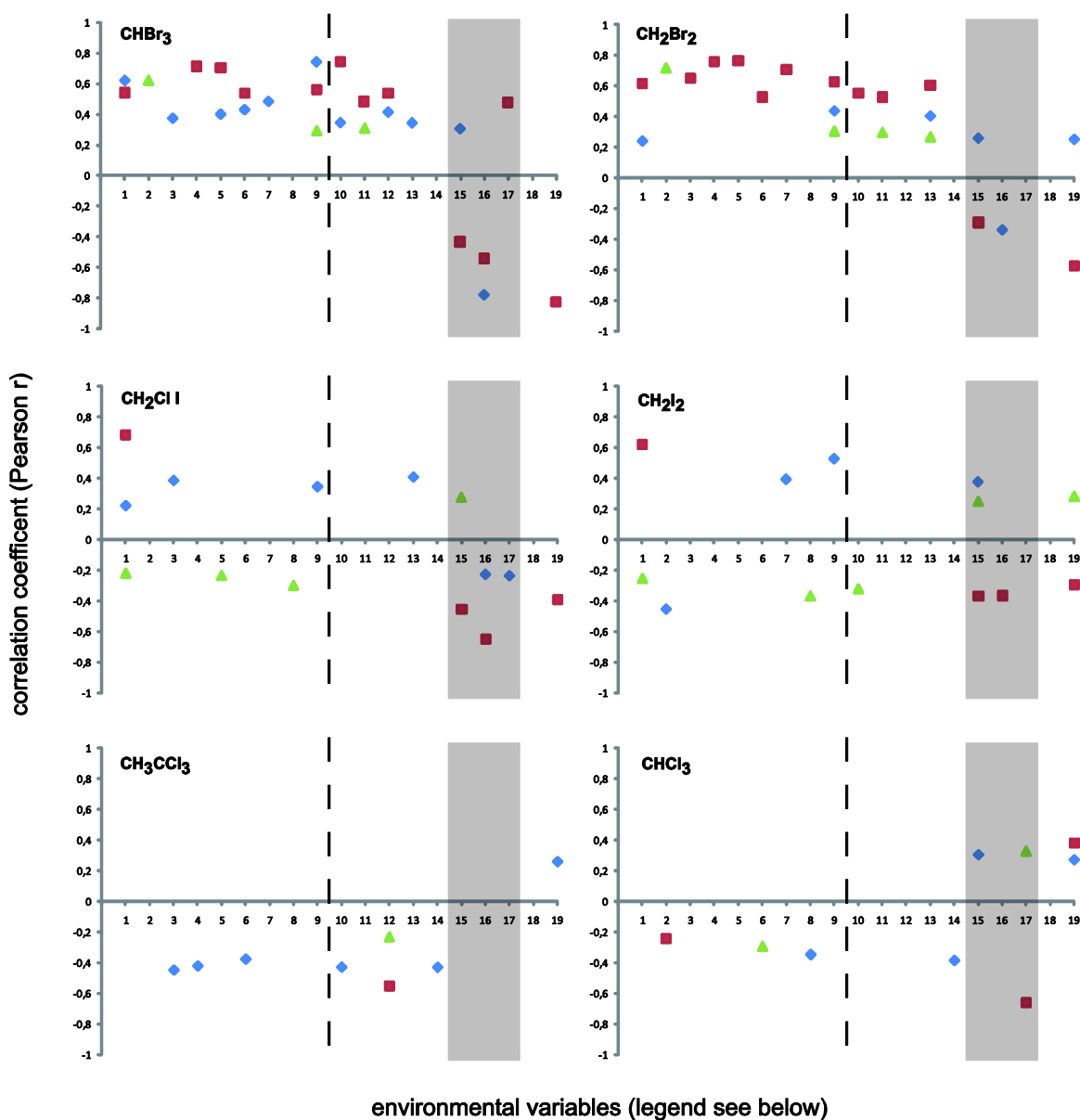


Figure 23. Correlations of selected VHOCs with environmental variables.

Results of cross-tabulation tables of Pearson r correlation coefficients for selected VHOCs and environmental variables. Data are clustered into three provinces: Upwelling (blue), Mixed water (green) and Open Ocean (red). Dashed line separate photosynthetic pigments and photoprotective pigments. Grey marks other biological marker. Variables 1-9: photosynthetic pigments (fluorimeter, chl a, chl b, chl c2, chl c3, fuco, but, per, hex). Variables 10-14: photoprotective pigments (diadino, allo, lut, zea, caro). Variables 15-17: N^* , AOU, CDOM. Variables 18-19: PAR, lighttransmission.

Correlations to various marker pigments were strong for brominated compounds mainly in the open ocean (Figure 23). Bromoform showed additionally weak correlations in the upwelling. The diversity of correlated pigments emphasise the involvement of different phytoplankton groups in the formation of bromocarbons. Fucoxanthin (Diatoms), Chl-*b* (green algae and prochlorophytes) as well as hexaxanthin and Chl-*c3* (prymnesiophytes) showed the highest correlations to bromocarbons.

Iodinated compounds did not correlate to marker pigments in samples with high iodocarbons concentrations (open ocean waters). Weak correlations to Chl-*b* (linked to prochlorophytes) and hex were observed in the upwelling. Chloriodomethane and diiodomethane likely have a biological origin, since they often correlate with biological markers (fluorescence, N* and AOU). Since phytoplankton is likely not a source for iodocarbons and at the same time N* and AOU correlations suggest a biological origin, it can be assumed, that bacteria are involved in the formation of those VHOCs. This assumption is in agreement with results by (Amachi 2005) who showed formation of both iodinated compounds by distinct groups of marine bacteria. As mentioned above, both iodocarbons might have additionally natural but non-biological sources (Martino et al. 2009).

Sun radiation (here expressed as PAR) did not correlate with the measured VHOC in any region. Thus a hypothesis of photolytic formation of iodinated compounds might be only a minor source. Light transmission values correlate negatively with bromoform, dibromomethane, chloriodomethane and diiodomethane in the open ocean. Since plankton has a negative effect on light transmission, plankton abundance may be the cause for elevated bromo- and iodocarbon concentrations.

Chlorinated compounds did not correlate to biological markers (Chl-*a*, N* or AOU). Correlations to marker pigments were weak or negative. Hence it can be assumed that main sources of chlorocarbons are of non-biological origin.

According to all correlations, brominated compounds were produced by microalgae in the open ocean. In the upwelling and in intermediate water masses this formation pathway is masked by strong external sources. Iodocarbons seem to have a bacterial origin and are mainly produced in the open ocean. Due to higher coastal concentrations and missing correlations to biological

markers, the main source of chlorinated compounds might be anthropogenic in origin. Since no correlation to radiation exposure were observed, photochemical formation might be a minor source for VHOC in the Iberian upwelling.

4.4.4 Near shore production: main source for brominated compounds in the upwelling?

We found the highest concentrations of bromocarbons in near-shore samples. This finding is in agreement with other studies. Carpenter et al. (2009) found a concentrations gradient in the order coastal region > upwelling > shelf > open ocean. We found lower dibromomethane/bromoform-ratios in near shore waters compared to oceanic waters. A different bromocarbon origin (phytoplankton dominated in open ocean and macroalgae dominated near coast) might be a reason for different ratios.

This is the first study which highlighted the influence of tide to offshore VHOC concentrations. We found strong effects for polybrominated compounds in the upwelling and no effects in the open ocean. Since concentrations are elevated with outgoing tide, it can be assumed that enriched waters are transported westwards thus highlighting the effect of tide on VHOC distribution. Hence, high near shore concentrations can be explained by a translocated macroalgae production.

In the Iberian area elevated concentrations of brominated compounds in the upwelling might be due to near shore production transported westward via a combination of tide and Ekman transport whereas open ocean concentrations could be explained by phytoplankton.

The effect of tide and lateral transport to iodinated compounds is weak and unclear. Concentrations are elevated at outgoing midtide in the upwelling and at incoming midtide in the intermediate waters. In the open ocean no statistically significant effect was observed. Thus the production of iodocarbons is less restricted to the coast and a phytoplankton production off shore can be assumed.

Our results show increased bromocarbon concentration after sunset and comparable low concentrations after sunrise. Generally halocarbons are reported to show elevated concentrations with an increase of irradiance (Ekdahl et al. 1998; Marshall et al. 1999; Wang et al. 2009). Since we assume that brominated compounds in the upwelling have a coastal source, it is likely that irradiance increased coastal macroalgae production.

4.5 Conclusion

Water samples taken in the Iberian Peninsula Upwelling System revealed that spatial distribution of halocarbons are related to sea surface temperature. Variations in sea surface temperatures can be explained by convections and advection processes; two typical processes in upwelling systems.

Statistical methods showed distinct similarities between three different clusters of VHOCs. In those clusters were usually halocarbons with the same halogens (bromocarbons, iodocarbons and chlorocarbons). Those groups were reflected in correlations patterns between VHOCs and environmental variables. Typical correlation patterns indicated that bromocarbons might have a phytoplanktonic source in the open ocean. Iodocarbons showed correlation patterns which were discussed to indicate a bacteria-related source in the open ocean. This idea is supported by the fact, that highest concentrations of iodocarbons were found off shore.

Furthermore it was shown that bromocarbon concentrations of near shore water samples were elevated several hours after high tide. This fact and the observed concentration gradient (lower values towards the open ocean) led us concludes, that the main source of bromocarbons is located in the upwelling and that water masses with elevated bromocarbon concentrations are translocated westwards .

The postulated high concentrations of VHOCs were not found during the campaign. In the upwelling, only weak correlations with marker pigments for phytoplankton were encountered. Hence we reject the idea that upwelling regions might be hot spots for VHOC formation due to diatoms. However the upwelling induced nutrient supply might have some effects on shore line macroalgae beds. We suggest that further studies between the shore line and the upwelling might contribute to a better understanding of sources within the upwelling areas.

5 Annual distribution of reactive halocarbons in a tide influenced estuary: Exchange fluxes between ocean and atmosphere

5.1 Introduction

The implications of halocarbons for atmospheric chemistry and their ozone depleting potential are discussed in the chapters above. Main source of short-lived reactive iodocarbons and bromocarbons are macroalgae. While iodocarbons are photolabile and broken down rapidly within the troposphere, bromocarbons are relatively photostable. These longer lives trace gases can be convected to the lower stratosphere and contribute up to 60% of stratospheric bromine (Sturges et al. 2000; Nielsen and Douglass 2001). Macroalgae release halocarbons at low tide directly to the atmosphere or influence atmospheric mixing ratios via air-sea exchange in the marine boundary layer (Carpenter et al. 1999).

Since macroalgae propagation is restricted to rocky shores, marine sources of VHOCs are highly localized. High concentrations can be found near coast, while open ocean concentrations are usually low. Consequently littoral zones are hot spots for halocarbons and are essential for global emission estimates. Several authors extrapolated local fluxes at large scale to attempt a global estimate of these fluxes (e.g. Moore and Groszko 1999; Quack and Wallace 2003; Butler et al. 2007). However those calculations remain uncertain because of the low temporal and spatial coverage of VHOC measurements.

Consequently, better global budget estimations can be achieved by high resolution measurements of VHOCs in hot spots of VHOC formation. Air and water concentrations were studied at various spots around the world, including:

- African coast and the Mauretaniien Upwelling (Class and Ballschmitter 1988; Quack et al. 2007a; Quack et al. 2007b; Carpenter et al. 2009),
- around the British Islands and the English Channel (Dawes and Waldock 1994; Nightingale et al. 1995; Carpenter et al. 1999; Carpenter et al. 2000; Archer et al. 2007; Bravo-Linares and Mudge 2009; Jones et al. 2009),
- in Californian coastal waters and salt marshes (Manley et al. 1992; Manley et al. 2006),

- in the North Sea (Klick 1992; Abrahamsson and Ekdahl 1996; Baker et al. 1999),
- in European estuaries (Christof et al. 2002),
- in a rock pool at Gran Canaria (Ekdahl et al. 1998),
- in the Pacific and Atlantic open ocean (Blake et al. 1997; Quack and Suess 1999; Nightingale et al. 2000a; Chuck et al. 2005; Wang et al. 2009),
- in Polar regions and the Southern ocean (Schall and Heumann 1993; Abrahamsson et al. 2004; Carpenter et al. 2007) and
- Iberian Peninsula waters (Martinez et al. 2002b, this work see chapter 5).

A comprehensive overview about published air and sea concentrations of halocarbons are given by Quack and Wallace (2003). Some studies reported seasonal variations of halocarbon concentrations (Blake et al. 1997; Carpenter et al. 2005; Tokarczyk and Moore 2006; Archer et al. 2007; MacDonald and Moore 2007; Hughes et al. 2009; Wang et al. 2009). However, the role of tidal influenced and nutrient enriched estuaries on VHOC distribution has been poorly explored. Some studies reported elevated halocarbon emissions during low tide in macroalgae beds (e.g. Pedersen et al. 1996). The authors attributed those findings to oxidative stress for the macroalgae. Therefore it can be assumed that tidal influenced coastal areas are characterized by elevated concentrations of iodocarbons and bromocarbons. River discharge creates large salinity and nutrient gradients in an estuary, those gradients have a great influence on species composition. Elevated nutrient levels for instance can stimulate the growth of macroalgae. At the same time a nutrient oversupply elevates the phyto- and bacterioplankton biomass production. As a consequence of this fact and together with high levels of suspended matter, photosynthetically active photon flux density (PFD) is decreased in highly productive estuaries. As a result macroalgae are outcompeted by phyto- and bacterioplankton with their high turn-over rates.

The present study contributes to a better global VHOC estimates by providing data for a poorly investigated halocarbon hotspot. The annual distribution of VHOCs was determined in a highly productive marine area in temperated coastal ecosystem in Western Europe.

In the following paragraphs data are presented and discussed showing a marked seasonality and high correlating to the sampling site. Fluxes to the atmosphere are calculated. Moreover we show results from a separate field campaign during a diurnal tidal cycle.

5.2 Methods

5.2.1 Sampling area

The sampling area was located in a region with one of the world highest tidal amplitudes (mega-tidal system). Samples were taken between May 2008 and May 2009 in the *Bay of Morlaix* at the south-western coast of the English Channel. Figure 24 show the sampling sites in a chart datum map.

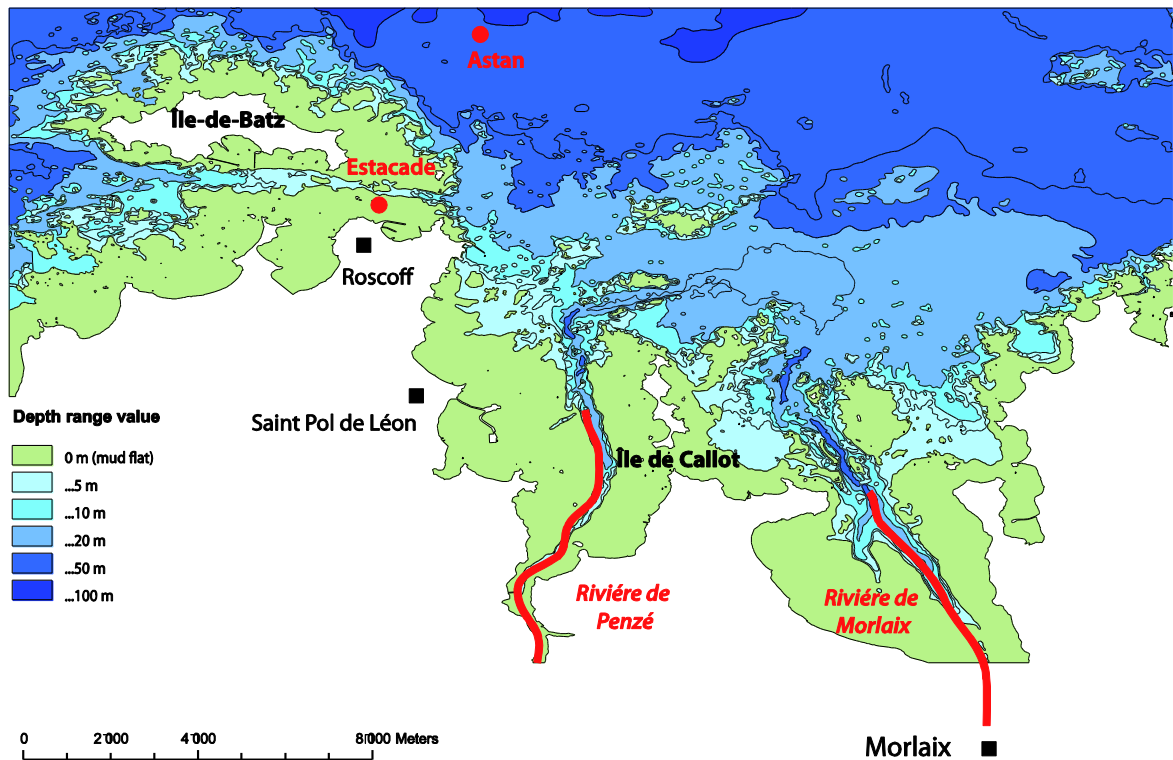


Figure 24. Chart datum map of the sampling area.

Sampling position in the river was based on the salinity. The sampling sites cover an area from 48°36' to 48.45°N and 3°50' to 3°58' W. (© SHOM contract no 178/2008).

It appears clearly from the map that large areas are exposed to the atmosphere at low tide during spring tide, when the tidal amplitude reaches 7.5 m. While the northern parts of the bay and around Batz island (*Île de Batz*) are predominated by high cover rates of macroalgae, the inner

parts of the bay are characterized by mudflats. Algal cover there is less pronounced and restricted to mainly *Fucaceae*.

Two rivers flow into the *Bay of Morlaix* estuary: the *Morlaix River* forms the eastern part of the estuary and has a north eastern branch (named *Le Dourduff*). On the western side of the estuary, the *Penzé River* discharge fresh water into the bay. The catchment areas of both rivers are characterized by high productive agriculture and a low localization degree of industry. As a result of intensive farming, the drainage basin discharge high amounts of nutrients to the estuary.

The climate has an influence on species composition and thereby an influence on potential halocarbon producer. The northern Breton coast is located in the temperate zone. Its climate is characterized by the Gulf Stream and the Westerlies with predominant south-westerly winds, low temperature amplitudes and an annual precipitation of about 650 mm. The climate is favourable for a great diversity in macroalgae species.

5.2.2 Sampling strategy

Samples were taken at neap tide at the *Penzé River*, the *Morlaix River* and the *ASTAN* point. The amplitude is 3.6 m during mean neap tide at Roscoff. Figure 25 shows the sampling during the field campaign from May 2008 to Mai 2009.

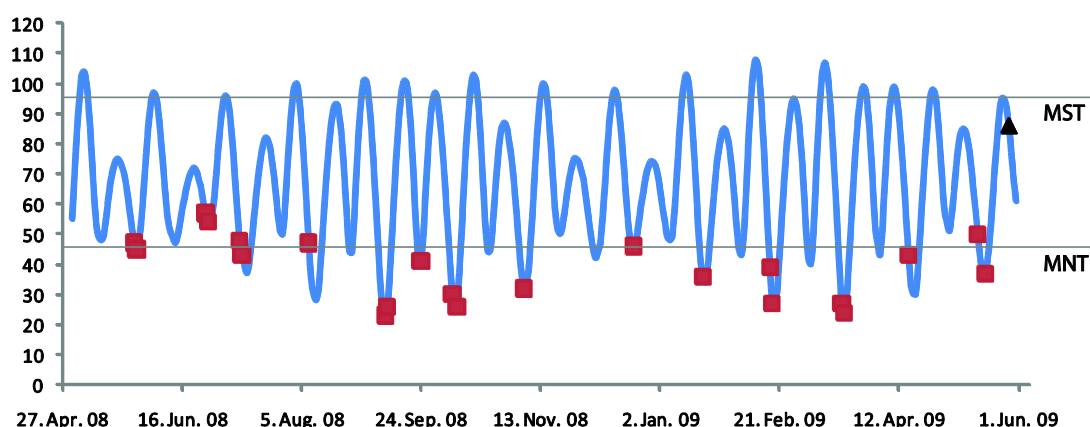


Figure 25. Tidal amplitude [expressed as tidal coefficient] and sampling strategy.

MST= mean spring tide (tidal coefficient of 95). MNT = mean neap tide (tidal coefficient of 45). Samples were taken at neap tide in the Bay of Morlaix (red square). A 24-h station was probed at spring tide.

Sampling took place at low tide in the inner part of the bay in order to minimize the mixing with incoming saltwater and was conducted with an inflatable motor vessel. Sampling always started at the point of highest salinity and thereafter followed the salinity gradient upstream. Sampling stations were predefined by salinity (2, 5, 10, 13, 17, 22, 27 and 33 PSU). Thus geographical positions changed at any sampling time. The lower salinity stations (2-17 PSU) were always located within the *Penzé River*.

Salinity, water temperature and geographical position were determined on board. Surface water was sampled with a Niskin bottle. Samples were taken for nutrient and pigment analysis (Chlorophyll *a* and phaeopigments). Additionally water was probed for high precision salinity determination. Air and water samples for VHOC determination were taken using the sampling devices described in paragraph 3.8.

The *ASTAN* point (oceanic waters, 35 PSU) was sampled on board the research vessels *Mysis* and *Neomysis*, at high tide during neap tide. Water masses at this point are characterized by intense currents. Those water masses sloshing between this point and the inner part of the estuary. High tide water masses are constantly translocated between the Channel and the inner part of the Bay.

During a separate field campaign at the *Estacade* point, samples were taken every two hours at spring tide over the course of a complete diurnal tidal cycle, at spring tide. The tidal amplitude was 7.5 m at the sampling site. Sampling at spring tide provides two advantages. Firstly, the studied factor (tide) was highly pronounced. Secondly, during spring tide the low tide occurs during noon. This provided the opportunity to study the effect of sun radiation for the formation of VHOCs.

5.2.3 Methods for physical, chemical and biological variables

Meteorological data

The measurements of the meteorological parameters were carried out with automated sensors located on the roof of the *Station Biologique de Roscoff*. The following parameters were determined:

- air temperature (Campbell sci., model HMP45C; precision: $\pm 0.2^\circ\text{C}$)
- atmospheric humidity (same sensor; precision: $\pm 1\%$ at 20°C)

- atmospheric pressure (Setra, model CS100; precision: ± 1 mbar)
- photosynthetically active photon flux density (400-700 nm; Quantum, model SKP215 SKYE; precision: $\pm 3\%$)
- wind velocity and direction (RM Young, model 05103; precision: $\pm 0.3 \text{ m} \cdot \text{s}^{-1}$ and $\pm 3^\circ$ at common wind conditions)

The sampling rate was 2 seconds; average values were automatically calculated for 15 and 60 minutes intervals. For wind velocity maxima values were determined for every 15 minutes interval.

SST, salinity, oxygen and suspended matter

Sea surface temperatures (SST) were determined onboard the research vessel. Water samples were taken for determination of salinity, oxygen and suspended matter. Measurements for dissolved oxygen were carried out by Winkler method. Suspended matter was determined by gravimetric analysis of the filter cake. High precision salinities measurements were carried out using a Guidline Portasal salinometer with a precision of ± 0.002 PSU, samples were analysed at the *Laboratoire de Chimie Océanographique de l'EPSHOM*, Brest.

Determination of nutrients

Samples were taken in 125 ml polyethylene bottles, pre-treated with hydrochloric acid and deionised water, and finally rinsed with the sea water to analyse. These bottles have been kept at -20°C in darkness until the analysis were carried out. For nutrient analysis a semi-automated system was used (TECHNICON, autoanalyser II). The following nutrients were determined:

- Silicic acid (Si(OH)_4): following the protocol of Fanning and Pilson (1973).
- Nitrate (NO_3^-) and nitrite (NO_2^-): as described by Bendschneider and Robinson (1952) and Wood et al. (1967). Firstly, nitrite concentrations were determined. Then, nitrate was reduced to nitrite and finally the nitrite concentration was measured. The difference between both gives the nitrates concentration.
- Phosphate (PO_4^{3-}): as defined by Murphy and Riley (1962).

Pigment analysis

Samples were kept in opaque nalgene bottles. A defined sample volume – depending of the particle load of the sample – was filtered passing a glass fibre filter (GF/F, whatman) at 0.2 bar low-pressure. Filters were kept at -20°C until the final analysis. Pigments were extracted by solid-liquid extraction with an acetone-water solution. Chlorophyll a and phaeopigment analysis was carried out following the protocol of Yentsch and Menzel (1963).

5.2.4 VHOC measurements

Volatile halogenated organic compounds were analysed using a purge-and-trap technique and GC-ECD (Chrompack CP 9000).

Volatiles were extracted from water samples by purging with ultra-pure helium for 20 min at a flow of $90 \cdot \text{ml min}^{-1}$. Purging took place at ambient temperature in a purge chamber. The vector gas formed minuscule froth bubbles after passing a glass frit (Pyrex 4). Air samples were purged for 80 minutes. The gas flow was dried downstream using a condenser (held at 2 °C) and a magnesium perchlorate trap.

Volatiles were concentrated by cryofocussing (-120°C), using a glass tube filled with glass beads. The trap was kept in a Dewar vessel. Low temperature were achieved by mixing liquid nitrogen with crude industrial glass beads. Volatiles were injected by thermodesorption (100°C, backflush). Several techniques were tested (electric resistance heater, heat guns etc). However boiling water showed best injection results.

Separation of the compounds was performed using a capillary column (fused silica megabore DB-624, 75 m, 0.53 mm id, 3 mm film thickness, J & W Scientific, flow: 6 ml min^{-1}) and a temperature program (10 min at 70°C, rising for 8 min to 150°C and stable for 7 min at 150°C). Quantification of volatiles was executed by external liquid standards (Carlo Erba, $1000 \text{ pg} \cdot \text{ml}^{-1}$). Detailed information are given in paragraph 3.8.

5.3 Results

5.3.1 Meteorological variables

The temperate climate determines meteorological variables. Air temperature and photosynthetically active photon flux density (PFD) are given in Figure 26. Both variables show a strong seasonality. Lowest daily mean air temperatures were observed in January (5.1 °C), while highest temperatures were measured in July and August (max: 18.1°C). The influence of the Gulf stream lowers the annual air temperature amplitude.

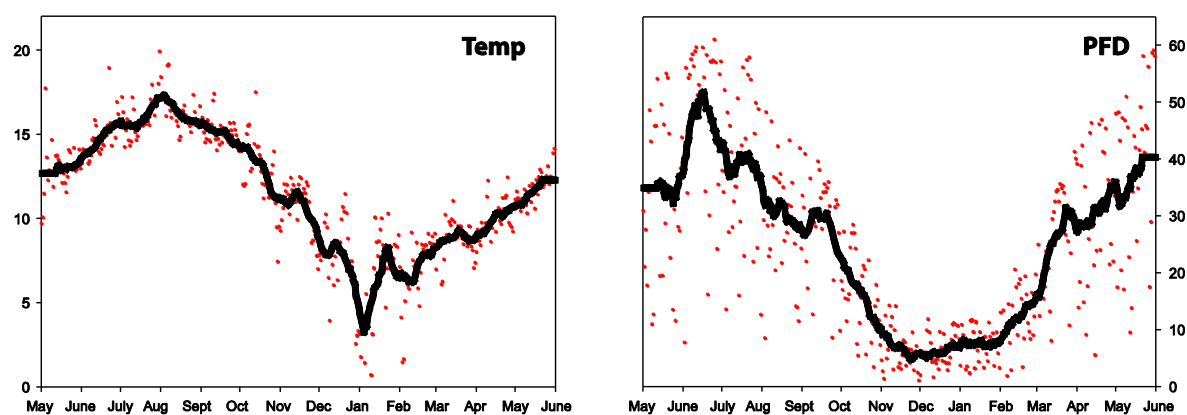


Figure 26. Air temperature and sun radiation at Roscoff between May 2008 and end of May 2009.

Red dots: Temperature given as daily mean [°C]. Photosynthetically Active Photon Flux Density (PFD) given as daily sum [$\text{mol photons} \cdot \text{m}^{-2} \cdot \text{d}^{-1}$]. Solid line: fitted curves of the daily values.

The PFD values are given as daily sum. Cloud cover caused high daily variability (up to a factor 9 between following days). Highest values were observed at highest sun declination in June ($61.0 \text{ mol photons} \cdot \text{m}^{-2} \cdot \text{d}^{-1}$). Lowest annual PFD values correspond to lowest sun declination in December ($1.1 \text{ mol photons} \cdot \text{m}^{-2} \cdot \text{d}^{-1}$). Air temperatures follow the solar radiation intensities with a delay of more than one month.

Wind velocity measured at Roscoff during the field campaign is shown in Figure 27. South-south-westerly winds are predominant during spring and summer. During storm season in fall and winter, predominant wind turned to north.

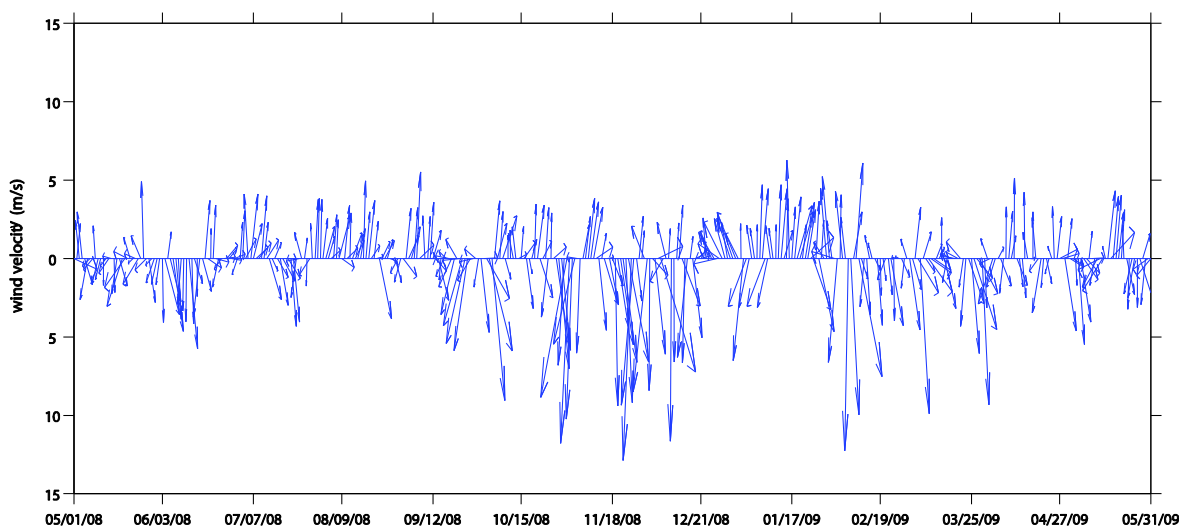


Figure 27. Wind velocity [$\text{m} \cdot \text{s}^{-1}$] and wind direction during the field campaign 2008/09.

5.3.2 Environmental data describing seasonality at ASTAN and ESTACADE point

Here we present environmental data from the northern most extent of the Bay of Morlaix. We decided to present those variables additionally to the data shown in paragraph 5.3.3. VHOC data will be described in the paragraph 5.3.4 to 5.3.6. Due to a high gradient in various parameters between the inner and outer part of the bay, annual variations are presented separated for the northern part of the bay. Moreover data acquisition took place with higher resolution at *ASTAN* and *ESTACADE* point. There, sea surface temperature (SST), salinity oxygen, suspended matter and nutrients were measured twice a month. Results are shown in Figure 28 and Figure 29.

SST values follow the air temperatures with a delay of about one month. Values in the Channel (*ASTAN* point) varied between 8.8 °C in February and 15.7°C in September. High tidal amplitude and tidal currents inhibited the formation of clear summer stratification. Profiles of various parameters showed deep mixing at the *ASTAN* and *ESTACADE* points (data not shown). Annual salinity variations are low. Salinities showed lowest values in June (35 PSU) and March (34.8 PSU) and can be explained by higher fresh water input from the catchment area and by precipitation. However there is a time delay between high river discharge and low salinities in the English Channel. This time delay between the higher river discharge and the lower salinity in the Channel

may be due to the residence time of the river inputs in the inner part of the bay and to the wind direction and speed.

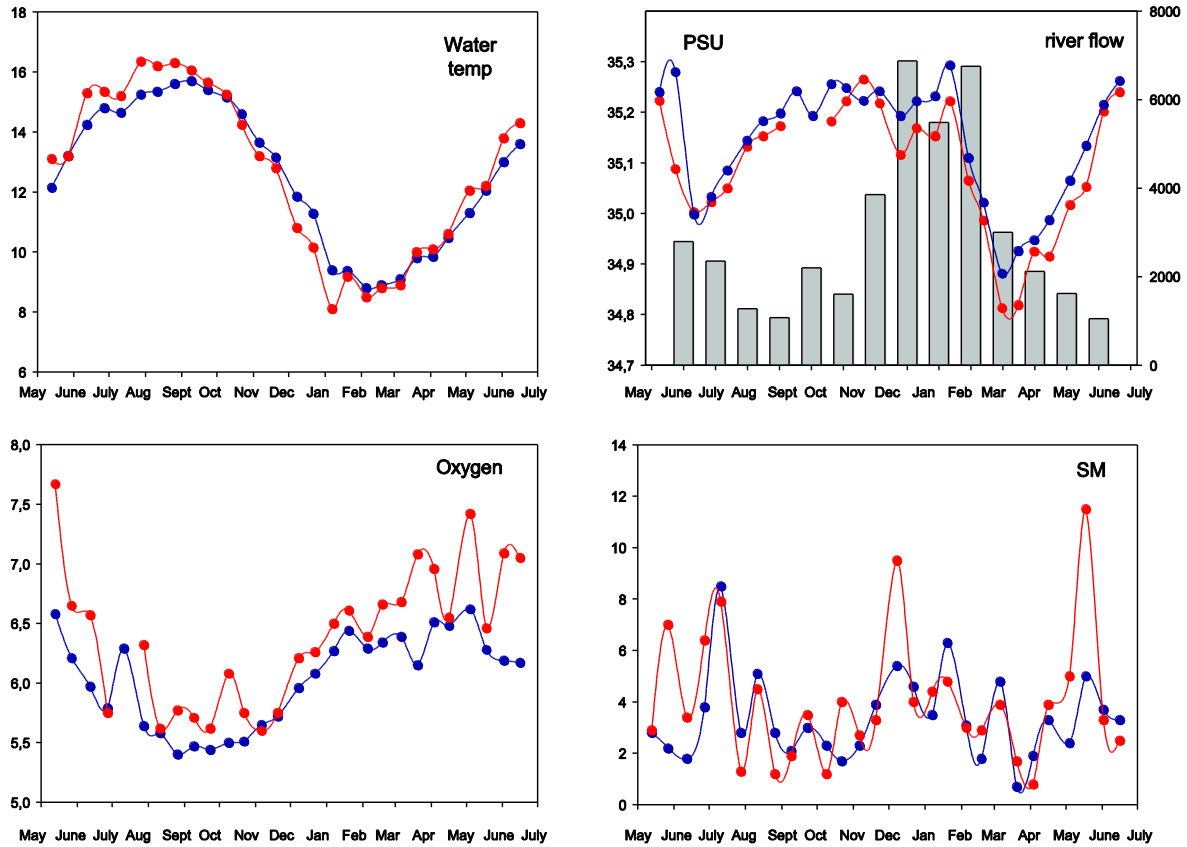


Figure 28. Seasonality of synoptic data at ASTAN and ESTACADE point.

Sea surface temperature [°C], salinity [PSU] and monthly average river flow [$\text{m}^3 \cdot \text{s}^{-1}$], oxygen [$\text{ml} \cdot \text{L}^{-1}$] and suspended matter [$\text{mg} \cdot \text{L}^{-1}$] in the Western English Channel, off Roscoff. Blue: ASTAN point. Red: ESTACADE point. Vertical bars: monthly average river flow of Penzé River, vales from www.hydro.eaufrance.fr

The annual oxygen concentration is inversely related to the SST. With an increase of the temperature, the solubility for oxygen in the water decrease. The annual variations at the *ESTACADE* point are more pronounced. This point is closely located to the shore line with a high macroalgae cover. During summer, biological formation of oxygen can cause super saturation. During the night however, the biological oxygen demand is increased and cause oxygen depletion. Hence measurements show high fluctuations at the *ESTACADE* point.

Suspended matter show high variability during the year. Highest values of suspended matter were measured in December 2008 and May 2009 at the *ESTACADE* point. Phytoplankton bloom, river discharge and storm events have an influence on this variable.

The annual nutrients levels are shown in Figure 29. Nitrate, phosphate and silicate concentrations are highest between December and April. Those high values can be explained by high fresh water input, decomposition of organic material and low biological nutrient uptake. Lowest values occur during spring at summer. Nutrient uptake by phytoplankton and macroalgae lower the water concentrations at this time of the year.

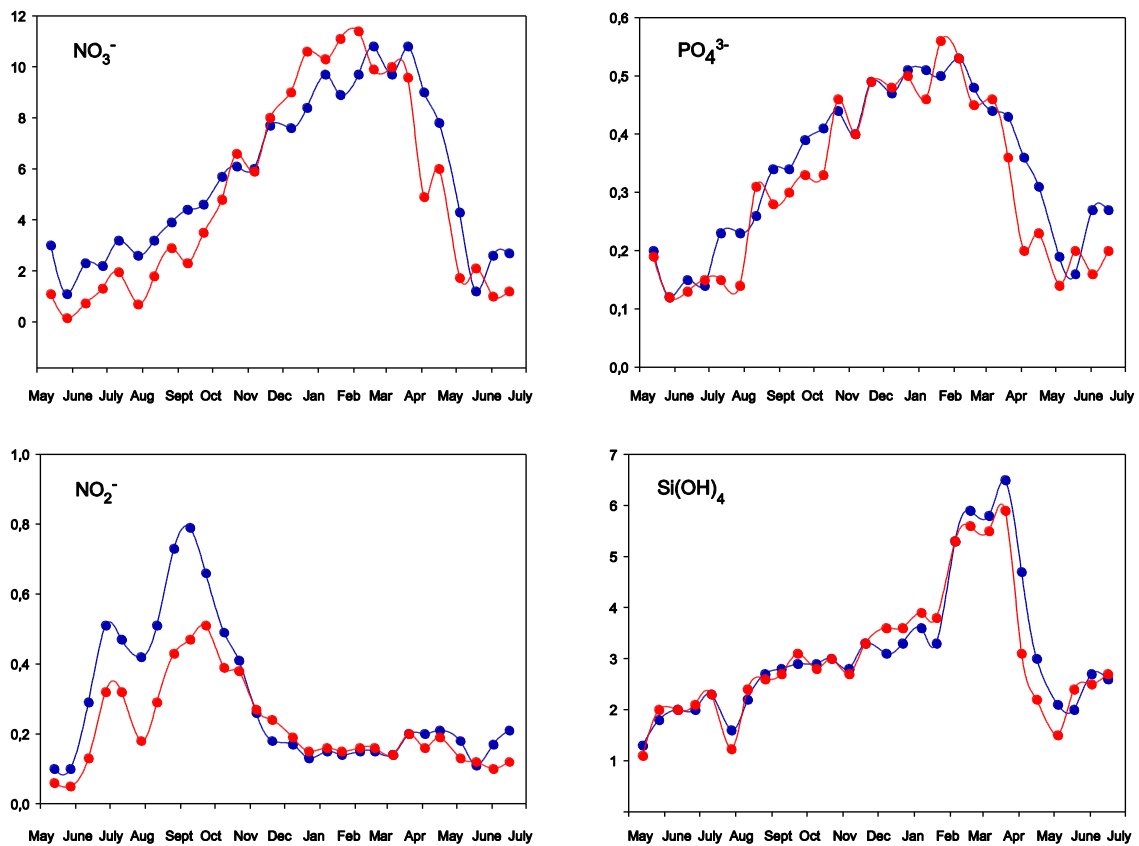


Figure 29. Annual nutrient levels [$\mu\text{mol} \cdot \text{L}^{-1}$] in the Western English Channel, off Roscoff.

Measurements from the stations *ASTAN* and *ESTACADE* between May 2008 and June 2009. Blue: *ASTAN* point. Red: *ESTACADE* point.

Silicate levels decrease several weeks before the occurrence of clear nitrate and phosphate depletion. Diatoms are able to consume large parts of the winter silicate pool. However the supply of phosphate and nitrate exceed their demand. Other photo-autotrophic groups (e.g. dinoflagellates) show later blooms and cause a final nutrient depletion in summer.

Nitrite formation occurs during decay of organic matter. Denitrifying bacteria are able to use nitrate as oxidant. Those processes are usually restricted to organic enriched and oxygen free sediments. Highest nitrite values were recorded in summer and fall and can be related to decomposition of sedimented phytoplankton from the spring bloom. Moreover high temperatures and low oxygen levels prefer the formation of nitrite during this time of the year.

In Figure 30 Chlorophyll *a* values are shown. Variances at both stations – *ASTAN* and *ESTACADE* point – show similar annual patterns.

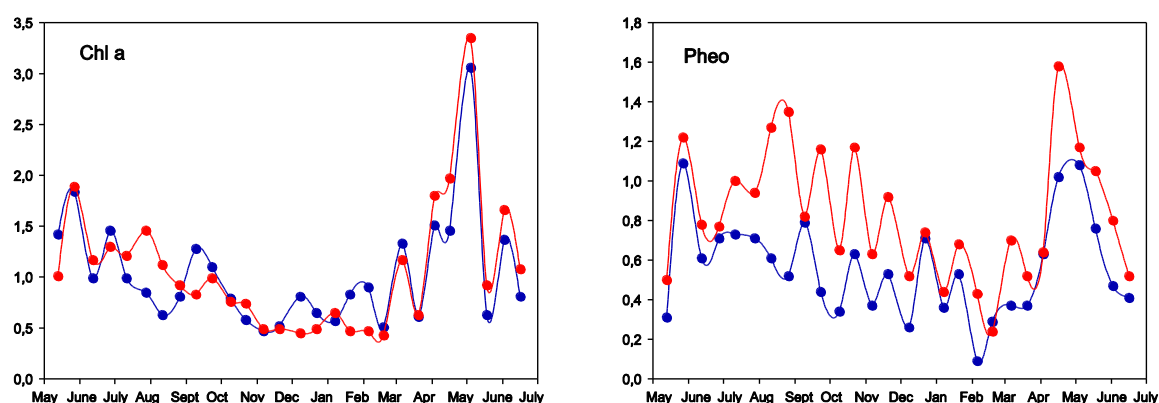


Figure 30. Annual distribution of pigments [$\mu\text{g L}^{-1}$] in the Western English Channel, off Roscoff. Measurements form the stations *ASTAN* and *ESTACADE* between May 2008 and June 2009. Blue: *ASTAN* point. Red: *ESTACADE* point.

In 2008, no clear phytoplankton bloom occurred during spring time. Chlorophyll *a* values decreased from spring 2008 to winter 2008/09. A clear phytoplankton bloom – most likely related to diatoms – is visible from April to May 2009. Phaeopigments are an indicator for the decay of Chlorophyll *a*. Values showed high variation during the field campaign. Values were higher in spring/summer 2008 and decreased until winter 2008/09. Values increase together with the increase of the phytoplankton density.

5.3.3 Environmental data describing seasonality along a salinity gradient in the Bay of Morlaix

Figure 31 and Figure 32 illustrate variations of different parameters along a salinity gradient during May 2008 and May 2009.

Highest chlorophyll *a* values were recorded in August 2008 ($22.6 \mu\text{g} \cdot \text{L}^{-1}$) and April 2009 ($18.4 \mu\text{g} \cdot \text{L}^{-1}$). In both cases high concentrations were obtained in the *Penzé River*. Annual maxima in the inner part of the bay exceeded the annual maxima in the other part (resulting from phytoplankton blooms in spring) by the factor 10. During fall and winter, chlorophyll *a* values were low in all parts of the bay. The annual phaeopigment distribution is closely related to chlorophyll *a*. Annual maxima were observed in August 2008 ($28.0 \mu\text{g} \cdot \text{L}^{-1}$) and April 2009 ($19.2 \mu\text{g} \cdot \text{L}^{-1}$) at the 2 PSU station. Maxima there exceeded the annual maxima in the Channel with a factor 25.

Sea surface temperature show a clear seasonality with highest values between June and August 2008, ranging from 17.4 to 18.8 °C. Along the gradient, temperature values are very similar and do not show a gradient.

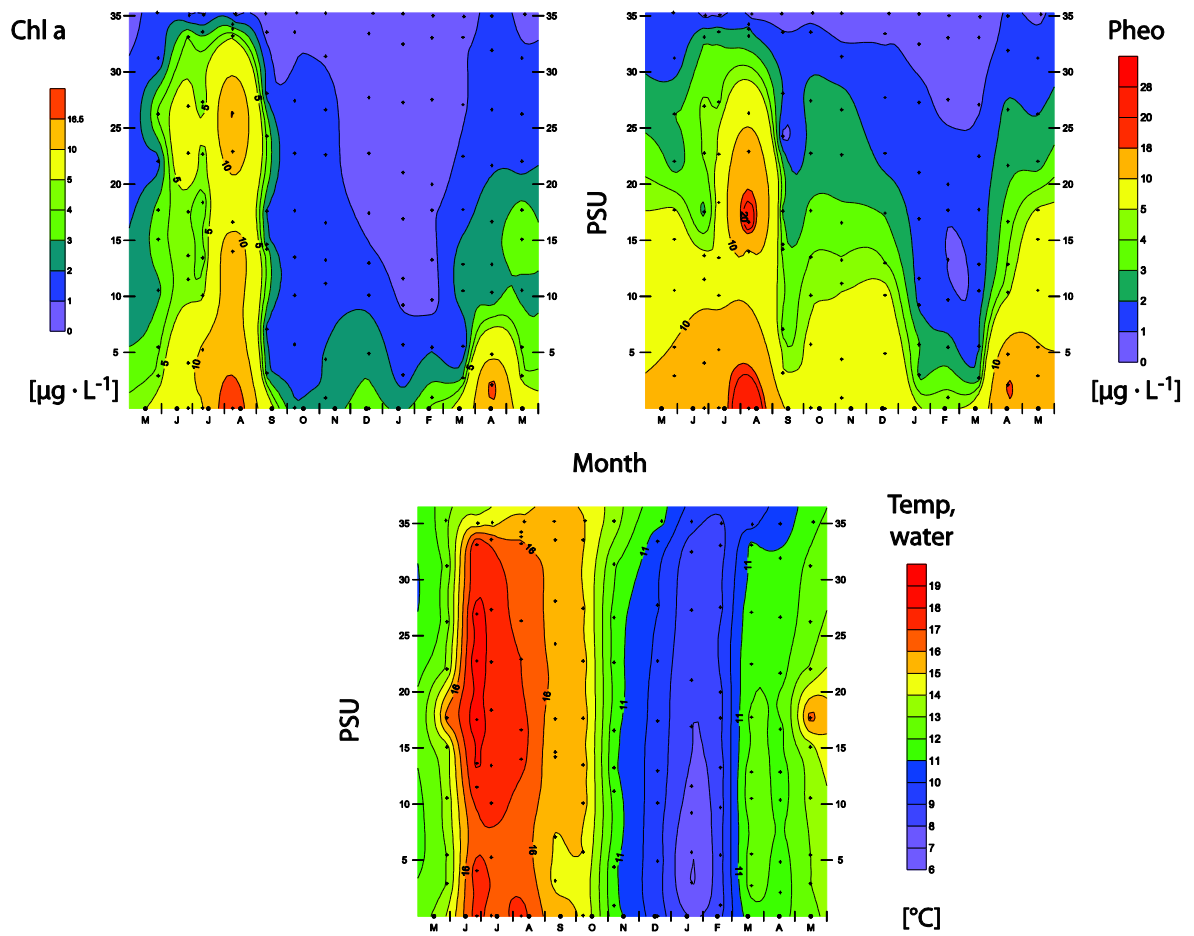


Figure 31. Annual distribution of Chlorophyll a, phaeopigments and water temperature in the Bay of Morlaix (May 2008 to May 2009) along the salinity gradient.

The annual nutrients levels in the bay are shown in Figure 32. Nitrate, phosphate and silicate concentrations are highest between December and April at low salinity stations. Maxima nitrate values ($718.8 \mu\text{mol} \cdot \text{L}^{-1}$) are 66.5 times higher at low salinity station than in the English Channel. Maxima phosphate values ($2.0 \mu\text{mol} \cdot \text{L}^{-1}$) from the inner part of the bay exceeded those one from the Channel by a factor 3.9. Silicate showed 24.4 fold higher maxima concentration in the bay ($158.9 \mu\text{mol} \cdot \text{L}^{-1}$) opposite to the winter maxima in the Channel. Enhanced nitrite values were recorded in summer and fall 2008 and spring 2009. Values were lower in the channel (factor 5.3) and at 2 PSU (factor 2.3).

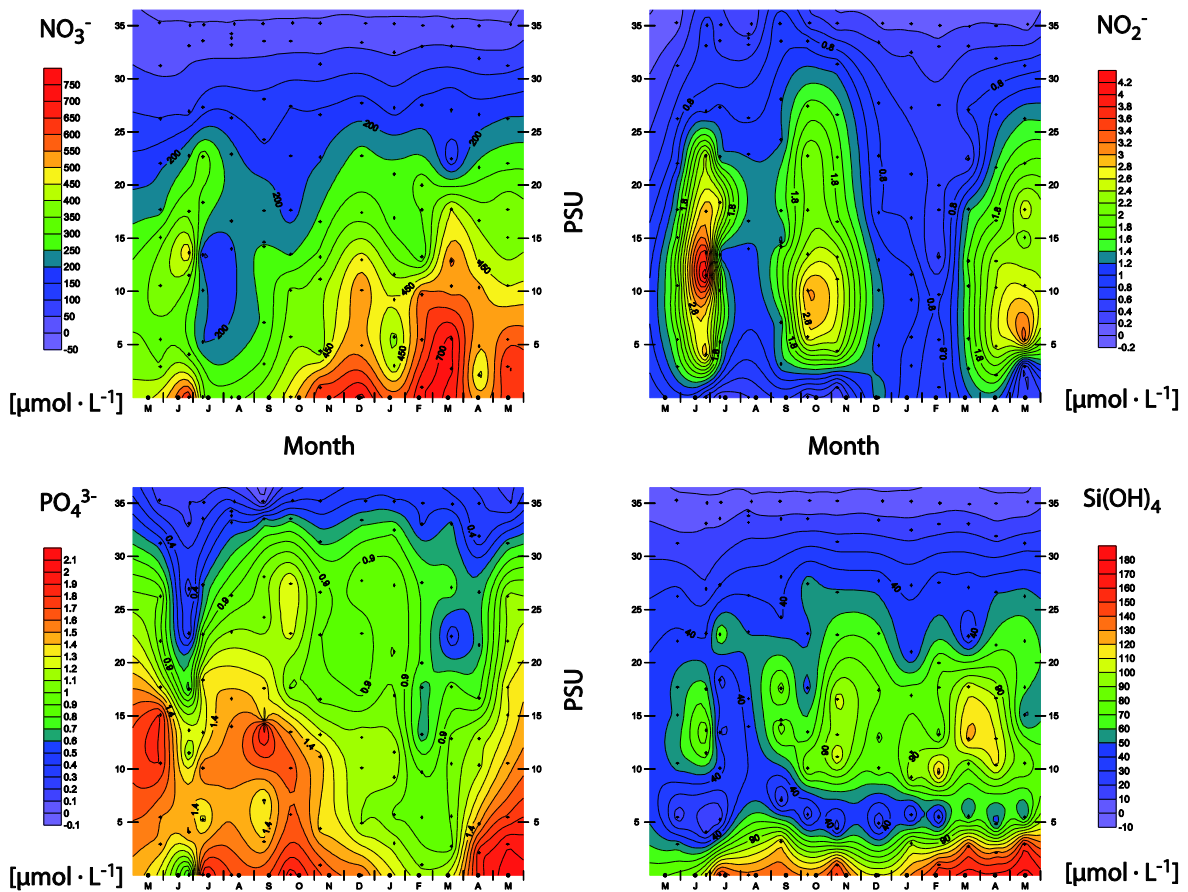


Figure 32. Annual distribution of nutrients in the Bay of Morlaix (May 2008 to May 2009).

5.3.4 Seasonality of VHOC surface concentrations

Bromocarbons

Bromoform and dibromochloromethane showed a concentration gradient which followed the salinity. Values were generally high in the outer bay (27-35 PSU) and exceeded the values from the inner bay by the factor 2 to 10. Concentrations of bromoform along the salinity gradient ranged between 34.7 in March 2009 and 1012.9 $\text{pmol} \cdot \text{L}^{-1}$ in June 2008. Highest dibromochloromethane concentrations were measured in June 2008 (44.6 pmol) and were lowest in March 2009 (2.3 $\text{pmol} \cdot \text{L}^{-1}$). Both compounds showed a clear seasonality with high concentrations in summer and low concentrations during winter.

Annual dibromomethane concentrations showed similar patterns compared to bromoform and dibromochloromethane: in summer concentrations were high (120.3 $\text{pmol} \cdot \text{L}^{-1}$ in September), whereas winter concentrations were low (5.9 $\text{pmol} \cdot \text{L}^{-1}$ in March). Along the salinity gradient however, highest values were not always found at the outer parts of the bay. While high summer values were related to salinities between 22 and 35 PSU, some high winter values were found at hypo saline sampling sites. For instance in January, February and April 2009, highest values were measured in at very low salinities (2-5 PSU).

Bromodichloromethane showed a distinct seasonality with highest values (18.7 $\text{pmol} \cdot \text{L}^{-1}$) measured between June and September 2008 and low values between November 2008 and May 2009. In contrast to other bromocarbons, the annual distribution of bromodichloromethane did not reveal a marked concentration gradient in the bay.

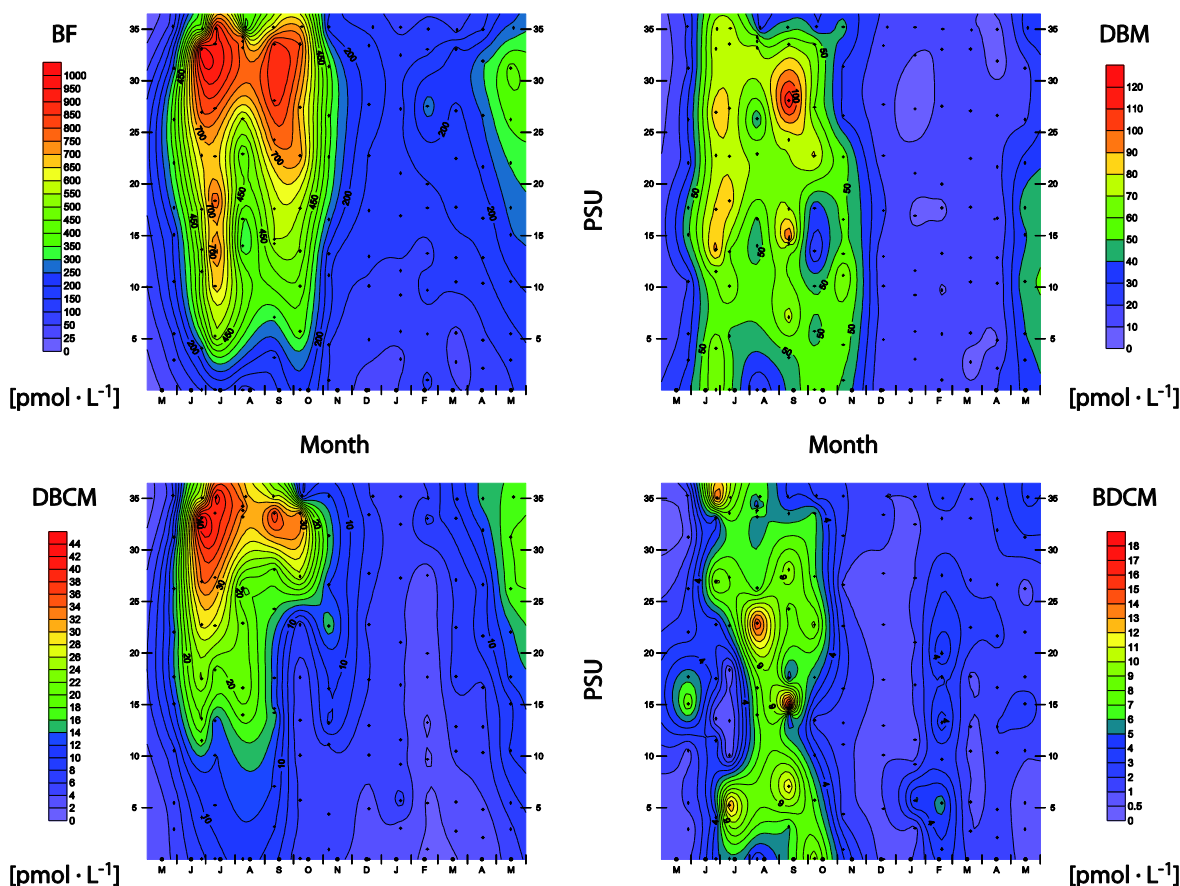


Figure 33. Annual distribution of brominated halocarbons along a salinity gradient in the Bay of Morlaix. BF (bromoform). DBM (dibromomethane). DBCM (dibromochloromethane). BDCM (bromodichloromethane)

Iodocarbons

As brominated compounds, iodocarbons showed a marked seasonality with high concentrations in early summer and low values in winter (Figure 34). Highest iodoethane concentrations were found in June 2008 ($14.7 \text{ pmol} \cdot \text{L}^{-1}$). Then values decrease until September and show a second peak in October ($7.4 \text{ pmol} \cdot \text{L}^{-1}$). Winter and spring values are low. Highest bromiodomethane concentrations were measured in June 2008 ($18.9 \text{ pmol} \cdot \text{L}^{-1}$), whereas those from diiodomethane were obtained in July ($24.6 \text{ pmol} \cdot \text{L}^{-1}$). Unlike most bromocarbons, iodocarbons showed no clear trend along the salinity gradient.

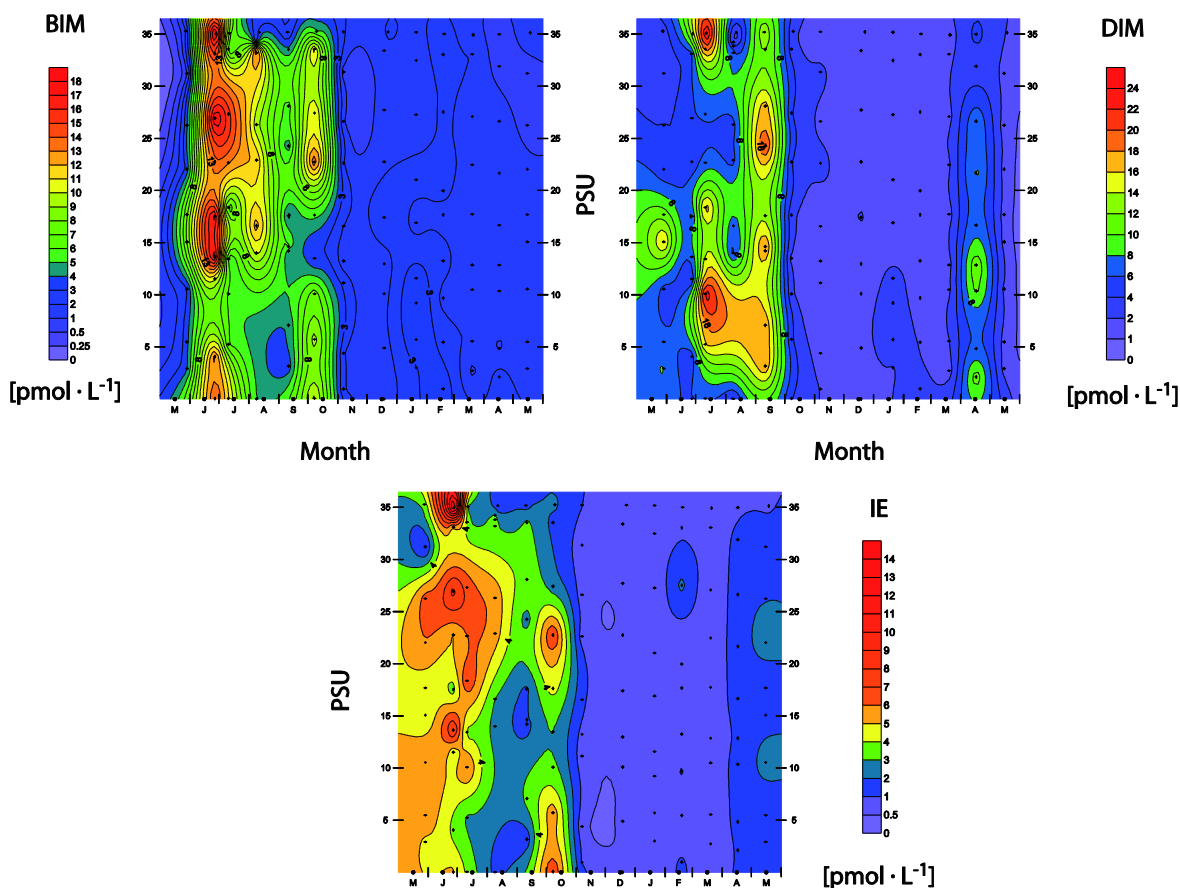


Figure 34. Annual distribution of iodinated halocarbons along a salinity gradient in the Bay of Morlaix.

IE: iodoethane. DIM: diiodomethane. BIM: bromiodomethane.

Chlorocarbons

Chlorocarbons showed an opposite pattern to brominated and iodinated compounds: values were high in winter and low in summer. Methyl chloroform concentrations ranged between 0.9 and 5.8 pmol L^{-1} . Highest tetrachloromethane were measured in the estuary in January (9.5 pmol L^{-1}). Summer values were low and showed increasing concentrations towards the Channel.

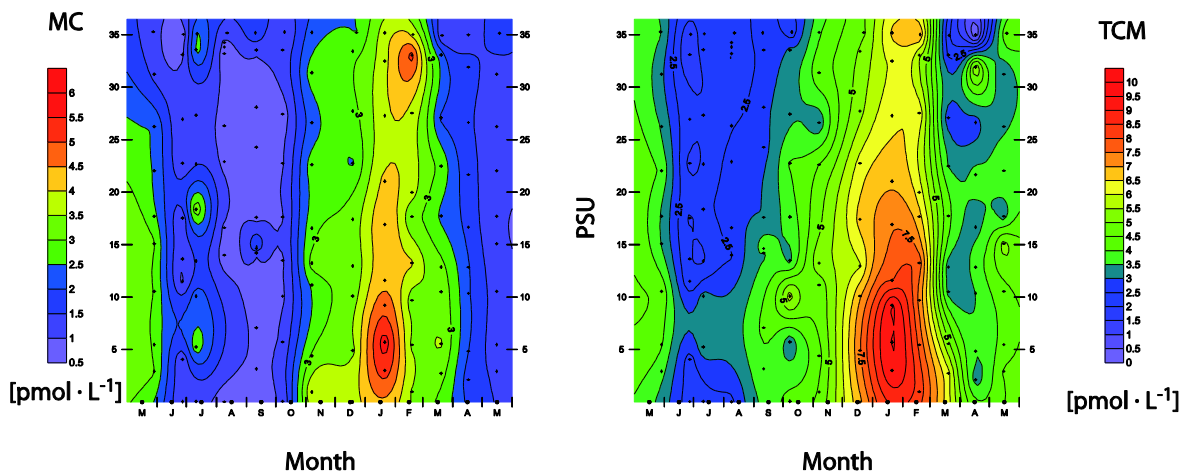


Figure 35. Annual distribution of chlorinated halocarbons along a salinity gradient in the Bay of Morlaix.

TCM: tetrachloromethane. MC: methyl chloroform.

5.3.5 Formation of halocarbons during a diurnal tidal cycle

The formation of halocarbons in an algae bed in front of the *ESTACADE* point was followed on 28th May 2009. Surface concentrations were measured every two hours. The tidal phase and the daylight length are shown in Figure 36. Water was low during highest solar altitude. The sampling day was sunny and calm.

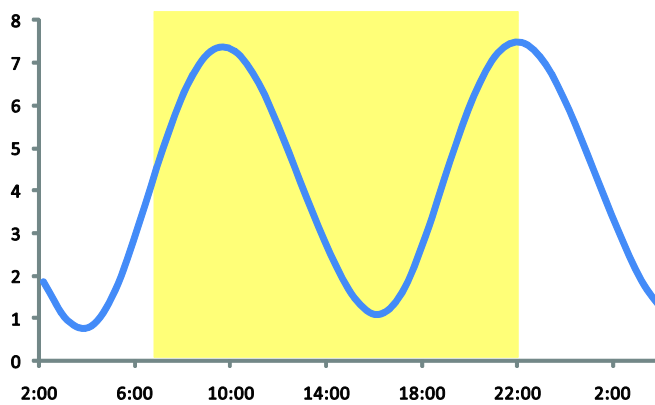


Figure 36. Diurnal tidal cycle and length of daylight at Roscoff during the field campaign at the *ESTACADE* point.

Figure 37 shows concentrations of methyl chloroform and tetrachloromethane measured on 28th May 2009. Diurnal variations did not show clear pattern and did not follow the tidal cycle.

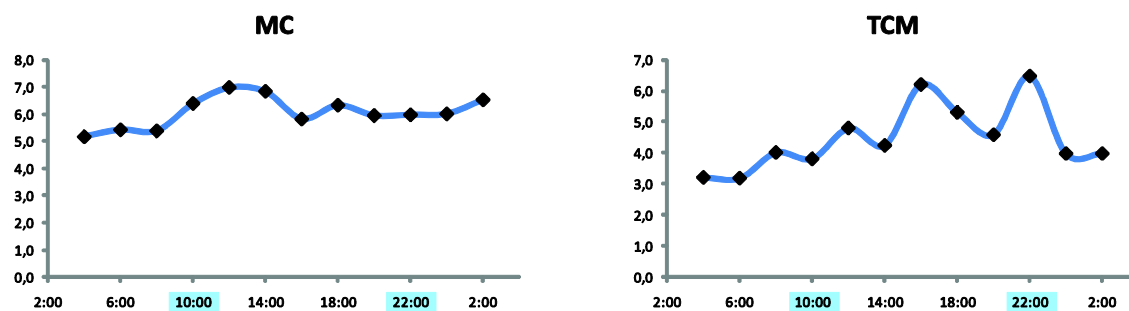


Figure 37. Concentrations of chlorinated compounds at *ESTACADE* point during diurnal tidal cycle. Halocarbon values in pmol · L⁻¹. High tides are marked in blue. MC: methyl chloroform. TCM: tetrachloromethane.

Diurnal concentrations of four bromocarbons are presented in Figure 38. Dibromomethane, bromoform and dibromochloromethane concentrations were elevated at low tide. Concentrations were 5-7 times higher at low tide compared to the lowest values. Bromodichloromethane showed highest concentrations two hours after the nightly high tide.

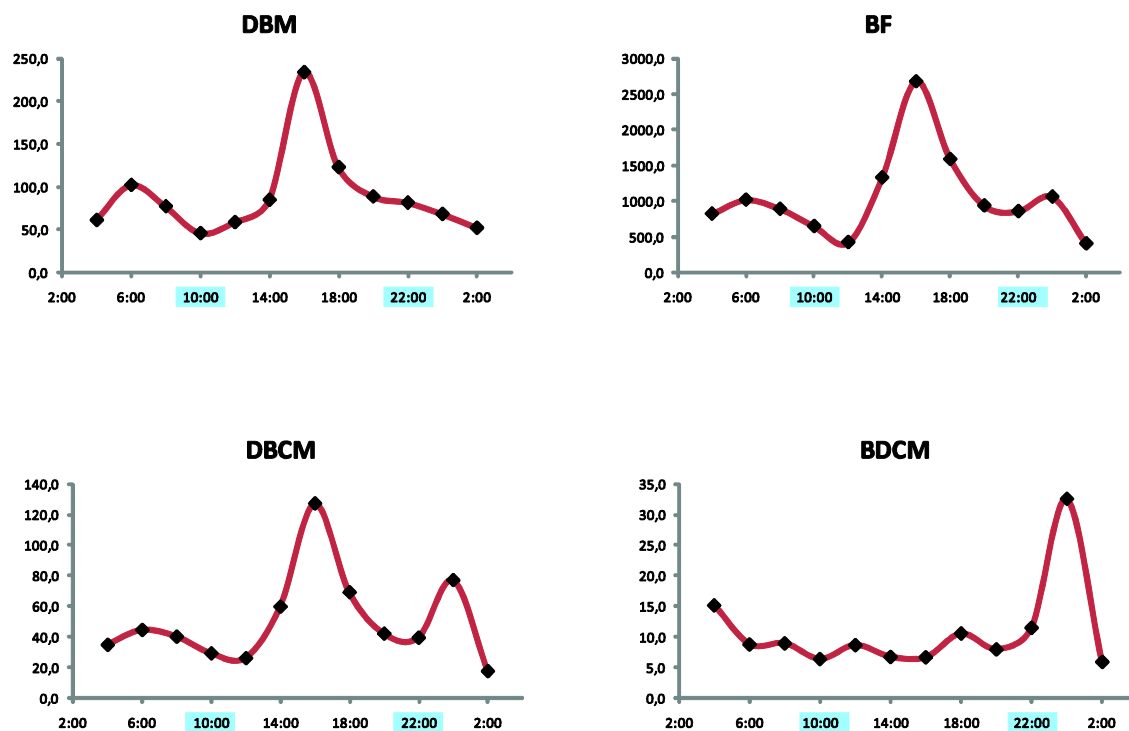


Figure 38. Concentrations of brominated compounds at *ESTACADE* point during diurnal tidal cycle.

Halocarbon values in pmol L⁻¹. High tides are marked in blue. DBM: dibromomethane. BF: bromoform. DBCM: dibromochloromethane. BDCM: bromodichloromethane.

Concentrations of three iodinated compounds are presented in Figure 39. Like for brominated compounds, highest values were measured at low tide during the day.

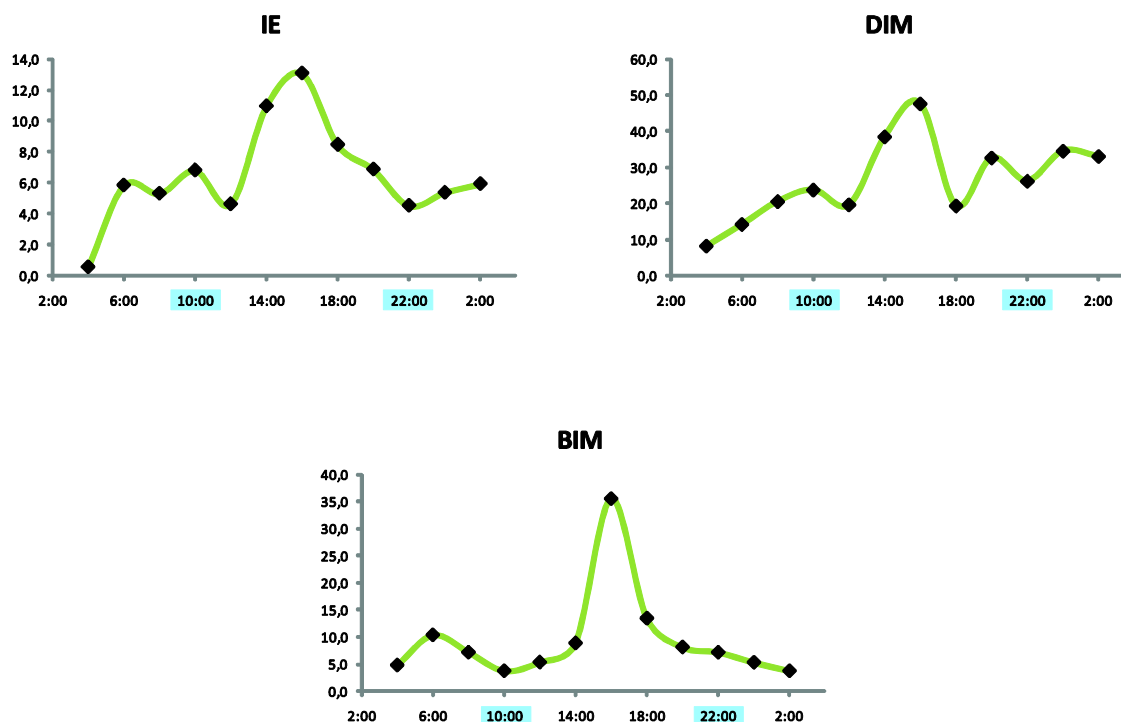


Figure 39. Concentrations of iodinated compounds at ESTACADE point during diurnal tidal cycle.

Halocarbon values in pmol L^{-1} . High tides are marked in blue. IE: iodoethane. DIM: diiodomethane. BIM: bromiodomethane.

5.3.6 Possible input of halocarbons by a sewage treatment plant at Morlaix

Wastewater treatment plants are known sources for halocarbons to the environment, especially for chlorinated compounds (Aucott et al. 1999). Additionally filed measurements in the *Morlaix River* was set out to elucidate possible inputs of halocarbons from the wastewater treatment plants of the city of Morlaix. Results are shown in Figure 40 and compared with measurements in the western part of the bay, several days later. Concentrations of all VHOCs between both sampling sites showed very similar values. No evidences were found for a distinct input of chlorinated compounds.

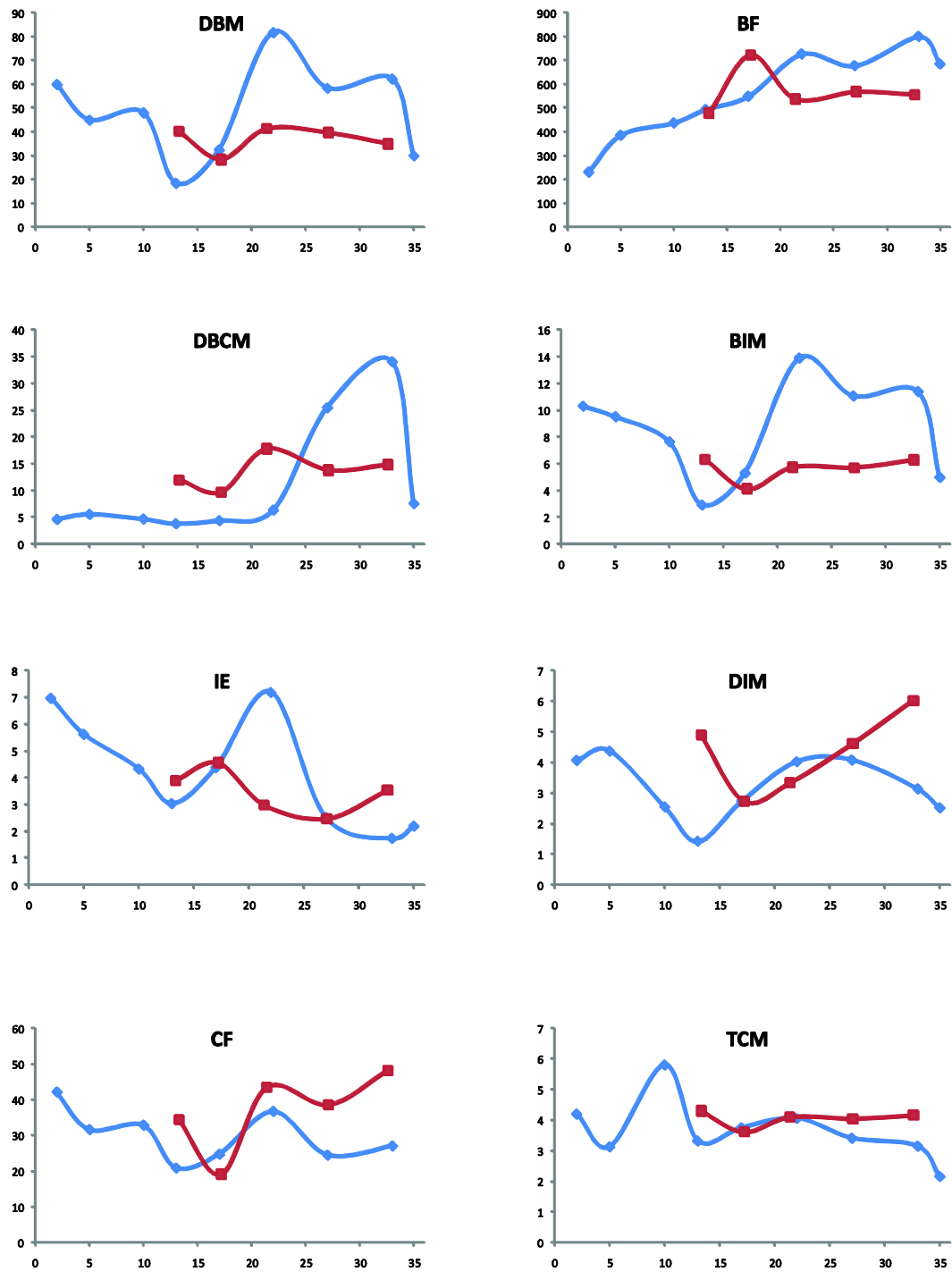


Figure 40. Comparison of halocarbon concentrations along two salinity gradients (PSU vs pmol L⁻¹).

Blue: Halocarbon distribution in the western part of the Bay of Morlaix, including the *Penzé River*. Red: halocarbons in the *Morlaix River*.

5.4 Discussion

5.4.1 Comparison to other costal measurements

This study has demonstrated that VHOC distribution patterns show a marked seasonality. Concentrations of some compounds (e.g. bromoform, dibromochloromethane) varying along the salinity gradient, whereas iodocarbons showed similar concentrations at different sampling sites in the Bay of Morlaix.

The comparison of published VHOC values reveals that halocarbon formation is highly localized. Saturations and sea-to-air fluxes decrease with increasing distance from coastal zones (Carpenter et al. 2009). Some costal studies were conducted in the Bay of Morlaix (Cocquempot 2004; Jones et al. 2009). While values of Cocquempot were comparable to our results (see Table 15), values from Jones et al. were much lower. This can be explained by the different sampling sites and the different temporal resolution (Jones et al. measured more westwards, during September 2006). A further comparison with other costal studies indicates that VHOC formation depends on position. Water samples from the Menai Strait showed highest concentrations. On the other side of the English Channel (Plymouth Sound), iodocarbons concentrations showed close agreements with our measurements.

Table 15. Range of halocarbon concentrations measured in water [$\mu\text{mol L}^{-1}$] and comparison with previous studies.

	English Channel Bay of Morlaix Roscoff (9/2006)		English Channel Bay of Morlaix nothern part (2000)		English Channel Bay of Morlaix nothern part (2008-2009) this work		Irish Sea Menai Strait (2004-2005) Bravo-Linares and Mudge 2009		English Channel Plymouth (2002-2004) Archer et al. 2007	
CH ₃ CH ₂ I	1,1	3,9	<LoD	5,13	0,2	4,8	0,4	31,2	<0.3	4.8
CH ₃ CCl ₃					0,8		<LoD	5,7		
CCl ₄			2,93	6,83	1,5		0,4	16,2		
CH ₂ Br ₂	8,3	34,4	14,42	143,04	6,0	77,9	<LoD	109,8		
CHBrCl ₂			1,83	14,04	<LoD	6,4	<LoD	161,5		
CHBr ₂ Cl			6,24	48,49	5,5	44,6	0,4	206,0		
CH ₂ BrI	1,9	18,9			0,4	15,0			0.2	7.0
CHBr ₃	142,8	519,4	77,95	1072,7	128,7	1012,9	3,0	3588,7		~1600
CH ₂ I ₂	0,1	4,5	<LoD	29,49	<LoD	18,8	<LoD	33,1	<0.3	15.3

A comparison with halocarbon mixing ratios in air [pptv] reveal high differences between the different studies (Table 16). Roscoff values from Jones et al. (2009) were about one order of magnitude lower compared to our results and up to two orders of magnitude lower compared to values from Lilia (Peters et al. 2005). Our results were in reasonable agreement with measurements from a previous study in the Bay of Morlaix and with those values from Lilia. The high variance between different studies indicates a high dependence of mixing ratios on wind direction and on the sampling site.

Additionally, different analytical procedures might be causal for those remarkable differences. This emphasises the concern of an inter calibration approach in between different research teams.

Table 16. Range of halocarbon mixing ratios [pptv] measured in air samples from different sampling sites.

	English Channel Bay of Morlaix Roscoff (9/2006) Jones et al. 2009		English Channel Bay of Morlaix nothern part (2000) Cocquempot 2004		English Channel Bay of Morlaix nothern part (2008-2009) this work		English Channel Lilia (Brittany) 2003 Peters et al. 2005	
CH ₃ CH ₂ I	0,21	0,82			0,02	4,10	2,22	96,9
CH ₃ CCl ₃					18,4	22,7		
CCl ₄			42	151	88,1	96,4		
CH ₂ Br ₂	0,28	1,36	1,3	17,6	0,4	17,2	2,36	262,0
CHBrCl ₂				14,9	0,2	3,6	12,5	246,0
CHBr ₂ Cl				11,3	2,0	36,6	3,47	128,2
CH ₂ BrI	0,01	0,13	3	4,1	0,0	5,8	0,55	9,9
CHBr ₃	0,56	5,35	1,9	121	12,2	128,1	10,5	396,0
CH ₂ I ₂	0,01	0,07			0,0	1,1	0,11	19,8

5.4.2 Temporal trends

An ANOVA (analysis of variance) was calculated in order to illustrate the influence of the factor time on the halocarbon concentration. The factor time partitioned the dataset in twelve parts (month). The mean values of each compartment were analyzed with the ANOVA. For each

halocarbon, time has a significant influence on the variances of the halocarbon concentrations (Figure 41). While iodinated and brominated compounds showed highest concentrations in summer and minima in winter, tetrachloromethane and methyl chloroform showed opposite patterns.

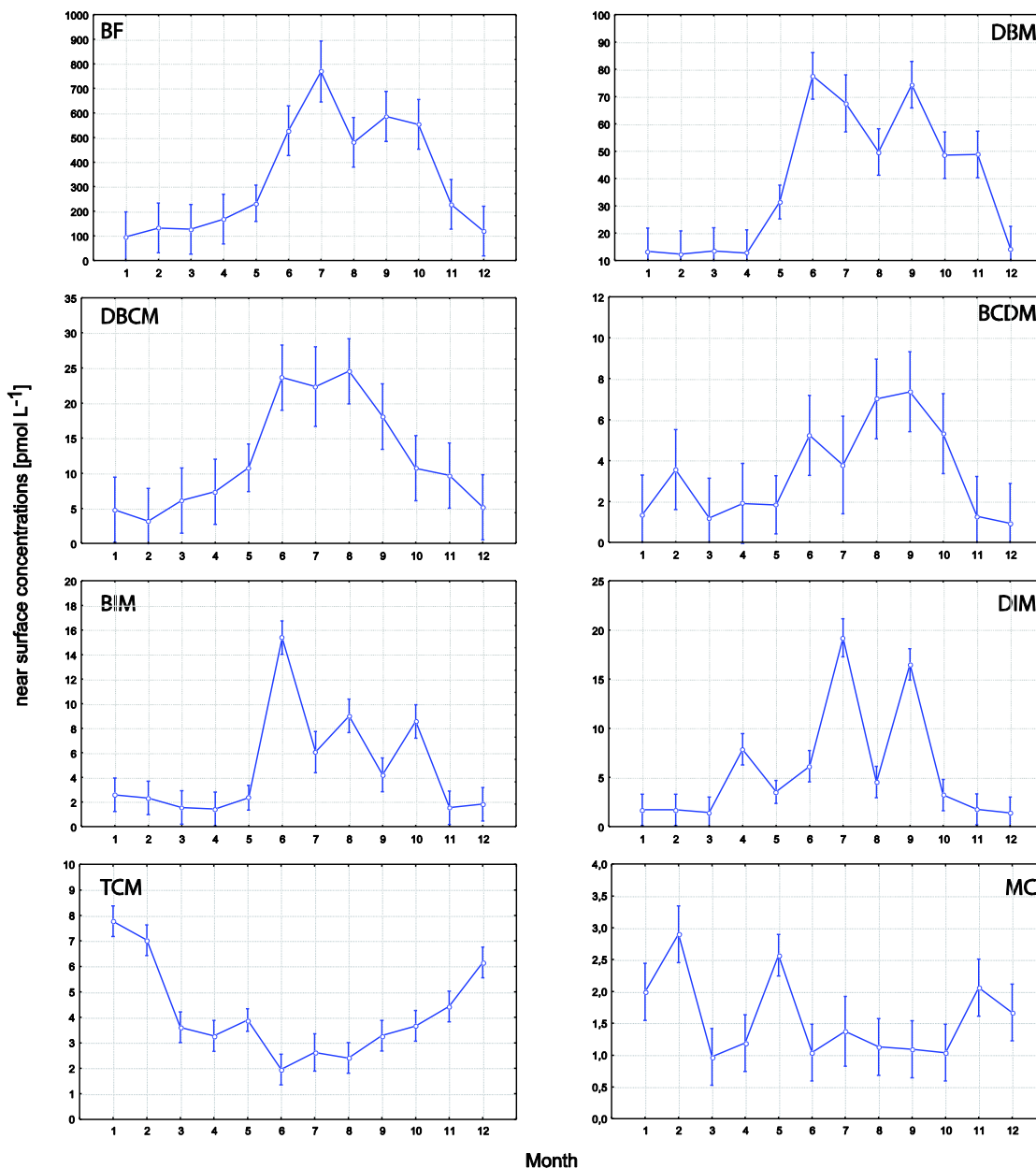


Figure 41. Seasonality of VHOCs in the Bay of Morlaix.

Mean values (circles) and 0.95 confidence intervals (vertical bars). ANOVAs indicated significant effect of time on the near surface concentrations of each VHOC (all p-values <0.01).

Seasonal patterns for halocarbons were shown only in few studies. In a recent study in the NW Atlantic, it was shown that iodomethane might be controlled by phytoplankton and/or photochemistry. Both factors can be causal for a marked seasonality (Wang et al. 2009). In a second study it was demonstrated that Antarctic water might have a strong source for dibromomethane and bromoform (Hughes et al. 2009). The authors found concomitant occurrence of the annual microalga bloom and high concentrations of those two bromocarbons during austral summer. A third study was conducted in a shallow bay in the West coast of Sweden (Klick 1992). The author reported summer maxima and winter minima for bromoform, dibromomethane and dibromochloromethane. Our results agree with those findings. Moreover the author described distinct concentration maxima in spring and fall for diiodomethane. We found two maxima at Roscoff; beginning of summer and end of summer. Klick (1992) attribute the seasonal pattern to macroalgae and phytoplankton occurrences. Additionally this author concluded that higher winter concentrations of tetrachloromethane are related to air-to-sea fluxes. Lower summer concentrations of this compound were explained with increased water temperatures in summer.

In a recent study it was revealed that iodocarbons show repeating seasonal cycles in temperate, shelf seas (Archer et al. 2007). The author found winter minima and, generally, late summer/autumn maxima in water samples from the English Channel.

It can be concluded that temporal trends are explained by different sun radiation levels, water temperature regimes or biological activity. The latter mentioned factor will be discussed in the following paragraph.

5.4.3 Biogenic sources

Several incubation experiments demonstrated species specific formation of VHOCs by phytoplankton (Tokarczyk and Moore 1994; Moore et al. 1996b), bacteria (Amachi et al. 2001) and macroalgae (Gschwend et al. 1985; Klick 1993; Nightingale et al. 1995; Pedersen et al. 1996; Carpenter et al. 2000).

An inventory of the macroalgae diversity and marine angiosperm distribution was conducted by Braud (1974) in the Bay of Morlaix. While north of *Ile de Callot* (island which is located in the center of the bay) macroalgae coverage and diversity are high, marine vegetation is less diverse in

the inner parts of the bay (south of the *Ile de Callot*). This island divides the bay in terms of salinity, nutrient supply (for latter see Figure 32) and biodiversity. The northern part is highly influenced by the Channel due to intense water mixing. Salinities are comparable with those from the English Channel and show only minor variations. The southern part shows strong variations in salinity during a diurnal tidal cycle. This salinity and nutrient gradation reflects macroalgae distribution. In the north, the dominant species are *Laminaria ochroleuca* and *L. hypoborea*. Furthermore Braud (1974) described the occurrence of *Laminaria digitata*, *L. saccharina*, *Halidrys siliquosa*, *Ascophyllum nodosum*, *Cystoseira sp.*, *Bifurcaria bifurcate*, *Saccorhiza polyschides*. The predominate species in the southern end of the bay are *Zostera sp.* (angiosperm) and *Fucus sp.*

No further detailed inventory of the macroalgae diversity was made up to now. Although it must be assumed that algae diversity and distribution were subject to changes, the general picture is still valid (personal communication with the scientific diving service at the *Station Biologique de Roscoff*). Those observations are in agreement with findings from Leigh et al. (2009) from the shore off Roscoff. Figure 42 illustrates the macroalgae cover around Roscoff and Île de Batz.

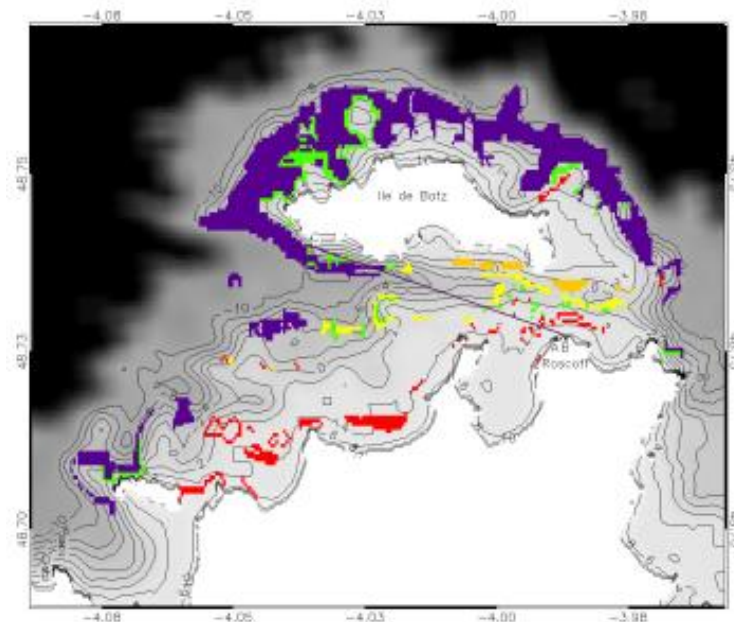


Figure 42. Macroalgae distribution off Roscoff and around Île de Batz (north western part of the Bay of Morlaix). Figure from (Leigh et al. 2009). Macroalgae cover coded with colours. Purple: *Laminaria hyperborean*. Green: *Laminaria digitata*, Orange: *Laminaria ochroleuca*. Yellow: *Saccharina latissima*. Red: *Ascophyllum sp.* / *Fucus sp.*

In a recent study, concentrations of halocarbons in seawater and mixing ratios in air were determinate along the shore line off Roscoff (Jones et al. 2009). The authors measured elevated concentrations generally during low tide and found maxima concentrations in waters directly over kelp beds (dominated by *Laminaria saccharina*, *L. digitata* and *L. ochroleuca*). Our measurements in the same area are consistent with those results. Figure 38 and Figure 39 clearly demonstrate the impact of tides on the seawater concentration of iodo- and bromocarbons. In contrary, anthropogenic trace gases as tetrachloromethane or methyl chloroform were not affected by tidal force. The study of Jones et al. (2009) revealed remarkable variances in seawater halocarbon concentrations in an area of few square kilometres. This agrees with our findings and emphasize that halocarbons have highly localized sources.

Table 17 show hourly iodine and bromine formation of different macroalgae. While bromocarbons are produced by a great variety of macroalgae species, iodinated compounds are released only by few species (*Laminaria sp.* and *Asparagopsis armata*). Those high effective VHOC producers can be found in the *Bay of Morlaix*. Moreover, cover rates of those macroalgae are higher in the northern end of the bay, which might responsible for the higher VHOC formation observed.

Table 17. Release of bromine and iodine from different macroalgae, reported by Carpenter et al. (2000).

Most effective producers are highlighted.

		Iodine release [$\mu\text{mol g}^{-1} \text{FW h}^{-1}$]								
		Total	CH ₃ I	CH ₃ CH ₂ I	CH ₂ ICI	CH ₂ IBr	CH ₂ I ₂	CHIBr ₂	CHI ₂ Cl	CHI ₂ Br
<i>Laminaria</i>	<i>digitata</i>	35.9	2.7	2.7	1.5	2.2	20.5	3.6	2.0	0.7
<i>Laminaria</i>	<i>saccharina</i>	6.5	0.5	0.4	0.9	0.8	3.7	0.1	0.02	0.03
<i>Ascophyllum</i>	<i>nodosum</i>	1.3	0.3	0.02	0.1	0.1	0.7	0.02	0.02	0.01
<i>Fucus</i>	<i>vesiculosus</i>	0.6	0.2	0.01	0.0	0.1	0.3	0.00	0.0	0.0
<i>Fucus</i>	<i>serratus</i>	0.1	0.01	0.01	0.01	0.02	0.1	0.01	0.0	0.0
<i>Pelvetia</i>	<i>canaliculata</i>	3.2	0.8	0.1	0.2	0.5	1.3	0.1	0.04	0.01
<i>Halidrys</i>	<i>siliquosa</i>	0.1	0.05	0.01	0.01	0.00	0.00	0.0	0.0	0.0
<i>Asparagopsis</i>	<i>armata</i>	232.6	3.5	3.5	0.2	4.4	2.8	216.3	1.6	0.2
<i>Chondrus</i>	<i>crispus</i>	0.4	0.2	0.04	0.1	0.03	0.1	0.01	0.0	0.0
<i>Enteromorpha</i>	<i>intestinalis</i>	0.9	0.1	0.1	0.1	0.2	0.2	0.1	0.1	0.01

Continued

		Bromine release [$\mu\text{mol g}^{-1} \text{FW h}^{-1}$]								
		Total	CH ₃ Br	CH ₃ CH ₂ Br	CH ₂ I ₂ Br	CHI ₂ Br ₂	CHI ₂ Br	CH ₂ Br ₂	CHBr ₂ Cl	CHBr ₃
<i>Laminaria</i>	<i>digitata</i>	627.6	0.0	0.0	1.9	6.9	0.6	14.4	13.8	589.3
<i>Laminaria</i>	<i>saccharina</i>	427.1	0.0	0.0	0.9	0.4	0.0	44.8	6.0	375.0
<i>Ascophyllum</i>	<i>nodosum</i>	31.8	0.0	0.0	0.1	0.03	0.0	2.7	0.9	28.1
<i>Fucus</i>	<i>vesiculosus</i>	61.5	0.0	0.0	0.1	0.0	0.0	1.9	1.2	58.3
<i>Fucus</i>	<i>serratus</i>	26.3	0.0	0.0	0.03	0.03	0.0	0.8	0.9	24.5
<i>Pelvetia</i>	<i>canaliculata</i>	332.6	0.0	0.0	0.7	0.3	0.0	23.6	6.3	302.0
<i>Halidrys</i>	<i>siliquosa</i>	9.0	0.02	0.01	0.0	0.0	0.0	0.3	0.8	7.8
<i>Asparagopsis</i>	<i>armata</i>	16900.0	0.0	0.0	0.0	439.4	0.0	169.0	1368.9	14922.7
<i>Chondrus</i>	<i>crispus</i>	19.7	0.04	0.0	0.04	0.02	0.0	1.5	2.2	16.0
<i>Enteromorpha</i>	<i>intestinalis</i>	1050.0	0.0	0.0	0.0	0.0	0.0	10.5	8.4	1031.1

Microalgae might be another biogenic source for halocarbons. As mentioned above several authors related their finding of elevated halocarbon concentrations with phytoplankton. Klick (19992) claimed a phytoplanktonic source for formation of diiodomethane and chloriodomethane (in contrast to that, she suggested that brominated compound have their origin in a macroalgae belt). Hughes et al. (2009), however, found correlations between high bromoform and dibromomethane concentrations and a phytoplankton bloom. Elevated iodomethane concentrations were found in the open ocean (Wang et al. 2009) and might be related to bacterioplankton (cyanobacteria).

Several aspects are in disfavor for the idea of a phytoplanktonic formation of bromocarbons in the *Bay of Morlaix*. No clear correlations between Chlorophyll a and VHOC concentrations were found. Moreover concentrations of various brominated compounds were generally higher in areas with high cover rates of macroalgae and lower in areas of low macroalgae densities. This implies that macroalgae were the major source of bromocarbons. However, due to rapid tidal influenced mixing processes, a clear distinction between macroalgae and phytoplankton is not evident.

5.4.4 Different sources along the gradient

Variations along the salinity gradient

The annual VHOC distribution is shown in Figure 33 to 26. Generally, brominated and iodinated compounds showed higher concentrations in summer. Maximum values of bromocarbons were measured in samples with higher salinity. In contrast, chlorinated compounds were generally higher concentrated in samples from lower salinities and iodinated compound did not show a dependence on salinity. In order to localize possible sources, VHOC concentrations along a salinity gradient are presented in Figure 43.

The *ASTAN* point is situated in the English Channel at the northern end of the *Bay of Morlaix* (see Figure 24), approximately two km from the shore of *Île de Batz* and 10 km from the estuary mouth of the *Penzé River*. The other sampling stations were predefined by salinity (2, 5, 10, 13, 17, 22, 27 and 33 PSU) and had therefore changing positions. While lower salinity stations were located in the estuary, higher salinity stations were situated in the centre of the bay

Bromoform and dibromomethane concentrations at higher salinity stations (27-35 PSU) were on average 2 to 2.5 fold higher than those from low salinity stations (2-10 PSU). During summer, a clear gradient is visible for both compounds. Dibromomethane summer concentrations were lowest at low salinity stations. At all other salinity stations, concentrations showed high variability along the salinity gradient, but no obvious trend could be observed. Winter concentrations of dibromomethane showed no tendency along the salinity gradient. Bromodichloromethane concentrations showed high variations during summer. Annual concentrations were 10% higher at the salinity range 13-22 PSU, compared with all other stations.

Iodinated compounds showed no clear tendency along the salinity gradient. In contrast to winter concentrations, summer values were highly variable. Average annual tetrachloromethane and methyl chloroform concentrations were 15 to 25% higher in the river, compared to high salinity stations.

Since some compounds showed a clear gradient along the bay, it can be concluded that those compounds do have a localized source. It is likely, that brominated compounds have their origin in large macroalgae beds in the northern part of the bay. Tetrachloromethane and methyl chloroform are anthropogenic and can be introduced via air-sea exchange in the ocean (Walker et

al. 2000). Due to legal ban in industry, mixing ratios in air decreasing since the 90th of the last century. Soils are described as important sink for those compounds (Happell and Roche 2003). Thus erosion in the catchment area could be causal for elevated concentrations in the estuary. Moreover increased water velocity in the river increase the air-sea flux (Abril et al. 2009).

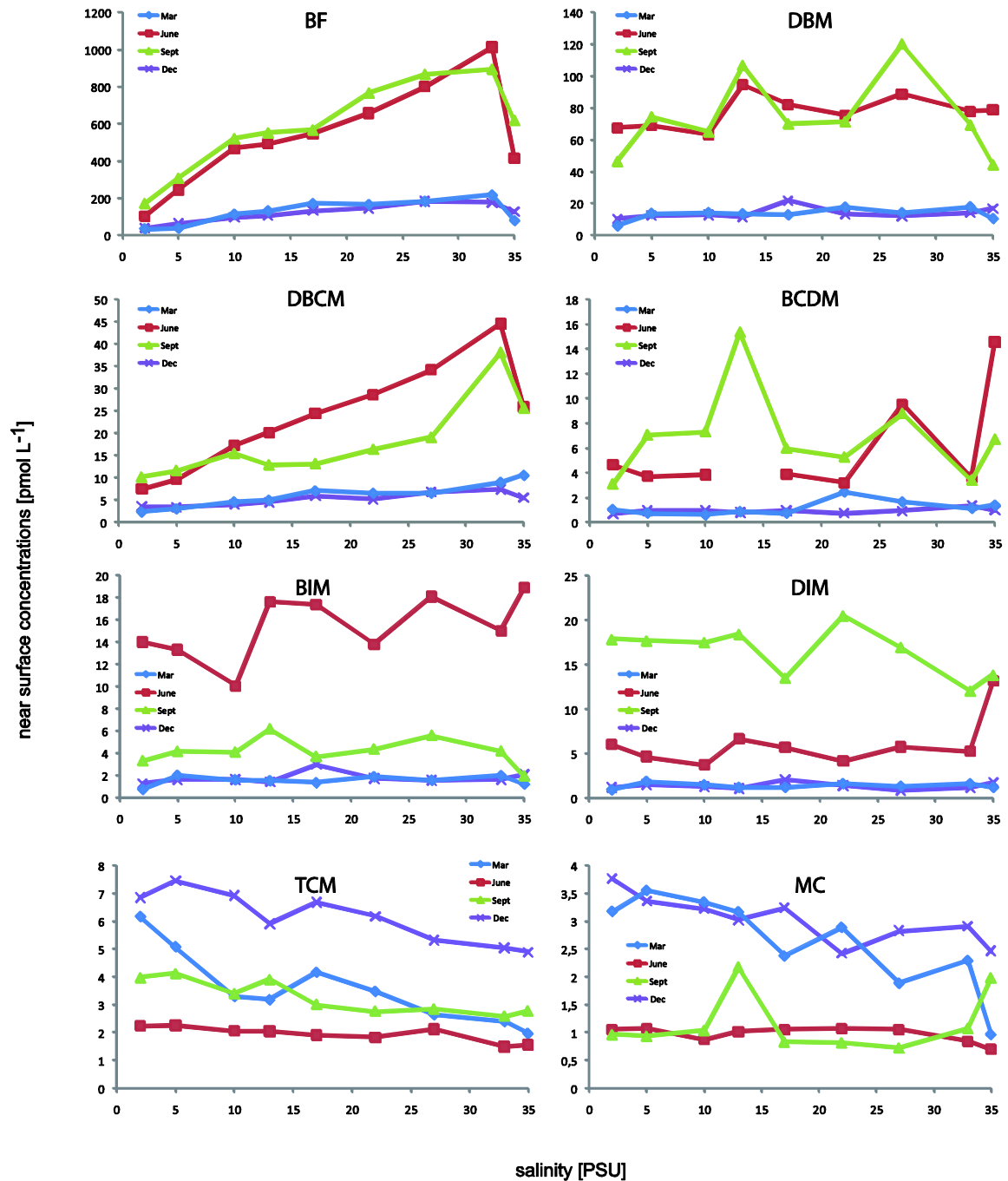


Figure 43. Influence of salinity on VHOC concentrations.

Iodocarbons did not show a clear pattern along the salinity gradient. Those compounds do not have localized sources. Due to low macroalgae cover rates in the inner part of the bay and in the estuary, an additional source must be supposed. As shown by Klick (1992), we can assume that formation of iodocarbons have a phytoplanktonic component.

The Bay of Morlaix is characterized by eutrophication due to large river discharge of nutrients. In contrast, the water body of English Channel range between meso- and oligotrophy and create a distinct nutrient gradient within the bay (see Figure 32). The high nutrient enables high primary production and created two maxima during the field campaign (July-August 2008 and April 2009, see Figure 31). Figure 44 show the pigment concentrations along the salinity gradient for the selected month and enable a direct comparison with Figure 43. Maxima values of Chlorophyll *a* do not show the same pattern than halocarbons. While winter and spring values show a clear gradient towards the estuary, summer values have two maxima (at very low salinities and at mesosaline conditions). Should phytoplankton be a source of VHOCs, formation might be limited to few species. It is therefore possible that high Chlorophyll *a* values are related to a minor VHOC producing species, while the planktonic VHOC producers are distributed differently to the main group of phytoplankton. Alternatively VHOC formation might be depending on physiological conditions of the phytoplankton. Stressed but less dense phytoplankton groups might be more effective VHOC producers.

Phaeopigment emerge from Chlorophyll *a* degradation. As shown in Figure 31, high phaeopigment values are correlated to high Chlorophyll *a* values. It has been shown that macroalgae produce VHOC as an agent against herbivore (Leblanc et al. 2006). Our results do not show a close agreement of high phaeopigment values with maxima of VHOC, thus high VHOC concentrations can not be linked to the presence of grazers.

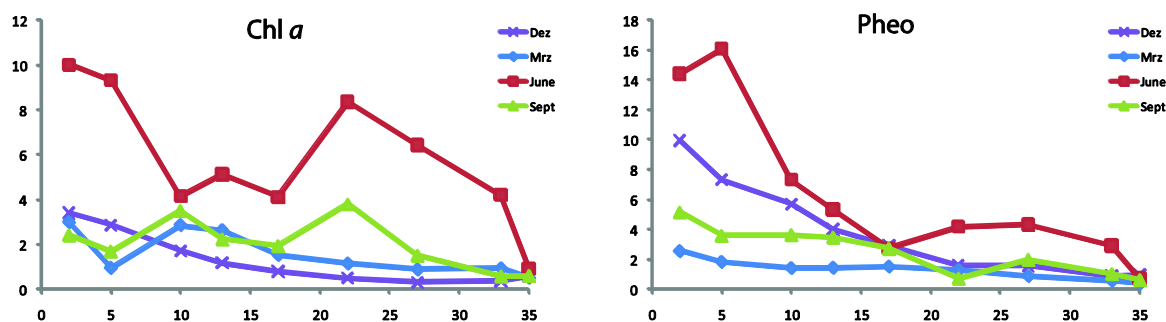


Figure 44. Pigment concentrations [$\mu\text{g L}^{-1}$] along the salinity gradient.

In order to determine common sources for different VHOCS, Spearman's rank coefficients were calculated and shown in Table 18. Highest correlations were obtained in between chlorocarbons ($\rho=0.65$ for methyl chloroform and tetrachloromethane), bromocarbons ($\rho=0.70$ for bromoform and dibromomethane; $\rho=0.79$ for bromoform and dibromochloromethane; $\rho=0.66$ for dibromochloromethane and dibromomethane) and iodocarbons ($\rho=0.65$ for diiodomethane and bromiodomethane). High correlation coefficients indicate similar sources or loss processes.

Table 18. Spearman's Rank Correlation (significance $p<0.01$).*

	IE	MC	TCM	DBM	BDCM	DBC	BIM	BF
MC	-0.26							
TCM	-0.63	0.65						
DBM	0.68	-0.33	-0.55					
BDCM	0.38	-0.26	-0.28	0.35				
DBC	0.55	-0.41	-0.72	0.66	0.34			
BIM	0.63	-0.25	-0.39	0.69	0.47	0.36		
BF	0.62	-0.45	-0.64	0.70	0.37	0.79	0.47	
DIM	0.65	-0.27	-0.47	0.57	0.38	0.40	0.65	0.45

* High correlation coefficients are highlighted and indicate similar sources.

Compounds with high correlations were plotted against each other and shown in Figure 45. Compounds which showed a concentration gradient within the bay were plotted at low and at high concentrations. Bromoform was well correlated with dibromomethane and

dibromochloromethane, respectively. The dibromomethane/bromoform -ratio at those stations was in agreement with the slope calculated by different authors (Carpenter and Liss 2000; Jones et al. 2009). The slope was higher at stations with highest concentrations of those compounds. This indicates a sink for bromoform and/or an additional source of dibromomethane and dibromochloromethane in the inner part of the bay (which reflect stations with lowest concentrations of bromocarbons). It can be speculated that different species with a different metabolism are producing either less bromoform, or, bromocarbons are produced in a different ratio. Alternatively, nucleophilic substitution can be a sink for bromoform and interfere with the bromocarbon ratio. Additionally, different bromocarbons ratios and correlations suggest the idea of a strong and localized source of bromocarbons, which is situated in the northern part of the bay and is likely related to macroalgae beds.

Bromoiodomethane was well correlated with diiodomethane and dibromomethane at all stations. Hence, those compounds have no localized sources and are produced in all parts of the bay. In the case of dibromomethane it was argued above that this halocarbon have a strong source in the north and an additional source in the inner parts of the bay.

Tetrachloromethane and methyl chloroform water concentrations show a gradient in the bay, with higher concentrations in the estuary. Above it was discussed, that air-to-sea flow may be the main source of those chlorocarbons in the bay. The slope at both parts of the bay (estuary and northern extend) are well comparable. This support the idea of a similar source of both gases and in all parts of the bay. A lower correlation coefficient in the estuary may indicate an additional input of one compound.

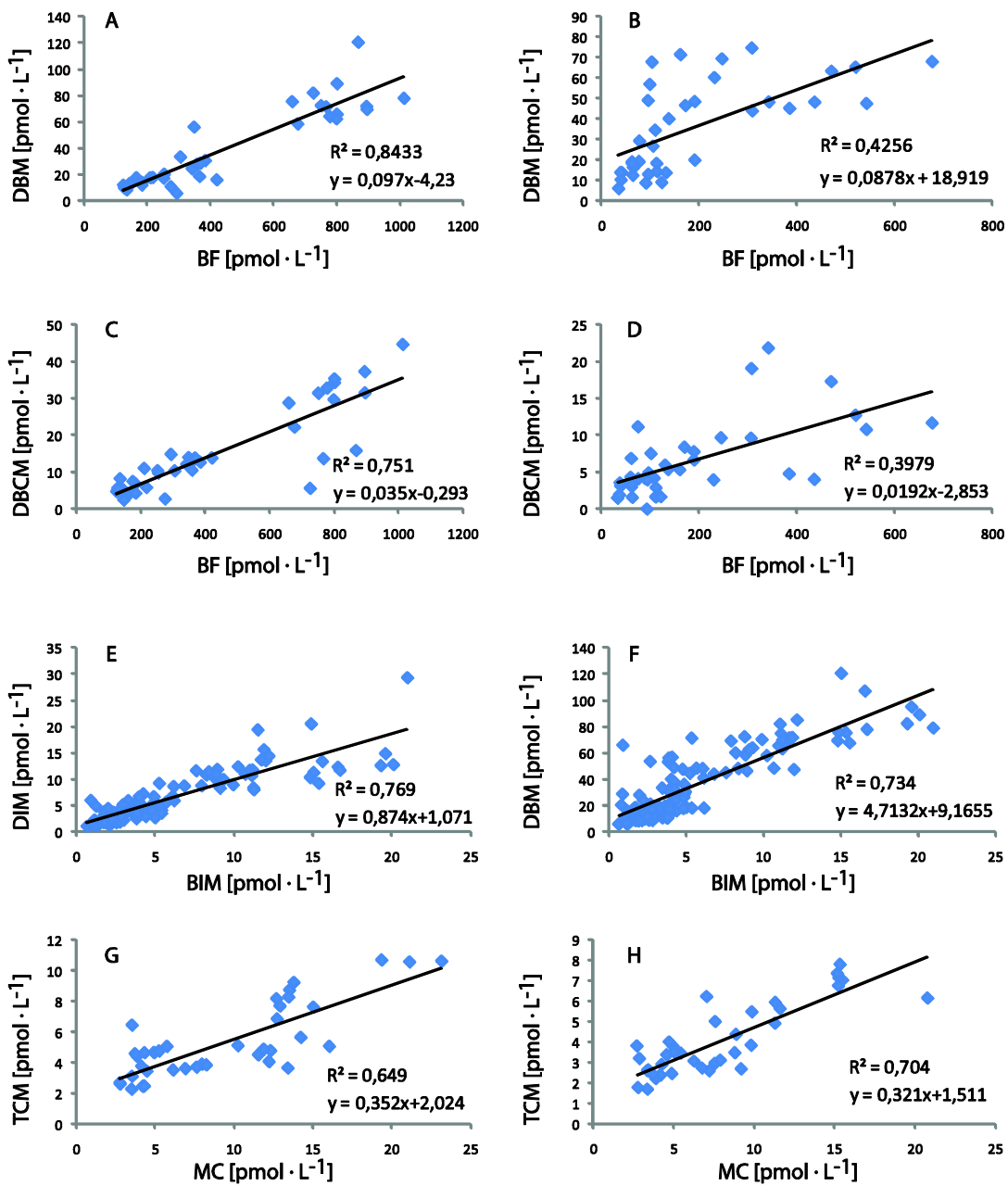


Figure 45. Correlation plots between seawater halocarbon concentrations.

A: Dibromomethane vs bromoform at stations with highest concentrations. B: Dibromomethane vs bromoform at stations with lowest concentrations. C: Dibromochloromethane vs bromoform at stations with highest concentrations. D: Dibromochloromethane vs bromoform at stations with lowest concentrations. E: Diiodomethane vs bromiodomethane at all stations. F: Dibromomethane vs bromiodomethane at all stations. G: Tetrachloromethane vs methyl chloroform at stations with highest concentrations. H: Tetrachloromethane vs methyl chloroform at stations with lowest concentrations.

Mixing of water masses with different origin

As shown in the paragraph above, VHOC can have localized sources. However, variations of VHOC concentrations along the salinity gradient can be explained by an intense tidal mixing, too. Since the Western English Channel is influenced by a large tidal amplitude, water mixes rapidly in the bay. The tidal stream can reach up to $1.5 \text{ m} \cdot \text{s}^{-1}$ during medium spring tide (this value can be higher during extraordinary spring tides and storms). The residence time of water within the inner estuary is depending on river discharge (see Figure 28) and tidal amplitude and varies between two and 13 days (Waeles et al. 2007). Figure 46 illustrates the evolution of surface currents during a half-diurnal tidal cycle.

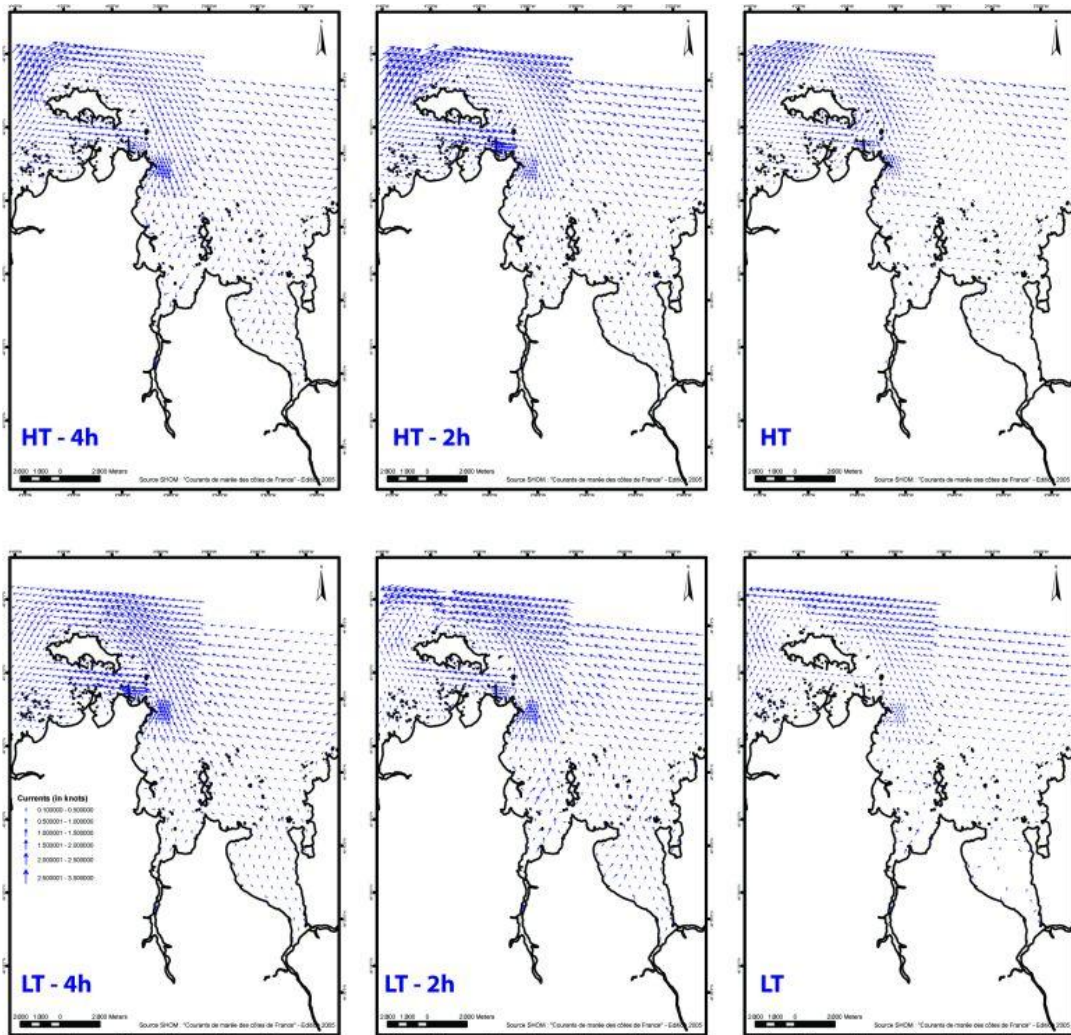


Figure 46. Currents in the Bay of Morlaix.

Model provided by SHOM. HT: High tide. LT: Low tide.

At low tide water masses move eastward, pass the *Île de Batz* and Roscoff and flow in the *Bay of Morlaix*. During the following hours, water flow velocity increases. Then, after high tide water masses flow back westwards. During a tidal cycle, currents are strong in the English Channel and less pronounced in the inner bay. Therefore, measurements at a specific sampling site do not always reflect a local VHOC formation. Water concentrations of VHOCs correspond to the formation and the loss of VHOC in specific water masses which, move forward and backward in the bay and in the estuary. As Figure 46 clearly demonstrates, samples from the *ASTAN* point (at high tide) are highly influenced by coastal (putitative macroalgae) production, mainly by nearshore formation westwards from the sampling station. Concentrations of brominated and iodinated compounds showed generally maxima values at high salinity stations. Those stations were located in the northern and central part of the bay. Lower values were usually measured in samples from low salinity stations, which were located in the inner estuary. Considering the translocation of the water masses, it can be assumed that highest biogenic VHOC formation occurred between the northern extend of the bay and the *Ile de Callot*. It is likely that biogenic-VHOC enriched water masses are pushed in the estuary during incoming high tide and are diluted there.

5.4.5 Sea-air Fluxes

As discussed above, biogenic VHOCs are known to have marine sources. Sea-to-air fluxes of VHOC represent the main sink for numerous halocarbons in the ocean. Those fluxes and their subsequent atmospheric photolysis results in the formation of reactive halocarbons, which have implications on atmospheric chemistry. Bromocarbons are an important source for reactive halocarbons and are accountable for a significant portion of the ozone depletion (Yang et al. 2005). Different authors estimated the global source strength of bromocarbons and focused mainly on bromoform. Nielsen and Douglass (2001) estimated an annual flux of 0.8 to 2.0 Gmol from marine areas towards the atmosphere. This estimate takes into account the marine source strength from atmospheric “background” bromoform mixing ratios and lifetimes. An alternative approach for flux calculations involves measurements of seawater concentrations (Fogelqvist and Krysell 1991; Quack and Wallace 2003), resulting in a global sea-to-air flux estimation of 0.9 to 7.0 Gmol $\text{CHBr}_3 \text{ a}^{-1}$.

Iodocarbons are characterized by short lifetimes and are photolytically degraded in the troposphere, resulting in the formation of reactive iodine atoms, which consequently react in the troposphere with ozone to form iodine oxide (Solomon et al. 1994). Iodine oxide contributes to the formation of particles (Hoffmann et al. 2001) and may play an important role in the formation of cloud condensation nuclei (O'Dowd et al. 2002). Global flux calculations for iodocarbons focused on iodomethane, leading to net emissions estimates of 0.9 to 2.5 Gmol CH₃I a⁻¹ (Moore and Groszko 1999; Bell et al. 2002). It is accepted by various authors that other iodocarbons (such as diiodomethane or bromoiodomethane) contribute to the global iodine flux (Klick and Abrahamsson 1992; Moore and Tokarczyk 1992; Carpenter et al. 1999; Archer et al. 2007). However no global flux calculations are computed for those iodocarbons.

All attempts to calculate global halocarbons emissions were aware of the uncertainties, resulting from limited data of local measurements and their tendency to measure during algae growing season. Our VHOC measurements of air and sea water samples confirm that latter objection: sea-to-air fluxes in the Bay of Morlaix are characterized by a clear seasonality (for selected VHOC see Figure 47). Fluxes of brominated and iodinated compounds are high in summer and show winter minima. Bromoform for instance showed a maximal flux in June 2008 of 6276 nmol m⁻² d⁻¹ (mean of different k_w-approaches), while in January 2009 the bay acted as a sink for bromoform (-27.9 nmol m⁻² d⁻¹). Diiodomethane fluxes towards the atmosphere showed maximum values in July 2008 (50.9 nmol m⁻² d⁻¹) and were reversed in November 2008, February 2009 and Mai 2009 (up to -25.6 nmol m⁻² d⁻¹). Chlorocarbons showed opposite seasonal fluxes. Oceanic methyl chloroform for instance was a source for the atmosphere in winter (4.8 nmol m⁻² d⁻¹ in February 2009). For most the year, surface waters of the bay can be described as sinks (up to -10.9 nmol m⁻² d⁻¹ in May 2009) for atmospheric chlorocarbons. Since elevated VHOC nearshore concentrations are claimed to have a strong (macro)algae source, it can be assumed that seasonality of biogenic VHOCs can be related to (macro)algae physiology: during algae growing season VHOC formation is elevated, while only little VHOC is produced during winter time.

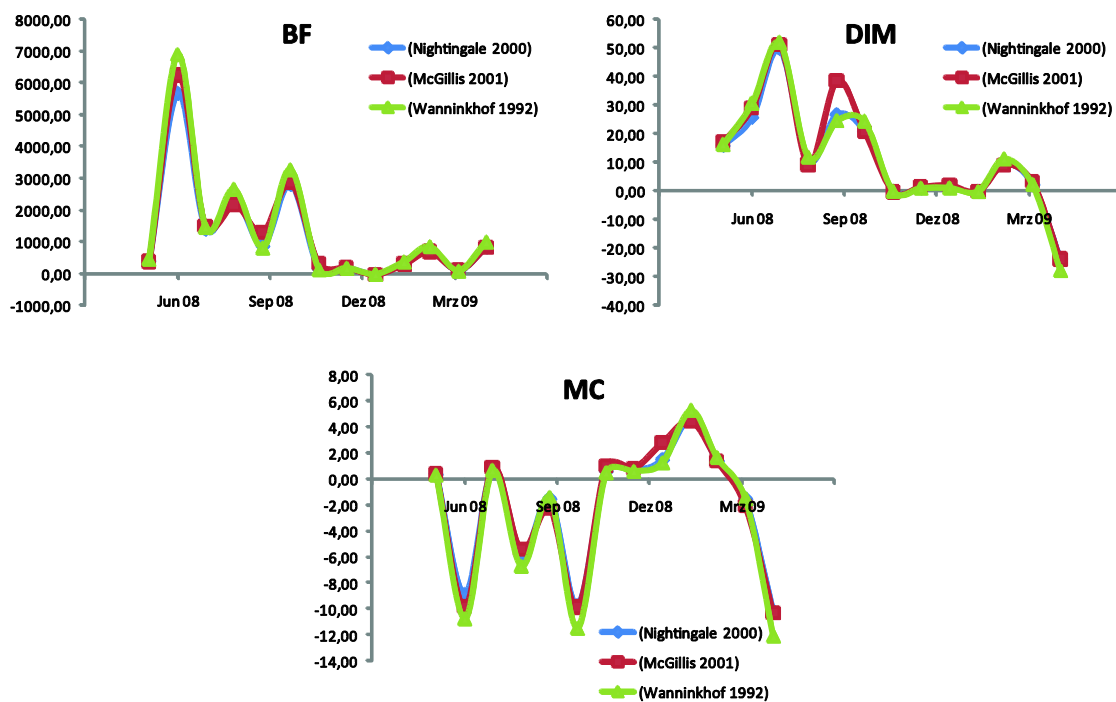


Figure 47. Sea-air flux [$\text{nmol m}^{-2} \text{d}^{-1}$] of selected VHOCS using different parameterization for the transfer velocity.

Sea-to-air fluxes of VHOCS highly depend on wind speed and direction (Figure 27) and vary with different parameterizations. Few studies (e.g. Yokouchi et al. 2001) applied the k_w -parameterization of Wanninkhof (1992). Most recent studies (e.g. Quack et al. 2007a; Hughes et al. 2009) used the approach from Nightingale et al. (2000b) or give results from different parameterizations (e.g. Archer et al. 2007). Since there is no agreement in the literature about single computations for sea-to-air fluxes, we choose to apply three different parameterisations to our data (Nightingale et al. 2000: N00; McGillis et al. 2001: MG01; Wanninkhof 1992: W92). Flux values of those three parameterizations are then directly comparable with other studies. Average sea-to-air fluxes are presented in Table 19 for three different regions in the *Bay of Morlaix*.

Table 19. Average annual daily [$\text{nmol m}^{-2} \text{day}^{-1}$] and total [$\mu\text{mol m}^{-2} \text{yr}^{-1}$] sea-to-air flux in the Bay of Morlaix. *

	35-27 PSU			22-13 PSU			10-02 PSU		
	W92	MG01	N00	W92	MG01	N00	W92	MG01	N00
	average daily sea-to-air flux [$\text{nmol m}^{-2} \text{day}^{-1}$]								
IE	12.8	12.4	11.3	23.7	21.2	20.2	18.5	16.5	16.0
MC	-1.2	-0.9	-1.0	-2.8	-2.4	-2.4	-3.8	-3.3	-3.2
TCM	-10.1	-9.6	-9.0	-14.3	-13.1	-12.4	-14.1	-13.0	-12.3
DBM	158.3	159.2	143.0	271.4	253.9	237.2	201.0	188.0	176.3
BDCM	9.4	9.2	8.5	15.3	13.7	14.0	10.2	8.7	9.2
DBCM	49.2	44.2	42.4	2.2	2.3	-0.4	-41.5	-38.3	-38.3
BIM	13.3	13.0	11.8	22.8	21.1	19.9	12.8	11.7	11.3
BF	1875.4	1808.0	1666.1	2010.5	1826.4	1741.4	490.0	442.3	425.0
DIM	8.9	10.4	8.6	13.4	14.1	12.6	11.9	12.1	11.3
	total sea-to-air flux [$\mu\text{mol m}^{-2} \text{a}^{-1}$]								
IE	5.0	4.9	4.4	9.4	8.4	8.0	7.4	6.6	6.4
MC	-0.5	-0.4	-0.4	-1.1	-1.0	-1.0	-1.5	-1.3	-1.3
TCM	-4.0	-3.8	-3.6	-5.7	-5.2	-4.9	-5.6	-5.2	-4.9
DBM	62.6	62.9	56.5	107.5	100.5	94.0	79.8	74.6	70.0
BDCM	3.7	3.6	3.4	6.1	5.4	5.6	4.1	3.5	3.7
DBCM	19.3	17.4	16.7	0.6	0.6	-0.4	-16.7	-15.4	-15.4
BIM	5.3	5.2	4.7	9.1	8.4	8.0	5.2	4.8	4.6
BF	741.8	714.8	659.3	799.0	725.0	692.2	195.1	175.8	169.2
DIM	3.5	4.1	3.4	5.3	5.6	5.0	4.8	4.8	4.5

* Comparison of different parameterization of the transfer velocity. W92: Wanninkof 1992. MG01: McGillis et al. 2001. N00: Nightingale et al. 2000. Schmidt numbers were calculated using the approach of DeBryn and Saltzman 1997 [for more details see paragraph 2.5].

Comparison of different approaches for transfer velocity clearly show that calculations with N00 resulted in the lowest values. MG01 and W92 values were in average 5% and 13% higher, respectively. The lowest values, given by N00 and the highest values given by W92, provide the range of values for the air-sea exchange of VHOCs in the bay.

The bay acted as a source of brominated and iodinated compounds. Bromoform and dibromomethane had the highest portion on the flux of bromine with a flux average of 79 and $541 \mu\text{mol m}^{-2} \text{a}^{-1}$ for the whole bay. Fluxes of iodocarbons were about one order of magnitude lower than fluxes of dibromomethane. During the field campaign the bay was a net sink for chlorinated compounds ($-0.9 \mu\text{mol m}^{-2} \text{a}^{-1}$ for methyl chloride and $-4.89 \mu\text{mol m}^{-2} \text{a}^{-1}$ for tetrachloromethane). Table 19 shows that fluxes depended largely on the location of the sampling site. Bromoform and dibromochloromethane had the highest fluxes in higher salinities. While marine waters with high salinity were a source for atmospheric dibromochloromethane, fluxes were reversed for those compounds in the estuary. Dibromomethane and

bromodichloromethane as well as iodinated compounds showed the highest fluxes values in medium salinities while at high and low salinities values were lower. Chlorinated compounds, such as tetrachloromethane and methyl chloroform showed highest annual air-to-sea fluxes at low salinities.

Our flux estimates are in agreement with other flux calculations computed for similar regions. Archer et al. (2007) calculated fluxes for iodinated compounds for an estuary in the Western English Channel. The authors calculated a total annual sea-to-air flux of $15.5 \mu\text{mol Iodine m}^{-2}$ and described chloriodomethane (39%), diiodomethane (33%) and iodomethane (22%) as the main components in the iodocarbons pool. Iodoethane (6%) and bromiodomethane (4%) formed a smaller proportion of the iodocarbon pool. Our results generally agree with those findings, but they did not show a prescind proportion of diiodomethane on the pool.

In another study Jones et al. (2009) calculated fluxes for iodo- and bromocarbons arising from air and few sea water samples, taken at Roscoff at high frequency during September 2006. They estimated a mean value of $1800 \text{ nmol m}^{-2} \text{ d}^{-1}$ for bromoform and $7.5 \text{ nmol m}^{-2} \text{ d}^{-1}$ for diiodomethane. While the mean value of bromoform is similar to our results, the value for dibromomethane was one order of magnitude lower compared to our calculations. This may be explained by the different temporal resolution of the measurements, a different habitat, and the different analytical system.

While Jones et al. (2009) sampled continuously during one month between 3 and 27 September 2006, in our work, the temporal resolution was lower (monthly) but with longer time duration (13 months). When comparing Figure 41 and Figure 47. Sea-air flux [$\text{nmol m}^{-2} \text{ d}^{-1}$] of selected VHOC using different parameterization for the transfer velocity. it becomes clear, that high VHOC water concentrations do not necessarily result in high fluxes. Values were high between June and October 2008, with a maximum in July. However high wind speed in June caused a high transfer velocity and resulting in a maximum sea-to-air-flux which was up to 8 times higher than other summer fluxes. In contrast, high concentrations of bromoform in water did not induce a high flux in July 2008. In this case, elevated air concentrations and low wind speed prevented a significant transfer to the atmosphere. The approach of Jones et al. (2009) is well suited for high precision flux determination for a limited time but requires high logistical expenses. Unfortunately, for a seasonal cycle this approach is hardly operable. Thus, better flux estimates can be achieved by an

increase in temporal measurement resolution and might decrease the risk of over- and underestimations due to unusual weather conditions.

In a review of the current literature Quack and Wallace (2003) calculated average sea-to-air fluxes of bromoform for different regions. According to the W92 approximation the authors estimated average global open ocean values of $9 \text{ nmol m}^{-2} \text{ d}^{-1}$ and a global average for near shore fluxes of $2426 \text{ nmol m}^{-2} \text{ d}^{-1}$. However this calculation was based on reported seawater surface concentrations and did not reflect seasonal aspects. Reported seawater concentrations are disproportionately limited to the main growing period of algae and hence suppress low winter fluxes. Sea-to-air fluxes from the *Bay of Morlaix* are highly comparable to near shore fluxes reported from Quack and Wallace (2003), when excluding winter values ($2201 \text{ nmol m}^{-2} \text{ d}^{-1}$ from May 2008 to October 2008 and May 2009; $250 \text{ nmol m}^{-2} \text{ d}^{-1}$ from November 2008 to April 2009).

Quack and Wallace (2003) stated that the narrow near shore regions represent only 0.3% of the global ocean area but contribute for about 23% of the global bromoform emissions. In contrast open ocean regions encompass 88% of the oceanic surface and may account for 29% of the global bromoform emission. Our results indicate that coastal hot spots for bromoform fluxes are restricted to macroalgae beds. It can be speculated that areas with low macroalgae cover, such as estuaries or sandy beaches, show significantly lower fluxes. Thus global estimates need a higher geographical resolution regarding the high productive coastal zones and their diverse habitats.

We showed that water concentrations of iodinated and brominated compounds are elevated during high tide (see Figure 38 and Figure 39). It can be concluded that global fluxes are overestimated when sampling at low tide and fluxes are underestimated when sampling at high tide. For further studies we suggest that measurements should be taken during a complete diurnal tidal cycle to avoid overestimations of fluxes resulting from measurements at low tide and underestimations arising from measurements at high tide.

5.5 Conclusion

All halocarbons displayed a marked seasonality in the *Bay of Morlaix*. Brominated and iodinated compounds showed summer maxima and winter minima. Both groups exhibited elevated concentrations in surface waters during low tide compared to high tide, caused presumably by biological activity. Chlorinated compounds showed winter maxima and summer minima. These annual distribution patterns were related to high air-to-sea fluxes in winter and low summer fluxes. Distinct concentration gradients of bromo- and chlorocarbons revealed the occurrence of high localized sources for both groups. Bromocarbons sources were related to macroalgae beds, whereas chlorocarbons have mostly airborne sources with higher inputs via the river side. The absence of marked concentration gradients of iodocarbons indicates that macroalgae beds in the northern part of the bay play only a minor role in the formation of those gases. Flux calculations revealed that tidal influenced and macroalgae dominated ecosystems contribute significantly to global halogen emissions, especially via bromoform and dibromomethane emissions. As seawater and air concentrations, sea-to-air fluxes showed a marked seasonality.

6 Physiological function of VHOCs for macroalgae

Although the exact purpose of the formation of volatile halocarbons is not fully understood, the idea of a halocarbon involvement in defence reactions in macroalgae is accepted by various authors (Itoh et al. 1997; Palmer et al. 2005; Leblanc et al. 2006; Weinberger et al. 2007; Küpper et al. 2008). Macroalgae inhabits rocky shores in all climates. Due to their sessile character, macroalgae developed defence strategies instead of escape strategies against pathogens. Among other defence strategies, the oxidative burst machinery creates a rapid and effective response to pathogen imminence. The apoplastic enzyme NADPH oxidase generates reactive oxygen species (ROS), such as hydroxyl radicals ($\cdot\text{OH}$), superoxide (O_2^-) or its dismutation product hydrogen peroxide (H_2O_2). Oxidative burst reactions were found in different red algae, including *Eucheuma platycladum* (Collen and Pedersen 1994), *Chondrus crispus* (Bouarab et al. 1999) and *Gracilaria conferta* (Weinberger et al. 1999). Only in the last decade, the oxidative burst machinery were reported in the brown algal species, *Laminaria digitata* (Küpper et al. 2001).

On a cellular level, ROS are released from the apoplast towards the surrounding seawater and have direct and toxic effects on the adversary organism. This early defence reaction is triggered by signal molecules from the grazer, the fouling organism or from components of an attacked neighbouring organism. Thus, Küpper et al. (2001) showed that oligogluluronates elicited the oxygen burst machinery in the kelp *Laminaria digitata*. Recently it was shown that those oligogluluronates also trigger gene expression of enzymes, which play a key role in defence reactions of *L. digitata* (Cosse et al. 2009). Oligogluluronate alginates are oligosaccharides and are the main component of cell wall of heterokontophyta. They are released to the water during digestion of algae material by grazers.

Besides this rapid primary defence reaction, the oxidative burst machinery regulates secondary defence responses that have been mainly documented for terrestrial plants:

- Formation of low molecular weight compounds. Those secondary metabolites have antibiotic qualities and belong to the phytoalexins (Ebel et al. 1995).
- Gene expression of pathogenesis inducing proteins (Fritig et al. 1998).
- Crosslinking of cell wall proteins (Brisson et al. 1994).
- Local limited necrosis (Tenhaken et al. 1995).

- Systemic acquired resistance (Chen et al. 1993).

For algae, the emission of VHOCs is discussed as secondary defence response (Mtolera et al. 1996). In this context, vanadium-dependent haloperoxidases (vHPOs) could play a key role in defence reactions of various algae (Butler and Carter-Franklin 2004). Apoplastic and extracellular vHPOs (linked to the cell wall) are likely to control the accumulation of halide ions. In *L. digitata* for instance, the iodine content can exceed the 30,000 fold concentration of seawater (Küpper et al. 1998). In *L. digitata*, most of iodide ions are located in the apoplast of peripheral tissue (Verhaeghe et al. 2008). The function of the halide ion accumulation is not fully understood. In kelps, iodide could serve as a powerful anti-oxidant pool (Küpper et al. 2008). Figure 48 illustrates the putative role of vHPOs for the control of halide-ion reservoir.

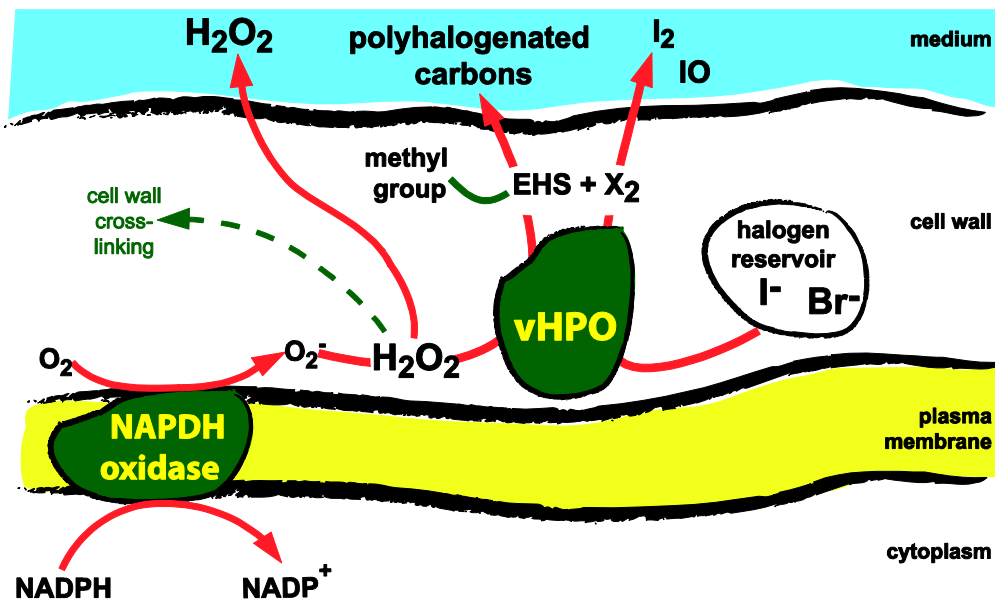


Figure 48. The putative role of vanadium-dependent haloperoxidases (vHPO) in the defence response of kelp.

Figure modified after Cosse (2007) and Verhaeghe et al. (2008). EHS: electrophilic halogen species.

The liberation of halide ions from the apoplast enables the oxidation of ROS. Intracellular ROS can be degraded by those reactions, too. However the extracellular formation of superoxide or hydrogen peroxide is made by the algae itself as a defence reaction. A drawback on ROS

formation is their limited life time. Hydrogen peroxide can be “transformed” in a more stable and very effective antibiotic detergent: In the presence of hydrogen peroxide, haloperoxidases oxidize halides and form electrophilic halogen species (XOH , X_2 , X_3^-). In a second step, those halogen intermediates react with methyl groups and form polyhalogenated carbons, which are relatively stable. The elevated release of VHOC during low tide can be discussed as a stress response to the exposure of seaweed to air (Pedersen et al. 1996; Bondu et al. 2008). Alternatively it can be discussed that VHOC are used to “impregnate” the cell wall. VHOC are highly hydrophobic and might be attached to the surface of the cell wall. During low tide and due to their volatility, VHOCs diffuse into the gas phase (atmosphere).

VHOC formation conditions are poorly investigated. This work highlights the role of plant-plant communication and their influence on VHOC formation. We show that the oligoguronates poly- α -1,4-L-guluronic acid (referred to as GG) trigger the formation of VHOC. Moreover we demonstrate that plant-plant communication orchestrates the formation of VHOCs: “forewarn” algae react less intense after perception of the GG signal. As far as VHOC are concerned, we conclude that this process might be beneficial for the algae in terms of cost efficiency.

The following paragraphs contain a publication from François Thomas et al. which was recently submitted in *New Phytologist*.

Waterborne signaling primes the expression of defense genes and buffers the elicitor-induced oxidative responses of the brown alga *Laminaria digitata*.

François Thomas^{1,2}, Audrey Cosse^{1,2}, Sophie Goulitquer³, Stefan Raimund^{4,5}, Pascal Morin^{4,5}, Catherine Leblanc^{1,2} and Philippe Potin^{1,2*}

¹UPMC Univ Paris 6, UMR 7139 Végétaux marins et Biomolécules, Station Biologique, F 29682, Roscoff, France

²CNRS, UMR 7139 Végétaux marins et Biomolécules, Station Biologique, F 29682, Roscoff, France

³Laboratoire de Biochimie « Epissage, Lipides, Cancer et Apoptose », INSERM U613, Faculté de Médecine, F-29285, Brest, France

⁴UPMC Univ Paris 6, UMR7144 Adaptation et Diversité en Milieu Marin, Station Biologique, F 29682, Roscoff, France

⁵CNRS, UMR 7144 Adaptation et Diversité en Milieu Marin, Station Biologique, F 29682, Roscoff, France

*Corresponding author: Dr Philippe POTIN

UMR 7139 CNRS/UPMC-Paris6, Station Biologique,

BP74, 29682 ROSCOFF Cedex, France

6.1 Summary

Like land plants, algae defend themselves upon biotic stress. Until now, there has been a lack of data concerning the occurrence of inter-individual communication, the so-called priming effect. This study aims to gain insight into the early steps of the defense responses of large marine brown algae (kelps), both in the laboratory and in the field and to investigate their potential to spread a warning message toward neighboring algae.

We compared the early responses of laboratory-grown and wild sporophytes of the brown alga *Laminaria digitata* upon elicitation with oligoguluronates. We followed the release of H₂O₂ and volatile organic compounds in the medium after elicitation. We used reverse transcription –

quantitative polymerase chain reaction (RT-qPCR) to monitor the kinetics of ten defense genes following the oxidative burst. Laboratory-grown algae were transplanted in natural habitats in order to reacclimate them and further evaluate how it affected their responses to elicitation. A novel conditioning procedure was further established to mimic field conditions in the laboratory.

Our experiments showed that *L. digitata* integrates waterborne cues released in the field and from elicited neighboring plants. It enhanced the management of the oxidative burst and volatile emissions, and potentiates algae for faster and stronger induction of specific defense genes.

Thus, waterborne signals shape the defense responses of kelps in nature through a priming effect, with important ecological consequences at the community level.

6.2 Introduction

In terrestrial plants, long-distance signaling mediating induced resistance against herbivores and pathogens was recently shown to be not only borne by systemic signals transported in the vascular system, but also caused by volatile compounds that move in the headspace outside the plant (Frost *et al.* 2007, Heil & Ton, 2008). Among these compounds, green-leaf volatiles and other herbivore-induced volatile organic compounds (VOCs) can mediate the systemic response of plants to local herbivore damage (Karban *et al.*, 2006; Frost *et al.*, 2007; Heil & Silva Bueno, 2007). Since such VOCs diffuse in the air, they may also reach neighboring plants and allow "plant-plant communication," which was reported first about 25 years ago in trees (Baldwin & Schutz, 1983; Baldwin *et al.* 2006) and is now a phenomenon described in numerous taxonomically unrelated plants (reviewed in Yi *et al.*, 2009). This inter-plant communication is reminiscent of the potentiation of defense responses in animals (Hayes *et al.*, 1995), a so-called primed state that is associated with a better or faster induction of defense upon biotic or abiotic stress.

In the marine aquatic environment, the exposure to air is time-limited and restricted to intertidal seaweeds. Therefore waterborne signaling has been hypothesized to represent the counterpart of airborne signaling. Waterborne signals from predators or predator-wounded conspecifics that can induce defensive changes in aquatic prey animals are well documented, especially in freshwater ecosystems (Vos *et al.* 2006, Van Donk 2007). In marine benthic communities, this type of

communication has been reported in rockweed (*Ascophyllum nodosum*), a common brown macroalga of North-Atlantic rocky shores, when it interacts with an herbivorous snail (Toth & Pavia 2000, Coleman *et al.*, 2007) and in other species of fucoids challenged with crustacean grazers (Rhode *et al.*, 2004, Haavisto *et al.*, 2009). However, only a direct induction of defenses has been shown to date. Furthermore, the fascinating challenge that remains is to delineate the steps that lead from the perception of these infochemicals to the actual defense response (Toth & Pavia 2000), which may express its features only after a secondary attack.

In comparison with the current knowledge on the transcriptional responses involved in the defense to attack by pathogens or herbivores in terrestrial plants, the changes in gene expression that lead to induced resistance phenomena has been hardly investigated in marine multicellular algae (Cosse *et al.*, 2008). Among the various traits that are expressed *de novo* or at much higher intensities to reduce or prevent further damage, the oxidative burst related responses (Potin 2008) and the activation of the synthesis of secondary metabolites (Pelletreau & Targett 2008, Lane & Kubanek 2008) have been most reported in the recent years.

The kelp *Laminaria digitata* provides an interesting marine algal model to study the defense responses and immunity traits in a eukaryotic lineage evolutionarily distant from plants and animals (Baldauf, 2003). Recognition of elicitors such as oligoguluronates (GGs), fragments of its major cell wall component (the polysaccharide alginate) that are possibly released during attack by pathogenic bacteria or herbivores, initiates a cascade of signaling events and leads to an oxidative burst (Küpper *et al.*, 2001) and pest resistance (Küpper *et al.*, 2002). Cosse *et al.* (2009) recently reported that GGs also induce a set of defense genes in *L. digitata*. It provided the first markers to monitor specific gene expression over time during elicitor-induced defense response in a macroalga. In addition, in response to both biotic (i.e. GG-perception) and abiotic oxidative stress, *L. digitata* naturally emits volatile aldehydes (Goullitquer *et al.*, 2009) and halocarbons (Palmer *et al.*, 2005) that are chemically related to VOCs which prime defense responses in terrestrial plants (Frost *et al.*, 2007; Ton *et al.*, 2007; Heil & Ton, 2008, Yi *et al.*, 2009).

Most of this knowledge on the responses induced by GGs was obtained on either laboratory-grown young sporophytes of about 5-15 cms in length or on sporophytes of similar size harvested from wild populations and reacclimated for a few days in laboratory controlled conditions (Küpper *et al.*, 2001; 2002; Cosse *et al.*, 2009; Goullitquer *et al.*, 2009; Palmer *et al.*, 2005). Most

experimental conditions involved the direct challenge of triplicates of a single plantlet without precise assumptions of the different origins of the material. A careful re-examination of these responses, integrating cell and gene-regulated mechanisms, in distinct and reliable physiological conditions is therefore required to better understand the ecological significance of defenses. Importantly also, now that gene defense markers are available, the search for waterborne, distance signaling is most accessible (Cosse *et al.*, 2009) and volatile aldehydes and halocarbons (Goulitquer *et al.*, 2009; Palmer *et al.*, 2005) are excellent candidates as communication molecules in kelps.

In this context, this study aims to gain insight into the early steps of the defense responses of kelps, both in the laboratory and in the field and to investigate their potential to spread a warning message toward neighboring algae. A first level consisted in comparing the oxidative burst induced by elicitation in laboratory-grown and freshly harvested or laboratory-acclimated wild sporophytes. The kinetics of expression of a set of ten defense genes specifically regulated following a GG elicitation was monitored by reverse transcription-quantitative polymerase chain reaction (RT-qPCR). Laboratory-grown algae were transplanted in natural habitats in order to reacclimate them and further evaluate how it affected their responses to elicitation. The effects of this transplantation were mimicked by a novel conditioning procedure in the laboratory based on co-incubation of naive “target” *L. digitata* sporophytes with “source” sporophytes that had previously been challenged with GGs (“conditioning pre-treatment”) or not (“control pre-treatment”). The results of oxidative burst monitoring, VOC measurements and gene expression studies strongly support the occurrence of stress-related waterborne communication in natural population of kelps.

6.3 Material and Methods

6.3.1 Algal material and elicitation procedures.

Young *Laminaria digitata* thalli were collected from the field (“wild sporophytes”) in two populations distant from 8 kilometers at Pointe Sainte Barbe (+48° 43' 3564, -3° 58' 697, Roscoff, Brittany, France) and Ile de Sieck (+48° 42' 2469, -4° 3' 5984, Santec). If not used immediately, they were maintained at 14°C in filtered seawater (FSW) as described in Cosse *et al.*, (2009).

Laboratory-grown sporophytes were obtained from unialgal cultures grown from meiospores taken from mature wild sporophytes collected in the same populations. Developing sporophytes were then transferred to larger flasks after 2 wk and grown with weekly changes of culture medium until they reached a size of c. 4–6 cm as previously described (Cosse *et al.*, 2009). Oligoguluronates (GGs) were prepared by acid hydrolysis of sodium alginate from *Laminaria hyperborea* (Danisco) according to Haug *et al.*, (1974) and used at a concentration of 100 $\mu\text{g}\cdot\text{mL}^{-1}$. Hydrogen peroxide concentrations in the seawater were monitored by luminometry as in Küpper *et al.*, (2001).

6.3.2 Conditioning procedure in the laboratory

Figure S1 shows the detailed design of the laboratory conditioning procedure. “Source” sporophytes were elicited by application of GG in FSW for 10 min, and rinsed twice to remove traces of elicitors. Control source sporophytes without elicitation were handled in the same way. Control and conditioned “target” sporophytes (ca. 0.2 – 1 g in weight) were introduced in Petri dishes (\varnothing 140 mm, 150 mL FSW) under agitation together with non-elicited or elicited source algae, respectively. After 24 hours, each target sporophyte was transferred to a new Petri dish for further experiments. Conditioned and control target sporophytes were elicited separately in 50 mL of FSW, and H_2O_2 concentrations were followed by luminometry. Seawater was sampled after 1 h to measure VOCs. Tissues were frozen in liquid nitrogen and stored at -80°C until RNA extraction.

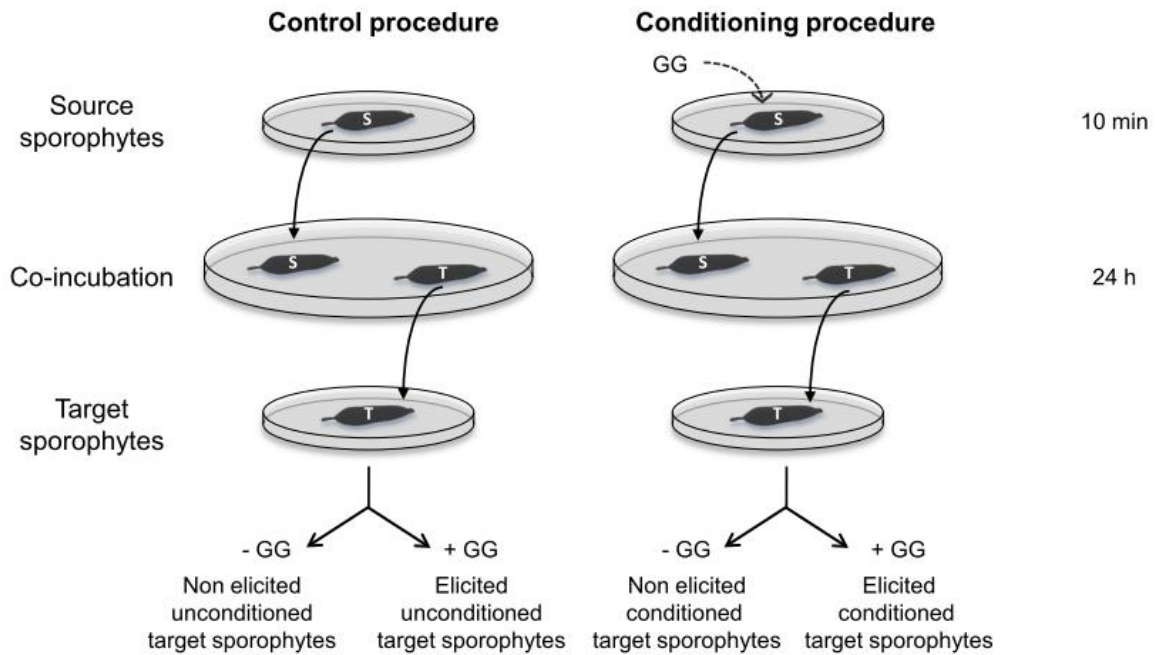


Figure S1: Design of the laboratory conditioning procedure. S: "Source" sporophytes which might produce a waterborne signal. T: "Target" sporophytes which receive a waterborne signal.

6.3.3 Transient transplantation in the field

The experiments took place at Pointe Sainte Barbe (Roscoff) in November 2007 and April 2008. Laboratory-grown sporophytes were introduced in tide pools using either a sealed transparent plastic bag filled with FSW or a nylon net allowing direct contact with natural seawater. After 1.5 h or 24h, laboratory-grown and wild sporophytes collected in the same kelp bed were taken back to the laboratory for further experiments.

6.3.4 Aldehydes and volatile halogenated organic compounds (VHOCs) measurements

Aldehydes were extracted from 25 mL seawater samples and analyzed according to Goulitquer et al., (2009). VHOC concentrations in seawater were determined as in Pruvost et al., (1999) with modifications. VHOCs were separated by purging with a purge-flow of $90 \text{ mL} \cdot \text{min}^{-1}$ ultra-pure nitrogen for 20 min, focused on a glass bead trap (Grace, DMCS treated, 80/100 mesh) at -120°C and subsequently injected by thermodesorption (100°C , backflush). VHOCs were identified and quantified by comparison with known standard solutions (Ultra Scientific and Supelco).

6.3.5 RNA extraction and RT-qPCR

Total RNA was extracted using an adapted protocol from Apt *et al.*, (1995) and treated with Turbo DNase (Ambion, Huntingdon, UK). 400 ng were reverse-transcribed using 2 μ L of RT Improm II (Promega, Madison, USA) and quantitative PCR was performed as in Cosse *et al.*, (2009).

6.4 Results

6.4.1 Wild and laboratory-grown algae display different defense responses

To investigate whether the containment in a laboratory could modify the defense patterns of algae, we compared the defense responses of laboratory-grown sporophytes of *L. digitata* and wild sporophytes of similar size freshly collected from the field. First, we followed the oxidative response induced by elicitation with oligoguluronates (GG) (Figure 1a).

In both types of algae, the challenge with GG was rapidly followed by an oxidative burst (within 10-15 minutes). Laboratory-grown sporophytes accumulated up to $6.26 \pm 0.46 \mu\text{mol.g}^{-1}$ FW of hydrogen peroxide 45 min after elicitation. In comparison, wild sporophytes produced a 30 times less intense oxidative burst ($p < 0.05$), reaching $0.22 \pm 0.15 \mu\text{mol.g}^{-1}$ FW of H_2O_2 ; it went back to the initial level within 40 min. In the same experiment, we profiled the expression kinetics of six previously identified defense-related genes, namely two thioredoxins (*prx* and *trx*), a key enzyme from the pentose phosphate pathway (glucose-6-phosphate dehydrogenase, *g6pd*), a mannitol-1-phosphate dehydrogenase (*mtld*) and two haloperoxidases (*ipo3* and *bpo3*). Figure 1b reports the fold variations of the gene expression after elicitation compared to unelicited sporophytes. In laboratory-grown sporophytes, *trx* and *bpo3* were induced and their expression was maximal 6 and 12 hours after elicitation, respectively. In wild sporophytes, the expression of the six defense marker genes was induced and maximal three hours after elicitation, getting back to the control level within 6 to 12 hours.

We elicited wild *L. digitata* sporophytes collected from the field either immediately, or after 2, 4, 5 and 8 days of incubation in FSW in the laboratory. The longer wild sporophytes had stayed in the laboratory, the more intense their oxidative response was (Figure 1c). Four days of incubation in FSW were sufficient to increase the accumulation of H_2O_2 by 165%, and it reached 400% after 5 days (Student's *t*-test, $P = 0.05$).

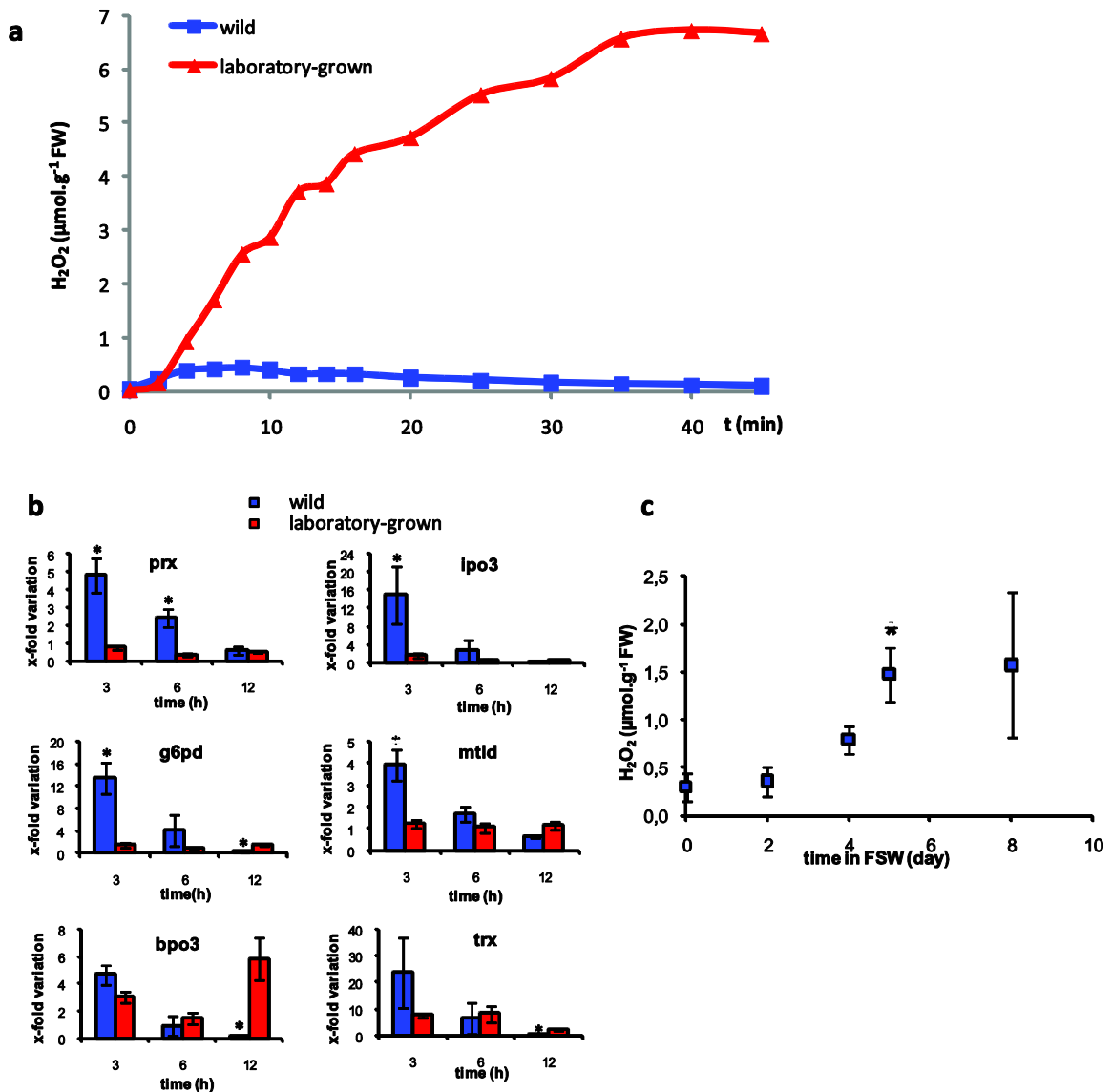


Figure 1: Defense patterns in laboratory-grown *L. digitata* are different from wild sporophytes.

a. Laboratory-grown and wild *Laminaria digitata* sporophytes were elicited with oligoguluronates in seawater and the concentration of H₂O₂ was recorded. Experiments were replicated three times and typical results are shown.

b. Kinetics of defense-related gene expression in laboratory-grown and harvested wild *L. digitata* sporophytes. Asterisk (*) denotes a significant difference between wild and laboratory-grown sporophytes at $\alpha = 5\%$.

c. Values of the maximum of H₂O₂ released during the oxidative burst by wild *L. digitata* sporophytes elicited either immediately after the harvest from their natural habitats or after laboratory incubation in FSW. Values were compared to $t = 0$ with t test (*, $P \leq 0.05$).

6.4.2 Effect of transient transplantation

To test whether the natural environment shapes the defense responses of *L. digitata*, laboratory-grown sporophytes were reintroduced for 1.5h in a net into a natural kelp bed to allow a direct contact with the environment, and taken back to the laboratory to analyze their response to an elicitation. As a control, laboratory-grown sporophytes were introduced into the same kelp bed in a sealed transparent plastic bag filled with filtered seawater (FSW) to prevent contact with water from the field. When taken back to the laboratory, upon challenge with GGs, the intensity of their oxidative burst reached $4.71 \pm 0.47 \mu\text{mol H}_2\text{O}_2 \cdot \text{g}^{-1} \text{FW}$ (Figure 2a) and was not significantly different from the one of algae that had stayed in the laboratory (Tukey-Kramer test, $P = 0.1$, $n = 3$). In contrast, the sporophytes reintroduced for 1.5h in a net displayed an oxidative burst reaching only $1.84 \pm 0.31 \mu\text{mol H}_2\text{O}_2 \cdot \text{g}^{-1} \text{FW}$ (Figure 2a), which represents 3-fold lower concentrations compared to algae from the same batch that had stayed in laboratory conditions. These experiments were repeated with longer transplantation periods of 24 h with similar trends. RT-qPCR was used to follow the gene expression three hours after the GG challenge (Figure 2b). In these laboratory-grown *L. digitata* that had stayed in the field in a net, the elicitation induced the expression of *g6pd*, *gst54*, *mtld*, *ipo3* and *bpo3* (between 1.5 and 3-fold variation compared to unelicited controls) and of *trx* in a higher extent (9-fold variation). In laboratory-grown *L. digitata* that had stayed in the field in a sealed plastic bag, the elicitation induced the expression of only *bpo3* and *trx* (3 and 5-fold variations compared to unelicited control, respectively). Contrarily to algae directly exposed to natural seawater, the expression of *g6pd*, *gst54*, *mtld* and *ipo3* was not induced (Figure 2b).

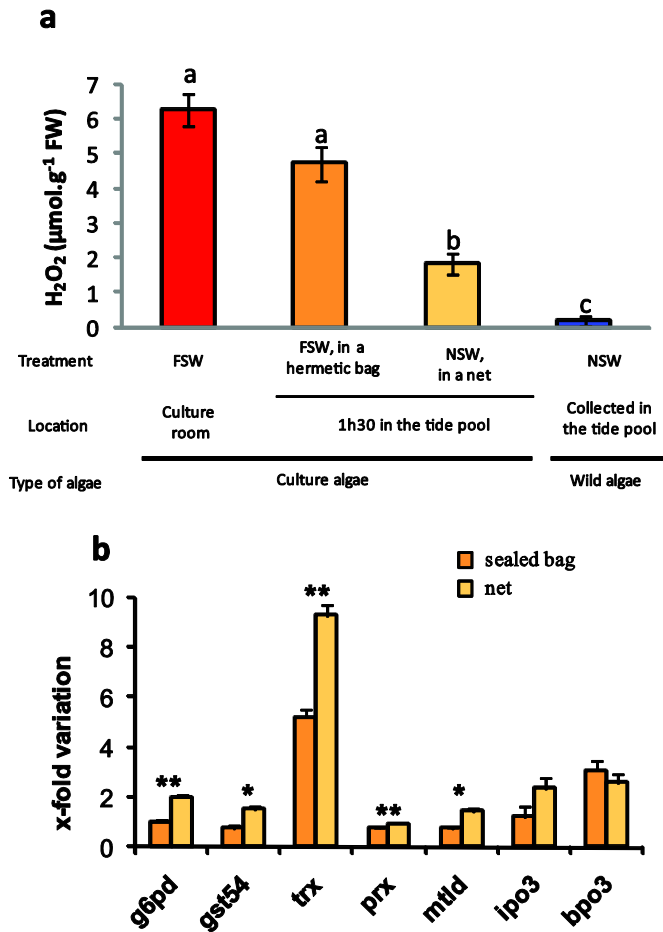


Figure 2: A primed state in laboratory-grown *L. digitata* sporophytes transferred to the field. Laboratory-grown sporophytes were kept in filtered seawater (FSW) in the laboratory (red) or transferred to a kelp bed, either in a sealed plastic bag filled with FSW (orange) or in a net allowing direct contact with natural seawater (NSW) (yellow). Wild sporophytes were harvested from the same kelp bed (blue). Algae were taken back to the laboratory and elicited with GGs. Values are mean \pm s.e.m. (n = 3).

a. Values of the maximum amount of H₂O₂ detected in the medium after elicitation in laboratory-grown, transferred for 1.5 h and wild-type *L. digitata* sporophytes. Letters denote a significant difference between groups as tested with the Tukey-Kramer test ($\alpha = 5\%$).

b. Expression of defense-related genes in laboratory-grown *L. digitata* sporophytes transplanted for 24 h or not in the field and later elicited with GGs for 3 h. Data were analysed for significant differences using a t-test (*, $P \leq 0.05$; **, $P \leq 0.01$).

6.4.3 Development of a conditioning procedure in the laboratory

We developed an original laboratory assay to further elucidate the phenomenon responsible for the discrepancy observed between wild and laboratory-grown sporophytes and the effect of transplantation in the field. Briefly, the principle was based on co-incubation of naive “target” *L. digitata* sporophytes with “source” sporophytes that had previously been challenged with GGs (“conditioning pre-treatment”) or not (“control pre-treatment”, see Figure S1 in Supp. Info. for details on experimental methods). After these treatments, target sporophytes were transferred alone into fresh filtered seawater and further experiments were conducted to characterize their defense responses. Neither the conditioned sporophytes nor the controls constitutively produced extracellular H₂O₂ (data not shown). A challenge with GGs triggered an oxidative burst in both conditioned and control sporophytes (Figure 3). However, maximum H₂O₂ accumulation was reached significantly earlier in conditioned sporophytes than in controls, after 7.7 ± 0.6 min and 12.0 ± 1.0 min, respectively (*t*-test, *P* = 0.031). External H₂O₂ concentrations tended to be lower in elicited conditioned sporophytes.

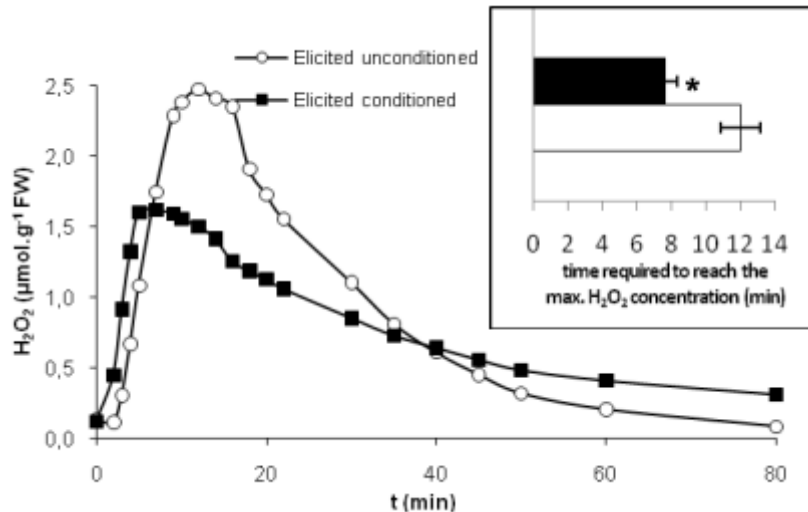


Figure 3: The GG-induced oxidative burst is detoxified faster in conditioned *L. digitata* sporophytes. Unconditioned and conditioned *L. digitata* sporophytes were elicited with oligoguluronates in seawater and the concentration of H₂O₂ was recorded. Experiments were replicated three times and typical results are shown. Inset: Time required to reach maximum H₂O₂ concentrations in the medium after elicitation. Values are mean ± s.e.m (n=3). Data were analyzed for significant difference with *t* test (*, *P* ≤ 0.05).

Using real-time quantitative PCR (RT-qPCR), we measured the relative transcript levels of 10 defense-related genes, namely two thioredoxins (*prx* and *trx*), two enzymes from the pentose phosphate pathway (*g6pd* and *6pgd*), three haloperoxidases (*ipo1*, *ipo3* and *bpo3*), the heat shock protein *hsp70*, a glutathione S transferase (*gst19*) and a methionine sulfoxide reductase (*msr*). Before challenging with GGs, the transcript levels were not significantly different in control and conditioned target sporophytes (*t*-test, $P > 0.40$, $n = 3$, see Table 1).

Table 1. Transcript levels of defense-related genes in conditioned and unconditioned *L. digitata* sporophytes, before elicitation. Values are mean \pm s.e.m. ($n = 3$).

	Transcripts level before elicitation		
	Control	Conditioning	Student test
	pre-treatment	pre-treatment	p-value
<i>trx</i>	0.018 \pm 0.009	0.016 \pm 0.009	0.88
<i>prx</i>	0.550 \pm 0.099	0.462 \pm 0.037	0.47
<i>g6pd</i>	0.395 \pm 0.138	0.280 \pm 0.112	0.55
<i>6pgd</i>	0.069 \pm 0.034	0.048 \pm 0.015	0.88
<i>ipo1</i>	0.094 \pm 0.033	0.068 \pm 0.037	0.51
<i>bpo1</i>	0.593 \pm 0.311	0.462 \pm 0.231	0.63
<i>bpo3</i>	0.034 \pm 0.015	0.022 \pm 0.016	0.43
<i>hsp70</i>	0.378 \pm 0.118	0.319 \pm 0.190	0.55
<i>gst19</i>	0.028 \pm 0.25	0.012 \pm 0.010	0.90
<i>msr</i>	0.010 \pm 0.004	0.013 \pm 0.007	0.88

However, depending on the pre-treatment, target sporophytes showed different response to elicitation. After the GG challenge, seven genes were significantly induced in conditioned sporophytes compared to five in unconditioned sporophytes considering all time points of the kinetic (Table 1). Induction reached higher levels in the conditioned sporophytes for the genes *trx*, *6pgd*, *bpo3*, *hsp70*, *msr* and three of them (*6pgd*, *bpo3*, *msr*) were induced earlier than in the unconditioned sporophytes. Thus, overall, the up-regulation of the defense-related transcriptome seems to be accelerated, as indicated by the greater number of significantly induced genes 1h30

after elicitation in conditioned algae compared to this number after 6 hours in control algae (Table 2, bottom line).

Table 2: Change in transcript levels of defense-related genes in conditioned and unconditioned *L. digitata* sporophytes, after elicitation with GGs in comparison to initial state

Genes	Elicited unconditioned sporophytes			Elicited conditioned sporophytes		
	1.5 h after elicitation	3 h after elicitation	6 h after elicitation	1.5 h after elicitation	3 h after elicitation	6 h after elicitation
<i>trx</i>	22.4 ± 7.3 P = 0.008	19.1 ± 6.5 P = 0.007	5.2 ± 0.5 P = 0.048	38.2 ± 6.3 P = 0.002	22.1 ± 4.6 P = 0.007	5.5 ± 0.5 P = 0.048
<i>prx</i>	1.0 ± 0.1 P = 0.491	1.0 ± 0.1 P = 0.495	0.6 ± 0.1 P = 0.049	1.3 ± 0.2 P = 0.099	1.2 ± 0.2 P = 0.163	0.9 ± 0.1 P = 0.203
<i>g6pd</i>	1.3 ± 0.4 P = 0.292	0.7 ± 0.2 P = 0.276	1.3 ± 0.4 P = 0.283	2.7 ± 0.9 P = 0.102	1.9 ± 0.3 P = 0.165	1.6 ± 1.0 P = 0.360
<i>6pgd</i>	1.1 ± 0.4 P = 0.353	nd	2.7 ± 0.6 P = 0.070	4.8 ± 1.8 P = 0.022	3.8 ± 2.2 P = 0.084	1.0 ± 0.1 P = 0.371
<i>ipo1</i>	1.7 ± 0.8 P = 0.357	0.5 ± 0.1 P = 0.108	0.3 ± 0.1 P = 0.052	3.0 ± 0.7 P = 0.045	0.5 ± 0.2 P = 0.288	0.5 ± 0.1 P = 0.193
<i>bpo1</i>	1.7 ± 0.7 P = 0.227	0.5 ± 0.1 P = 0.296	1.9 ± 1.1 P = 0.248	2.2 ± 0.8 P = 0.171	0.8 ± 0.0 P = 0.348	0.8 ± 0.3 P = 0.394
<i>bpo3</i>	2.6 ± 1.0 P = 0.160	2.1 ± 0.8 P = 0.132	3.4 ± 0.6 P = 0.034	4.4 ± 1.8 P = 0.079	4.3 ± 3.9 P = 0.242	2.4 ± 0.8 P = 0.105
<i>hsp70</i>	4.1 ± 1.5 P = 0.027	13.3 ± 2.8 P = 0.001	6.6 ± 0.6 P = 0.002	7.0 ± 2.0 P = 0.016	17.0 ± 5.5 P = 0.018	7.5 ± 0.6 P = 0.031
<i>gst19</i>	3.0 ± 0.3 P = 0.124	2.3 ± 1.3 P = 0.125	4.3 ± 2.7 P = 0.090	6.6 ± 2.9 P = 0.046	2.3 ± 1.5 P = 0.184	2.8 ± 1.0 P = 0.090
<i>msr</i>	1.0 ± 0.4 P = 0.358	1.6 ± 0.4 P = 0.019	0.5 ± 0.2 P = 0.347	2.5 ± 0.4 P = 0.052	5.5 ± 2.3 P = 0.046	1.1 ± 0.1 P = 0.256
number of induced genes	2	3	4	7	3	2

Conditioned and control *L. digitata* sporophytes were challenged with GGs as elicitors. Transcript levels were quantified by RT-qPCR before elicitation (t = 0) and after 1.5 h, 3 h and 6 h for 10 defense-related genes, namely a thioredoxin (*trx*), a peroxiredoxin (*prx*), a glucose-6-phosphate dehydrogenase (*g6pd*), a 6-phosphogluconate dehydrogenase (*6pgd*), a iodoperoxidase (*ipo1*), two bromoperoxidases (*bpo1* and *bpo3*), a heat shock protein (*hsp70*), a glutathione-S-transferase (*gst19*) and a methionine sulfoxide reductase (*msr*) genes. Values are means ± s.e.m. (n = 3) of the fold changes in relative transcript levels after elicitation compared to t = 0. P-values are the results of Student's t-tests; values in bold represent a significant difference of the expression level compared to t = 0 (α = 8%). Gray cells denote a significantly different fold variation compared to elicited unconditioned sporophytes for the same time period (median test, α = 8%). Abbreviations: nd, not determined.

6.4.4 The conditioning procedure down-regulated the oligogulonates-induced release of VOCs

We applied this novel conditioning procedure to further explore other early responses of the conditioned and unconditioned *L. digitata* sporophytes. We monitored the release of volatile organic compounds (VOCs) in the seawater surrounding target sporophytes one hour after GG-elicitation. Elicitation of unconditioned sporophytes enhanced the emission of most VOCs measured (Figure 4) compared to unelicited controls. Among aldehydes, the highest fold variations were recorded for 4-HDDE (6-fold increase) and hexanal, 2,4(t,t)-decadienal, dodecadienal, 4-HHE and 4-HNE (3- to 4-fold increases). Of the volatile halocarbons, iodoethane ($\text{CH}_3\text{CH}_2\text{I}$) and diiodomethane (CH_2I_2) showed the highest increases (6- and 3.7-fold increases, respectively, compared to unelicited controls). This induction was less pronounced for brominated compounds, the most responsive being bromodichloromethane (CHBrCl_2) and dibromomethane (CH_2Br_2) with a 2-fold increase. In conditioned algae, the one-hour elicitation was not followed by such an increase in the amount of VOCs. The production of most aldehydes by the elicited conditioned sporophytes was equal to or even lower than by non-elicited controls. Exceptions were hexanal, 4-HNE and 2,4(t,t)-decadienal and these were only induced 2-fold compared to controls. The overall elicitation-induced production of halocarbons was lower in conditioned sporophytes compared to unconditioned sporophytes (Figure 4).

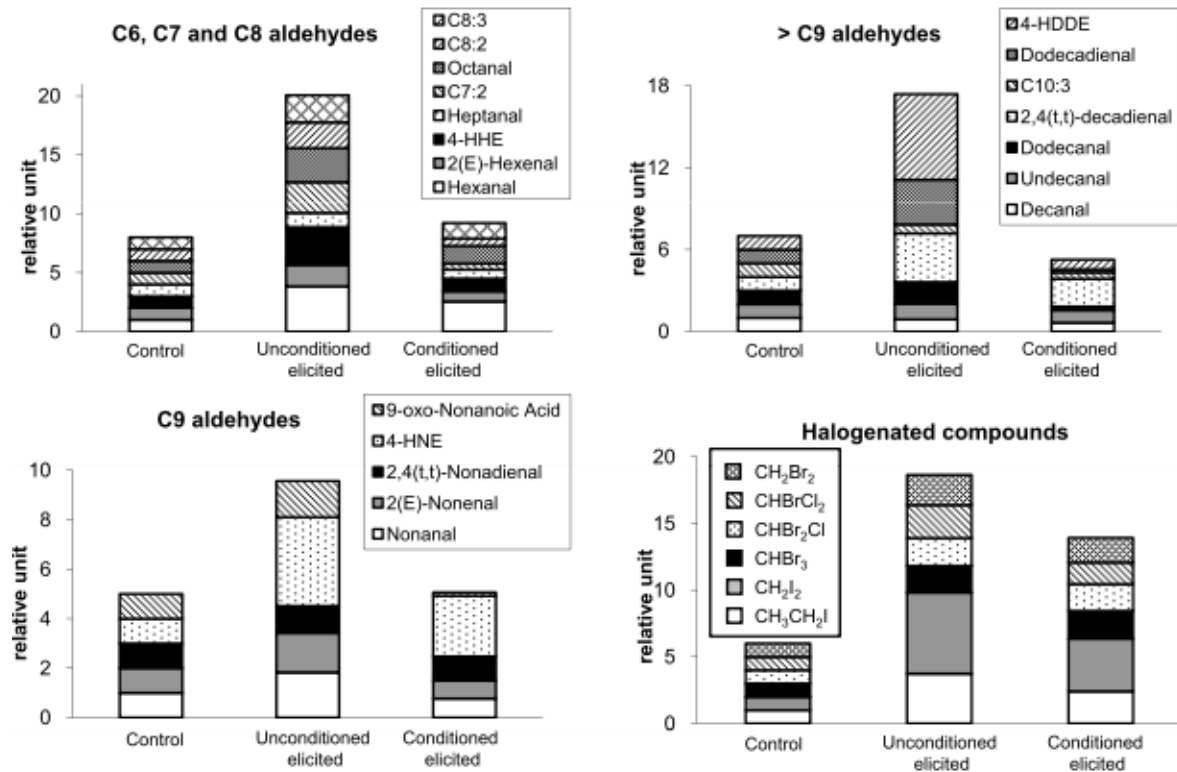


Figure 4: Conditioned *L. digitata* sporophytes release fewer amounts of VOCs after elicitation. VOCs were quantified in the medium surrounding *L. digitata* control and conditioned sporophytes 1 h after challenge or not with GGs. For each compound, the control level was set to a relative unit of 1 to express the fold-variation in the other conditions. 4-HHE, 4-hydroxy-(E)-2-hexenal; C7:2, (E,E)-2,4-heptadienal; C8:2, 2,4-octadienal; C8:3, 2,4,7-octatrienal; 4-HNE, 4-hydroxy-(E)-2-nonenal; C10:3, 2,4,7-decatrienal; 4-HDDE, 4-hydroxydodecadienal; CH₃CH₂I, iodoethane; CH₂I₂, diiodomethane; CHBr₃, bromoform; CHBr₂Cl, dibromochloromethane; CHBrCl₂, bromodichloromethane; CH₂Br₂, dibromomethane. Values are means of three independent replicates.

6.5 Discussion

Three main conclusions emerge from our observations and experiments: first, our results showed that *L. digitata* sporophytes grown in the laboratory display altered defense responses compared to wild conspecifics. Secondly, laboratory-grown sporophytes that were transplanted in the field exhibited a response that resembles the one of wild specimens. It suggests that a direct contact with the seawater from the field affected the algae responses to subsequent elicitation with GG. Thirdly, we established a conditioning procedure which mimics the field effects. In this context, target sporophytes reacted differently to GG-elicitation whether source sporophytes had been

elicited or not before the co-incubation (conditioning or control procedure, respectively). Taken together, these results indicate that waterborne signals shape the defense responses of kelps in nature or in laboratory conditions that induce a priming effect.

Upon elicitation with oligoguluronates, laboratory-grown and wild sporophytes exhibited an oxidative burst, concordant with the literature (Küpper et al., 2001). However, we showed that H₂O₂ levels reached concentrations 30 times lower with wild sporophytes (Figure 1a). Such a tendency of a more pronounced oxidative burst in laboratory-grown sporophytes could not be related to inter-individual variability as it was already observed with other culture batches from meiospores isolated from mature sporophytes originating from populations of Helgoland in Germany (Küpper et al., 2002). This phenomenon cannot be linked to a desensitization of wild sporophytes to GG elicitation, as shown by the gene expression analysis. Indeed, we showed that even if their oxidative responses appears less intense, wild sporophytes still perceive the stress signal and activate the expression of defense genes (Figure 1b). Furthermore, our data indicate that this response involves more genes and is more intense in wild sporophytes than in laboratory-grown specimens. In terms of kinetics, induction in wild algae was systematically rapidly repressed, getting back to the control level within 12 hours after elicitation. The return to the initial expression levels took a longer time in laboratory-grown algae. Together, these results support the hypothesis that wild and laboratory-grown *L. digitata* sporophytes are in a different state, which may be explained by their different living conditions, i.e. natural environment vs. controlled culture conditions. This is supported by the fact that the elicitation-induced oxidative response of wild specimens removed from the field tends to get closer to the one of laboratory-grown sporophytes (Figure 1c).

To investigate the possibility of an effect of the natural environment on the defense capacities of *L. digitata* sporophytes, we conducted transplantation experiments of laboratory-grown algae into a natural kelp bed. We showed that a direct contact with the seawater from the field affected the algae responses to subsequent elicitation. Under GG stress, transplanted laboratory-grown sporophytes displayed a response that resembles the one of wild specimens. The oxidative burst appeared to be 3 times less intense (Figure 2a), and still more genes were induced compared to non-transplanted controls (Figure 2b). This was not the case when algae were introduced into the same kelp bed in a sealed transparent plastic bag to prevent contact with water from the field. In

this case, the intensity of the elicitation-induced oxidative burst was not significantly different from the non-transplanted controls (Figure 2a). The gene response was also less pronounced than in transplanted algae that had a direct contact with the seawater. This shows that the observed effect of the natural environment on the defense capacities cannot be related to physical parameters such as light or temperature. A direct contact with the natural seawater seems to explain the discrepancy observed between wild and laboratory-grown algae. Since 1.5 hour of transplantation was sufficient to obtain detectable differences, it is unlikely that small arthropods or pathogens could come through the net to attach the algae in such a short time and be responsible for our observations. Thus, we propose that *L. digitata* sporophytes could be able to perceive water-borne infochemicals present in the natural environment, enhancing their capacities to efficiently react to further stress.

To test this hypothesis and identify a mechanism of external vectorisation of defense signals in kelps, we developed a novel experimental assay. We used *L. digitata* sporophytes as sources of potential signals to be perceived by target sporophytes (Figure S1). We show that target sporophytes react differently to GG-elicitation whether source sporophytes had been elicited or not before the co-incubation (conditioning or control procedure, respectively). Conditioned target sporophytes produced less intense oxidative burst (Figure 3). This can be explained by a faster trigger of the ROS detoxification process, as H₂O₂ concentration begins to decrease significantly earlier in conditioned sporophytes. We also demonstrated that conditioned sporophytes show a higher and faster up-regulation of the defense marker genes in response to elicitation, compared to unconditioned algae (Table 2). Before challenging with GGs, the transcript levels were not significantly different in unconditioned and conditioned sporophytes (Table 2). This indicates that the enhanced transcriptional response in conditioned sporophytes was not based on primary induction of defense mechanisms during conditioning but resulted from increased reactivity to elicitation. This is redolent of the priming effect known in the terrestrial environment (Conrath *et al.*, 2002). In plant cells, this sensitization to react more rapidly and/or more strongly to environmental stresses upon appropriate stimulation can be induced biologically by beneficial rhizobacteria and mycorrhizal fungi or through the emission of VOCs during plant interactions with pathogens (Yi *et al.*, 2009) or insects (Frost *et al.*, 2008a). It is also chemically mediated by application of low doses of salicylic acid (SA), its synthetic analog benzothiadiazole (BTH), jasmonates or β -aminobutyric acid (BABA) (Conrath *et al.*, 2006; Frost *et al.*, 2008b)

In *L. digitata* sporophytes, the perception of putative waterborne molecules potentiates the gene response to elicitation. Potentiated algae display faster and stronger elicitation-dependent induction of specific defense genes. These results resemble the priming effects on the expression of defense genes already shown in terrestrial plants. In particular, Ton *et al.*, (2007) found an earlier and/or stronger transcriptional induction of six defense-related genes in maize plants that had previously been in contact with airborne signals from herbivore-infested neighbours. In addition, our results suggest that the priming-like mechanism of *L. digitata* sporophytes affects the way they manage oxidative stress. It has been shown previously that the oxidative burst was an important prerequisite for induced resistance against a bacterial pathogen (Küpper *et al.*, 2002) and that reactive oxygen species (ROS) could act as signaling agents to trigger the defense reactions (Cosse *et al.*, 2008). However, high levels of ROS can have deleterious effects on the algal cells if their production and detoxification is not strictly controlled (Dring, 2006). We propose that perception of the putative signal could potentiate the detoxifying capacities of ROS in primed sporophytes. This would reduce the damage to algal cells while keeping the effect of ROS as toxic compounds against attackers and/or as defense-signaling agents. This hypothesis is supported by the observation that the priming-affected genes are implicated in the management of the oxidative stress.

In response to both biotic and abiotic oxidative stress, it has been shown that *L. digitata* naturally emits volatile aldehydes (Goulitquer *et al.*, 2009) and halocarbons (Palmer *et al.*, 2005) in large amounts. The biological significance of distance signaling in primed *L. digitata* was further analysed by monitoring the volatile organic compounds (VOC) released in response to elicitation. We show that primed (i.e. conditioned) sporophytes released lower amounts of VOCs in response to GG-elicitation compared to unconditioned algae (Figure 4). As VOC emissions are dependent upon oxidative stress in kelps (Palmer *et al.*, 2005, Goulitquer *et al.*, 2009), their lower production supports the fact that primed algae display enhanced ROS detoxification mechanisms.

Altogether, these data demonstrate that priming-like mechanisms exist in kelps, suggesting it could be a conserved feature of innate immunity among eukaryotic lineages. The primed sporophytes managed oxidative stress better after elicitation, as shown by H₂O₂ (Figures 1a and 3) and VOC (Figure 4) levels, and display faster and/or stronger transcriptional responses (Table 2). Defense-related waterborne communication in marine algal models has already been reported.

Previous studies have demonstrated that external cues released either directly from the brown algae *Ascophyllum nodosum* and *Fucus vesiculosus* under herbivory or from feeding grazers were able to directly induce chemical defenses in unharmed conspecifics (Toth & Pavia, 2000; Rhode *et al.*, 2004). However, merely late defense responses were studied so far and only direct induction of defenses could be evidenced. In the present study, we investigated for the first time earlier steps of the defense responses and showed that waterborne signals also have a potentiating effect, preparing sporophytes to better respond to further attack without directly triggering defense reactions. It is believed that this priming phenomenon excludes the costly direct allocation of resources to a defense that may eventually not be required, while increasing resistance in case of further attack (van Ulten *et al.*, 2006; Walters & Heil, 2007). In addition to conditioning in the laboratory, the field transplantation experiments we conducted reveal that a stay in the natural environment can potentiate the defense responses of *L. digitata*, confirming that priming mediated by waterborne signals released from *L. digitata* occurs in nature. This may explain the drastic differences observed for the elicitation-induced oxidative burst (Figure 1a) and transcriptional responses (Figure 1b) of wild algae compared to laboratory-grown sporophytes. The primed state of wild algae is at least partly reversible, as demonstrated by the effect of removal from their natural environment on the oxidative response to elicitation. However, even after 8 days of isolation from putative environmental signals, the oxidative response of wild sporophytes did not reach the very high levels of the laboratory-grown algae (Figure 1c), suggesting that the effect of signal perception may persist for longer periods. This observation fits the emerging concept of plant memory or “stress imprint” (Bruce *et al.*, 2007, Gàlis *et al.*, 2009). Overall, the results reported in the present study demonstrate that waterborne cues induce priming and greatly shape the defense responses of kelps. It raises the question as to the effects at the community level. The coastal environment provides kelps with a wealth of potential infochemicals. Measurements in rock pools containing *L. digitata* detected the presence of a cocktail of volatile aldehydes (Goulitquer *et al.*, 2009), alkenes (Broadgate *et al.*, 2004) and halogenated compounds (Carpenter *et al.*, 2000). In nature, wild sporophytes are thereby likely to integrate infochemicals to control oxidative burst, production of VOCs and defense-related gene expression. Kelp forests represent both important habitats and food sources for a wide range of consumers and are subjected to multiple biotic (i.e. herbivores, pathogens, etc.) and abiotic stresses (i.e. dessication, UV, etc.). Recent studies on the *A. nodosum* algal model have shown

that waterborne signaling affects the population dynamics of herbivores and predators in controlled laboratory conditions (Coleman *et al.*, 2007, Borell *et al.*, 2004). It was also recently suggested that resistance to herbivores may be induced in advance by waterborne cues and spread effectively throughout a *Fucus vesiculosus* belt (Haavisto *et al.*, 2009). In terrestrial plants, priming was reported to occur in different types of induced resistance and is considered as an important ecological adaptation to resist environmental stress (Heil & Silva Bueno, 2007; Pieterse & Dicke, 2007; Walters *et al.*, 2006, Yi *et al.*, 2009). Interestingly, it was shown in *Arabidopsis thaliana* that the fitness costs of priming are lower than those of constitutively activated defenses (Van Hulst *et al.*, 2006).

Based on these laboratory and field experiments, we hypothesize that inter-individual communication via stress-related signals may influence the structuring of marine communities in coastal ecosystems. The novel conditioning procedure described in this work to prime kelps in the laboratory will facilitate further study of this mechanism, such as the identification of the putative signal(s) and of their impacts on herbivore or pathogen resistance.

6.6 Acknowledgements

This work was partially funded by the ECOKELP program of the French Agence Nationale de la Recherche (ANR) (ANR 06 BDIV 012). PhD fellowships to F.T. and S.G. were awarded by the Ministère de l'Enseignement Supérieur et de la Recherche. A.C. was supported by a PhD fellowship from the Brittany Regional Council and a post-doctoral fellowship from ECOKELP. S.R. received funding from the European community's Sixth Framework Programme (ESTeam MESTCT 2005-020737). This work was conducted in the Laboratoire International Associé "Dispersal and Adaptation of Marine Species" (LIA DIAMS) PUC, Chile and CNRS-UPMC, France.

6.7 References

- Apt KE, Clendennen SK, Powers DA, Grossman AR. 1995. The gene family encoding the fucoxanthin chlorophyll proteins from the brown alga *Macrocystis pyrifera*. *Mol Gen Genet* **246**, 455-464
- Baldauf SL. 2003. The deep roots of eukaryotes. *Science* **300**: 1703–1706.
- Baldwin IT, Schultz JC 1983 Rapid changes in tree leaf chemistry induced by damage: evidence for communication between plants. *Science* **221**, 277-279
- Baldwin IT, Halitschke R, Paschold A, von Dahl CC, Preston CA. 2006 Volatile signaling in plant-plant interactions: "talking trees" in the genomics era. *Science* **311**, 812-815
- Borell EM, Foggo A, Coleman RA. 2004. Induced resistance in intertidal macroalgae modifies feeding behaviour of herbivorous snails. *Oecologia* **140**, 328-334
- Broadgate WJ, Malin G, Küpper FC, Thompson A, Liss PS. 2004. Isoprene and other non-methane hydrocarbons from seaweeds: a source of reactive hydrocarbons to the atmosphere. *Marine Chem* **88**, 61-73
- Bruce TJA, Matthes MC, Napier JA, Pickett JA. 2007. Stressful "memories" of plants: Evidence and possible mechanisms. *Plant Sci.* **173**, 603-608
- Carpenter LJ, Malin G, Liss PS, Küpper FC. 2000. Novel biogenic iodine-containing trihalomethanes and other short-lived halocarbons in the coastal East Atlantic. *Global Biogeochem Cycles* **14**, 1191-1204
- Coleman RA, Ramchunder SJ, Davis KM, Moody AJ, Foggo A. 2007. Herbivore-induced infochemicals influence foraging behaviour in two intertidal predators. *Oecologia* **151**, 454-463
- Conrath U, Pieterse CMJ, Mauch-Mani B. 2002. Priming in plant-pathogen interactions. *Trends Plant Sci.* **7**: 210–216.
- Conrath U, Beckers GJM, Flors V, Garcia-Agustin P, Jakab G, Mauch F, Newman MA, Pieterse CMJ, Poinssot B, Pozo MJ et al 2006. Priming: Getting ready for battle. *Mol. Plant-Microbe Interact.* **19**, 1062-1071
- Cosse A, Leblanc C, Potin P. 2008 . Dynamic defense of marine macroalgae against pathogens: from early activated to gene-regulated responses. *Adv. Bot. Res.* **46**: 221–266
- Cosse A, Potin P, Leblanc C. 2009. Patterns of gene expression induced by oligoguluronates reveal conserved and environment-specific molecular defense responses in the brown alga *Laminaria digitata*. *New Phytol* **182**, 239–250
- Dring MJ 2006. Stress resistance and disease resistance in seaweeds: the role of reactive oxygen metabolism. *Adv Bot Res* **43**:175–207

Frost CJ, Appel HM, Carlson JE, De Moraes CM, Mescher MC, Schultz JC. 2007. Within-plant signalling via volatiles overcomes vascular constraints on systemic signalling and primes responses against herbivores. *Ecol Lett* **10**, 490-498

Frost CJ, Mescher MC, Dervinis C, Davis JM, Carlson JE, De Moraes CM. 2008a. Priming defense genes and metabolites in hybrid poplar by the green leaf volatile cis-3-hexenyl acetate. *New Phytol.* **180**:722-34.

Frost CJ, Mescher MC, Carlson JE, De Moraes CM. 2008b. Plant defense priming in plant-herbivore interactions: getting ready for a different battle. *Plant Physiol.* **146**: 818–824.

Gális I, Gaquerel E, Pandey SP, Baldwin IT. 2009. Molecular mechanisms underlying plant memory in JA-mediated defence responses. *Plant, Cell Environ.* **32**, 617-627

Goultquer S, Ritter A, Thomas F, Ferec C, Salaün JP, Potin P. 2009. Release of volatile aldehydes by the brown algal kelp *Laminaria digitata* in response to both biotic and abiotic stress. *Chembiochem* **10**, 977-982

Haavisto F, Välikangas T, Jormalainen V. 2009. Induced resistance in a brown alga: phlorotannins, genotypic variation and fitness costs for the crustacean herbivore. *Oecologia*. 2009 Nov 18. [Epub ahead of print]

Haug A, Larsen B, Smidsrod O. 1974. Uronic acid sequence in alginate from different sources. *Carbohydrate Research* **32**: 217–225.

Hayes MP, Freeman SL, Donnelly RP. 1995. IFN- α priming of monocytes enhances LPS-induced TNF production by augmenting both transcription and mRNA stability. *Cytokine* **7**, 427-435

Heil M, Silva Bueno JC 2007. Within-plant signaling by volatiles leads to induction and priming of an indirect plant defense in nature. *Proc Natl Acad Sci USA* **104**: 5467–5472

Heil M, Ton J. 2008. Long-distance signalling in plant defence. *Trends Plant Sci* **13**: 264–272

Karban R, Shiojiri K, Huntzinger M, McCall AC. 2006. Damage-induced resistance in sagebrush: Volatiles are key to intra- and interplant communication. *Ecology* **87**:922-30.

Küpper FC, Kloareg B, Guern J, Potin P. 2001. Oligoguluronates elicit an oxidative burst in the brown algal kelp *Laminaria digitata*. *Plant Physiol* **125**, 278-291

Küpper FC, Müller DG, Peters AF, Kloareg B, Potin P. 2002. *J Chem Ecol* **28**, 2057-2081

Lane AL, Kubanek J. (2008) Secondary metabolite defenses against pathogens and biofoulers. In pp. 229-243, *Algal Chemical Ecology*. C.D. Amsler, Ed. Springer-Verlag, Berlin.

Palmer CJ, Anders TL, Carpenter LJ, Küpper FC, McFiggans GB. 2005. Iodine and halocarbon response of *Laminaria digitata* to oxidative stress and links to atmospheric new particle production. *Environ Chem* **2**, 282-290

Pelletreau KN, Targett NM. 2008. New perspectives for addressing patterns of secondary metabolites in marine macroalgae. In: pp. 121-146, *Algal Chemical Ecology*, C. D. Amsler Ed. Springer-Verlag, Berlin.

- Pieterse CMJ, Dicke M 2007. Plant interactions with microbes and insects: from molecular mechanisms to ecology. *Trends Plant Sci* **12**: 564–569
- Potin P. 2008. Oxidative burst and related Responses in biotic interactions of algae; in pp.245–272, *Algal Chemical Ecology*, C. D. Amsler Ed. Springer-Verlag, Berlin.
- Pruvost J, Connan O, Marty Y, Le Corre P. 1999. A sampling device for collection and analysis of volatile halocarbons in coastal and oceanic waters. *The Analyst* **124**, 1389-1394
- Rohde S, Molis M, Wahl M. 2004. Regulation of anti-herbivore defence by *Fucus vesiculosus* in response to various cues. *J Ecol* **92**, 1011-1018
- Ton J, D'Allesandro M, Jourdie V, Jakab G, Karlen D, Held M, Mauch-Mani B, Turlings TCJ 2007. Priming by airborne signals boosts direct and indirect resistance in maize. *Plant J* **49**: 16–26
- Toth, G. B., Pavia, H. 2000. Water-borne cues induce chemical defense in a marine alga (*Ascophyllum nodosum*). *Proc. Natl. Acad. Sci. USA* **97**, 14418-14420
- van Donk, E. 2007. Chemical information transfer in freshwater plankton. *Ecol Informatics* **2**, 112-120
- van Hulten M, Pelsler M, van Loon LC, Pieterse CMJ, Ton J 2006. Costs and benefits of priming for defense in *Arabidopsis*. *Proc Natl Acad Sci USA* **103**: 5602–5607
- Vos M, Vet LEM, Wackers FL, Middelburg JJ, Van Der Putten WH, Mooij WM, Heip CHR, Van Donk E. 2006. Infochemicals structure marine, terrestrial and freshwater food webs: Implications for ecological informatics. *Ecological Informatics* **1**, 23-32
- Walters DR, Cowley T, Weber H 2006. Rapid accumulation of trihydroxy oxylipins and resistance to the bean rust pathogen *Uromyces fabae* following wounding in *Vicia faba*. *Ann Bot (Lond)* **97**: 779–784
- Walters D, Heil M. (2007). Costs and trade-offs associated with induced resistance. *Physiol. Mol. Plant Pathol.* **71**, 3-17
- Yi HS, Heil M, Adame-Alvarez RM, Ballhorn DJ, Ryu CM. 2009. Airborne induction and priming of plant defenses against a bacterial pathogen. *Plant Physiol.* **151**:2152-61.

7 Conclusions and perspectives

During this thesis we designed an analytical system for measurements of halocarbons. New sampling devices were successfully developed for fieldwork. These instruments showed high performance, both at sea and during laboratory analyses.

Two highly productive marine areas were studied for VHOC distribution and air-sea fluxes: a diatom dominated upwelling region and a nutrient enriched coastal region with an important macroalgae cover and a mega-tidal regime. Additionally, the role of plant-plant communication and its influence on VHOC formation was investigated in a separate laboratory study.

The main conclusions of this thesis are (1) upwelling regions are not characterized by high internal VHOC formation, (2) in tidal-influenced marine areas tides have significant effects on the formation of iodo- and bromocarbons but no influence on the formation of chlorocarbons (with the exception of chloroform, which showed minor dependence on tides in the Iberian upwelling), (3) bromocarbons have strong and highly localized coastal sources (4) iodocarbons have sources that are not strictly related to macroalgae, (5) main sources of chlorocarbons might have an anthropogenic origin, (6) formation of halocarbons and their fluxes to the atmosphere show a marked seasonality and (7) a unknown signal molecule orchestrates the defence response and formation of VHOCs in kelp.

To better understand the halocarbon cycle and to achieve better halocarbon budgets, future studies are necessary clasping (a) the biochemical background, (b) the species and inter-species level, (c) formation in (changing) ecosystems and (d) large scale distribution patterns.

Our work contributed to the understanding of VHOC formation in the kelp algae *Laminaria digitata* by highlighting the role of plant-plant communication and its influence on halocarbon formation. In a general perspective, the biological role and the enzymatic formation of VHOC in different species are poorly investigated. To date no study has shown a direct involvement of haloperoxidases in the formation of VHOC in a marine organism. A functional study should be designed to highlight the exact purpose of haloperoxidases in different species and could provide answers on this topic.

To the best of our knowledge, no study showed the defence potential of VHOCs against grazers or fouling organisms. As discussed above, VHOC formation is described for various species. The ecology of those species is usually well studied and therefore possible grazers or fouling organisms are known. Incubation experiments should show at which extent grazing/fouling contributes to VHOC release from algae.

Several incubation experiments demonstrated species specific formation of VHOCs by phytoplankton (Tokarczyk and Moore 1994; Moore et al. 1996b), bacteria (Amachi et al. 2001) and macroalgae (Gschwend et al. 1985; Klick 1993; Nightingale et al. 1995; Pedersen et al. 1996; Carpenter et al. 2000). However species-specific responses to different stress levels remain unclear. Ocean acidification and elevated SST are processes that are related to global change and might have some influence on VHOC formation. UV radiation, nutrient levels and osmotic stress have consequences for algae physiology and are therefore interesting variables to investigate for future research.

In this work we showed that coastal zones are strong sources for bromo- and iodocarbons and are subjected to a marked seasonality. We discussed that sea-to-air flux calculations are associated with considerable uncertainties both at global and local scale. Global estimates could be improved by a higher number of studies in numerous geographical regions and diverse ecosystems. Moreover, a high temporal resolution could improve sea-to-air estimates in a given area.

Considering the high impact of coastal zones for the global cycle of halogens, those areas are of great interest for future research. Previous studies and our current work in highly productive marine areas suggest that daily and seasonal variations and variations arising from different spots and habitats within the area have consequences on VHOC distribution and sea-to-air-fluxes. It is obvious that additional studies with a high temporal measurement resolution are essential for better budget global calculations. Finally, intercalibration of different instruments would help to obtain better halocarbon budgets.

8 Literature

- Abrahamsson, K., S. Bertilsson, et al. (2004). "Variations of biochemical parameters along a transect in the Southern Ocean, with special emphasis on volatile halogenated organic compounds." Deep-Sea Research Part II-Topical Studies in Oceanography **51**(22-24): 2745-2756.
- Abrahamsson, K. and A. Ekdahl (1996). "Volatile halogenated compounds and chlorophenols in the Skagerrak." Journal of Sea Research **35**(1-3): 73-79.
- Abrahamsson, K. and S. Klick (1990). "Determination of Biogenic and Anthropogenic Volatile Halocarbons in Sea-Water by Liquid-Liquid-Extraction and Capillary Gas-Chromatography." Journal of Chromatography **513**: 39-45.
- Abril, G., M. V. Commarieu, et al. (2009). "Turbidity limits gas exchange in a large macrotidal estuary." Estuarine Coastal and Shelf Science **83**(3): 342-348.
- Adams, F. C., M. Heisterkamp, et al. (1998). "Speciation of organometal and organohalogen compounds in relation to global environmental pollution." Analyst **123**(5): 767-772.
- Amachi, S. (2005). "Microbial Influences on the Mobility and Transformation of Radioactive Iodine in the Environment." Journal of Nuclear and Radiochemical Sciences **6**(1).
- Amachi, S., Y. Kamagata, et al. (2001). "Bacteria mediate methylation of iodine in marine and terrestrial environments." Applied and Environmental Microbiology **67**(6): 2718-2722.
- Andreae, M. O., E. Atlas, et al. (1996). "Methyl halide emissions from savanna fires in southern Africa." Journal of Geophysical Research-Atmospheres **101**(D19): 23603-23613.
- Archer, S. D., L. E. Goldson, et al. (2007). "Marked seasonality in the concentrations and sea-to-air flux of volatile iodocarbon compounds in the western English Channel." Journal of Geophysical Research-Oceans **112**(C8): -.
- Asplund, G., J. V. Christiansen, et al. (1993). "A Chloroperoxidase-Like Catalyst in Soil - Detection and Characterization of Some Properties." Soil Biology & Biochemistry **25**(1): 41-46.
- Atkins, P. W. (1986). Physical chemistry. Acford, Chichester, Great Britain, W H Freeman & Co: 857.
- Atlas, E. and S. Schauffler (1991). "Analysis of Alkyl Nitrates and Selected Halocarbons in the Ambient Atmosphere Using a Charcoal Preconcentration Technique." Environmental Science & Technology **25**(1): 61-67.
- Attieh, J. M., A. D. Hanson, et al. (1995). "Purification and Characterization of a Novel Methyltransferase Responsible for Biosynthesis of Halomethanes and Methanethiol in Brassica-Oleracea." Journal of Biological Chemistry **270**(16): 9250-9257.
- Aucott, M. L., A. McCulloch, et al. (1999). "Anthropogenic emissions of trichloromethane (chloroform, CHCl₃) and chlorodifluoromethane (HCFC-22): Reactive Chlorine Emissions Inventory." Journal of Geophysical Research-Atmospheres **104**(D7): 8405-8415.
- Baker, J. M., C. E. Reeves, et al. (1999). "Biological production of methyl bromide in the coastal waters of the North Sea and open ocean of the northeast Atlantic." Marine Chemistry **64**(4): 267-285.
- Bell, N., L. Hsu, et al. (2002). "Methyl iodide: Atmospheric budget and use as a tracer of marine convection in global models." Journal of Geophysical Research-Atmospheres **107**(D17): -.
- Bendschneider, K. and R. J. Robinson (1952). "A New Spectrophotometric Method for the Determination of Nitrite in Sea Water." Journal of Marine Research **11**(1): 87-96.

- Bianchi, A. P., M. S. Varney, et al. (1991). "Analysis of Volatile Organic-Compounds in Estuarine Sediments Using Dynamic Headspace and Gas-Chromatography Mass-Spectrometry." Journal of Chromatography **542**(2): 413-450.
- Blake, N. J., D. R. Blake, et al. (1997). "Distribution and seasonality of selected hydrocarbons and halocarbons over the western Pacific basin during PEM-West A and PEM-West B." Journal of Geophysical Research-Atmospheres **102**(D23): 28315-28331.
- Blake, N. J., D. R. Blake, et al. (1999). "Aircraft measurements of the latitudinal, vertical, and seasonal variations of NMHCs, methyl nitrate, methyl halides, and DMS during the First Aerosol Characterization Experiment (ACE 1)." Journal of Geophysical Research-Atmospheres **104**(D17): 21803-21817.
- Bondu, S., B. Cocquempot, et al. (2008). "Effects of salt and light stress on the release of volatile halogenated organic compounds by *Solieria chordalis*: a laboratory incubation study." Botanica Marina **51**(6): 485-492.
- Bouarab, K., P. Potin, et al. (1999). "Sulfated oligosaccharides mediate the interaction between a marine red alga and its green algal pathogenic endophyte." Plant Cell **11**(9): 1635-1650.
- Braud, J.-P. (1974). Etude de quelques parametres ecologiques, biologiques et biochimiques chez une pheophycee des cotes bretonnes *Laminaria ochroleuca*. Marseille, Aix-Marseille Université.
- Bravo-Linares, C. M. and S. M. Mudge (2009). "Temporal trends and identification of the sources of volatile organic compounds in coastal seawater." Journal of Environmental Monitoring **11**(3): 628-641.
- Brisson, L. F., R. Tenhaken, et al. (1994). "Function of Oxidative Cross-Linking of Cell-Wall Structural Proteins in Plant-Disease Resistance." Plant Cell **6**(12): 1703-1712.
- Bullister, J. L. and D. P. Wisegarver (2008). "The shipboard analysis of trace levels of sulfur hexafluoride, chlorofluorocarbon-11 and chlorofluorocarbon-12 in seawater." Deep-Sea Research Part I-Oceanographic Research Papers **55**(8): 1063-1074.
- Bulsiewicz, K., H. Rose, et al. (1998). "A capillary-column chromatographic system for efficient chlorofluorocarbon measurement in ocean waters." Journal of Geophysical Research-Oceans **103**(C8): 15959-15970.
- Butler, A. and J. N. Carter-Franklin (2004). "The role of vanadium bromoperoxidase in the biosynthesis of halogenated marine natural products." Natural Product Reports **21**(1): 180-188.
- Butler, J. H. (1995). "Ozone Depletion - Methyl-Bromide under Scrutiny." Nature **376**(6540): 469-470.
- Butler, J. H., D. B. King, et al. (2007). "Oceanic distributions and emissions of short-lived halocarbons." Global Biogeochemical Cycles **21**(1): -.
- Camel, V. and M. Caude (1995). "Trace Enrichment Methods for the Determination of Organic Pollutants in Ambient Air." Journal of Chromatography A **710**(1): 3-19.
- Carpenter, L. J., C. E. Jones, et al. (2009). "Air-sea fluxes of biogenic bromine from the tropical and North Atlantic Ocean." Atmospheric Chemistry and Physics **9**(5): 1805-1816.
- Carpenter, L. J. and P. S. Liss (2000). "On temperate sources of bromoform and other reactive organic bromine gases." Journal of Geophysical Research-Atmospheres **105**(D16): 20539-20547.
- Carpenter, L. J., G. Malin, et al. (2000). "Novel biogenic iodine-containing trihalomethanes and other short-lived halocarbons in the coastal East Atlantic." Global Biogeochemical Cycles **14**(4): 1191-1204.

- Carpenter, L. J., W. T. Sturges, et al. (1999). "Short-lived alkyl iodides and bromides at Mace Head, Ireland: Links to biogenic sources and halogen oxide production." Journal of Geophysical Research-Atmospheres **104**(D1): 1679-1689.
- Carpenter, L. J., D. J. Wevill, et al. (2005). "Atmospheric bromoform at Mace Head, Ireland: seasonality and evidence for a peatland source." Atmospheric Chemistry and Physics **5**: 2927-2934.
- Carpenter, L. J., D. J. Wevill, et al. (2007). "Depth profiles of volatile iodine and bromine-containing halocarbons in coastal Antarctic waters." Marine Chemistry **103**(3-4): 227-236.
- Chameides, W. L. and D. D. Davis (1980). "Iodine - Its Possible Role in Tropospheric Photochemistry." Journal of Geophysical Research-Oceans and Atmospheres **85**(Nc12): 7383-7398.
- Chen, Z. X., H. Silva, et al. (1993). "Active Oxygen Species in the Induction of Plant Systemic Acquired-Resistance by Salicylic-Acid." Science **262**(5141): 1883-1886.
- Christof, O. (2002). Leichtflüchtige halogenierte Kohlenwasserstoffe - Vorkommen, Verhalten und Bedeutung in Küstengebieten. Hamburg, University of Hamburg. **PhD**.
- Christof, O., R. Seifert, et al. (2002). "Volatile halogenated organic compounds in European estuaries." Biogeochemistry **59**(1-2): 143-160.
- Chuck, A. L., S. M. Turner, et al. (2005). "Oceanic distributions and air-sea fluxes of biogenic halocarbons in the open ocean." Journal of Geophysical Research-Oceans **110**(C10): -.
- Clark, J. F., P. Schlosser, et al. (1995). "Gas Transfer Velocities for S₆ and He-3 in a Small Pond at Low Wind Speeds." Geophysical Research Letters **22**(2): 93-96.
- Class, T. and K. Ballschmiter (1987). "Chemistry of Organic Traces in Air .9. Evidence of Natural Marine Sources for Chloroform in Regions of High Primary Production." Fresenius Zeitschrift Fur Analytische Chemie **327**(1): 40-41.
- Class, T. H. and K. Ballschmiter (1988). "Chemistry of Organic Traces in Air .8. Sources and Distribution of Bromochloromethanes and Bromochloromethanes in Marine Air and Surfacewater of the Atlantic-Ocean." Journal of Atmospheric Chemistry **6**(1-2): 35-46.
- Clerbaux, C. and D. Cunnold (2006). Long-Lived Compounds. World Meteorological Organization Global Ozone Research and Monitoring Project - Report No. 50.
- Cocquempot, B. (2004). Composés organiques halogénés volatils en milieu marin. Origines biologiques et flux vers l'atmosphère. Brest, UBO. **PhD**.
- Coelho, H. S., R. J. J. Neves, et al. (2002). "A model for ocean circulation on the Iberian coast." Journal of Marine Systems **32**(1-3): 153-179.
- Collen, J. and M. Pedersen (1994). "A Stress-Induced Oxidative Burst in Eucheuma-Platykladum (Rhodophyta)." Physiologia Plantarum **92**(3): 417-422.
- Cosse, A., C. Leblanc, et al. (2007). Dynamic Defense of Marine Macroalgae Against Pathogens: From Early Activated to Gene[hyphen (true graphic)]Regulated Responses. Advances in Botanical Research. K. Jean-Claude and D. Michel, Academic Press. **Volume 46**: 221-266.
- Cosse, A., P. Potin, et al. (2009). "Patterns of gene expression induced by oligoguluronates reveal conserved and environment-specific molecular defense responses in the brown alga *Laminaria digitata*." New Phytologist **182**(1): 239-250.
- Coulter, C., J. T. G. Hamilton, et al. (1999). "Halomethane : bisulfide/halide ion methyltransferase, an unusual corrinoid enzyme of environmental significance isolated from an aerobic methylotroph using chloromethane as the sole carbon source." Applied and Environmental Microbiology **65**(10): 4301-4312.

- Crusius, J. and R. Wanninkhof (2003). "Gas transfer velocities measured at low wind speed over a lake." Limnology and Oceanography **48**(3): 1010-1017.
- Davis, D., J. Crawford, et al. (1996). "Potential impact of iodine on tropospheric levels of ozone and other critical oxidants." Journal of Geophysical Research-Atmospheres **101**(D1): 2135-2147.
- Dawes, V. J. and M. J. Waldock (1994). "Measurement of Volatile Organic Compounds at UK National Monitoring Plan Stations." Marine Pollution Bulletin **28**(5): 291-298.
- DeBruyn, W. J. and E. S. Saltzman (1997a). "Diffusivity of methyl bromide in water." Marine Chemistry **57**(1-2): 55-59.
- DeBruyn, W. J. and E. S. Saltzman (1997b). "The solubility of methyl bromide in pure water, 35 parts per thousand sodium chloride and seawater." Marine Chemistry **56**(1-2): 51-57.
- Dewulf, J., D. Drijvers, et al. (1995). "Measurement of Henry's Law Constant as Function of Temperature and Salinity for the Low-Temperature Range." Atmospheric Environment **29**(3): 323-331.
- Dewulf, J., D. Ponnet, et al. (1996). "Measurement of atmospheric monocyclic aromatic hydrocarbons and chlorinated C-1- and C-2-hydrocarbons at ng.m(-3) concentration levels." International Journal of Environmental Analytical Chemistry **62**(4): 289-301.
- Dewulf, J. and H. VanLangenhove (1995). "Simultaneous determination of C-1- and C-2-halocarbons and monocyclic aromatic hydrocarbons in marine water samples at NG/L concentration levels." International Journal of Environmental Analytical Chemistry **61**(1): 35-46.
- Dewulf, J. and H. VanLangenhove (1997). "Chlorinated C-1- and C-2-hydrocarbons and monocyclic aromatic hydrocarbons in marine waters: An overview on fate processes, sampling, analysis and measurements." Water Research **31**(8): 1825-1838.
- Doskey, P. V. (1991). "The Effect of Treating Air Samples with Magnesium Perchlorate for Water Removal during Analysis for Nonmethane Hydrocarbons." Hrc-Journal of High Resolution Chromatography **14**(11): 724-728.
- Drewer, J., K. V. Heal, et al. (2008). "Methyl bromide emissions to the atmosphere from temperate woodland ecosystems." Global Change Biology **14**(11): 2539-2547.
- Duinker, J. C. (1993). "Chlorinated biphenyls in open waters: sampling, extraction, clean-up and instrumental determination." UNESCO. Intergovernmental Oceanographic Commission. Manuals and guides **27**: 1-36.
- Ebel, J., A. A. Bhagwat, et al. (1995). "Elicitor Binding-Proteins and Signal-Transduction in the Activation of a Phytoalexin Defense Response." Canadian Journal of Botany-Revue Canadienne De Botanique **73**: S506-S510.
- Ekdahl, A. and K. Abrahamsson (1997). "A simple and sensitive method for the determination of volatile halogenated organic compounds in sea water in the amol 1(-1) to pmol 1(-1) range." Analytica Chimica Acta **357**(3): 197-209.
- Ekdahl, A., M. Pedersen, et al. (1998). "A study of the diurnal variation of biogenic volatile halocarbons." Marine Chemistry **63**(1-2): 1-8.
- Eklund, G., B. Josefsson, et al. (1978). "Determination of Chlorinated and Brominated Lipophilic Compounds in Spent Bleach Liquors from a Sulfite Pulp-Mill - Glass Capillary Column Gas Chromatography-Mass Spectrometry Computer Analysis and Identification." Journal of Chromatography **150**(1): 161-169.
- Fahey, D. W. (2006). Twenty Questions and Answers about the Ozone Layer: 2006 Update.

- Fanning, K. A. and M. E. Q. Pilson (1973). "Spectrophotometric Determination of Dissolved Silica in Natural Waters." Analytical Chemistry **45**(1): 136-140.
- Farman, J. C., B. G. Gardiner, et al. (1985). "Large Losses of Total Ozone in Antarctica Reveal Seasonal Clox/Nox Interaction." Nature **315**(6016): 207-210.
- Fogelqvist, E. and M. Krysell (1991). "Naturally and Anthropogenically Produced Bromoform in the Kattegatt, a Semienclosed Oceanic Basin." Journal of Atmospheric Chemistry **13**(4): 315-324.
- Frew, N. M., R. K. Nelson, et al. (2002). "Spatial Variations in Surface Microlayer Surfactants and Their Role in Modulating Air-Sea Exchange." Gas Transfer at Water Surfaces. pp. **127**: 153-159.
- Fritig, B., T. Heitz, et al. (1998). "Antimicrobial proteins in induced plant defense." Current Opinion in Immunology **10**(1): 16-22.
- Frost, T. and R. C. Upstill-Goddard (2002). "Meteorological controls of gas exchange at a small English lake." Limnology and Oceanography **47**(4): 1165-1174.
- Giese, B., F. Larnus, et al. (1999). "Release of volatile iodinated C-1-C-4 hydrocarbons by marine macroalgae from various climate zones." Environmental Science & Technology **33**(14): 2432-2439.
- Gotz, R., O. H. Bauer, et al. (1998). "Organic trace compounds in the water of the River Elbe near Hamburg - Part I." Chemosphere **36**(9): 2085-2101.
- Gribble, G. W. (1996). "Naturally occurring organohalogen compounds--a comprehensive survey." Fortschr Chem Org Naturst **68**: 1-423.
- Gribble, G. W. (1998). "Naturally occurring organohalogen compounds." Accounts of Chemical Research **31**(3): 141-152.
- Gribble, G. W. (1999). "The diversity of naturally occurring organobromine compounds." Chemical Society Reviews **28**(5): 335-346.
- Gribble, G. W. (2003). "The diversity of naturally produced organohalogens." Chemosphere **52**(2): 289-297.
- Grob, K. and A. Habich (1983). "Trace Analysis of Halocarbons in Water - Direct Aqueous Injection with Electron-Capture Detection." Journal of High Resolution Chromatography & Chromatography Communications **6**(1): 11-15.
- Groszko, W. (1999). An estimate of the global air-sea flux of methyl chloride, methyl bromide and methyl iodide. Halifax, Canada, Dalhousie University.
- Grote, C., E. Belau, et al. (1999). "Development of a SPME-GC method for the determination of organic compounds in wastewater." Acta Hydrochimica Et Hydrobiologica **27**(4): 193-199.
- Gruber, N. and J. L. Sarmiento (1997). "Global patterns of marine nitrogen fixation and denitrification." Global Biogeochemical Cycles **11**(2): 235-266.
- Gschwend, P., O. C. Zafiriou, et al. (1980). "Volatile Organic-Compounds in Seawater from the Peru Upwelling Region." Limnology and Oceanography **25**(6): 1044-1053.
- Gschwend, P. M., J. K. Macfarlane, et al. (1985). "Volatile Halogenated Organic-Compounds Released to Seawater from Temperate Marine Macroalgae." Science **227**(4690): 1033-1035.
- Hamilton, J. T. G., W. C. McRoberts, et al. (2003). "Chloride methylation by plant pectin: An efficient environmentally significant process." Science **301**(5630): 206-209.
- Happell, J. D. and M. P. Roche (2003). "Soils: A global sink of atmospheric carbon tetrachloride." Geophysical Research Letters **30**(2): -.

- Happell, J. D. and D. W. R. Wallace (1997). "Gravimetric preparation of gas phase working standards containing volatile halogenated compounds for oceanographic applications." Deep-Sea Research Part I-Oceanographic Research Papers **44**(9-10): 1725-1738.
- Helz, G. R. and R. Y. Hsu (1978). "Volatile Chlorocarbons and Bromocarbons in Coastal Waters." Limnology and Oceanography **23**(5): 858-869.
- Hoekstra, E. J., F. J. M. Verhagen, et al. (1998). "Natural production of chloroform by fungi." Phytochemistry **49**(1): 91-97.
- Hoffmann, T., C. D. O'Dowd, et al. (2001). "Iodine oxide homogeneous nucleation: An explanation for coastal new particle production." Geophysical Research Letters **28**(10): 1949-1952.
- Holmen, K. and P. Liss (1984). "Models for Air Water Gas Transfer - an Experimental Investigation." Tellus Series B-Chemical and Physical Meteorology **36**(2): 92-100.
- Hu, Z. and R. M. Moore (1996). "Kinetics of methyl halide production by reaction of DMSP with halide ion." Marine Chemistry **52**: 147-155.
- Hughes, C., A. L. Chuck, et al. (2009). "Seasonal cycle of seawater bromoform and dibromomethane concentrations in a coastal bay on the western Antarctic Peninsula." Global Biogeochemical Cycles **23**: -.
- Hughes, C., G. Malin, et al. (2008). "The production of volatile iodocarbons by biogenic marine aggregates." Limnology and Oceanography **53**(2): -.
- Hunter-Smith, R. J., P. W. Balls, et al. (1983). "Henry Law Constants and the Air-Sea Exchange of Various Low-Molecular Weight Halocarbon Gases." Tellus Series B-Chemical and Physical Meteorology **35**(3): 170-176.
- Itoh, N., M. Tsujita, et al. (1997). "Formation and emission of monohalomethanes from marine algae." Phytochemistry **45**(1): 67-73.
- Jahne, B. (1980). Zur Parametrisierung des Gasaustausches mit Hilfe von Laborexperimenten. Heidelberg, University of Heidelberg.
- Jakubowska, N., B. Zygmunt, et al. (2009). "Sample preparation for gas chromatographic determination of halogenated volatile organic compounds in environmental and biological samples." Journal of Chromatography A **1216**(3): 422-441.
- James, K. J. and M. A. Stack (1997). "Rapid determination of volatile organic compounds in environmentally hazardous wastewaters using solid phase microextraction." Fresenius Journal of Analytical Chemistry **358**(7-8): 833-837.
- Janicki, W., L. Wolska, et al. (1993). "Simple Device for Permeation Removal of Water-Vapor from Purge Gases in the Determination of Volatile Organic-Compounds in Aqueous Samples." Journal of Chromatography A **654**(2): 279-285.
- Jones, C. E., K. E. Hornsby, et al. (2009). "Coastal measurements of short-lived reactive iodocarbons and bromocarbons at Roscoff, Brittany during the RHaMBLe campaign." Atmospheric Chemistry and Physics **9**(22): 8757-8769.
- Jordan, A., J. Harnisch, et al. (2000). "Volcanogenic halocarbons." Environmental Science & Technology **34**(6): 1122-1124.
- Kepler, F., R. Borchers, et al. (2003). "Formation of volatile iodinated alkanes in soil: results from laboratory studies." Chemosphere **52**(2): 477-483.
- Kepler, F., R. Eiden, et al. (2000). "Halocarbons produced by natural oxidation processes during degradation of organic matter." Nature **403**(6767): 298-301.
- Key, B. D., R. D. Howell, et al. (1997). "Fluorinated organics in the biosphere." Environmental Science & Technology **31**(9): 2445-2454.

- Khalil, M. A. K. and R. A. Rasmussen (1998). Ocean-air exchange of atmospheric trace gases. Portland State Univ., Portland, Oreg., Rep. 01-1097, Dep. of Phys.
- King, D. B., J. H. Butler, et al. (2000). "Implications of methyl bromide supersaturations in the temperate North Atlantic Ocean." Journal of Geophysical Research-Atmospheres **105**(D15): 19763-19769.
- King, D. B., J. H. Butler, et al. (2002). "Predicting oceanic methyl bromide saturation from SST." Geophysical Research Letters **29**(24): -.
- Klamm, S. W. and G. W. Scheil (1989). "Sample Volume Measurement Errors Caused by Co₂ Adsorption in Desiccants." Environmental Science & Technology **23**(11): 1420-1422.
- Klick, S. (1992). "Seasonal-Variations of Biogenic and Anthropogenic Halocarbons in Seawater from a Coastal Site." Limnology and Oceanography **37**(7): 1579-1585.
- Klick, S. (1993). "The Release of Volatile Halocarbons to Seawater by Untreated and Heavy-Metal Exposed Samples of the Brown Seaweed *Fucus-Vesiculosus*." Marine Chemistry **42**(3-4): 211-221.
- Klick, S. and K. Abrahamsson (1992). "Biogenic Volatile Iodated Hydrocarbons in the Ocean." Journal of Geophysical Research-Oceans **97**(C8): 12683-12687.
- Koppmann, R., K. Czapiewski, et al. (2005). Natural and human induced biomass burning in Africa: an important source for volatile organic compounds in the troposphere. Climate Change and Africa. P. S. Low, Cambridge University Press: 68-78.
- Krysell, M. and P. D. Nightingale (1994). "Low-Molecular-Weight Halocarbons in the Humber and Rhine Estuaries Determined Using a New Purge-and-Trap Gas-Chromatographic Method." Continental Shelf Research **14**(12): 1311-1329.
- Kuivinen, J. and H. Johnsson (1999). "Determination of trihalomethanes and some chlorinated solvents in drinking water by headspace technique with capillary column gas-chromatography." Water Research **33**(5): 1201-1208.
- Küpper, F. C., L. J. Carpenter, et al. (2008). "Iodide accumulation provides kelp with an inorganic antioxidant impacting atmospheric chemistry." Proceedings of the National Academy of Sciences of the United States of America **105**(19): 6954-6958.
- Küpper, F. C., B. Kloareg, et al. (2001). "Oligogulonates elicit an oxidative burst in the brown algal kelp *Laminaria digitata*." Plant Physiology **125**(1): 278-291.
- Küpper, F. C., N. Schweigert, et al. (1998). "Iodine uptake in Laminariales involves extracellular, haloperoxidase-mediated oxidation of iodide." Planta **207**(2): 163-171.
- Kuß, J. (1994). Volatile halogenated hydrocarbons: Exchange processes between atmosphere and seawater. Kiel, Christian-Albrechts Universität zu Kiel. **PhD**.
- Laternus, F. (1995). "Release of Volatile Halogenated Organic-Compounds by Unialgal Cultures of Polar Macroalgae." Chemosphere **31**(6): 3387-3395.
- Laternus, F. (2001). "Marine macroalgae in polar regions as natural sources for volatile organohalogenes." Environmental Science and Pollution Research **8**(2): 103-108.
- Laternus, F., B. Giese, et al. (2000). "Low-molecular-weight organoiodine and organobromine compounds released by polar macroalgae - The influence of abiotic factors." Fresenius Journal of Analytical Chemistry **368**(2-3): 297-302.
- Laternus, F., T. Svensson, et al. (2004). "Ultraviolet radiation affects emission of ozone-depleting substances by marine macroalgae: Results from a laboratory incubation study." Environmental Science & Technology **38**(24): 6605-6609.

- Law, C. S. and W. T. Sturges (2006). Halogenated Very Short-Lived Substances. World Meteorological Organization Global Ozone Research and Monitoring Project - Report No. 50.
- Leblanc, C., C. Colin, et al. (2006). "Iodine transfers in the coastal marine environment: the key role of brown algae and of their vanadium-dependent haloperoxidases." Biochimie **88**(11): 1773-1785.
- Legendre, L. (1998). Numerical ecology, Elsevier Science.
- Leigh, R. J., S. M. Ball, et al. (2009). "Measurements and modelling of molecular iodine emissions, transport and photodestruction in the coastal region around Roscoff." Atmos. Chem. Phys. Discuss. **9**(5): 21165-21198.
- Lepine, L. and J. F. Archambault (1992). "Parts-Per-Trillion Determination of Trihalomethanes in Water by Purge-and-Trap Gas-Chromatography with Electron-Capture Detection." Analytical Chemistry **64**(7): 810-814.
- Li, H. J., Y. Yokouchi, et al. (1999). "Measurement of methyl halides in the marine atmosphere." Atmospheric Environment **33**(12): 1881-1887.
- Li, H. J., Y. Yokouchi, et al. (2001). "Distribution of methyl chloride, methyl bromide, and methyl iodide in the marine boundary air over the western Pacific and southeastern Indian Ocean." Geochemical Journal **35**(2): 137-144.
- Liss, P. S. and L. Merlivat (1986). Air-sea gas exchange rates: introduction and synthesis. The role of air-sea exchange in geochemical cycling. P. Buat-Ménard. Dordrecht: 113-128.
- Liss, P. S. and P. G. Slater (1974). "Flux of Gases across Air-Sea Interface." Nature **247**(5438): 181-184.
- Lobert, J. M., W. C. Keene, et al. (1999). "Global chlorine emissions from biomass burning: Reactive Chlorine Emissions Inventory." Journal of Geophysical Research-Atmospheres **104**(D7): 8373-8389.
- Lobert, J. M., S. A. YvonLewis, et al. (1997). "Undersaturation of CH₃Br in the Southern Ocean." Geophysical Research Letters **24**(2): 171-172.
- Lovelock, J. E. (1958). "A Sensitive Detector for Gas Chromatography." Journal of Chromatography **1**(1): 35-46.
- Lovelock, J. E. (1974). "Electron-Capture Detector - Theory and Practice." Journal of Chromatography **99**(Nov6): 3-12.
- MacDonald, S. and R. M. Moore (2007). "Seasonal and spatial variations in methyl chloride in NW Atlantic waters." Journal of Geophysical Research-Oceans **112**(C5): -.
- Mackay, D. and W. Y. Shiu (1981). "A Critical-Review of Henrys Law Constants for Chemicals of Environmental Interest." Journal of Physical and Chemical Reference Data **10**(4): 1175-1199.
- Mackay, D., W. Y. Shiu, et al. (1979). "Determination of Air-Water Henrys Law Constants for Hydrophobic Pollutants." Environmental Science & Technology **13**(3): 333-337.
- Manley, S. L. (2002). "Phytogenesis of halomethanes: A product of selection or a metabolic accident?" Biogeochemistry **60**(2): 163-180.
- Manley, S. L. and M. N. Dastoor (1987). "Methyl Halide (CH₃X) Production from the Giant-Kelp, *Macrocystis*, and Estimates of Global CH₃X Production by Kelp." Limnology and Oceanography **32**(3): 709-715.
- Manley, S. L. and J. L. de la Cuesta (1997). "Methyl iodide production from marine phytoplankton cultures." Limnology and Oceanography **42**(1): 142-147.

- Manley, S. L., K. Goodwin, et al. (1992). "Laboratory Production of Bromoform, Methylene Bromide, and Methyl-Iodide by Macroalgae and Distribution in Nearshore Southern California Waters." Limnology and Oceanography **37**(8): 1652-1659.
- Manley, S. L., N. Y. Wang, et al. (2006). "Coastal salt marshes as global methyl halide sources from determinations of intrinsic production by marsh plants." Global Biogeochemical Cycles **20**(3): -.
- Marshall, R. A., D. B. Harper, et al. (1999). "Volatile bromocarbons produced by *Falkenbergia* stages of *Asparagopsis* spp. (Rhodophyta)." Limnology and Oceanography **44**(5): 1348-1352.
- Martinez, E., S. Lacorte, et al. (2002a). "Multicomponent analysis of volatile organic compounds in water by automated purge and trap coupled to gas chromatography-mass spectrometry." Journal of Chromatography A **959**(1-2): 181-190.
- Martinez, E., I. Llobet, et al. (2002b). "Patterns and levels of halogenated volatile compounds in Portuguese surface waters." Journal of Environmental Monitoring **4**(2): 253-257.
- Martino, M., G. P. Mills, et al. (2009). "A new source of volatile organoiodine compounds in surface seawater." Geophysical Research Letters **36**: -.
- McGillis, W. R., J. B. Edson, et al. (2001). "Direct covariance air-sea CO₂ fluxes." Journal of Geophysical Research-Oceans **106**(C8): 16729-16745.
- Miermans, C. J. H., L. E. van der Velde, et al. (2000). "Analysis of volatile organic compounds, using the purge and trap injector coupled to a gas chromatograph/ion-trap mass spectrometer: Review of the results in Dutch surface water of the Rhine, Meuse, Northern Delta Area and Westerscheldt, over the period 1992-1997." Chemosphere **40**(1): 39-48.
- Molina, M. J. and F. S. Rowland (1974). "Stratospheric Sink for Chlorofluoromethanes - Chlorine Atomic-Catalysed Destruction of Ozone." Nature **249**(5460): 810-812.
- Moore, R. (2003). Marine Sources of Volatile Organohalogens. Natural Production of Organohalogen Compounds: 85-101.
- Moore, R. M., C. E. Geen, et al. (1995). "Determination of Henry Law Constants for a Suite of Naturally-Occurring Halogenated Methanes in Seawater." Chemosphere **30**(6): 1183-1191.
- Moore, R. M. and W. Groszko (1999). "Methyl iodide distribution in the ocean and fluxes to the atmosphere." Journal of Geophysical Research-Oceans **104**(C5): 11163-11171.
- Moore, R. M., W. Groszko, et al. (1996a). "Ocean-atmosphere exchange of methyl chloride: Results from NW Atlantic and Pacific Ocean studies." Journal of Geophysical Research-Oceans **101**(C12): 28529-28538.
- Moore, R. M. and R. Tokarczyk (1992). "Chloro-Iodomethane in North-Atlantic Waters - a Potentially Significant Source of Atmospheric Iodine." Geophysical Research Letters **19**(17): 1779-1782.
- Moore, R. M. and R. Tokarczyk (1993). "Volatile Biogenic Halocarbons in the Northwest Atlantic." Global Biogeochemical Cycles **7**(1): 195-210.
- Moore, R. M., M. Webb, et al. (1996b). "Bromoperoxidase and iodoperoxidase enzymes and production of halogenated methanes in marine diatom cultures." Journal of Geophysical Research-Oceans **101**(C9): 20899-20908.
- Moore, R. M. and O. C. Zafiriou (1994). "Photochemical Production of Methyl-Iodide in Seawater." Journal of Geophysical Research-Atmospheres **99**(D8): 16415-16420.

- Mossinger, J. C., D. E. Shallcross, et al. (1998). "UV-VIS absorption cross-sections and atmospheric lifetimes of CH₂Br₂, CH₂I₂ and CH₂BrI." Journal of the Chemical Society-Faraday Transactions **94**(10): 1391-1396.
- Mtolera, M. S. P., J. Collen, et al. (1996). "Stress-induced production of volatile halogenated organic compounds in *Eucheuma denticulatum* (Rhodophyta) caused by elevated pH and high light intensities." European Journal of Phycology **31**(1): 89-95.
- Mudge, S. M. (2007). "Multivariate statistical methods in environmental forensics." Environmental Forensics **8**(1-2): 155-163.
- Murphy, C. D., R. M. Moore, et al. (2000). "An isotopic labeling method for determining production of volatile organohalogenes by marine microalgae." Limnology and Oceanography **45**(8): 1868-1871.
- Murphy, J. and J. P. Riley (1962). "A Modified Single Solution Method for Determination of Phosphate in Natural Waters." Analytica Chimica Acta **26**(1): 31-&.
- Ni, X. H. and L. P. Hager (1999). "Expression of *Batis maritima* methyl chloride transferase in *Escherichia coli*." Proceedings of the National Academy of Sciences of the United States of America **96**(7): 3611-3615.
- Nielsen, J. E. and A. R. Douglass (2001). "Simulation of bromoform's contribution to stratospheric bromine." Journal of Geophysical Research-Atmospheres **106**(D8): 8089-8100.
- Nightingale, P. D. (2003). Air-Sea Interaction - Gas Exchange. Encyclopedia of Atmospheric Sciences. R. H. James. Oxford, Academic Press: 84-93.
- Nightingale, P. D., P. S. Liss, et al. (2000a). "Measurements of air-sea gas transfer during an open ocean algal bloom." Geophysical Research Letters **27**(14): 2117-2120.
- Nightingale, P. D., G. Malin, et al. (2000b). "In situ evaluation of air-sea gas exchange parameterizations using novel conservative and volatile tracers." Global Biogeochemical Cycles **14**(1): 373-387.
- Nightingale, P. D., G. Malin, et al. (1995). "Production of Chloroform and Other Low-Molecular-Weight Halocarbons by Some Species of Macroalgae." Limnology and Oceanography **40**(4): 680-689.
- Novak, J., J. Zluticky, et al. (1973). "Analysis of Organic Constituents Present in Drinking-Water." Journal of Chromatography **76**(1): 45-50.
- O'Doherty, S. J., P. G. Simmonds, et al. (1993). "Analysis of Replacement Chlorofluorocarbons Using Carboxen Microtraps for Isolation and Preconcentration in Gas-Chromatography Mass-Spectrometry." Journal of Chromatography A **657**(1): 123-129.
- O'Dowd, C. D., J. L. Jimenez, et al. (2002). "Marine aerosol formation from biogenic iodine emissions." Nature **417**(6889): 632-636.
- O'Hagan, D. and D. B. Harper (1999). "Fluorine-containing natural products." Journal of Fluorine Chemistry **100**(1-2): 127-133.
- Omenetto, N., G. A. Petrucci, et al. (1996). "Absolute and/or relative detection limits in laser-based analysis: The end justifies the means." Fresenius Journal of Analytical Chemistry **355**(7-8): 878-882.
- Page, B. D. and G. Lacroix (1993). "Application of Solid-Phase Microextraction to the Headspace Gas-Chromatographic Analysis of Halogenated Volatiles in Selected Foods." Journal of Chromatography **648**(1): 199-211.
- Palmer, C. J., T. L. Anders, et al. (2005). "Iodine and halocarbon response of *Laminaria digitata* to oxidative stress and links to atmospheric new particle production." Environmental Chemistry **2**(4): 282-290.

- Pankow, J. F. (1991). "Technique for Removing Water from Moist Headspace and Purge Gases Containing Volatile Organic-Compounds - Application in the Purge with Whole-Column Cryotrapping (P/Wcc) Method." Environmental Science & Technology **25**(1): 123-126.
- Pedersen, M., J. Collen, et al. (1996). "Production of halocarbons from seaweeds: An oxidative stress reaction?" Scientia Marina **60**: 257-263.
- Perez, F. F., C. G. Castro, et al. (2001). "Coupling between the Iberian basin - scale circulation and the Portugal boundary current system: a chemical study." Deep-Sea Research Part I- Oceanographic Research Papers **48**(6): 1519-1533.
- Peters, C., S. Pechtl, et al. (2005). "Reactive and organic halogen species in three different European coastal environments." Atmospheric Chemistry and Physics **5**: 3357-3375.
- Pfeilsticker, K., W. T. Sturges, et al. (2000). "Lower stratospheric organic and inorganic bromine budget for the Arctic winter 1998/99." Geophysical Research Letters **27**(20): 3305-3308.
- Popp, P. and A. Paschke (1997). "Solid phase microextraction of volatile organic compounds using carboxen-polydimethylsiloxane fibers." Chromatographia **46**(7-8): 419-424.
- Potin, P., K. Bouarab, et al. (2002). "Biotic interactions of marine algae." Current Opinion in Plant Biology **5**(4): 308-317.
- Pruvost, J. (2001). Etude des composés organiques halogénés volatils en milieu marin. Origines biologiques et anthropiques, échanges avec l'atmosphère – Utilisation comme traceurs transitoires de la circulation dans l'atlantique du Nord-Est. Chimie appliquée : chimie marine. Brest, Université de Bretagne Occidentale. **PhD**.
- Pruvost, J., O. Connan, et al. (1999). "A sampling device for collection and analysis of volatile halocarbons in coastal and oceanic waters." Analyst **124**(9): 1389-1394.
- Quack, B. (1994). Leichtflüchtige Halogenkohlenwasserstoffe in der marinen Atmosphäre: Bestand, Herkunft und Massenbilanzen über der Nord- und Ostsee. Kiel, Christian-Albrechts-Universität.
- Quack, B., E. Atlas, et al. (2004). "Oceanic bromoform sources for the tropical atmosphere." Geophysical Research Letters **31**(23): -.
- Quack, B., E. Atlas, et al. (2007a). "Bromoform and dibromomethane above the Mauritanian upwelling: Atmospheric distributions and oceanic emissions." Journal of Geophysical Research-Atmospheres **112**(D9): -.
- Quack, B., I. Peeken, et al. (2007b). "Oceanic distribution and sources of bromoform and dibromomethane in the Mauritanian upwelling." Journal of Geophysical Research-Oceans **112**(C10): -.
- Quack, B. and E. Suess (1999). "Volatile halogenated hydrocarbons over the western Pacific between 43 degrees and 4 degrees N." Journal of Geophysical Research-Atmospheres **104**(D1): 1663-1678.
- Quack, B. and D. W. R. Wallace (2003). "Air-sea flux of bromoform: Controls, rates, and implications." Global Biogeochemical Cycles **17**(1): -.
- Ras, M. R., F. Borrell, et al. (2009). "Sampling and preconcentration techniques for determination of volatile organic compounds in air samples." Trac-Trends in Analytical Chemistry **28**(3): 347-361.
- Reid, R. C., J. M. Prausnitz, et al. (1987). The properties of gases and liquids. New York, McGraw-Hill Publishing Company: 52-55.
- Richter, U. and D. W. R. Wallace (2004). "Production of methyl iodide in the tropical Atlantic Ocean." Geophysical Research Letters **31**(23): -.

- Rook, J. J. (1977). "Chlorination Reactions of Fulvic Acids in Natural-Waters." Environmental Science & Technology **11**(5): 478-482.
- Salawitch, R. J., D. K. Weisenstein, et al. (2005). "Sensitivity of ozone to bromine in the lower stratosphere." Geophysical Research Letters **32**(5): -.
- Sanchez, J. M. and R. D. Sacks (2003). "On-line multibed sorption trap and injector for the GC analysis of organic vapors in large-volume air samples." Analytical Chemistry **75**(4): 978-985.
- Sander, R. (1999). Compilation of Henry's Law constants for inorganic and organic species of potential importance in environmental chemistry
- Saxena, D., S. Aouad, et al. (1998). "Biochemical characterization of chloromethane emission from the wood-rotting fungus *Phellinus pomaceus*." Applied and Environmental Microbiology **64**(8): 2831-2835.
- Schall, C. and K. G. Heumann (1993). "GC Determination of Volatile Organoiodine and Organobromine Compounds in Arctic Seawater and Air Samples." Fresenius Journal of Analytical Chemistry **346**(6-9): 717-722.
- Simmonds, P. G. (1984). "Analysis of Trace Halocarbons in Natural-Waters by Simplified Purge and Cryotrap Method." Journal of Chromatography **289**(Apr): 117-127.
- Singh, H. B., L. J. Salas, et al. (1983a). "Methyl Halides in and over the Eastern Pacific (40-Degrees-N-32-Degrees-S)." Journal of Geophysical Research-Oceans and Atmospheres **88**(Nc6): 3684-3690.
- Singh, H. B., L. J. Salas, et al. (1983b). "Selected Man-Made Halogenated Chemicals in the Air and Oceanic Environment." Journal of Geophysical Research-Oceans and Atmospheres **88**(Nc6): 3675-3683.
- Smethie, W. M., T. Takahashi, et al. (1985). "Gas-Exchange and Co₂ Flux in the Tropical Atlantic-Ocean Determined from Rn-222 and Pco₂ Measurements." Journal of Geophysical Research-Oceans **90**(Nc4): 7005-7022.
- Smyth, T. J., P. I. Miller, et al. (2001). "Remote sensing of sea surface temperature and chlorophyll during Lagrangian experiments at the Iberian margin." Progress in Oceanography **51**(2-4): 269-281.
- Smythe-Wright, D., S. M. Boswell, et al. (2006). "Methyl iodide production in the ocean: Implications for climate change." Global Biogeochemical Cycles **20**(3): -.
- Sokal, R. and F. Rohlf (1995). Biometry: the principles and practice of statistics in biological research, WH Freeman.
- Solomon, S., R. R. Garcia, et al. (1994). "On the Role of Iodine in Ozone Depletion." Journal of Geophysical Research-Atmospheres **99**(D10): 20491-20499.
- Staudinger, J. and P. V. Roberts (2001). "A critical compilation of Henry's law constant temperature dependence relations for organic compounds in dilute aqueous solutions." Chemosphere **44**(4): 561-576.
- Stringer, R. and P. Johnston (2001). "Chlorine and the environment: An overview of the chlorine industry." Environmental Science and Pollution Research **8**(2): 146-146.
- Sturges, W. T., G. F. Cota, et al. (1992). "Bromoform Emission from Arctic Ice Algae." Nature **358**(6388): 660-662.
- Sturges, W. T., D. E. Oram, et al. (2000). "Bromoform as a source of stratospheric bromine." Geophysical Research Letters **27**(14): 2081-2084.
- Swinerton, J. W., C. H. Cheek, et al. (1962). "Determination of Dissolved Gases in Aqueous Solutions by Gas Chromatography." Analytical Chemistry **34**(4): 483-&.

- Tanzer, D. and K. G. Heumann (1992). "Gas-Chromatographic Trace-Level Determination of Volatile Organic Sulfides and Selenides and of Methyl-Iodide in Atlantic Surface-Water." International Journal of Environmental Analytical Chemistry **48**(1): 17-31.
- Tenhaken, R., A. Levine, et al. (1995). "Function of the Oxidative Burst in Hypersensitive Disease Resistance." Proceedings of the National Academy of Sciences of the United States of America **92**(10): 4158-4163.
- Tessier, E., D. Amouroux, et al. (2002). "Formation and volatilisation of alkyl-iodides and -selenides in macrotidal estuaries." Biogeochemistry **59**(1-2): 183-206.
- Theiler, R., J. C. Cook, et al. (1978). "Halohydrocarbon Synthesis by Bromoperoxidase." Science **202**(4372): 1094-1096.
- Tokarczyk, R. and R. M. Moore (1994). "Production of Volatile Organohalogenes by Phytoplankton Cultures." Geophysical Research Letters **21**(4): 285-288.
- Tokarczyk, R. and R. M. Moore (2006). "A seasonal study of methyl bromide concentrations in the North Atlantic (35 degrees-60 degrees N)." Journal of Geophysical Research-Atmospheres **111**(D8): -.
- Tokarczyk, R. and E. S. Saltzman (2001). "Methyl bromide loss rates in surface waters of the North Atlantic Ocean, Caribbean Sea, and eastern Pacific Ocean (8 degrees-45 degrees N)." Journal of Geophysical Research-Atmospheres **106**(D9): 9843-9851.
- Tsai, W. T. and K. K. Liu (2003). "An assessment of the effect of sea surface surfactant on global atmosphere-ocean CO₂ flux." Journal of Geophysical Research-Oceans **108**(C4).
- Urhahn, T. and K. Ballschmiter (1998). "Chemistry of the biosynthesis of halogenated methanes: C1-organohalogenes as pre-industrial chemical stressors in the environment?" Chemosphere **37**(6): 1017-1032.
- Urhahn, T. and K. Ballschmiter (2000). "Analysis of halogenated C-1/C-2-trace compounds in marine atmosphere." Fresenius Journal of Analytical Chemistry **366**(4): 365-367.
- Verhaeghe, E. F., A. Fraysse, et al. (2008). "Microchemical imaging of iodine distribution in the brown alga *Laminaria digitata* suggests a new mechanism for its accumulation." Journal of Biological Inorganic Chemistry **13**(2): 257-269.
- Vollmer, M. K. and R. F. Weiss (2002). "Simulations determination of sulfur hexafluoride and three chlorofluorocarbons in water and air." Marine Chemistry **78**(2-3): 137-148.
- Waeles, M., R. D. Riso, et al. (2007). "Distribution and seasonal changes of lead in an estuarine system affected by agricultural practices: The Penze estuary, NW France." Estuarine Coastal and Shelf Science **74**(3): 570-578.
- Walker, S. J., R. F. Weiss, et al. (2000). "Reconstructed histories of the annual mean atmospheric mole fractions for the halocarbons CFC-11, CFC-12, CFC-113, and carbon tetrachloride." Journal of Geophysical Research-Oceans **105**(C6): 14285-14296.
- Wallace, D. W. R., P. Beining, et al. (1994). "Carbon-Tetrachloride and Chlorofluorocarbons in the South-Atlantic Ocean, 19-Degrees-S." Journal of Geophysical Research-Oceans **99**(C4): 7803-7819.
- Wang, L., R. M. Moore, et al. (2009). "Methyl iodide in the NW Atlantic: Spatial and seasonal variation." Journal of Geophysical Research-Oceans **114**: -.
- Wanninkhof, R. (1992). "Relationship between Wind-Speed and Gas-Exchange over the Ocean." Journal of Geophysical Research-Oceans **97**(C5): 7373-7382.
- Wanninkhof, R., J. R. Ledwell, et al. (1985). "Gas-Exchange Wind-Speed Relation Measured with Sulfur-Hexafluoride on a Lake." Science **227**(4691): 1224-1226.

- Wanninkhof, R. and W. R. McGillis (1999). "A cubic relationship between air-sea CO₂ exchange and wind speed." Geophysical Research Letters **26**(13): 1889-1892.
- Weinberger, F., B. Coquempot, et al. (2007). "Different regulation of haloperoxidation during agar oligosaccharide-activated defence mechanisms in two related red algae, *Gracilaria* sp and *Gracilaria chilensis*." Journal of Experimental Botany **58**(15-16): 4365-4372.
- Weinberger, F., M. Friedlander, et al. (1999). "Oligoagars elicit a physiological response in *Gracilaria conferta* (Rhodophyta)." Journal of Phycology **35**(4): 747-755.
- Werkhoff, P. and W. Bretschneider (1987). "Dynamic Headspace Gas-Chromatography - Concentration of Volatile Components after Thermal-Desorption by Intermediate Cryofocusing in a Cold Trap .2. Effect of Sampling and Desorption Parameters on Recovery." Journal of Chromatography **405**: 99-106.
- Wever, R., M. G. M. Tromp, et al. (1991). "Brominating Activity of the Seaweed *Ascophyllum-Nodosum* - Impact on the Biosphere." Environmental Science & Technology **25**(3): 446-449.
- Wevill, D. J. and L. J. Carpenter (2004). "Automated measurement and calibration of reactive volatile halogenated organic compounds in the atmosphere." Analyst **129**(7): 634-638.
- White, R. H. (1982). "Analysis of Dimethyl Sulfonium Compounds in Marine-Algae." Journal of Marine Research **40**(2): 529-536.
- Whitman, W. G. (1923). "The two-film theory of gas absorption." Chem. & Metall. Eng. **29**: 146-148.
- Wilke, C. R. and P. Chang (1955). "Correlation of Diffusion Coefficients in Dilute Solutions." Aiche Journal **1**(2): 264-270.
- Wishkerman, A., S. Gebhardt, et al. (2008). "Abiotic methyl bromide formation from vegetation, and its strong dependence on temperature." Environmental Science & Technology **42**(18): 6837-6842.
- Wood, E. D., Armstrong, Fa, et al. (1967). "Determination of Nitrate in Sea Water by Cadmium-Copper Reduction to Nitrite." Journal of the Marine Biological Association of the United Kingdom **47**(1): 23-&.
- Wright, S. W., S. W. Jeffrey, et al. (1991). "Improved Hplc Method for the Analysis of Chlorophylls and Carotenoids from Marine-Phytoplankton." Marine Ecology-Progress Series **77**(2-3): 183-196.
- Wuosmaa, A. M. and L. P. Hager (1990). "Methyl-Chloride Transferase - a Carbocation Route for Biosynthesis of Halometabolites." Science **249**(4965): 160-162.
- Yang, X., R. A. Cox, et al. (2005). "Tropospheric bromine chemistry and its impacts on ozone: A model study." Journal of Geophysical Research-Atmospheres **110**(D23): -.
- Yentsch, C. S. and D. W. Menzel (1963). "A Method for the Determination of Phytoplankton Chlorophyll and Phaeophytin by Fluorescence." Deep-Sea Research **10**(3): 221-231.
- Yokouchi, Y., Y. Nojiri, et al. (2001). "Atmospheric methyl iodide: High correlation with surface seawater temperature and its implications on the sea-to-air flux." Journal of Geophysical Research-Atmospheres **106**(D12): 12661-12668.
- Yvon-Lewis, S. A. and J. H. Butler (2002). "Effect of oceanic uptake on atmospheric lifetimes of selected trace gases." Journal of Geophysical Research-Atmospheres **107**(D20): -.
- Zafiriou, O. C. (1974). "Photochemistry of Halogens in Marine Atmosphere." Journal of Geophysical Research **79**(18): 2730-2732.
- Zafiriou, O. C. (1975). "Reaction of Methyl Halides with Seawater and Marine Aerosols." Journal of Marine Research **33**(1): 75-81.

- Zlatkis, A., Lichtens.Ha, et al. (1973). "Concentration and Analysis of Volatile Urinary Metabolites." Journal of Chromatographic Science **11**(6): 299-302.
- Zoccolillo, L. and M. Rellori (1994). "Halocarbons in Antarctic Surface Waters." International Journal of Environmental Analytical Chemistry **55**(1-4): 27-32.